THE USE OF FUNCTIONALIZED ZIRCONOCENES AS PRECURSORS TO SILICA-SUPPORTED ZIRCONOCENE OLEFIN POLYMERIZATION CATALYSTS

by

Cheng, Xu

A Dissertation Submitted to the Faculty of
the Virginia Polytechnic Institute and State University
in Partial Fulfillment of the Requirements for the Degree of

Doctor of Philosophy

in

Chemistry

Paul A. Deck, Chairman

Karen J. Brewer

Brian E. Hanson

Timothy E. Long

James M. Tanko

Dec. 10th, 2001

Department of Chemistry
Virginia Tech
Blacksburg, Virginia

Keywords: Synthesis, Organometallic, Zirconocene, Stannyl, Silyl, Electrophilic Substitution, Hydrolysis, Polyolefin Catalyst, MAO, Immobilization, Silica, Leaching

Abstract

Me_3Si substituents adjacent to Cp_2MCl_2 (M = Ti, Zr, Hf) are converted to $BrMe_2Si$ groups using BBr_3. The high reactivity of the Si-Br bonds toward nucleophiles such as water suggested that these substituents could react with hydroxylated silica surfaces, immobilizing the metallocenes. This dissertation concerns the syntheses of electrophile-functionalized zirconocene dihalide complexes and their use as precursors to silica-supported metallocene olefin polymerization catalysts.

First we extended the metallocene "functionalization" chemistry to obtain substituents bearing more than one electrophilic bond. $(Me_3Sn)_2C_5H_4$ combined with $CpZrCl_3$ in toluene to afford (η^5-Me_3Sn-C_5H_4)$CpZrCl_2$ (**A**). Reactions of **A** with electrophiles (E-X = Cl_2B-Cl, I-Cl, and I-I) afforded (η^5-XMe_2Sn-C_5H_4)$CpZrCl_2$ (and E-Me) cleanly. The reaction of **A** with BBr_3 afforded either (η^5-$BrMe_2Sn$-C_5H_4)$CpZrBr_2$ (25 °C, 10 min) or (η^5-Br_2MeSn-C_5H_4)$CpZrBr_2$ (25 °C, 15 h). Ph_2MeSi-C_5H_4Li combined with $ZrCl_4$•2THF to afford (η^5-Ph_2MeSi-C_5H_4)$_2ZrCl_2$ (**B**). The reaction of **B** with BCl_3 led to incomplete cleavage of the Ph-Si bonds, however treatment of **B** with BBr_3 afforded (η^5-Br_2MeSi-C_5H_4)$_2ZrBr_2$ (**C**) efficiently. X-ray crystal structures of (η^5-$ClMe_2Sn$-C_5H_4)$CpZrCl_2$•½toluene, (η^5-Br_2MeSn-C_5H_4)$CpZrBr_2$•THF, **B**, and **C** were obtained.

Metallocene **C** reacts with water to afford an oligosiloxane-supported zirconocene dibromide. Spectroscopic characterization suggested a stereoregular structure in which the metallocene units have *meso* symmetry. The oligomeric substance showed high activity for homogeneous ethylene polymerization.

Supported metallocene olefin polymerization catalysts were prepared by combining a functionalized metallocene precursor (Cp_2ZrBr_2 bearing either $BrMe_2Si$ or Br_2MeSi groups) and partially dehydroxylated silica. The activities of the immobilized zirconocene catalysts

decreased and the stabilities increased with increasing number of tethers. The immobilized catalyst prepared from (η^5-Br_2MeSi-$C_5H_4)_2ZrBr_2$, which is assumed to form two "double-tethers" to silica, was significantly more active than the catalyst prepared from [η^5-1,3-$(BrMe_2Si)_2C_5H_3]_2ZrBr_2$, which is assumed to form four "single-tethers" to silica. Catalyst leaching was observed in all the immobilized zirconocene catalysts.

Finally we report model studies on the stability of the Si-O-Si bonds toward methylaluminoxane (MAO). The reaction of (η^5-$BrMe_2Si$-$C_5H_4)CpZrBr_2$ with $^tBuMe_2SiOH$ results in the formation of Si-O-Si bonds; addition of NEt_3 results in further reaction to afford Si-O-Zr bonds. The reaction of Me_3Si-O-$SiMe_3$ with MAO showed that Si-O-Si bonds can be cleaved under the conditions of our polymerization reactions.

Acknowledgements

I sincerely thank my advisor, Prof. Paul A. Deck, for his great support and guidance in my graduate research for the Ph. D. degree at Virginia Tech. Under his supervision, I learned a lot of synthetic organometallic methods and techniques, as well as methods and techniques for heterogeneous catalytic olefin polymerization. It has been a great opportunity and experience for me to work in his group. I sincerely appreciate his great help.

I am grateful to my committee members, Professors Karen Brewer, Brian Hanson, Timothy Long, and James Tanko, for their kind help during the course of my research and graduate study.

I also want to thank William Bebout and Tom Glass of the Analytical Service for their help with the NMR instrument, and Ms. Judy Gunderson of Dow Chemical for her kind work in obtaining the GPC data of polyethylene samples.

I also got a lot of help in my research from my group partners in the past two years. They are Francisco Cavadas, Eric Hawrelak, Owen Lofthus, Matthew Thornberry, and Andrea Warren. Their friendship encouraged me to overcome many difficulties. I wish to take this opportunity to thank them.

This research was supported by the National Science Foundation (CHE-9875446) and Research Corporation (CS0567). I appreciate their financial support.

Finally, without the edification, support, and endless love from my parents, I would not have been the person I am. They were, are, and will be forever the most important source of encouragement to me. This dissertation is dedicated to them.

Table of Contents

List of Schemes

List of Tables

List of Figures

List of Abbreviations

Ac: acetate
b.p.: boiling point
Bu: butyl
Cp: cyclopentadienyl
CPMAS: cross-polarization magic-angle spinning
DME: 1,2-dimethyloxyethane
EAO: ethylaluminoxane
EHMO: extended Hückel molecular orbit
ESR: electron spin resonance
Et: ethyl
Flu: fluorenyl
FT-IR: Fourier transform infrared
GPC: gel permeation chromatography
HDPE: high density polyethylene
ICP-OES: inductively coupled plasma-optical emission spectroscopy
Ind: indenyl
LDPE: low density polyethylene
LLDPE: linear low density polyethylene
MALDI: matrix-assisted laser desorption ionization
MAO: methylaluminoxane
Me: methyl
M_n: number average molecular weight
M_p: peak molecular weight of the molecular weight distribution curve from GPC
MW: molecular weight
M_w: weight average molecular weight
MWD: molecular weight distribution
M_z: z-average molecular weight
NMR: nuclear magnetic resonance
PDI: polymer dispersity index
PE: polyethylene
PP: polypropylene
Ph: phenyl
R_p: polymerization rate
TBAO: t-butyl aluminoxane
tbp: triangular bipyramid
TEA: triethyl aluminum
THF: tetrahydrofuran
T_m: temperature of the melting point
TMA: trimethyl aluminum
TOF MS: time-of-flight mass spectroscopy
UV: ultra-violet

Chapter 1 Introduction

1.1 Polyethylenes and Methods to Produce Polyethylenes

Polymers are widely used everywhere in the world. Polyethylenes compose of one-third of the world's total production of polymeric thermoplastics.[1] This section describes the most common types of polyethylene and compares their most important physical properties.

1.1.1 Classification of Polyethylenes and Their Applications

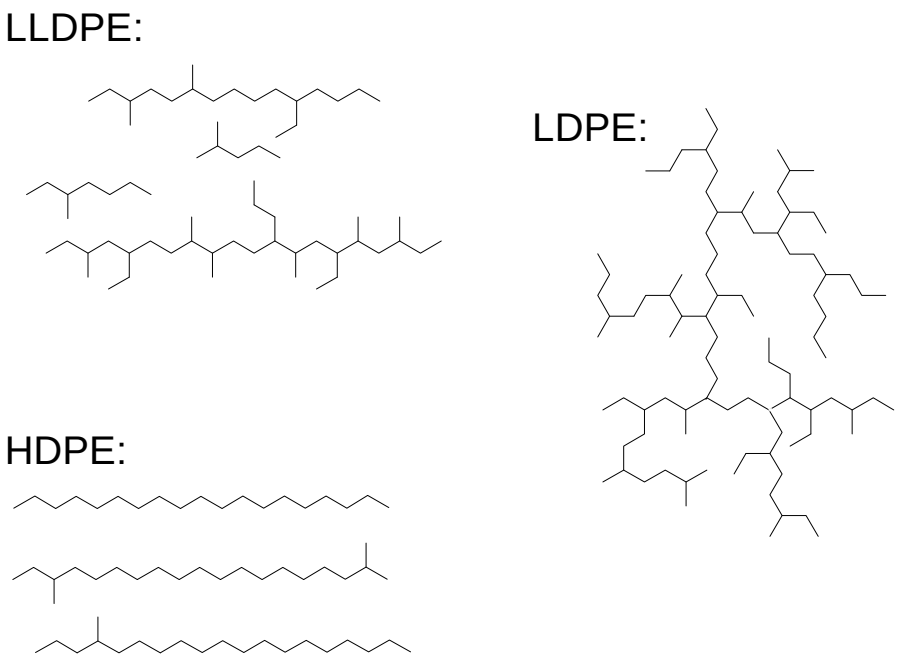

Figure 1-1 Chain Structures of LDPE, HDPE and LLDPE

Generally speaking, polyethylenes can be divided into two categories, i.e., low-density polyethylene (LDPE) and high-density polyethylene (HDPE). LDPE refers to the polyethylene of density between 0.910 g/cm^3 and 0.940 g/cm^3, and HDPE is polyethylene of density higher than 0.940 g/cm^3.[2] LDPE can be further divided into normal LDPE and linear low-density

[1] Foxley, D.: *Chem. & Ind.* (**Apr. 20)**, 305-308 (1998).
[2] Xie, T.-Y.; McAuley, K. B.; Hsu, J. C.-C.; Bacon, D. W.: *Ind. Eng. Chem. Res.* **33(3)**, 449-479 (1994).

polyethylene (LLDPE) based on the microstructures of the polyethylene chains. In most cases,[3] normal LDPE is made by a free-radical polymerization process. As a result, LDPE contains short-chain branches, as well as long-chain branches in the polymer chains (Figure 1-1), which lower the crystallinity, the melting point, and the density of LDPE compared to HDPE. As a result, LDPE is flexible and has high impact strength.

LLDPE is made by copolymerization of ethylene with an α-olefin (e.g., 1-butene, 1-hexene, or 1-octene) using Ziegler-Natta catalysts.[4] Incorporation of an α-olefin unit into a polymer chain introduces a short-chain branch, but the chain structure is linear (Figure 1-1). Although the density of LLDPE is in the same range as LDPE, LLDPE has much improved impact strength, puncture resistance, and tear strength compared to LDPE.[5]

HDPE is made by homopolymerization of ethylene using Ziegler-Natta catalysts.[4] HDPE comprises linear polyethylene chains with few branches (Figure 1-1). This microstructure results in better packing of polymer chains in solid state, so HDPE has higher density and crystallinity than LDPE. As a result, HDPE is a rigid thermoplastic.

LDPE, LLDPE, and HDPE have many applications. Due to their flexibility and toughness, the predominant application of LDPE and LLDPE is to make flexible blown films and soft extruded components such as tubing. HDPE is more useful as a structural material due to its rigidity. Applications of HDPE include formed packaging (such as milk bottles), pipe, and molded pieces such as kitchenware and toys.

---

[3] Recent results showed that long-chain branching polyethylene could also be produced using metallocene catalysts. Lai, S.-Y.; Wilson, J. R.; Knight, G. W.; Stevens, J. C.; Chum, P.-W. S.: *US Appl.* 301948 (1993).

[4] Phillips developed chromium oxide based catalysts, e.g., CrO_3/SiO_2. a) Clark, A.; Hogan, J. P.; Banks, R. L.; Lanning, W. C.: *Ind. Eng. Chem.* **48(7)**, 1152-1155 (1956). b) Hogan, J. P.; Banks, R. L.: *Belg. Pat.* 530617 (1955).

[5] James, D. E.: *Encyclo. of Polym. Sci. and Eng. 2nd ed.*, J. I. Kroschwitz Ed.-in-Chief, Wiley: New York 1986, **6**, 429-454.

1.1.2 Free Radical Polymerization

Free radical polymerization of ethylene is used to produce LDPE. The process was discovered by accident in the ICI laboratories in the UK in 1933.[6] Commercial production requires high temperatures (130-350 ^{o}C) and high pressures (122-303 MPa or 1200-3000 atm).[7] Generally, the polymerization is initiated by introducing a radical source, such as oxygen or peroxides, into the reactor. A free radical generated by thermal decomposition of the initiator attacks and adds to an ethylene molecule to form a new radical with an additional -CH_2CH_2- unit, which further attacks other monomers to develop a polymer chain. Growth of a polymer chain radical can be terminated by several mechanisms, including combination or disproportionation with another polymer chain radical, β-scission of the polymer chain radical itself, or chain transfer to ethylene, transfer agent, or polymer chain (Scheme 1-1).[7] Chain transfer to a polymer chain may proceed by either intramolecular or intermolecular routes. Intramolecular chain transfer refers to the abstraction of a hydrogen atom, usually from the fifth carbon back in the same chain by the chain radical. This "back-biting" mechanism terminates the original chain radical but creates a new radical in the middle of the same chain, where the chain continues to grow to form a branch. Therefore, intramolecular chain transfer causes short-chain branches (Scheme 1-1). Intermolecular chain transfer refers to the abstraction of a hydrogen atom from another polymer chain by the chain radical, which terminates the original chain radical but creates a new radical somewhere in the middle of the other polymer chain, where a new branch chain grows. Therefore, intermolecular chain transfer causes long-chain branches (Scheme 1-1).

[6] Fawcett, E. W.; Gibson, R. O.; Perrin, M. W.; Paton, J. G.; Williams, E. G.: *Brit. Pat.* 471590 (1937).
[7] Doak, K. W.: *Encyclo. of Polym. Sci. and Eng. 2nd ed.*, J. I. Kroschwitz Ed.-in-Chief, Wiley: New York 1986, **6**, 386-429.

Scheme 1-1 Free Radical Polyethylene Chain Termination Mechanisms [7]

combination:

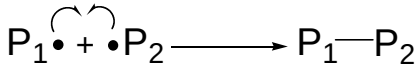

disproportionation:

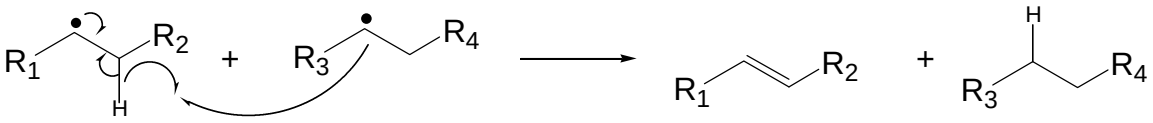

b-scission:

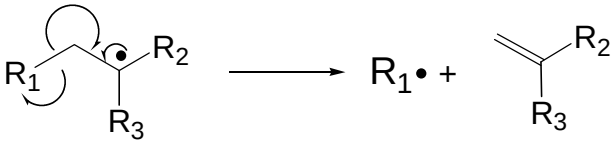

chain transfer to solvent:

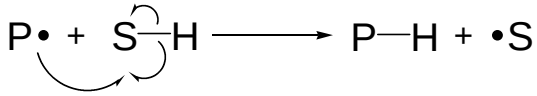

chain transfer to ethylene:

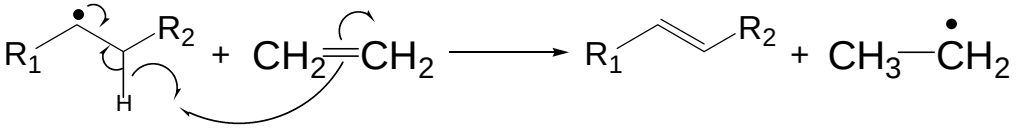

chain transfer to polymer chain:

intermolecular:

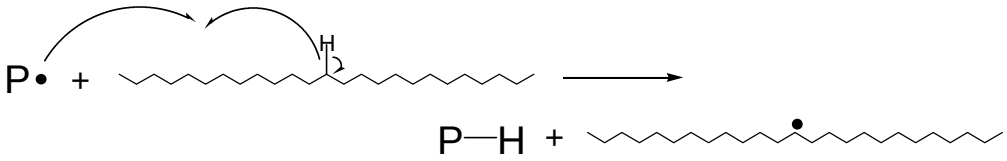

intramolecular:

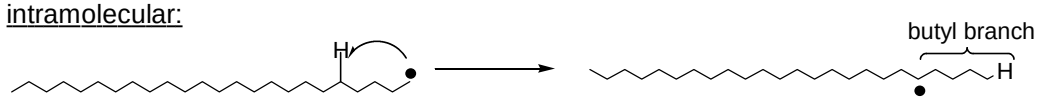

Free radical polymerization is the first commercial method to produce polyethylene. However, this method has some limitations. The process can only produce LDPE,[8] which has few (but relatively large scale) applications. Also, the required high temperature and high pressure consume a lot of energy and cause safety problems.

1.1.3 Coordination Polymerization Using Ziegler-Natta Catalysts

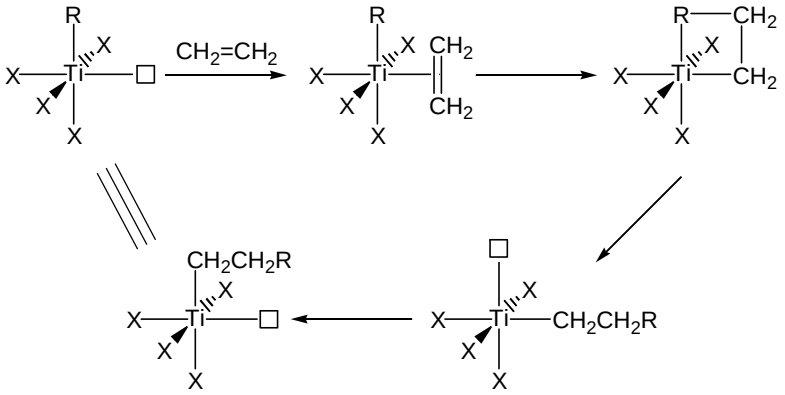

Scheme 1-2 Cossee-Arlman Mechanism [9]

An alternative method to make polyethylenes is coordination polymerization using Ziegler-Natta catalysts.[4] A Ziegler-Natta catalyst is normally a group 4 compound in combination with an aluminum alkyl compound. Ziegler and coworkers discovered that polyethylene could be made at 50-100 ^{o}C and atmospheric pressure using a catalyst system composed of titanium halides and aluminum alkyls.[10] The polyethylene made using his catalysts had higher density and crystallinity than LDPE from free radical polymerization. Natta and coworkers discovered that stereoregular polypropylene could be made using $TiCl_3$/electron

[8] It was found in DuPont that linear polyethylene can be made by free radical polymerization at 50-80 ^{o}C and 707 MPa (7000 atm), but the condition is not commercially feasible. Larchar, A. W.; Pease, D. C.: *US Pat.* 2816883 (1957).

[9] Hamielec, A. E.; Soares, J. B. P.: *Prog. Polym. Sci.* **21(4)**, 651-706 (1996).

[10] a) Ziegler, K.; Holzkamp, E.; Breil, H.; Martin, H.: *Angew. Chem.* **67**, 541-547 (1955). b) Ziegler, K.: *Belg. Pat.* 533362 (1954). c) Ziegler, K.: *Angew. Chem.* **76(13)**, 545-553 (1964).

donor/$AlEt_3$.[11] After decades of development, Ziegler-Natta catalysts have become the most important commercial catalysts to make HDPE and LLDPE.[12]

Most commercial Ziegler-Natta catalysts are heterogeneous systems. Typically, $TiCl_3$ is combined with $Al(C_2H_5)_3$ as the cocatalyst. A generally accepted mechanism to explain the mechanism of olefin polymerization using Ziegler-Natta catalysts is the Cossee-Arlman mechanism (Scheme 1-2).[13] The basic idea is that an active site contains a transition metal atom (Ti^{3+}) in an octahedral configuration. Five of the six coordination sites are occupied by four chlorine atoms from the crystal lattice and one alkyl group that originated from the cocatalyst. The remaining coordination site is a vacancy, where the double bond of an olefin monomer (e.g., ethylene) can coordinate and then insert in between the alkyl group and the metal center by a four-membered-ring intermediate (or transition state), resulting in two-carbon homologation of the alkyl group. The coordination and insertion cycle continues, and the alkyl group becomes a polymer chain. Several reactions can separate a polymer chain from the active center, i.e., spontaneous chain transfer, chain transfer to monomer, chain transfer to aluminum, and chain transfer to hydrogen (Scheme 1-3).[14] Spontaneous chain transfer and chain transfer to monomer both include b-hydride elimination process, in which the b-hydrogen on the polymer chain s-coordinated to the metal center is extracted by the metal center. The polymer chain becomes an olefin p-coordinated to the metal center through a p bond. The polymer chain can then leave the metal center to form a terminated polymer molecule, and an olefin monomer can coordinate to grow a new chain. Chain transfer to aluminum is through a four-centered metathesis mechanism,

[11] a) Natta, G.: *Angew. Chem.* **68**, 393-403 (1956). b) Natta, G.: *Angew. Chem.* **76(13)**, 553-566 (1964). c) Natta, G.: *J. Polym. Sci.* **16**, 143-154 (1955).
[12] Boor, J. Jr.: *Ziegler-Natta Catalysts and Polymerizations*, Academic: New York 1979.
[13] a) Cossee, P.: *Tetrahedron Lett.* **(17)**, 12-16 (1960). b) Cossee, P.: *J. Catal.* **3(1)**, 80-88 (1964). c) Arlman, E. J.; Cossee, P.: *J. Catal.* **3(1)**, 99-104 (1964).

in which a metal center with a polymer chain and an Al atom in AlR_3 exchange their ligands, so the polymer chain is coordinated to the Al atom and an R group is coordinated to the metal center after metathesis. Chain transfer to H_2 is also a metathesis process, which terminates the coordinated polymer chain and makes the metal center coordinate with a hydride. Chain transfer to H_2 provides a method to control the molecular weight of the polymer product.

spontaneous chain transfer:

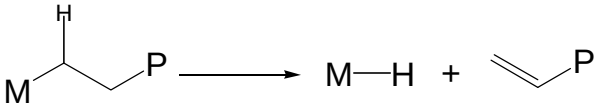

chain transfer to monomer:

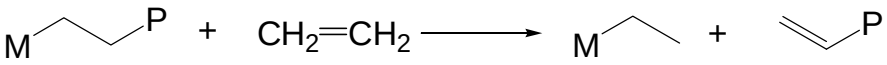

chain transfer to organometallic compound:

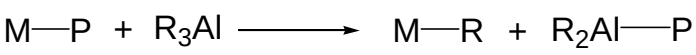

chain transfer to hydrogen:

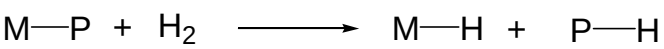

Scheme 1-3 Chain Termination Mechanisms in Coordination Polymerization of Ethylene [14]

Natta and coworkers found that only a very small portion of Ti atoms in $TiCl_3$ particles are actually involved in the polymerization.[15] Therefore, to improve efficiency, Ziegler-Natta catalysts are usually supported on inorganic (or, less frequently, organic) supports. The best support is $MgCl_2$. Because Mg and Ti have similar atomic size, shape, and coordination number, $MgCl_2$ has a similar crystalline structure to that of $TiCl_3$. Therefore, Ti(III) active centers have the best coordination and stability on $MgCl_2$ surfaces.[2] $MgCl_2$-supported (so-called "second generation") Ziegler-Natta catalysts are 2-3 orders of magnitude more active than their

[14] Beach, D. L.; Kissin, Y. V.: *Encyclo. of Polym. Sci. and Eng. 2nd ed.*, J. I. Kroschwitz Ed.-in-Chief, Wiley: New York 1986, **6**, 454-490.

unsupported counterparts, which has the important technological effect of reducing the "ash content" of the polymer and improving the clarity and tear resistance of film resins.

Ziegler-Natta catalysts also have some disadvantages. Because they are supported catalysts, characterization of the active species and detailed investigation of mechanisms and structure-property relationships are difficult. In addition, the solid surface is not uniform. The surface contains active metal centers having different catalytic properties. Some active centers have larger rate constant than others. Some active centers allow the α-olefin comonomer to coordinate and insert into polymer chain easier than others. Therefore, the HDPE produced has a broad molecular weight distribution (MWD), and the LLDPE produced has a non-uniform distribution of the incorporated α-olefin units among the polymer chains. This non-uniformity is called “multi-site” behavior. Although inhomogeneity of HDPE and LLDPE produced by the “multi-site” Ziegler-Natta catalysts limits some applications, Ziegler-Natta resins have processing advantages that might otherwise be achieved only by blending two or more metallocene resins. A "multi-site" Ziegler-Natta resin is, in effect, a "molecular" polyethylene blend. As long as formation of highly volatile, highly soluble, or highly crystalline chains (and subsequent phase separation) can be avoided, Ziegler-Natta resins are ideal for many molding and film-blowing applications.

There are four industrial processes to produce HDPE and LLDPE using Ziegler-Natta catalysts, i.e., the solution process, the bulk process, the slurry (suspension) process, and the gas-phase process.

---

[15] a) Natta, G.; Pasquon, I.: *Adv. in Catal. and Related Subjects* **11**, 1-66 (1959). b) Natta, G.; Mazzanti, G.; DeLuca, D.; Giannini, U.; Bandini, F.: *Makromol. Chem.* **76**, 54-65 (1964).

1.1.3.1 The Solution Polymerization Process

The solution process was the first industrial process using Ziegler-Natta catalysts. Though mostly replaced by the slurry and gas-phase processes, solution polymerization is still used to produce polyethylene by some companies. Advantages include a relatively small reactor (short residence time) and easy control of polymer properties. The process operates at above 120-130 ^{o}C,[14] so polyethylene is melted and soluble in hydrocarbon solvent (e.g., cyclohexane). Ethylene, solvent, catalyst, and hydrogen are fed into a reactor continuously. The polymerization is allowed to continue for a period of time. Then the hot polymer solution is discharged, and the solvent is removed by vaporization. The solution process is used to produce low molecular weight (MW) polyethylene. As the MW of polyethylene increases, the viscosity of the polymer solution increases, which causes stirring and homogeneity problems in the solution process. Besides the viscosity limitation, the solution process has another major disadvantage: Solvent volatilization requires huge energy consumption.

1.1.3.2 The Bulk Polymerization Process

The bulk process resembles the solution process, but it does not use any solvent. It operates at 170-350 ^{o}C and 30-200 MPa,[16] so that polyethylene is a melt. Ethylene monomer and catalyst dissolve in the melt, where the polymerization occurs.

1.1.3.3 The Slurry Polymerization Process

Due to its maturity and flexibility in the process engineering, the slurry (suspension) process is widely employed to produce polyethylene. The process is similar to the solution process. However, it operates at a relatively low temperature (e.g., 85-110 ^{o}C),[17] below the melting point of polyethylene, so that the polymer is essentially insoluble in the inert solvent

[16] Machon, J. P.; Hermant, R.; Houzeaux, J. P.: *J. Polym. Sci. Polym. Symp.* **52**, 107-117 (1975).

(e.g., hexane). In the reactor, the ethylene monomer is dissolved in the solvent; the catalyst particles and the polymer formed are suspended in the solvent. The polymerization occurs on the surface of the suspended catalyst particles. The slurry process is limited for not being able to produce LLDPE, especially that of density below 0.930 g/cm^3.[2] Low-density polyethylene has increased solubility in the solvent, and the dissolved polymer increases viscosity and causes reactor fouling. In addition, solvent removal in the slurry process also consumes energy. Slurry and solution processes are still used for polymers where the cost of the resin offsets the process costs. Elastomer resins are an important example.

1.1.3.4 The Gas-Phase Polymerization Process

Union Carbide set up the first commercial plant to produce polyethylene using the gas-phase process in 1968 under the brand name "Unipol".[18] The "Unipol" process uses a fluidized-bed reactor. Catalyst particles are introduced into the reactor by an inert gas flow. The particles are kept in the reaction zone in the reactor by a strong ethylene flow. Due to the ethylene flow, the particles are flowing and separated from each other in the reaction zone, so it is called a fluidized bed. Under the polymerization conditions (a temperature below 100 ^{o}C and a pressure below 2 MPa),[5] ethylene polymerizes on the particles, and gradually the particles grow into tiny polymer corpuscles. Polymer particles above certain size can not keep flowing in the reaction zone, so they fall down to the bottom of the reactor, where they are removed as product. Ethylene has three process functions: the monomer for the polymerization, the medium to remove heat generated in the polymerization, and the gas flow to keep particles flowing and separated. One major difficulty for academic laboratories is the enormous difficulty and cost of

[17] Short, J. N.: *Transition Metal Catalyzed Polymerizations: Alkenes and Dienes Part B*, R. P. Quirk Ed., Harwood Academic Publishers: New York 1983, 651-669.

[18] a) Rasmussen, D. M.: *Chem. Eng.* **79(21)**, 104-105 (1972). b) Miller, A. R.: *US Pat.* 4003712 (1977). c) Wagner, B. E.; Goeke, G. L.; Karol, F. J.: *US Pat.* 4303771 (1981).

designing and building even a small-scale version of a Unipol reactor in order to study this kind of polymerization process.

The gas-phase process has many advantages over the liquid processes. The shapes of the polymer particles produced resemble the shapes of the catalyst particles, so it is easy to control polymer particle shapes. In addition, the polymer particles removed from the reactor can be directly packed as final product. In contrast, in the liquid processes, the particles are poorly shaped and need to be further pelletized.

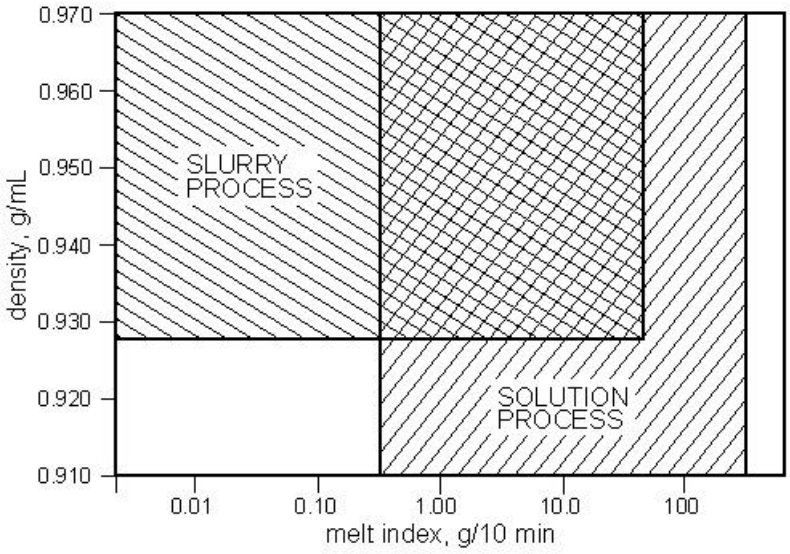

Figure 1-2 Production Capabilities of the Liquid Polymerization Processes [2]

The gas-phase process does not include any solvent, so the solubility and viscosity problems encountered in the liquid processes do not arise in the gas-phase process. Therefore, the gas-phase process is able to produce polyethylene of a broad range of densities and melt indices (inversely related to the weight average molecular weight, M_w). Figure 1-2 shows how the production capabilities of the liquid processes are limited to produce polyethylenes of certain range of densities and melt indices.[2] In contrast, the gas-phase process is able to produce

polyethylenes of densities and melt indices covering the whole map (i.e., density from 0.910 to 0.970 g/cm^3, melt index from less than 0.01 up to 200 g/10min).[5]

In the liquid processes, the comonomer content is limited due to the viscosity problem from the dissolved copolymer and comonomer.[19,20] The problem does not exist in the gas-phase process. Therefore, copolymer of higher comonomer content can be produced.

An efficient method to control polymer MW in the Ziegler-Natta polymerization is to introduce certain amount of hydrogen into the reactor. In the liquid processes, hydrogen needs to dissolve into the liquid and diffuse to the active sites to act, but there are solubility problem at high temperature and homogeneity problem in the diffusion process. In the gas-phase process, the solubility problem does not exist, so the hydrogen concentration is not limited. The diffusion problem in the gas phase is also minimized. Hydrogen molecules react with active sites directly on the surface of the particles to control MW of the polymer.

The gas-phase process also has some disadvantages. The operating temperature is limited by the polymer softening point. Therefore, the productivity of the catalyst is limited. The heat transfer efficiency of gas phase is poor, so an additional inert heat transfer agent is required to keep a stable operating environment. Otherwise, local hot spots cause polymer sintering and agglomeration problems. Significant progress has been made to overcome these disadvantages. The distinct economic and technological advantages of the gas-phase process over the liquid processes have revolutionized the polyolefin industry worldwide. Commercial production capability of polyolefins using the gas-phase process has grown rapidly in the past thirty years, and it has become the most important method to produce polyolefins.

[19] Rhee, S. J.; Baker, E. C.; Edwards, D. N.; Lee, K. H.; Moorhouse, J. H.; Scarola, L. S.; Karol, F. J.: *US Pat.* 4994534 (1991).
[20] Burdett, I. D.: *CHEMTECH* **22(10)**, 616-623 (1992).

1.2 Metallocene Catalysts

1.2.1 Development of Metallocene Catalysts

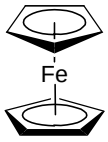

Scheme 1-4 Molecular Structure of Ferrocene

Although most commercial Ziegler-Natta catalysts are heterogeneous catalysts, there are some homogeneous Ziegler-Natta catalysts that were discovered in the early stage of the development of Ziegler-Natta catalysts.[12] An important family of homogeneous Ziegler-Natta catalysts is the metallocene catalysts. The term "metallocene" traditionally refers to organometallic compounds having two cyclopentadienyl (Cp) ligands and, optionally, one or more additional ligands such as alkyl or halide. In common usage, however, "metallocene" refers to the broader category of compounds containing one or more Cp (or, less frequently, arene ligands) and their derivatives. Cp ligands have an "aromatic" π-electron system, and they coordinate to the metal centers using these π frontier orbitals. The coordination bonding is distributed equally among the five atoms.[21] The famous sandwich compound, ferrocene or dicyclopentadienyliron (Cp_2Fe, Scheme 1-4) is the first metallocene compound, discovered in 1951.[22] Metallocene compounds important for olefin polymerization are the group 4 (Ti, Zr, Hf) metallocene compounds with cyclopentadienyl ligands. The first example of a metallocene catalyst for olefin polymerization, titanocene dichloride, was discovered by Breslow and Newburg.[23] They found that a solution of Cp_2TiCl_2 and a trialkylaluminum cocatalyst (AlR_3) polymerizes ethylene. Another example is the zirconium analog (zirconocene dichloride),

[21] Johnson, J. C.: *Metallocene Technology*, Noys Data Corporation: Park Bridge, New Jersey 1973.
[22] Kealy, T. J.; Pauson, P. L.: *Nature* **168**, 1039-1040 (1951).
[23] Breslow, D. S.; Newburg, N. R.: *J. Am. Chem. Soc.* **79(18)**, 5072-5073 (1957).

Cp_2ZrCl_2/AlR_3.[24] Initially, the activities of metallocene catalysts were poor, the catalysts lacked stereospecificity for propylene polymerization, and their kinetic lifetimes were short, but the polyethylene product had narrow molecular weight distribution.[25] For these reasons, metallocenes did not attract much interest for over 20 years, but attempts to improve the performance of the metallocene catalysts continued in a few laboratories anyway.

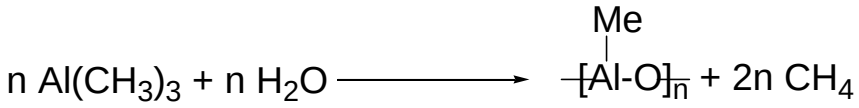

Scheme 1-5 Synthesis of MAO

In 1973, Reichert and Meyer found that the polymerization activity of the $Cp_2TiEtCl/AlEtCl_2$ catalyst system was significantly enhanced when some water was present in the system.[26] The result was supported by similar results about different titanocene catalyst systems from different groups.[27,28,29] Long and Breslow proposed that a bridged compound from the reaction of alkylaluminum and water, $ClR_2Al\text{-}O\text{-}AlR_2Cl$, formed a stable complex with Cp_2TiCl_2, which showed high activity for polymerization.[27] Araki, et al. found that trialkylaluminum reacts with water to produce an oligomeric alkylaluminoxane, e.g., methylaluminoxane (MAO) formed by the reaction of trimethylaluminum (TMA) and water (Scheme 1-5).[30] Prompted by these results, Sinn and Kaminsky directly used alkylaluminoxane as the cocatalyst instead of alkylaluminum with additional water, and they observed similarly high activities. Therefore, they concluded that the oligomeric aluminoxane is responsible for the

[24] Resconi, L.; Giannini, U.; Albizzati, E.; Piemontesi, F.; Fiorani, T.: *Polym. Prepr.* **32(1)**, 463-464 (1991).
[25] Reddy, S. S.; Sivaram, S.: *Prog. Polym. Sci.* **20(2)**, 309-367 (1995).
[26] Reichert, K. H.; Meyer, K. R.: *Makromol. Chem.* **169**, 163-176 (1973).
[27] Long, W. P.; Breslow, D. S.: *Justus Liebigs Ann. Chem.* **(3)**, 463-469 (1975).
[28] Andresen, A.; Cordes, H. G.; Herwig, J.; Kaminsky, W.; Merck, A.; Mottweiler, R.; Pein, J.; Sinn, H.; Vollmer, H. J.: *Angew. Chem.* **88(20)**, 689-690 (1976).
[29] a) Cihlář, J.; Mejzlik, J.; Hamřik, O.: *Makromol. Chem.* **179(10)**, 2553-2558 (1978). b) Cihlář, J.; Mejzlik, J.; Hamřik, O.; Hudec, P.; Majer, J.: *Makromol. Chem.* **181(12)**, 2549-2561 (1980).
[30] Ueyama, N.; Araki, T.; Tani, H.: *Macromolecules* **7(2)**, 153-160 (1974).

high activities.[31] Additional studies showed that MAO is more effective than other alkylaluminoxanes.[32] Kinetic studies by Mejzlik and coworkers indicated that the great activity-enhancing effect of MAO was due to the tremendous increase of the chain propagation rate constant caused by the aluminate anions rather than an increase in the number of the active sites.[29]

Triggered by the discovery of the highly active metallocene/MAO catalysts, studies on homogeneous metallocene catalysts boomed.[9,25,33,34] Scientists continue to be attracted by many distinct advantages of the metallocene catalysts over the conventional Ziegler-Natta catalysts.

1.2.2 Synthesis, Structure and Property of Aluminoxanes

Aluminoxanes are a group of compounds derived from aluminum alkyls. Their general structure can be represented by $[\text{-O-Al(R)-}]_n$.[25] The characteristic structure component of aluminoxanes is the Al-O-Al linkage. Depending on the alkyl group of the precursor aluminum alkyl, aluminoxanes include methylaluminoxane (MAO), ethylaluminoxane (EAO), t-butyl-aluminoxane (TBAO), etc. MAO is the most difficult to prepare as well as the most reactive aluminoxane and the most active cocatalyst for metallocene catalysts. An additional problem of MAO is that the trimethylaluminum, which is prepared from chloromethane, is considerably more expensive than triethylaluminum, which can be made directly from ethylene.

1.2.2.1 Synthesis of Aluminoxanes

Aluminoxanes are prepared by the controlled partial hydrolysis of corresponding aluminum alkyls. Several methods have been developed. Based on the way water is introduced

[31] a) Sinn, H.; Kaminsky, W.: *Adv. Organomet. Chem.* **18**, 99-149 (1980). b) Sinn, H.; Kaminsky, W.; Vollmer, H. J.; Woldt, R.: *Angew. Chem. Int. Ed. Engl.* **19(5)**, 390-392 (1980).
[32] Kaminsky, W.; Steiger, R.: *Polyhedron* **7(22-23)**, 2375-2381 (1988).
[33] Olabisi, O.; Atiqullah, M.; Kaminsky, W.: *J.M.S.-Rev. Macromol. Chem. Phys.* **C37(3)**, 519-554 (1997).
[34] Kaminsky, W.; Arndt, M.: *Applied Homogeneous Catalysis with Organometallic Compounds*, B. Cornils and W. A. Herrmann Eds., VCH: New York 1996, **1**, 220-236.

in the preparation, the methods are generally divided into three categories: i.e., direct hydrolysis methods, crystallized water methods, and other methods.

In the direct hydrolysis methods, water is introduced directly with or without some carrier. Water can be dispersed in a solvent, e.g., benzene or toluene, and the alkylaluminum is then mixed with the "wet" solvent to form aluminoxane.[35] Sakharovskaya and coworkers used a nitrogen stream to introduce water vapor into their reaction.[36] Water vapor can also be directly condensed into a cooled solution of alkylaluminum.[37] In contrast, Kaminsky and Haehnsen simply used ice as the source of water, but they kept the reaction temperature low to avoid the presence of any liquid water.[38] In the direct methods, the physical bonds between water and the carrier are weak and water is easily released, so the reaction conditions are difficult to control.

Salt hydrates are good sources of water. The water is crystallized and chemically bonded in the crystal lattice stoichiometrically, so using salt hydrates allows more accurate control of the quantity of water in the reaction system. Salt hydrates that have been used in the syntheses of aluminoxanes include $CuSO_4 \cdot 5H_2O$, $Al_2(SO_4)_3 \cdot 18H_2O$, $Al_2(SO_4)_3 \cdot 15H_2O$, $FeSO_4 \cdot 7H_2O$, $LiBr \cdot 2H_2O$, etc.[25] A typical process to prepare MAO using $CuSO_4 \cdot 5H_2O$ as the water source was described by Giannetti and coworkers.[39] To a two-liter round-bottom flask with a mechanical stirrer protected by nitrogen flow, fine pulverized $CuSO_4 \cdot 5H_2O$ of 55 g and 200 mL toluene were added. The temperature was decreased to -20 ^oC, then, a toluene solution of $Al(CH_3)_3$ (510 mL, 1.438 M) was added to the flask dropwise through a dropping funnel under nitrogen protection. The mixture was under sufficient stirring, and the temperature was slowly

[35] Vandenberg, E. J.: *J. Polym. Sci.* **47(149)**, 486-491 (1960).
[36] Sakharovskaya, G. B.; Korneev, N. N.; Popov, A. F.; Larikov, E. I.; Zhigach, A. F.: *Zh. Obshch. Khim.* **34(10)**, 3435-3438 (1964).
[37] Storr, A.; Jones, K.; Laubengayer, A. W.: *J. Am. Chem. Soc.* **90(12)**, 3173-3177 (1968).
[38] a) Kaminsky, W.; Haehnsen, H.: *DE Pat.* 3240383 (1982). b) Haehnsen, H.: *Ph.D. Dissertation*, University of Hamburg: Hamburg 1984.
[39] Giannetti, E.; Nicoletti, G. M.; Mazzocchi, R.: *J. Polym. Sci. Polym. Chem. Ed.* **23(8)**, 2117-2134 (1985).

raised to 20 ^{o}C over 24 hours. The mixture was then filtered, and a clear solution was obtained. The solvent (toluene) was removed by vacuum from the clear solution, and a caramel-like solid residue was obtained. A 1 : 1 mixture of toluene and n-hexane was added to the residue and stirred, then, the solvent was removed by vacuum. The process was repeated several times to remove any distillable $Al(CH_3)_3$ completely. The final product was dried at 40 ^{o}C and $1x10^{-6}$ mmHg to yield 12.6 g of a white solid.

Some other methods to prepare aluminoxanes include the reaction of PbO with an alkylaluminum,[40] the reaction between methoxyaluminum ($Me_x(OMe)AlCl_{2-x}$, x=0, 1, 2) and methylaluminum chlorides (Me_yAlCl_{3-y}, y=1, 2, 3).[41]

1.2.2.2 Structures and Properties of Aluminoxanes

As residues obtained from removal of solvent, aluminoxanes are white amorphous powders or glassy solids. They are soluble in toluene and benzene but insoluble in n-hexane. X-ray powder diffraction confirms that MAO is amorphous. The degree of oligomerization is generally between 5 and 30. The C/Al ratio varies from 1.1 to 1.6, and the aluminum content is around 45%. Analysis by ^{1}H NMR spectroscopy reveals that unreacted TMA always exists in MAO. Repeated extraction or vacuum evaporation can merely reduce the TMA concentration. Besides the TMA signal, the ^{1}H NMR spectrum of MAO in toluene-d_8 shows a broad band centered at -0.35 ppm.[42] Gel permeation chromatography (GPC) data presented by Cam and coworkers showed that MAO is a mixture containing many compounds with molecular weights ranging from 250 to 1500.[43]

[40] Bolesławski, M.; Pasynkiewicz, S.: *J. Organomet. Chem.* **43(1)**, 81-93 (1972).
[41] Kosińska, W.; Kunicki, A.; Bolesławski, M.; Pasynkiewicz, S.: *J. Organomet. Chem.* **161(3)**, 289-297 (1978).
[42] Resconi, L.; Bossi, S.; Abis, L.: *Macromolecules* **23(20)**, 4489-4491 (1990).
[43] Cam, D.; Albizzati, E.; Cinquina, P.: *Makromol. Chem.* **191(7)**, 1641-1647 (1990).

Figure 1-3 The Cyclic and Linear Structures of MAO [25]

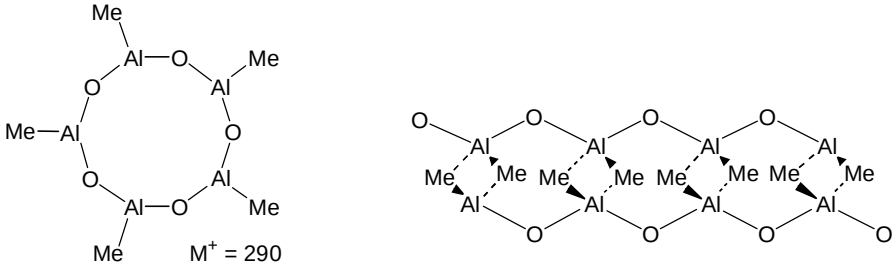

Oligomeric aluminoxanes are usually represented by a general formula, $[\text{-O-Al(R)-}]_n$. However, this proposed linear-chain structure[44] could only represent the approximate composition of aluminoxanes. The structures of aluminoxanes are actually very complicated and can vary with synthetic conditions and isolation methods. Based on a mass spectroscopy study, Sinn and Kaminsky reported a cyclic MAO structure of a MAO fraction isolated by fractional precipitation.[31a] An M^+ peak at 290 amu was assigned to a cyclic structure containing five aluminum atoms (Figure 1-3). However, aluminum atoms are rarely tricoordinate in solution or in solid state species. The observed species at 290 amu was probably a fragment of a linear or cage species. Aluminum compounds without bulky ligands tend to maximize the coordination number of aluminum at four by forming oligomers, in which two or more aluminum atoms share bridging ligands. Therefore, most other authors have proposed structures in which aluminum atoms have a coordination number of four. A linear double-chain structure of MAO containing four-coordinated aluminum atoms (Figure 1-3) was proposed independently by Giannetti[39] and Sugano.[45] Atwood and Zaworotko presented the crystallographic molecular structure of $[Al_7O_6(CH_3)_{16}]^-$, a separated fraction of MAO, which shows clearly four-coordinated aluminum

[44] Pasynkiewicz, S.: *Polyhedron* **9(2-3)**, 429-453 (1990).
[45] Sugano, T.; Matsubara, K.; Fujita, T.; Takahashi, T.: *J. Mol. Catal.* **82(1)**, 93-101 (1993).

atoms (Figure 1-4).[46] Barron also demonstrated molecular structures of some isolated t-butyl-aluminoxanes, e.g., $[(^tBu)Al(\mu_3\text{-}O)]_6$, $[(^tBu)Al(\mu_3\text{-}O)]_9$, which are three-dimensional with four-coordinated aluminum atoms (Figure 1-5).[47] Barron also proposed a plausible molecular structure for $[(^tBu)Al(\mu_3\text{-}O)]_{12}$ as shown in Figure 1-5.

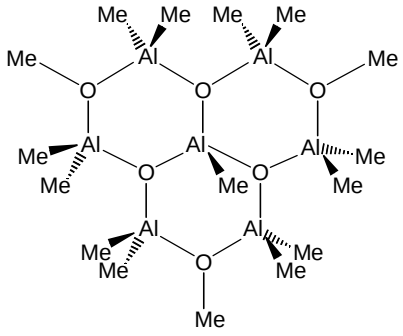

Figure 1-4 The Structure of $[Al_7O_6(CH_3)_{16}]^-$ [46]

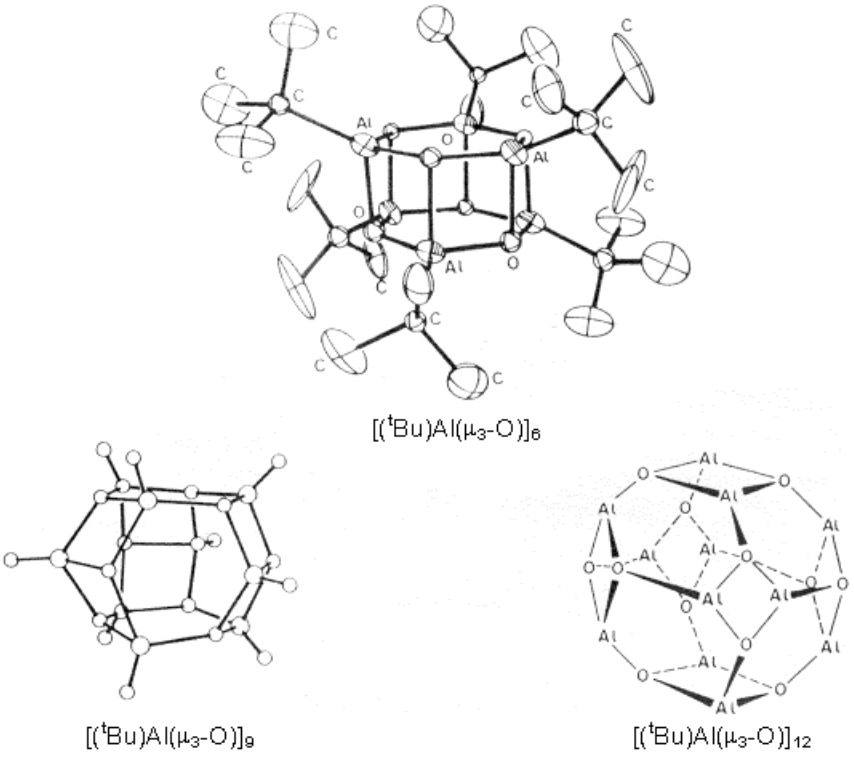

Figure 1-5 Structures of Some Three-dimensional MAO Molecules [47] (Courtesy of ACS)

[46] Atwood, J. L.; Hrncir, D. C.; Priester, R. D.; Rogers, R. D.: *Organometallics* **2(8)**, 985-989 (1983).
[47] Mason, M. R.; Smith, J. M.; Bott, S. G.; Barron, A. R.: *J. Am. Chem. Soc.* **115(12)**, 4971-4984 (1993).

1.2.3 Advantages of Metallocene Catalysts

Initially, homogeneous metallocene catalysts were less attractive because of their low activities for olefin polymerization compared to the conventional heterogeneous Ziegler-Natta catalysts. However, the discovery of aluminoxane cocatalysts tremendously increased the activities of metallocene catalysts. Some modified metallocene catalysts even have higher activities than the conventional Ziegler-Natta catalysts.[48] One of the most active metallocene catalysts for ethylene polymerization is the ethylene-bridged bis(4,5-dimethyl-fluorenyl) zirconium dichloride (Scheme 1-6).[49] This compound showed an activity of 2.85×10^4 kg PE/g(Zr)/h, when mixed with MAO (Al/Zr = 20000) in n-pentane at 60 ^oC with 10.0 bar ethylene. In comparison, the activities of supported Ziegler-Natta catalysts are in the range of 500-1000 kg PE/g(M)/h.[25] Among the metallocenes of the three group 4 elements, zirconocene catalysts are the most active and stable.[32] High activity not only increases efficiency and productivity, but it also makes the catalyst removal from the polymer product unnecessary, since the catalyst concentration in the polymer is too low to affect the polymer properties or to appreciably contaminate packaged foods.

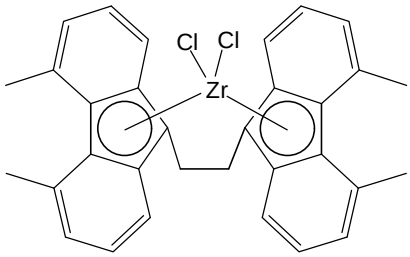

Scheme 1-6 Molecular Structure of [(μ-C_2H_4)(η^5-4,5-Me_2Flu)$_2$]ZrCl_2 [49]

Modified metallocene catalysts can also produce stereoregular polyolefins, e.g., isotactic and syndiotactic polypropylene.[33] Most iso-specific metallocene precursors are C_2 symmetrical,

[48] Alt, H. G.; Köppl, A.: *Chem. Rev.* **100(4)**, 1205-1221 (2000).
[49] Alt, H. G.: *J. Chem. Soc., Dalton Trans.* **(11)**, 1703-1709 (1999).

and most syndio-specific metallocene precursors are of C_s symmetry,[33,48,50] but there are important exceptions. For example, highly isotactic polypropylene (95% mm triads determined by ^{13}C NMR) can be produced using the C_2-symmetric rac-ethylene[bis(4,5,6,7-tetrahydroindenyl)zirconium] dichloride (Scheme 1-7) with MAO.[51] On the contrary, the C_s-symmetric isopropylidene(cyclopentadienyl)(fluorenyl)-zirconium dichloride (Scheme 1-7) produces highly syndiotactic polypropylene (94.6% r sequences).[48] Due to its excellent rigidity, toughness, and temperature resistance, isotactic polypropylene is used in some injection molding and extrusion processes. Syndiotactic polypropylene is more resistant to ultraviolet radiation than isotactic polypropylene and it is used to make medical apparati that require UV sterilization.[9]

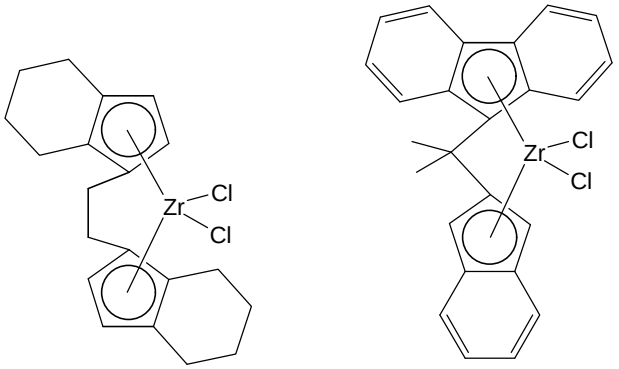

rac-[(μ-C_2H_4)(H_4Ind)$_2$]$ZrCl_2$ [(μ-Me_2C)(Ind)(Flu)]$ZrCl_2$

Scheme 1-7 Molecular Structures of rac-[(m-C_2H_4)(H_4Ind)$_2$]$ZrCl_2$ and [(m-Me_2C)(Ind)(Flu)]$ZrCl_2$ [48,51]

The homogeneous metallocene catalysts are "single-site" catalysts. The term "single-site" means that all the active sites are of the same properties, e.g., same structure, same activity, same selectivity, same chain-transfer rate, etc., so the polymer produced has narrow MWD (PDI

[50] Soga, K.; Shiono, T.: *Prog. Polym. Sci.* **22(7)**, 1503-1546 (1997).
[51] Kaminsky, W.; Külper, K.; Brintzinger, H. H.; Wild, F. R. W. P.: *Angew. Chem. Int. Ed. Engl.* **24(6)**, 507-508 (1985).

~ 2.0), the theoretical value predicted by the Shultz-Flory distribution.[52] In contrast, the conventional Ziegler-Natta catalysts are "multi-site" catalysts, as discussed in Section 1.1.3, leading to broad MWD.[53]

Similarly, "single-site" metallocene catalysts are able to produce high quality LLDPE, which has a narrow distribution of short-chain branches among the polymer chains and a random distribution of short-chain branches in a polymer chain. The narrow distribution of short-chain branches minimizes crystallization in the polymer, making the LLDPE an excellent elastomer free of crystallinity. An example presented by Kaminsky and Schlobohm showed that the LLDPE produced by copolymerization of ethylene and 1-butene using Cp_2ZrCl_2/MAO had a significantly lower melting point than that obtained using a heterogeneous Ziegler-Natta catalyst, $TiCl_4/AlEt_3$, with the same degree of 1-butene incorporation.[54] Due to the improved properties, LLDPE produced by metallocene catalysts is expected for many applications.[55]

Theoretically, metallocene catalysts can produce polyethylene of very high MW, especially when the polymerization temperature is low. At -20 ^oC, the rates of chain transfer reactions, e.g., β-hydride elimination reaction, are so low that the polymerization becomes essentially a living polymerization, i.e., the MW of the polymer is only a function of polymerization time, providing there is a sufficient supply of the monomers.[56]

Control of MW of polymer produced by a metallocene catalyst can be easily achieved by introducing hydrogen to the polymerization system or increasing its temperature. Unlike conventional Ziegler-Natta catalysts, metallocenes require only a trace of hydrogen to

[52] Flory, P. J.: *Principles of Polymer Chemistry*, Cornell University: Ithaca, New York 1953.
[53] Soares, J. B. P.; Hamielec, A. E.: *Polymer* **36(11)**, 2257-2263 (1995).
[54] Kaminsky, W.; Schlobohm, M.: *Makromol. Chem., Macromol. Symp.* **4**, 103-108 (1986).
[55] Tullo, A. H.: *Chem. & Eng. News* **78(32)**, 35-46 (2000).
[56] Kaminsky, W.: *Catalytic Polymerization of Olefins*, T. Keii and K. Soga Eds., Kodansha-Elsevier: Tokyo 1985, **25**, 293-304.

significantly reduce the MW of polymer produced.[57] On the contrary, a large excess of hydrogen is required to produce oligomers using conventional Ziegler-Natta catalysts, and the oligomers produced are saturated.[9] In addition, oligomers with unsaturated terminal vinyl or vinylidene groups can be produced by metallocene catalysts by increasing the polymerization temperature, because b-hydride elimination becomes the primary chain transfer pathway. The unsaturated oligomers can be further functionalized to make many useful chemicals.[58] Using certain "constrained geometry" catalysts, the unsaturated oligomers can undergo appreciable insertion into growing polymer chains, leading to long-chain branched polymers having unusual rheological properties.[3]

The "single-site" nature of metallocenes simplifies mechanistic studies. Many powerful techniques are available for solution characterization of chemical structure. Although relatively inactive, the early metallocene catalysts with aluminum alkyl cocatalysts provide good systems for mechanistic study. The development of the aluminum-free cationic metallocene catalysts using borane compounds such as $B(C_6F_5)_3$ as cocatalysts, provides ideal systems to study the mechanism and understand the structures of active species.[59,60]

The distinct features of the metallocene catalysts make it possible for chemists to design and make polymers of desired structures. The bright future of the metallocene catalysts has encouraged great efforts from many companies to commercialize them for polyolefin production. The first commercial process using metallocene catalysts is Exxon's "Exxpol" solution process. The LLDPE from the "Exxpol" process showed significantly different properties from those of

[57] Kaminsky, W.; Lüker, H.: *Makromol. Chem. Rapid Commun.* **5(4)**, 225-228 (1984).
[58] Hungenberg, K.-D.; Kerth, J.; Langhauser, F.; Müller, H.-J.; Müller, P.: *Angew. Makromol. Chem.* **227**, 159-177 (1995).
[59] Hlatky, G. G.; Turner, H. W.; Eckman, R. R.: *J. Am. Chem. Soc.* **111(7)**, 2728-2729 (1989).
[60] a) Yang, X.-M.; Stern, C. L.; Marks, T. J.: *J. Am. Chem. Soc.* **113(9)**, 3623-3625 (1991). b) Marks, T. J.: *Acc. Chem. Res.* **25(2)**, 57-65 (1992).

the LLPDE from the conventional Ziegler-Natta catalysts.[61] Commercial production capacity of polyolefins using metallocene catalysts continues to grow rapidly (Table 1-1).[62]

Table 1-1 Worldwide Metallocene Polyolefins Capacity Commitments [62]

company	region	year of commercialization	capacity(ton/year)
polyethylene			
Dow	U.S.	1993	50,000
Exxon	U.S.	1995	100,000
Mitsui	Japan	1995	100,000
Mitsubishi	Japan	1994	100,000
Union Carbide	U.S.	1995	300,000
polypropylene			
Chisso	Japan	--	20,000
Exxon	U.S.	1996	100,000
Hoechst	Europe	1995	100,000
Mitsui Toatsu	Japan	1994-1995	75,000-100,000

1.2.4 Disadvantages of Metallocene Catalysts

Metallocene catalysts do have some disadvantages. The activities of the metallocene catalysts for olefin polymerization are highly dependent on the Al/M ratio.[63,64] Metallocenes require large excesses of MAO (high Al/M ratio) to achieve high activities. For example, Chien

[61] Schut, J. H.: *Plast. Technol.* **37(12)**, 15 (1991).
[62] Baker, J.: *Euro. Chem. News* **(Oct.18)**, 22 (1993).
[63] Chien, J. C. W.; Razavi, A.: *J. Polym. Sci. Part A, Polym. Chem.* **26(9)**, 2369-2380 (1988).
[64] Chien, J. C. W.; Wang, B.-P.: *J. Polym. Sci. Part A, Polym. Chem.* **26(11)**, 3089-3102 (1988).

and Wang found that Cp_2ZrCl_2/MAO only exhibited an activity of $1.66x10^2$ kg/g(Zr)/h/MPa for ethylene polymerization when the Al/Zr ratio was 521 and the Zr concentration was $4.8x10^{-5}$ mol/L. The activity increased dramatically when the Al/Zr ratio increased, and it reached $4.9x10^3$ kg/g(Zr)/h/MPa when the Al/Zr ratio reached 92730 and the Zr concentration was reduced to $1.1x10^{-6}$ mol/L.[65] The cost of MAO is high, so the costs of the polyolefins made by metallocene catalysts are also high, if the Al/M ratios are high. Too much aluminoxane also increases the ash content (which is mainly alumina) in the product resin. In order to compete in price with the polyolefins produced by conventional Ziegler-Natta catalysts, either the cost of MAO or the ratio of Al/M in the polymer production processes using metallocene catalysts needs to be significantly reduced.

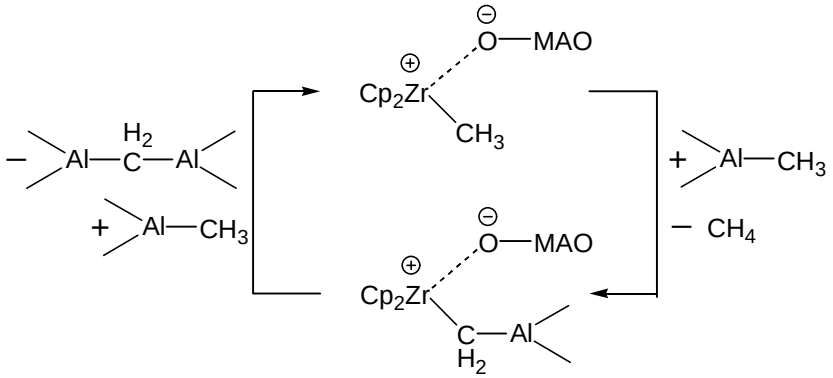

Scheme 1-8 The Deactivation Mechanism of Cp_2ZrCl_2/MAO Proposed by Kaminsky and Coworkers [67]

Kinetics studies showed decay-type kinetic profiles for ethylene polymerization using metallocene catalysts.[65,66] In the Cp_2ZrCl_2/MAO system, the polymerization rate (R_p) reaches a maximum about one minute after the introduction of the catalyst. Then, R_p follows a gradual decay to about one half of the maximum value.[65] This feature limits the productivity of the catalysts. The mechanism of deactivation of metallocene catalysts is not fully understood. One

[65] Chien, J. C. W.; Wang, B.-P.: *J. Polym. Sci. Part A, Polym. Chem.* **28(1)**, 15-38 (1990).

deactivation process of Cp_2ZrCl_2/MAO proposed by Kaminsky involves the formation of an inactive Zr-CH_2-Al structure (Scheme 1-8).[67]

The homogeneous nature of the metallocene catalysts also has some disadvantages from practical point of view. As discussed in Section 1.1.3.4, the gas-phase process for polyolefin production has many economic and technological advantages. However, the gas-phase process requires solid catalyst particles, so the metallocene catalysts, which are pure compounds and occur as crystalline solids, can not be used in gas-phase processes without immobilization. Besides, unlike in the gas-phase process, it is difficult to control polymer morphology in the solution process using homogeneous metallocene catalysts.

1.2.5 Mechanism of Metallocene Catalyzed Olefin Polymerization

Since the discovery of the conventional Ziegler-Natta catalysts and the metallocene catalysts for olefin polymerization, many mechanisms have been proposed. Two major steps are involved in the polymerization mechanism: i.e., the coordination of monomer to the active center and the insertion of the coordinated monomer into the growing polymer chain. Different mechanisms differ primarily in the structural details of the coordination and the insertion. Among the proposed mechanisms, the Cossee-Arlman mechanism, the trigger mechanism, and the Brookhart-Green mechanism are the three most important.

1.2.5.1 Some Proposed Mechanisms

The Cossee-Arlman mechanism (Scheme 1-2)[13] was originally proposed to explain the mechanism of the conventional heterogeneous Ziegler-Natta catalysts (see Section 1.1.3), but it is also applies to metallocene catalysts. When it is used to explain the mechanism of olefin polymerization using the metallocene catalysts, e.g., Cp_2TiCl_2/MAO, the active site is a cationic

[66] Fischer, D.; Mülhaupt, R.: *J. Organomet. Chem.* **417(1-2)**, C7-C11 (1991).
[67] Kaminsky, W.; Bark, A.; Steiger, R.: *J. Mol. Catal.* **74(1-3)**, 109-119 (1992).

species in solution, $Cp_2Ti^{\oplus}Me$ (Scheme 1-9), which has a vacant coordination site for the coordination of an α-olefin monomer. The Cossee-Arlman mechanism can not fully explain the iso-specificity of some metallocene catalysts. In addition, it can not explain some observations that the reaction order of the olefin monomer is higher than one.[68] However, there are still disputes on the polymerization reaction orders.[69]

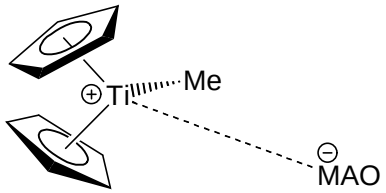

Scheme 1-9 The Active Species of Cp_2TiCl_2/MAO in Solution

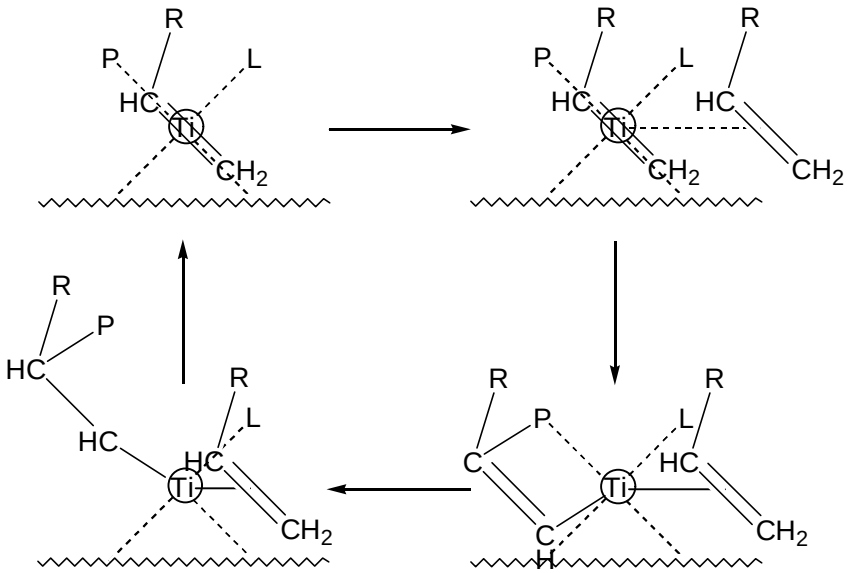

Scheme 1-10 Trigger Mechanism [68]

The trigger mechanism was proposed by Ystenes to overcome some defects of the Cossee-Arlman mechanism.[68] The trigger mechanism involves a two-monomer transition state, in which the insertion of one monomer is triggered by a second monomer (Scheme 1-10). The

[68] Ystenes, M.: *J. Catal.* **129(2)**, 383-401 (1991).
[69] Liu, Z.-X.; Somsook, E.; White, C. B.; Rosaaen, K. A.; Landis, C. R.: *J. Am. Chem. Soc.* **123(45)**, 11193 -11207 (2001).

trigger mechanism has three assumptions: 1) the site for monomer incorporation is always occupied by a monomer, since the insertion of one monomer is triggered by the incorporation of another monomer; 2) the insertion of a monomer will be retarded if a second incoming monomer is absent; 3) the two monomer units interact with each other and with the metal center in the transition state. The trigger mechanism rationalizes a reaction order between one and two for the olefin monomer.

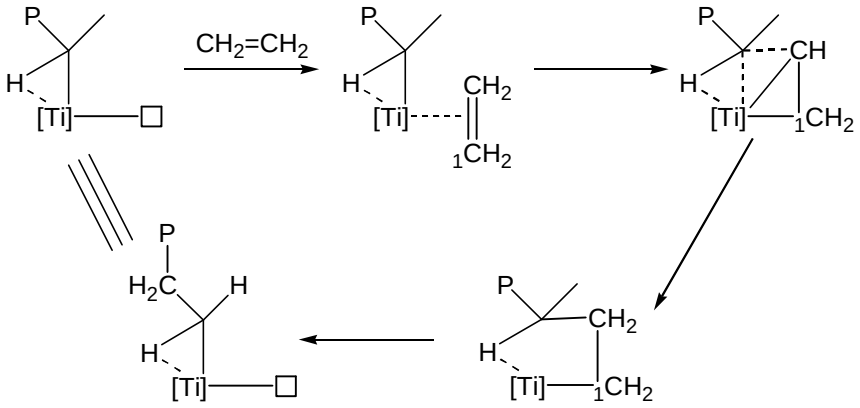

Scheme 1-11 Brookhart-Green Mechanism [50]

Brookhart and Green proposed a mechanism involving an α-H agostic interaction between one of the hydrogen atoms on the α carbon atom of the alkyl (growing polymer) chain and the metal center. The α-H agostic interaction assists the insertion of an olefin monomer.[70] The mechanism is supported by the α-H isotope effects observed by Krauledat and Brintzinger,[71] Piers and Bercaw,[72] as well as the ab initio calculation by Ahlrichs and coworkers.[73] The Brookhart-Green mechanism is shown in Scheme 1-11, the major difference between this mechanism and the Cossee-Arlman mechanism is that the olefin insertion is assisted by the α-H agostic interaction. The α-H interaction also accounts for stereoregularities much more

[70] a) Brookhart, M.; Green, M. L. H.: *J. Organomet. Chem.* **250(1)**, 395-408 (1983). b) Brookhart, M.; Green, M. L. H.; Wong, L.-L.: *Prog. Inorg. Chem.* **36**, 1-124 (1988).
[71] Krauledat, H.; Brintzinger, H.-H.: *Angew. Chem. Int. Ed. Engl.* **29(12)**, 1412-1413 (1990).
[72] Piers, W. E.; Bercaw, J. E.: *J. Am. Chem. Soc.* **112(25)**, 9406-9407 (1990).

effectively. For some time, most scientists agreed that steric effects of the ligands alone were responsible for the orientation of prochiral olefin insertion (enantiomorphic site control). However, Bercaw has used α-H interactions to introduce some chain-end character into the stereoregulation model, resulting in a highly consistent mechanistic picture.

1.2.5.2 Formation of Active Sites and the Role of MAO

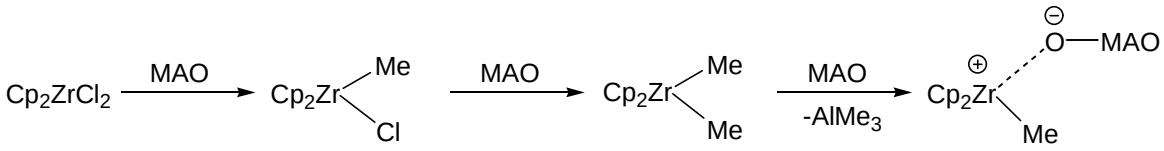

Scheme 1-12 Kaminsky's Mechanism [67]

MAO is the critical component that tremendously increases the catalytic activities of metallocene catalysts. Considerable effort has been expended to study the role of MAO in the mechanism of olefin polymerization using metallocene catalysts. The generally accepted mechanism proposed by Kaminsky and coworkers shows the major functions of MAO in the formation of an active center (Scheme 1-12).[67] MAO is very reactive towards water and oxygen, so the first function of MAO in a polymerization system is to act as a scavenger to get rid of trace amounts of water or oxygen, which are harmful to the polymerization. As shown in Scheme 1-12, in the formation process of an active center of the Cp_2ZrCl_2/MAO system, MAO methylates Cp_2ZrCl_2 to form the dimethylated species $Cp_2Zr(CH_3)_2$. After the methylation, MAO further extracts one of the two methyl groups on the metal center to form a highly polarized species with Cp_2ZrCH_3 partially positively charged. The cationic-like Cp_2ZrCH_3 is the active species for olefin monomer coordination and insertion.

Giannetti and coworkers proposed a different active species.[39] They thought that the active species contained a highly polarized Zr-O-Al linkage with the partial positive charge on

[73] Weiss, H.; Ehrig, M.; Ahlrichs, R.: *J. Am. Chem. Soc.* **116(11)**, 4919-4928 (1994).

the zirconium atom and the partial negative charge on the neighboring aluminum atom of MAO (Scheme 1-13). However, it is hard to believe that the partial negative charge is located on the aluminum atom instead of the oxygen atom, since the latter is much more electronegative than the former. Chien and coworkers proposed a mechanism including two kinds of active species, C_i^* and C_i^{*+}, in the Cp_2ZrCl_2/MAO system.[65] The subscript "i" corresponds to the number of coordination sites of a metal center occupied by MAO. C_i^* is a neutral species and C_i^{*+} is the corresponded cationic species. Chien thought that C_2^* was the most active and stable species. According to Chien, C^{*+} is produced by the reaction between Cp_2ZrCl_2 and MAO (Scheme 1-14). In the Giannini's mechanism, the TMA remaining in MAO is the actual alkylation agent.[74] It alkylates Cp_2ZrCl_2 to produce $Cp_2Zr(CH_3)Cl$, which further reacts with MAO to form a highly polarized structure (Scheme 1-15).

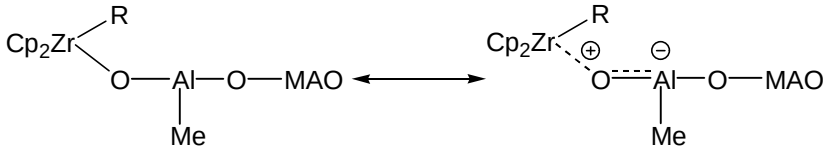

Scheme 1-13 Giannetti's Mechanism [39]

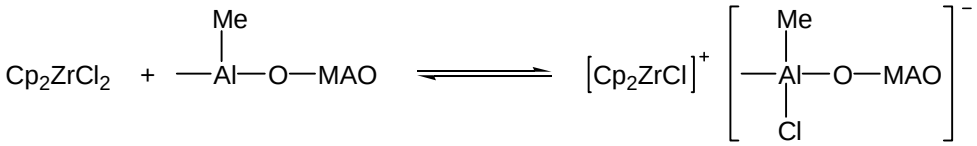

Scheme 1-14 Chien's Mechanism [65]

[74] Cam, D.; Giannini, U.: *Makromol. Chem.* **193(5)**, 1049-1055 (1992).

Scheme 1-15 Giannini's Mechanism [74]

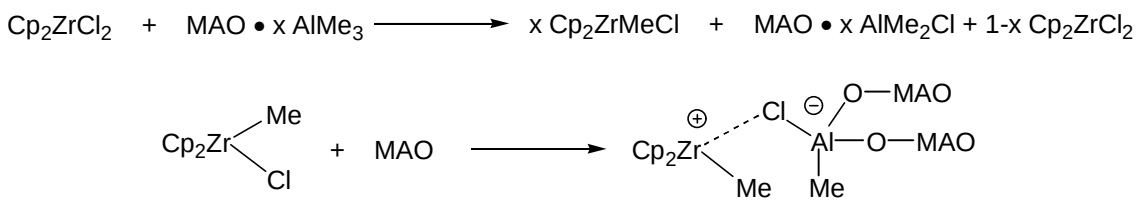

Another function of MAO in the polymerization process is to stabilize the active metal centers by preventing bimolecular deactivation (Scheme 1-16).[75,76] This is also one of the reasons why a large excess of MAO is required to achieve high activity for homogeneous metallocene catalysts, since a large excess of MAO isolates metallocene molecules from each other.

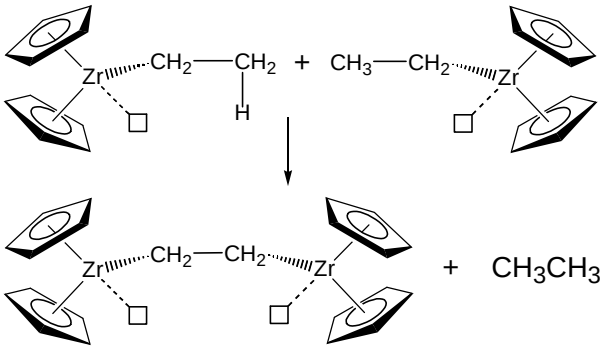

Scheme 1-16 Bimolecular Deactivation of Active Metallocene Catalyst [64]

1.3 Supported Metallocene Catalysts

As discussed in Section 1.2.4, homogeneous catalysts can not be used in industrial gas-phase processes for olefin polymerization. As a result, the range of MW and density of polymers that homogeneous catalysts can produce are limited by the viscosity and solubility problems in the liquid processes, and the shapes of the polymer particles are poor due to the poor control of particle shape in the liquid processes.

[75] Chien, J. C. W.; Rieger, B.; Sugimoto, R.; Mallin, D. T.; Rausch, M. D.: *Catalytic Olefin Polymerization*, T. Keii and K. Soga Eds., Elsevier-Kodansha: Tokyo 1990, **56**, 535-574.

Conventional Ziegler-Natta catalysts are heterogeneous catalysts. In solid catalyst particles, there are always precursor species buried in the particles that can not contact with cocatalyst to become active species and contribute to activity for olefin polymerization. In the supported Ziegler-Natta catalysts, the precursor species are dispersed on the surfaces of the support particles, so theoretically, they can all be activated and contribute to the activity.

Encouraged by the success of the supported Ziegler-Natta catalysts, many research groups started to explore techniques to support metallocene catalysts on some solid supports, so that the supported metallocene catalysts can be used in the gas-phase processes. A good supporting technique should not only immobilize a metallocene catalyst firmly, i.e., no leaching of active species from the support, but it also preserve the most useful features of the catalyst, e.g., high activity and stereospecificity, as well as lifetime, comonomer incorporation, and hydrogen response.

Many types of solid materials have been investigated as support materials for the immobilization of metallocene compounds.[77] The support materials can be classified into two categories: inorganic materials and polymeric materials. Inorganic materials include SiO_2, $MgCl_2$, Al_2O_3, zeolite, and more. Organic materials include polystyrene, polysiloxane, and more.

1.3.1 Supported Metallocene Catalysts on Silica

Silica is the most commonly used inorganic support material for supported metallocene catalysts. Silica is chemically inert to common solvents and most organic and organometallic compounds, being attacked only by strong bases (hot alkalis), strong nucleophiles (main group alkyls such as methyllithium), and fluoride. Silica is inexpensive, and silica products of various

[76] Chien, J. C. W.; He, D.-W.: *J. Polym. Sci. A Polym. Chem.* **29(11)**, 1603-1607 (1991).
[77] Hlatky, G. G.: *Chem. Rev.* **100(4)**, 1347-1376 (2000).

specifications are available commercially. The porous structure of silica can afford an enormous surface area, which enhances the efficiency of the supported catalysts. The silica surface also contains hydroxyl and siloxane functional groups, which are useful in surface modification and catalyst immobilization (Section 1.3.1.1). Many techniques have been developed to prepare supported metallocene catalysts on silica. The next section describes some of the general descriptive chemistry of silica, while the following three sections discuss the three main techniques for metallocene immobilization on silica: direct deposition, pre-alumination, and covalent tethering.

1.3.1.1 General Features of Silica

Silica (SiO_2) has many phases, including anhydrous crystalline phases (quartz, tridymite, cristobalite, etc.) and amorphous phases (vitreous silica from fused quartz, silica M from neutron-irradiated silica, micro-amorphous silica prepared by vapor condensation, solution deposition, etc.).[78] The micro-amorphous silica can be further divided into special microscopic forms (sheets, ribbons, and fiber-like) by special processes, a common amorphous form (spherical particles of less than 1000 Å in diameter, or their three-dimensional aggregates), hydrated amorphous silica, and biogenic silica. Though it was once proposed that amorphous silica actually contains extremely small crystallites in the cristobalite phase,[79] ordinary characterizations of amorphous silica only show typical features of an amorphous phase. The silica commonly used to prepare supported catalysts is that in the common amorphous form, which includes anhydrous amorphous silica and surface-hydroxylated amorphous silica.

Anhydrous amorphous silica is made in vapor phase.[78] It can be made by vaporizing SiO_2 using an arc or plasma and then condensing the vapor in a stream of dry inert gas. A

[78] Iler, R. K.: *The Chemistry of Silica*, Wiley: New York 1979, 15-29.

second method is to oxidize volatile silicon monoxide in gas phase with air. Anhydrous amorphous silica is also prepared by oxidizing silicon compounds in the gas phase, e.g., SiH_4, $SiCl_4$, etc., with dry oxygen. These "fume" silicas are used as inert fillers, e.g., in rubber. Surface-hydroxylated amorphous silica is normally prepared by the condensation/dehydration reaction of $Si(OH)_4$ in saturated aqueous solution. It can also be made using the vapor phase methods, if water vapor is present in the system.

Common amorphous silica particles are spherical. The particles' sizes vary with the preparation conditions. Sub-micron particles may spontaneously aggregate to form micrometer-sized "particles".[80] These large "particles" are actually aggregates of much smaller silica particles. Therefore, the aggregates have porous structures, and their surface areas are large.

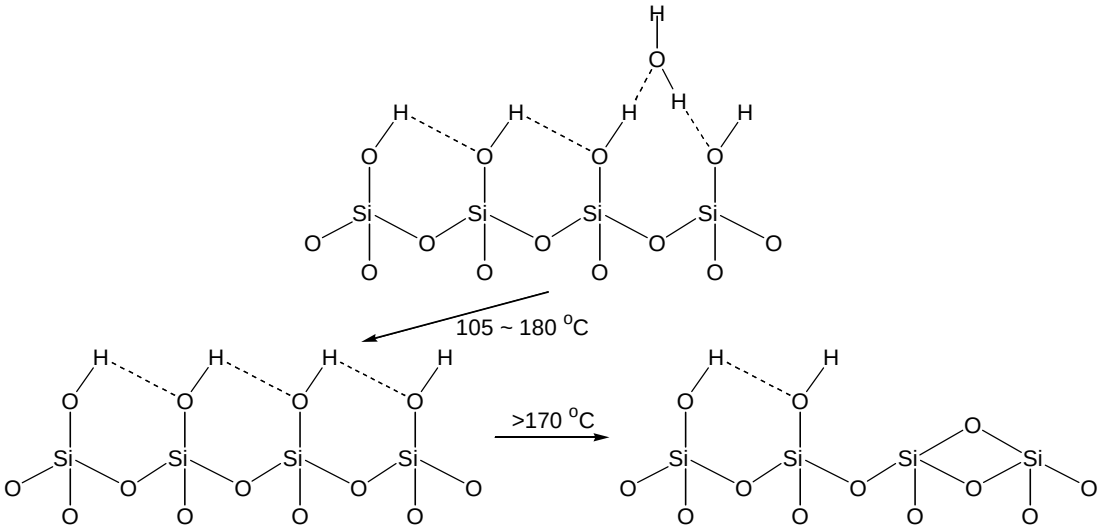

Scheme 1-17 Dehydration of Silica [82]

Unmodified silica may have a fully hydroxylated surface, which means that the solid structure terminates in silanol (SiOH) groups on the surface. Water molecules can easily adsorb on this type of surface. The opposite of a fully hydroxylated surface is a siloxane surface, on

[79] Dana, E. S.: *The System of Mineralogy of J. D. Dana: Descriptive Mineralogy 6th ed.*, Wiley: New York 1892, 183-197.

which, oxygen atoms are each bonded to two neighboring silicon atoms, though a small fraction of silanol groups is always present. A fully hydroxylated surface can be converted to a siloxane surface by dehydration at elevated temperatures. The density of silanol groups on silica surface depends on the dehydration temperature. The dehydration curves may vary with types of silica samples. Generally speaking, physically adsorbed water molecules desorb at 25-105 ^{o}C, and chemically adsorbed (hydrogen-bonded) water molecules desorb at 105-180 ^{o}C.[81] Adjacent silanol groups undergo condensation to form siloxane groups and give off water molecules above about 170 ^{o}C (Scheme 1-17). Almost half of the hydroxyl groups on silica surface are removed at around 400 ^{o}C. Above 750 ^{o}C, only isolated SiOH groups still exist on the surface.[82] According to the calculation based on a simple model considering only geometry and density of amorphous silica, Iler proposed that there should be about 7.8 OH groups per nm^2 on an amorphous silica surface.[83] The densities of OH groups on amorphous silica surfaces at elevated temperatures have been studied. A fully hydroxylated surface of smooth and non-porous heat-stabilized (stored at 120-150 ^{o}C) amorphous silica has an OH density of 4-5 per nm^2.[84,85] The OH density values at elevated temperatures vary somehow with measurement methods or types of silica. Table 1-2 and Table 1-3 present some of the data obtained by Bastick[83,86] and Curthoys,[87] respectively.

---

[80] Iler, R. K.: *The Chemistry of Silica*, Wiley: New York 1979, 462-463.
[81] Lange, K. R.: *J. Colloid Sci.* **20(3)**, 231-240 (1965).
[82] Iler, R. K.: *The Chemistry of Silica*, Wiley: New York 1979, 637-645.
[83] Iler, R. K.: *The Colloid Chemistry of Silica and Silicates*, Cornell University: Ithaca, New York 1955, 242-247.
[84] Snoeyink, V. L.; Weber, W. J. Jr.: *Progress in Surface and Membrane Science*, J. F. Danielli, M. D. Rosenberg, and D. A. Cadenhead Eds., Academic: New York 1972, **5**, 63-119.
[85] Barby, D.: *Characterization of Powder Surfaces*, G. D. Parfitt and K. S. W. Sing Eds., Academic: New York 1976, 353-425.
[86] Bastick, J.: *Bull. Soc. Chim. France* **20**, 437-440 (1953).
[87] Curthoys, G.; Davydov, V. Y.; Kiselev, A. V.; Kiselev, S. A.; Kuznetsov, B. V.: *J. Colloid & Interface Sci.* **48(1)**, 58-72 (1974).

Table 1-2 Calculated Water Content of Silica Gel [86]

temperature ^{o}C	$\%H_2O$	specific surface m^2/g	OH groups per nm^2	degree of OH coating [(b)]
100	5.5	710	5.1	0.64
200	5.1	714	4.7	0.59
300	4.0	697	3.8	0.48
400	2.9	689	2.8	0.35
500	1.9	663	1.9	0.24
600	1.3	636	1.3	0.16
800	0.7	523	0.9	0.11
900	0.6	427	0.9	0.11

(a) The values were calculated from the data obtained by Bastick for silica gel of pore diameter of 2.5 μm dried at ordinary temperature using P_2O_5.
(b) The complete coverage of the surface is assumed to require 8 OH groups per nm^2.

Table 1-3 Concentration of Surface OH Groups of Silica in the High Temperature Range [87]

temperature (oC)	OH /nm^2
700	1.2
800	0.9
900	0.65
1000	0.4

1.3.1.2 Direct Deposition

Direct deposition (also called grafting or impregnation) is the most convenient method of metallocene immobilization. In a typical process, some pretreated (calcined and partially thermally dehydroxylated) silica is stirred with a solution of a metallocene compound in inert atmosphere at room temperature or elevated temperatures for a period of time. Then, the slurry is filtered, and the remaining solid product is washed with solvent several times to remove weakly adsorbed metallocene molecules. The washed product is dried under vacuum to remove the solvent. The metallocene compound is believed to react with hydroxyl groups on silica surface and bond to the surface though an M-O-Si bond (Scheme 1-18). Kaminsky and Renner supported (μ-C_2H_4)Ind_2ZrCl_2 on silica dehydrated at 100 ^oC under vacuum.[88] The supported catalyst was active for propylene polymerization at 50 ^oC with only 35-200 equivalents of MAO cocatalyst and produced isotactic polypropylene of much higher melting point (157-161 ^oC) and MW ($5x10^5$-$8x10^5$) than those from the homogeneous analog (T_m = 122 ^oC and MW = $2x10^4$).

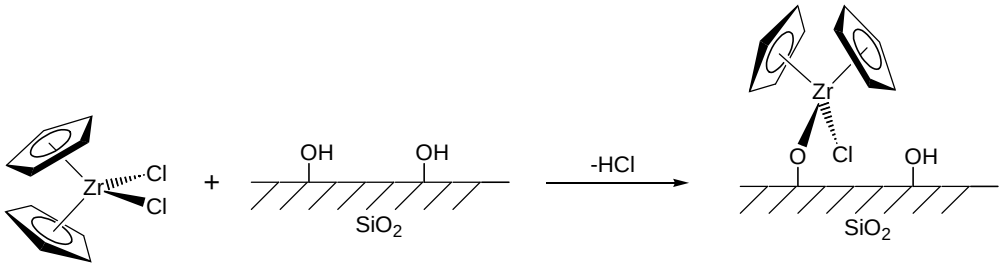

Scheme 1-18 Immobilization of Zirconocene Compound Directly on Silica

Many parameters need to be considered in the direct deposition method, such as metal loading, silica activation temperature, grafting temperature and time, solvent, etc. A comprehensive effort to optimize the preparation of silica-supported bis(n-butyl cyclopentadienyl) zirconium dichloride, (n-Bu-η^5–$C_5H_4)_2ZrCl_2$, was carried out by dos Santos

[88] Kaminsky, W.; Renner, F.: *Makromol. Chem. Rapid Commun.* **14(4)**, 239-243 (1993).

and coworkers.[89] They found that the maximum Zr loading on silica decreased with increasing pretreatment temperature of silica under vacuum.[90] The supported catalyst prepared using silica pretreated at room temperature only gave a minor activity for olefin polymerization when activated by MAO, though it had the highest Zr concentration. The low activity was attributed to the formation of a large number of inactive bidentate Zr species on the silica surface instead of the monodentate species (Scheme 1-19), since the concentration of residual surface hydroxyl groups is high if silica is dehydrated at room temperature. The highest activity for ethylene polymerization with MAO cocatalyst was achieved with the supported catalysts prepared using silica dehydrated at 723 K in vacuum. The MWD of the polymer produced by the silica-supported catalyst decreased with increasing dehydration temperature of the silica support. Longer grafting time or higher grafting temperature in the immobilization process yielded deactivated species. The highest activity for ethylene polymerization was achieved using a supported catalyst prepared after grafting at 353 K for one hour in toluene solution.[89]

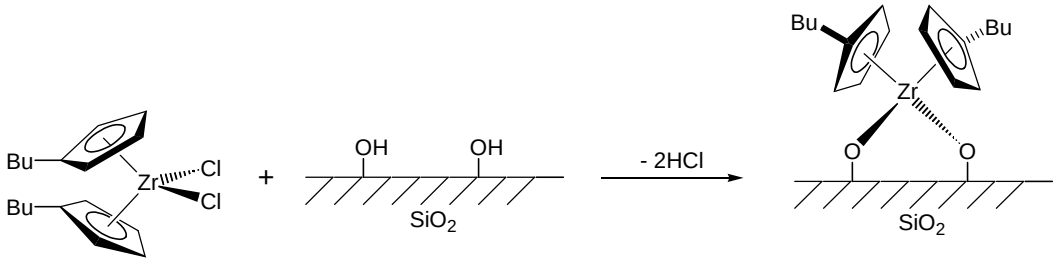

Scheme 1-19 Bidentate Surface Metallocene Species [90]

Supported metallocene catalysts prepared using the direct deposition method usually exhibit low activities for olefin polymerization. Low activity is attributed to (a) the steric demand of the surface, which prevents monomers from accessing the active sites, (b) the

[89] dos Santos, J. H. Z.; Larentis, A.; da Rosa, M. B.; Krug, C.; Baumvol, I. J. R.; Dupont, J.; Stedile, F. C.; Forte, M. de C.: *Macromol. Chem. Phys.* **200(4)**, 751-757 (1999).
[90] dos Santos, J. H. Z.; Krug, C.; da Rosa, M. B.; Stedile, F. C.; Dupont, J.; Forte, M. de C.: *J. Mol. Cat. A Chemical* **139(2-3)**, 199-207 (1999).

donating/poisoning effect of the oxygen atom in the M-O-Si linkage, and (c) the bimolecular deactivation of two adjacent surface metal centers, when the surface metallocene loading is high. Several modified methods were developed to solve the problems. One modification is to put spacers between silica surface and the supported metallocene molecules to enhance the accessibility of the active sites and to avoid the poisoning effect of the direct contact between metal centers and silica surface. This modification leads to the covalent tethering method (Section 1.3.1.4). The other modification is to put spacers among the metallocene molecules on a silica surface to reduce the propensity for two metallocene molecules on the surface to be located close enough together to enable bimolecular deactivation.

Lee and coworkers modified silica with trisiloxane or pentamethylene spacers before impregnating $CpIndZrCl_2$. The supported catalyst showed higher polymerization activity than that prepared with unmodified silica.[91] Dos Santos and coworkers used silyl chlorides, e.g., Ph_3SiCl, Me_3SiCl, Me_2SiHCl, as spacers among metallocene molecules supported on silica surface.[92] In their process, silica was first reacted with a silyl chloride solution. Then, a metallocene compound, $(n\text{-}Bu\text{-}\eta^5\text{–}C_5H_4)_2ZrCl_2$, was impregnated on the modified silica support. The maximum Zr loading on the modified silica decreased with increased silyl chloride loading. The activity of the supported catalyst for ethylene polymerization with MAO cocatalyst increased with silyl chloride loading and reached a maximum at 0.3wt% Si/SiO_2. The maximum activity was twice as much as that of the same metallocene compound supported on bare silica.

1.3.1.3 Pre-alumination

The term “pre-alumination” refers to an immobilization process in which silica is treated with MAO before impregnating with a metallocene compound. In one process, silica is stirred

[91] Lee, D.-H.; Yoon, K.-B.; Noh, S.-K.: *Macromol. Rapid Commun.* **18(5)**, 427-431 (1997).
[92] dos Santos, J. H. Z.; Greco, P. P.; Stedile, F. C.; Dupont, J.: *J. Mol. Catal. A Chem.* **154(1-2)**, 103-113 (2000).

with a solution of MAO and then filtered. The solid portion is washed and dried in vacuum to obtain the MAO-modified silica. A minor modification of this process is to add n-decane to the slurry of silica and MAO in toluene to precipitate the MAO onto the silica.[93] In another process, supported MAO is generated in situ by reacting TMA with water in the presence of silica, or by reacting TMA with water adsorbed on the surface of silica without dehydration.[94,95] The subsequent metallocene impregnation process is similar to that of the direct deposition method.

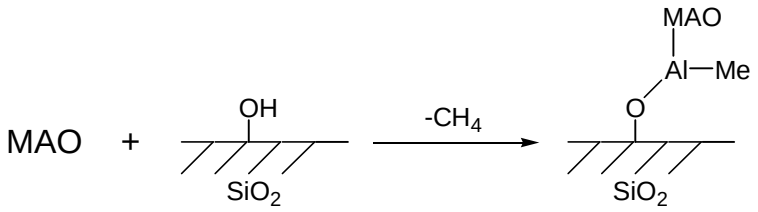

Scheme 1-20 Reaction of Silica with MAO

When silica is treated with MAO, the surface hydroxyl groups react with MAO and release CH_4 (Scheme 1-20), so MAO is bonded to silica through Si-O-Al bonds. The bonded MAO can methylate and extract methyl groups from metallocene molecules during the impregnation of a metallocene compound, and the metallocene molecules are thus immobilized on silica by ionic interaction with the bonded MAO and become active catalytic species at the same time (Scheme 1-21). The ionic interaction is weak, so the active species may be able to migrate over the MAO covered silica surface, resulting in a similar environment of the active species as that in homogeneous solution.[96] Therefore, the polymers produced by these supported catalysts have similar properties as those produced by corresponding homogeneous metallocene catalysts.

[93] Kioka, M.; Kashiwa, N.: *US Pat.* 4874734 (1989).
[94] Tsutsui, T.; Ueda, T.: *US Pat.* 5234878 (1993).
[95] Gürtzgen, S.: *US Pat.* 5446001 (1995).

Scheme 1-21 Immobilization of Zirconocene Compound on MAO-treated Silica

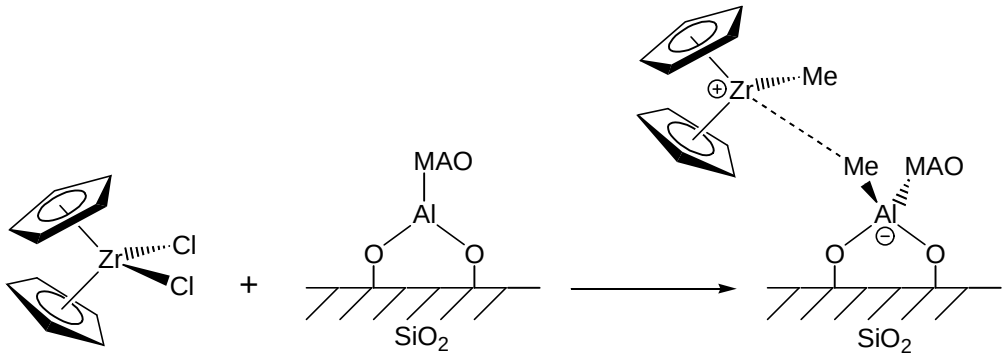

Chien and He immobilized (μ-C_2H_4)Ind_2ZrCl_2 on silica pretreated with MAO.[76] They found that the supported catalyst was active for ethylene/propylene polymerization with MAO cocatalyst. It required only about one-tenth or less of MAO that was required by the homogeneous analog to achieve the same polymerization activity. The copolymer produced by the supported catalyst had similar properties as that produced by the homogeneous analog. Kaminsky and Renner compared the pre-alumination method with the direct deposition method.[88] They found that the silica-supported (μ-C_2H_4)Ind_2ZrCl_2 prepared using the direct deposition method produced isotactic polypropylene of much higher MW and melting point than those of the isotactic polypropylene produced by the homogeneous (μ-C_2H_4)Ind_2ZrCl_2. However, the isotactic polypropylene produced by the silica-supported (μ-C_2H_4)Ind_2ZrCl_2 prepared using the pre-alumination method resembled that produced by the homogeneous (μ-C_2H_4)Ind_2ZrCl_2. They attributed the difference to the stronger interaction of the metal centers with unmodified silica surface in the direct deposition method and the solution-like weaker interaction of the metal centers with MAO-modified silica surface in the pre-alumination method.

---

[96] Chen, Y.-X.; Rausch, M. D.; Chien, J. C. W.: *J. Polym. Sci. A Polym. Chem.* **33(13)**, 2093-2108 (1995).

Some authors described a method to immobilize a metallocene and MAO on silica that is close to the pre-alumination method. In this method, a solution of metallocene and MAO is prepared first; then silica is added to the solution. The slurry is stirred and dried to form the supported catalyst.[97,98] Since the metallocene compound has been activated in solution by MAO, the immobilization should occur between excess MAO and silica surface. The structure of the supported catalyst prepared using this method should resemble that of the supported catalyst using the pre-alumination method.

1.3.1.4 Covalent Tethering

An alternative to impregnation is to immobilize metallocene compounds on silica support through covalent tethers. One end of such a tether is covalently bonded to silica surface, and the other end is covalently bonded to an ancillary ligand on the metallocene molecule. The covalent tethers not only serve as ties to bind the metallocene molecules to the support, they also function as spacers between the metallocene molecules and the support to minimize the steric hindrance and the poisoning effect of the support surface as described in Section 1.3.1.2. A flexible tether should allow the bonded metallocene molecule to have rotational (but not translational) freedom on the support surface, so that the environment of the supported active center is similar to that of a homogeneous active center.

Many kinds of covalent tethers have been used to immobilize metallocene catalysts on silica. The immobilization methods can be divided into two general approaches. In the first approach, silica is modified with tethering ligand first; then the modified silica reacts with some metallocene-forming compound to generate the tethered metallocene compound on silica. A disadvantage of this approach is that it is unable to control the steric configuration of the

[97] Fraaije, V.; Bachmann, B.; Winter, A.: *Eur. Pat. Appl.* 780402 (1997).
[98] Wasserman, E. P.; Lynn, T. R.; Smale, M. W.; Brady, R. C. III; Karol, F. J.: *US Pat.* 5648310 (1997).

immobilized metallocene compound on silica. For example, it is hard to ensure that two tethered Cp ligands have reacted with a reagent like $ZrCl_4$, and it would be nearly impossible to achieve diastereoselective coordination of two tethered ligands such as indenyl, which has enantiotopic ligand faces. Another disadvantage is that it is very difficult to characterize or purify the intermediates on support in every step in the preparation – and there are often three or more steps. In the other approach, a functionalized metallocene compound with tether-forming substituents is synthesized first; then the substituents react with silica to generate the tethered metallocene compound on silica. It is possible to control the steric configuration of an immobilized metallocene compound by designing, synthesizing, purifying, and characterizing the specific functionalized metallocene compound before immobilization.

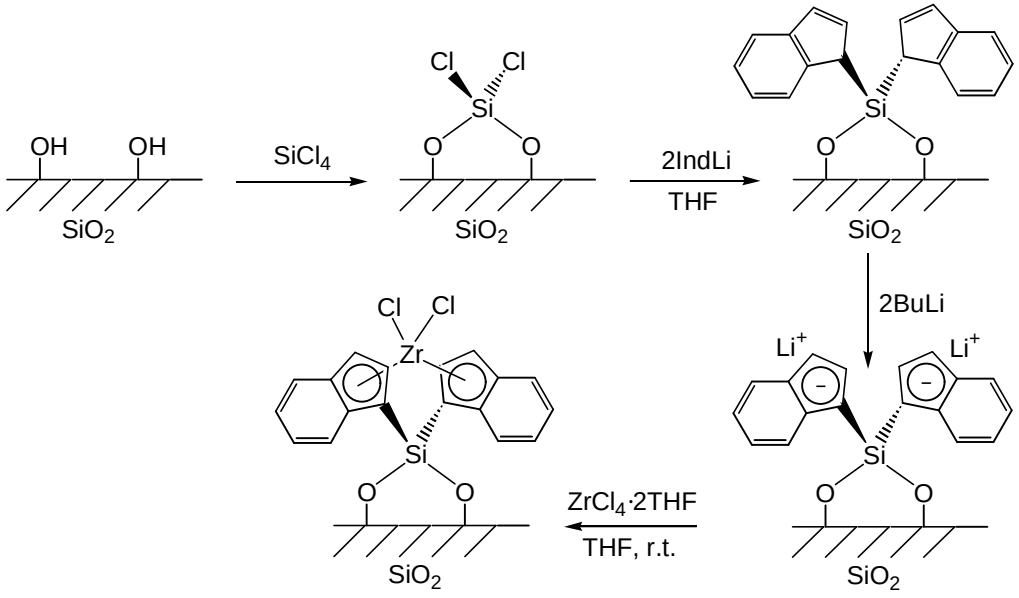

Scheme 1-22 Preparation of Silica-supported ansa-Ind_2ZrCl_2 [99]

Soga and coworkers immobilized some ansa-zirconocene catalysts on silica using covalent tethers bonded to the bridging atoms.[99] They constructed covalently bonded ansa-ligands on silica first; then they reacted the supported ligands with $ZrCl_4$•2THF to make the

zirconocene compounds supported on silica. A typical process for the preparation of a supported ansa-Ind_2ZrCl_2 is illustrated in Scheme 1-22. Silica was treated with $SiCl_4$, so that surface hydroxyl groups were converted to doubly anchored $SiCl_2$ groups. Addition of IndLi followed by BuLi converted the $SiCl_2$ groups to $Si(IndLi)_2$ groups, which further reacted with $ZrCl_4$•2THF to get the supported ansa-Ind_2ZrCl_2 with one double-tether. The supported catalysts produced highly isotactic polypropylene with MAO or TMA. However, the observed catalytic activities were more than ten times lower than those of the homogeneous analogs. Iiskola and coworkers used an alkyl siloxane tether.[100] They reacted $C_5H_5(CH_2)_3Si(OCH_2CH_3)_3$ with partially dehydrated silica using a saturated gas-solid method (Scheme 1-23). The surface hydroxyl group or Si-O-Si group broke one of the Si-O-C linkages in the molecule, and the molecule was thus bonded to silica by a siloxane linkage. The modified silica was further treated with BuLi to convert the cyclopentadiene groups to cyclopentadienyl anions, which reacted with $CpZrCl_3$ in a slurry to form the supported zirconocene compound. They claimed that the supported catalyst was highly active for ethylene polymerization in the presence of MAO. The activity was five times more than that of supported $CpZrCl_3$ prepared using the direct deposition method and twice more than that of homogeneous $CpZrCl_3$. However, their catalyst was still much less active than homogeneous Cp_2ZrCl_2. The polyethylenes produced had narrow MWDs, comparable to those of the polyethylenes produced by the homogeneous analogs. Pakkanen and coworkers[101] immobilized constrained-geometry group 4 metallocene compounds on silica through similar covalent tethers. They also modified silica with a tethering ligand before making the metallocene compounds supported on silica.

---

[99] Soga, K.; Kim, H.-J.; Shiono, T.: *Macromol. Chem. Phys.* **195(10)**, 3347-3360 (1994).

[100] a) Iiskola, E. I.; Timonen, S.; Pakkanen, T. T.; Härkki, O.; Seppälä, J. V.: *Appl. Surf. Sci.* **121-122**, 372-377 (1997). b) Iiskola, E. I.; Timonen, S.; Pakkanen, T. T.; Härkki, O.; Lehmus, P.; Seppälä, J. V.: *Macromolecules* **30(10)**, 2853-2859 (1997).

Scheme 1-23 Preparation of Silica-supported Cp_2ZrCl_2 through Alkyl Siloxane Tethers [100]

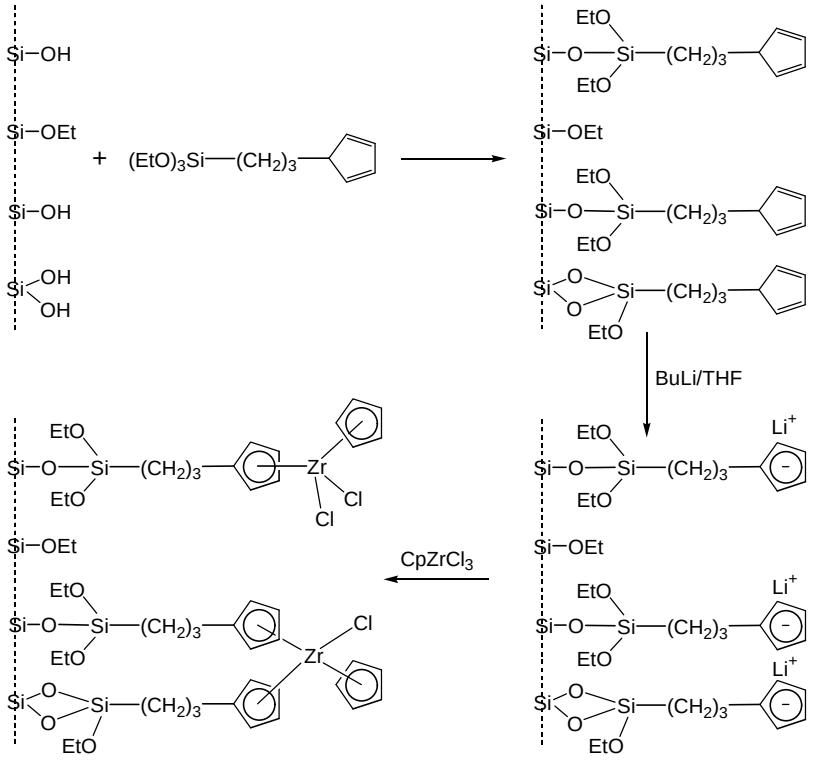

Scheme 1-24 Immobilization of a Constrained-geometry Titanocene Compound on Silica through Alkyl Siloxane Tethers [102]

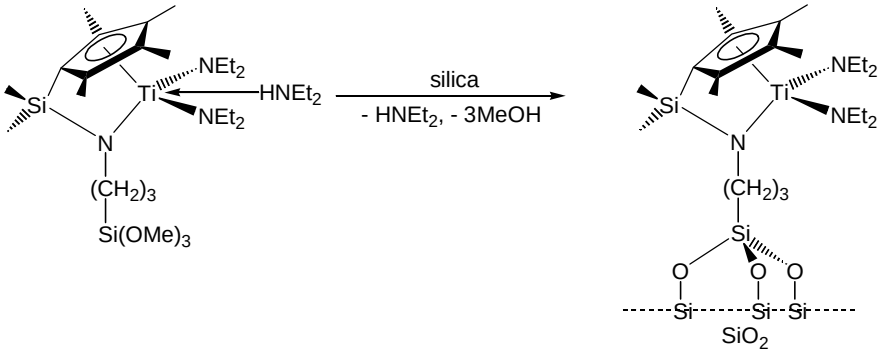

[101] Juvaste, H.; Pakkanen, T. T.; Iiskola, E. I.: *Organometallics* **19(23)**, 4834-4839 (2000).

Scheme 1-25 Immobilization of a C_2-symmetric Silylene-bridged Zirconocene Compound on Silica though an Alkylsilyl Tether [103]

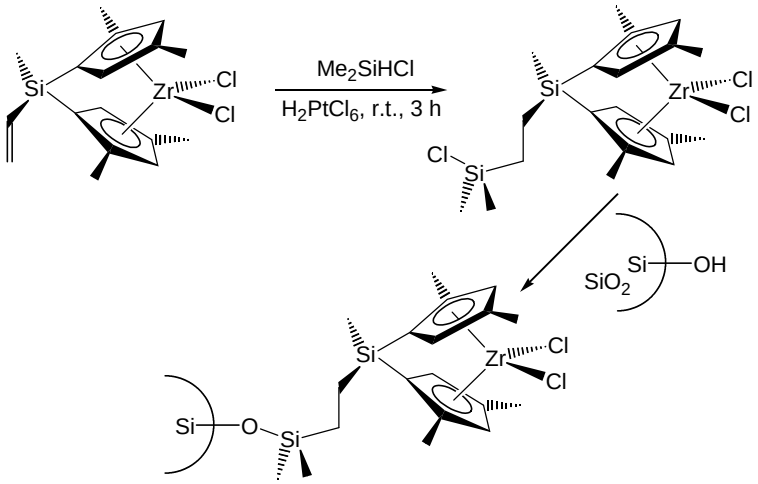

Eisen and coworkers immobilized a constrained-geometry titanocene compound on silica using the same alkyl siloxane tether as that used by Iiskola and coworkers (Scheme 1-24).[102] However, they synthesized the substituted titanocene compound with the tether first; then they immobilized the compound onto silica. The supported catalysts produced syndiotactic polystyrene, and the polymers produced had higher MW than those produced by the homogeneous analogs. Suzuki and coworkers made a C_2 symmetric silylene-bridged zirconocene compound with a chlorodimethylsilylethyl group attached on the bridging silicon atom.[103] The chlorosilyl functional group can react with a hydroxyl group on silica to make immobilized ansa-zirconocene compound (Scheme 1-25). A model study for the immobilization reaction was also carried out using $^{t}BuMe_2SiOH$ instead of silica. They obtained the modified zirconocene compound with Si-O-Si linkage as expected (Scheme 1-26). The supported catalyst showed a much higher activity for propylene polymerization than a similar supported catalyst

[102] Galan-Fereres, M.; Koch, T.; Hey-Hawkins, E.; Eisen, M. S.: *J. Organomet. Chem.* **580(1)**, 145-155 (1999).
[103] Suzuki, N.; Asami, H.; Nakamura, T.; Huhn, T.; Fukuoka, A.; Ichikawa, M.; Saburi, M.; Wakatsuki, Y.: *Chem. Lett.* **(4)**, 341-342 (1999).

prepared by direct deposition method. The polypropylene produced was isotactic. Lee and Oh prepared several zirconocene derivatives with alkoxyhexyl substituents on the cyclopentadienyl rings.[104] The ether linkages of these compounds were expected to break in the reaction with dehydrated silica to generate the supported zirconocene compounds. They studied the reaction between t-butyl decyl ether and dehydrated silica as a model for the metallocene immobilization reaction. The results supported the proposed cleavage of the ether linkage by dehydrated silica (Scheme 1-27). The supported catalysts exhibited activities for ethylene polymerization higher than the analogous supported catalysts prepared using the direct deposition method. Lee, et al. prepared silica-supported $CpIndZrCl_2$ with covalent pentamethylene tethers using different immobilization methods.[105] They found that the supported catalysts had ethylene polymerization activities comparable to that of homogeneous $CpIndZrCl_2$ with MAO cocatalyst.

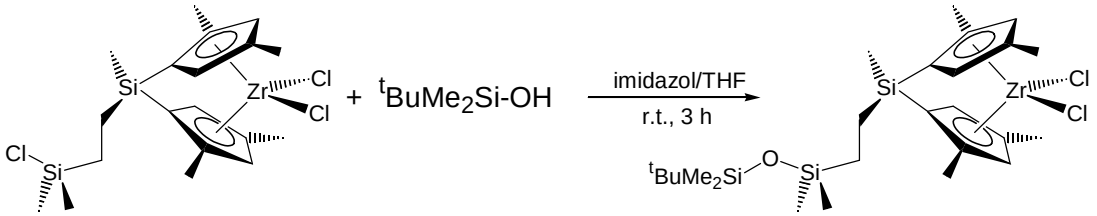

Scheme 1-26 Model Study of the Immobilization of the C_2-symmetric Silylene-bridged Zirconocene Compound [103]

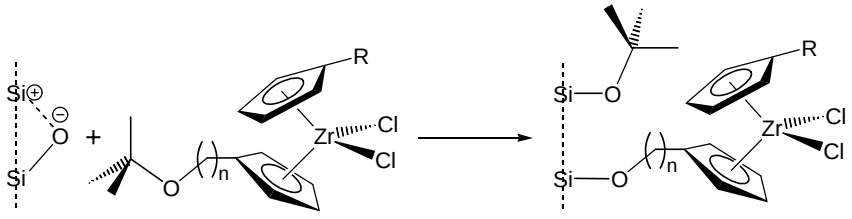

Scheme 1-27 Immobilization of Zirconocene Compound through Alkyl Tethers [104]

[104] Lee, B.-Y.; Oh, J.-S.: *Macromolecules* **33(9)**, 3194-3195 (2000).

1.3.2 Metallocene Catalysts Supported on Other Materials

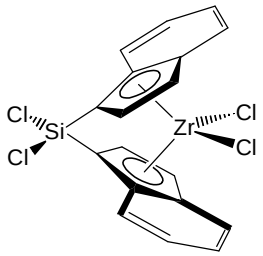

Scheme 1-28 Molecular Structure of rac-[(m-Cl_2Si)Ind_2]$ZrCl_2$ [106]

Because $MgCl_2$ is a widely used inorganic material in the preparation of supported Ziegler-Natta catalysts,[2,50] some researchers chose $MgCl_2$ as a support for metallocene catalysts. Soga and coworkers immobilized μ-dichlorosilylene bisindenyl zirconium dichloride (Scheme 1-28) on $MgCl_2$ using an impregnation method.[106] They found that the supported catalyst showed fairly high activity (226 kg(PP)/mol(Zr)/h) for propylene polymerization with MAO cocatalyst (Al/Zr = 5000) at 40 ^oC. The polypropylene product was highly isotactic (%mmmm = 91.8%). Kang and coworkers investigated $MgCl_2$-supported half-sandwich metallocene catalysts, i.e., $CpZrCl_3$ and $CpTiCl_3$.[107] They observed more than a 100-fold activity increase for ethylene polymerization using MAO as the cocatalyst under similar polymerization conditions, after $CpZrCl_3$ and $CpTiCl_3$ were immobilized on $MgCl_2$. The molecular weights of the polymers produced by the supported catalysts were also much higher than that produced by the homogeneous $CpZrCl_3$ and $CpTiCl_3$ catalysts, but the molecular weight distributions were poorer. Through an electron spin resonance (ESR) spectroscopy study, Xu and coworkers found two kinds of active species in $MgCl_2$-supported $CpTiCl_3$ catalysts. One species could not be removed from the support by interaction with MAO, and the other species was readily removed

[105] Lee, D.-H.; Lee, H.-B.; Noh, S.-K.; Song, B.-K.; Hong, S.-M.: *J. Appl. Polym. Sci.* **71(7)**, 1071-1080 (1999).
[106] Soga, K.; Arai, T.; Uozumi, T.: *Polymer* **38(19)**, 4993-4995 (1997).
[107] Kang, K.-K.; Oh, J.-K.; Jeong, Y.-T.; Shiono, T.; Ikeda, T.: *Macromol. Rapid Commun.* **20(6)**, 308-311 (1999).

and formed the same active site as that in the homogeneous $CpTiCl_3$/MAO system.[108] Juan and coworkers also carried out a semi-empirical computational study of the adsorption of metallocene compounds on β-$MgCl_2$ crystalline planes using an extended Hückel molecular orbital method (EHMO).[109] The calculated energy curves showed the formation of stable adsorbed species on the crystalline planes.

Soga and Kaminaka extensively investigated several inorganic metallocene supports including Al_2O_3, SiO_2, MgO, $MgCl_2$, MgF_2, CaF_2, and AlF_3.[110] The metallocene compounds investigated were (μ-C_2H_4)($IndH_4$)$_2ZrCl_2$, (μ-Me_2C)$FluCpZrCl_2$, and Cp_2ZrCl_2 ($IndH_4$ = 4,5,6,7-tetrahydro-1-indenyl, Flu = fluorenyl). The supported catalysts were prepared by impregnation. They found that the supported catalysts prepared using Al_2O_3, $MgCl_2$, MgF_2, CaF_2, and AlF_3 as support materials were easily activated by TMA or TEA. The supported catalysts exhibited fairly high activities in propylene polymerization. The tacticities of the polypropylenes produced by the supported catalysts resembled those by the corresponding homogeneous metallocene catalysts. The catalysts directly supported on SiO_2 or MgO did not show polymerization activity with alkylaluminum cocatalysts. However, if SiO_2 was treated with a little MAO before impregnation, the supported catalysts on SiO_2 were highly active with alkylaluminum cocatalysts.

Zeolites are aluminosilicates having highly ordered and well characterized crystal structures, which contain large channels and cages. These channels and cages give zeolites very large surface areas and can serve as hosts for small guest molecules. The most commonly used zeolite for supported metallocene catalysts is HY/NaY zeolite. Woo and coworkers prepared

[108] Xu, J.-T.; Zhao, J.; Fan, Z.-Q.; Feng, L.-X.: *European Polym. J.* **35(1)**, 127-132 (1999).
[109] Ferreira, M. L.; Damiani, D. E.; Juan, A.: *Comput. Mater. Sci.* **9(3-4)**, 357-366 (1998).
[110] Soga, K.; Kaminaka, M.: *Makromol. Chem.* **194(6)**, 1745-1755 (1993).

NaY-supported Cp_2ZrCl_2 and Cp_2TiCl_2 catalysts.[111] They reacted the NaY zeolite with MAO or TMA first, and then the pretreated NaY further reacted with the metallocene compounds. The amount of MAO required for highly active catalysts was greatly reduced (Al/Zr = 186), and the molecular weights and melting points of the polyethylene products from the supported catalysts were higher than those from the corresponding homogeneous catalysts. Extraction experiments showed that the metallocene catalysts were stable on NaY. Woo and coworkers attributed the stability to the entrapment of the metallocene molecules inside the large cages in the NaY zeolite. Sbrana and coworkers prepared supported Cp_2ZrCl_2/Cp_2ZrMe_2 catalysts on a TMA-modified HY zeolite. The supported catalysts exhibited the same activities as the homogeneous analogs but with higher stability.[112] Michelotti and coworkers found that the activities for polymerization and copolymerization of ethylene and α-olefins decreased, but the molecular weights of the copolymers were increased and the stabilities improved, when bridged or non-bridged metallocene catalysts, e.g., Cp_2ZrCl_2, Ind_2ZrCl_2, and $(\mu\text{-}C_2H_4)Ind_2ZrCl_2$ (Ind = indenyl), were supported on HY zeolite.[113] Coutinho and coworkers used Y zeolites with different sodium contents (NaY, NaHY, HY) and a sodium mordenite (NaM) zeolite to prepare supported Cp_2ZrCl_2 catalysts.[114] They found lower activities but higher molecular weights in ethylene polymerization using the supported catalysts than those using the homogeneous Cp_2ZrCl_2/MAO catalyst. The activities increased as the concentration of aluminum in the zeolite framework increased, and the supported catalyst on NaM exhibited the highest activity. The results indicated that the aluminum concentration was the dominant factor. Rahiala, et al. used MCM-

[111] Woo, S.-I.; Ko, Y.-S.; Han, T.-K.: *Macromol. Rapid. Commun.* **16(7)**, 489-494 (1995).
[112] Braca, G.; Sbrana, G.; Raspolli-Galletti, A. M.; Altomare, A.; Arribas, G.; Michelotti, M.; Ciardelli, F.: *J. Mol. Catal. A Chem.* **107(1-3)**, 113-121 (1996).
[113] a) Michelotti, M.; Altomare, A.; Ciardelli, F.; Roland, E.: *J. Mol. Catal. A Chem.* **129(2-3)**, 241-248 (1998). b) Michelotti, M.; Arribas, G.; Bronco, S.; Altomare, A.: *J. Mol. Catal. A Chem.* **152(1-2)**, 167-177 (2000).

41, a mesoporous silicate, as the support.[115] They found that Cp_2ZrCl_2 supported on Al-modified MCM-41 exhibited higher ethylene polymerization activity than that on pure MCM-41 and silica.

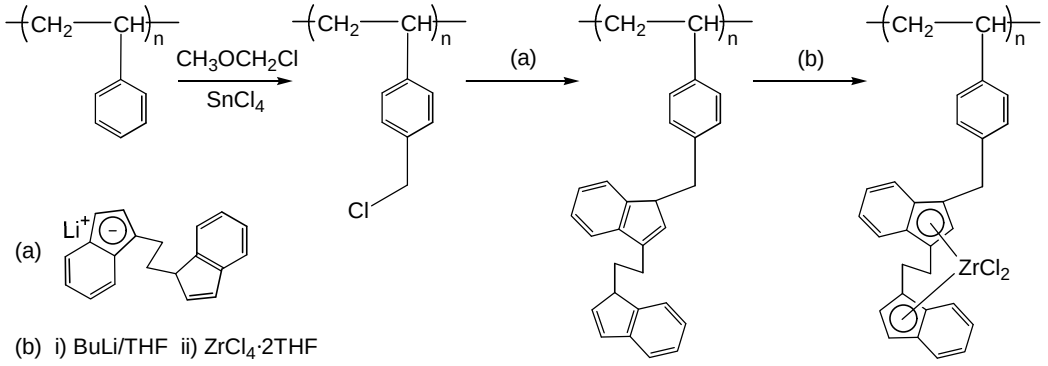

Scheme 1-29 Synthesis of Polystyrene-supported [(m-C_2H_4)Ind_2]$ZrCl_2$ [116]

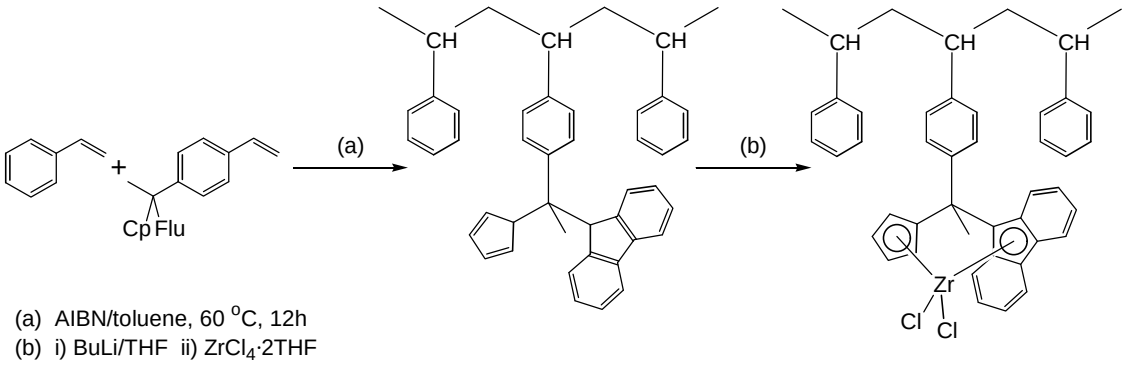

Scheme 1-30 Synthesis of Polystyrene-supported [(m-(MePhC)CpFlu]$ZrCl_2$ [117]

Organic polymers have also been used as support materials for supported metallocene catalysts. The major advantage of organic polymer supports is that they will not create inorganic content in the polymers produced by the supported catalysts, so the properties of the polymers are improved. A commonly used polymeric support material is polystyrene. Soga and

[114] Marques, M. F. V.; Henriques, C. A.; Monteiro, J. L. F.; Menezes, S. M. C.; Coutinho, F. M. B.: *Macromol. Chem. Phys.* **198(11)**, 3709-3717 (1997).
[115] Rahiala, H.; Beurroies, I.; Eklund, T.; Hakala, K.; Gougeon, R.; Trens, P.; Rosenholm, J. B.: *J. Catal.* **188(1)**, 14-23 (1999).

coworkers prepared several different polystyrene-supported zirconocene catalysts by modifying the phenyl rings on the polystyrene chains.[116] A typical process included functionalizing some of the phenyl rings, followed by incorporation of indene or its derivatives covalently (Scheme 1-29). Then the incorporated indene groups were deprotonated to make indenyl ligands, which further reacted with $ZrCl_4$ to produce the supported zirconocene catalysts. The polystyrene-supported zirconocene catalysts were stable even at 70 ^oC and were fairly active for olefin polymerization at high temperature. Soga and coworkers also prepared a copolymer of styrene and 1-vinyl-4-(1-cyclopentadienyl-1-fluorenyl)ethyl benzene, then they reacted the polymer-supported ligand with $ZrCl_4$ to make a supported catalyst that could produce syndiotactic polypropylene (Scheme 1-30) with MAO cocatalyst.[117] Uozumi and coworkers made polystyrene-supported tetra(pentafluorophenyl)borate (Scheme 1-31), which further reacted with $(\mu\text{-}C_2H_4)Ind_2ZrCl_2$ or $(\mu\text{-}Ph_2C)FluCpZrCl_2$ to form supported catalysts.[118] With $Al(i\text{-}Bu)_3$ as cocatalyst, the supported catalysts had activities for ethylene polymerization comparable to those of the corresponding homogeneous catalysts. Liu and coworkers immobilized Cp_2ZrCl_2 on MAO-modified poly(styrene-co-acrylamide) using directly impregnation.[119] Some other polymeric supports used include, poly(styrene-co-divinylbenzene),[120,121] poly(4-vinyl-pyridine),[122] poly[p-(silylene)phenylene],[123] poly(styrene-co-4-vinylpyridine).[124]

[116] Nishida, H.; Uozumi, T.; Arai, T.; Soga, K.: *Macromol. Rapid Commun.* **16(11)**, 821-830 (1995).
[117] Kitagawa, T.; Uozumi, T.; Soga, K.; Takata, T.: *Polymer* **38(3)**, 615-620 (1997).
[118] Kishi, N.; Ahn, C.-H.; Jin, J.; Uozumi, T.; Sano, T.; Soga, K.: *Polymer* **41(11)**, 4005-4012 (2000).
[119] Liu, S.-S.; Meng, F.-H.; Yu, G.-Q.; Huang, B.-T.: *J. Appl. Polym. Sci.* **71(13)**, 2253-2258 (1999).
[120] Roscoe, S. B.; Fréchet, J. M. J.; Walzer, J. F.; Dias, A. J.: *Science* **280(5361)**, 270-273 (1998).
[121] Hong, S.-C.; Ban, H.-T.; Kishi, N.; Jin, J.-Z.; Uozumi, T.; Soga, K.: *Macromol. Chem. Phys.* **199(7)**, 1393-1397 (1998).
[122] Musikabhumma, K.; Uozumi, T.; Sano, T.; Soga, K.: *Macromol. Rapid Commun.* **21(10)**, 675-679 (2000).
[123] Ban, H.-T.; Uozumi, T.; Sano, T.; Soga, K.: *Macromol. Chem. Phys.* **200(8)**, 1897-1902 (1999).

Scheme 1-31 Synthesis of Polystyrene-supported Activator [118]

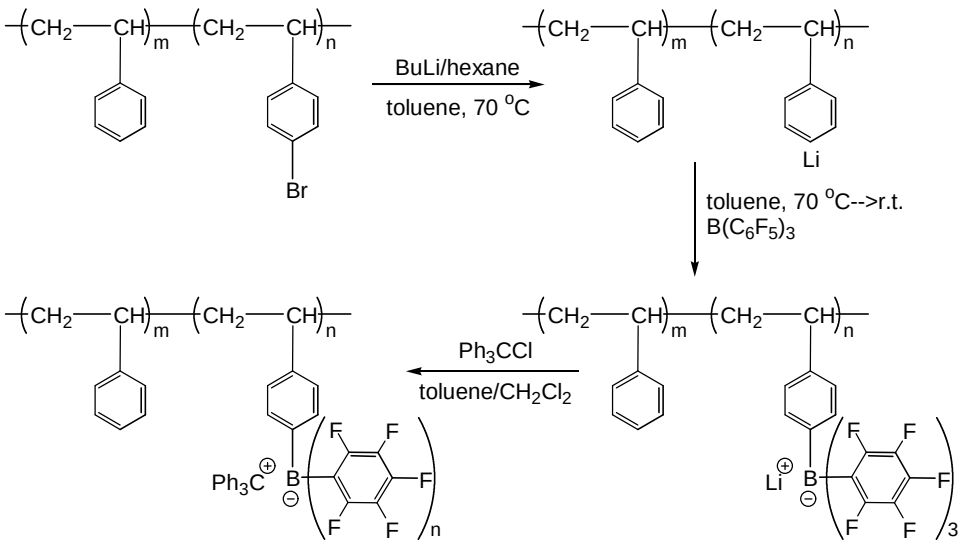

Scheme 1-32 Preparation of Immobilized Zirconocene Compound on Double-strand Polysiloxane Chains [125]

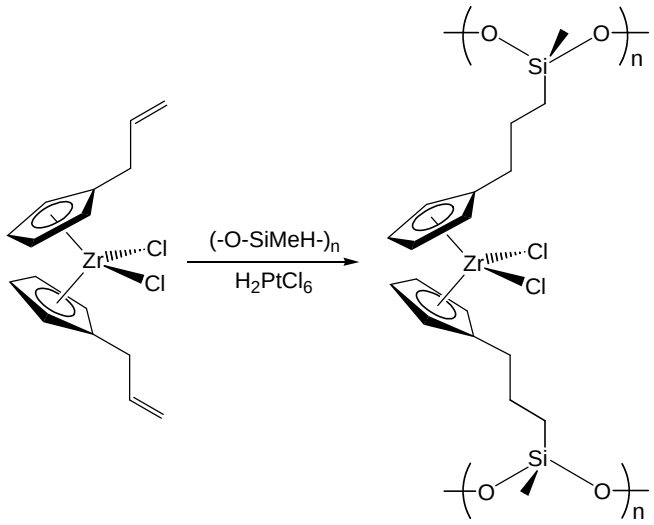

[124] Meng, F.-H.; Yu, G.-Q.; Huang, B.-T.: *J. Polym. Sci. A Polym. Chem.* **37(1)**, 37-46 (1999).

Polysiloxanes were also used as support materials for supported metallocene catalysts. Antberg and coworkers used a hydrosilylation reaction to prepare supported metallocenes on polysiloxanes (Scheme 1-32).[125] In a typical preparation, they reacted poly(methyl siloxane) with 1,1'-allyl-substituted cyclopentadienyl zirconium dichloride. Hydrosilylation catalyzed by H_2PtCl_6 of the double bonds of the allyl groups with the Si-H bonds of the polysiloxane made the zirconocene covalently bonded to the polysiloxane chains. Soga, et al. developed a different method (Scheme 1-33).[126] They synthesized indenyl- or fluorenyl-substituted polysiloxanes and used the indenyl or fluorenyl substituents as ligands to synthesize metallocene catalysts supported on polysiloxanes. The polysiloxane precursors and the supported catalysts are soluble in common organic solvents. Propylene polymerization results showed that the supported catalysts on indenyl-methyl-polysiloxane backbone or bisindenyl-polysiloxane backbone had much higher activities than the corresponding silica-supported bis(indenyl)zirconocene dichlorides with MAO cocatalyst. The propylene polymerization activity of the supported catalyst with fluorenyl-methyl-polysiloxane backbone was about 100 times lower than the other two, but it was the most active for ethylene polymerization. Alt and coworkers made polysiloxane microgel and used it as support material.[127] Their microgels were functionalized with chlorosilanes containing fluorenyl groups, which reacted with $(\eta^5\text{-}C_5Me_5)ZrCl_3$ or $ZrCl_4$ to produce the polysiloxane-micro-gel-supported zirconocene compounds (Scheme 1-34). The micro-gel-supported zirconocene catalysts showed similar activities for ethylene polymerization as those of their silica-supported analogs with MAO cocatalyst.

---

[125] Antberg, M.; Böhm, L.; Rohrmann, J.: *US Pat.* 5071808 (1991);

[126] a) Soga, K.; Arai, T.; Hoang, B.-T.; Uozumi, T.: *Macromol. Rapid Commun.* **16(12)**, 905-911 (1995). b) Arai, T.; Ban, H.-T.; Uozumi, T.; Soga, K.: *J. Polymer Sci. Part A: Polymer Chem.* **36(3)**, 421-428 (1998). c) Arai, T.; Ban, H.-T.; Uozumi, T.; Soga, K.: *Macromol. Chem. Phys.* **198(2)**, 229-237 (1997). d) Soga, K.; Ban, H.-T.; Arai, T.; Uozumi, T.: *Macromol. Chem. Phys.* **198(9)**, 2779-2787 (1997).

[127] Alt, H. G.; Schertl, P.; Köppl, A.: *J. Organomet. Chem.* **568(1-2)**, 263-269 (1998).

Scheme 1-33 Preparation of Polysiloxane-supported Zirconocene Compounds with Cyclopentadienyl, Indenyl, or Fluorenyl Ligands [126]

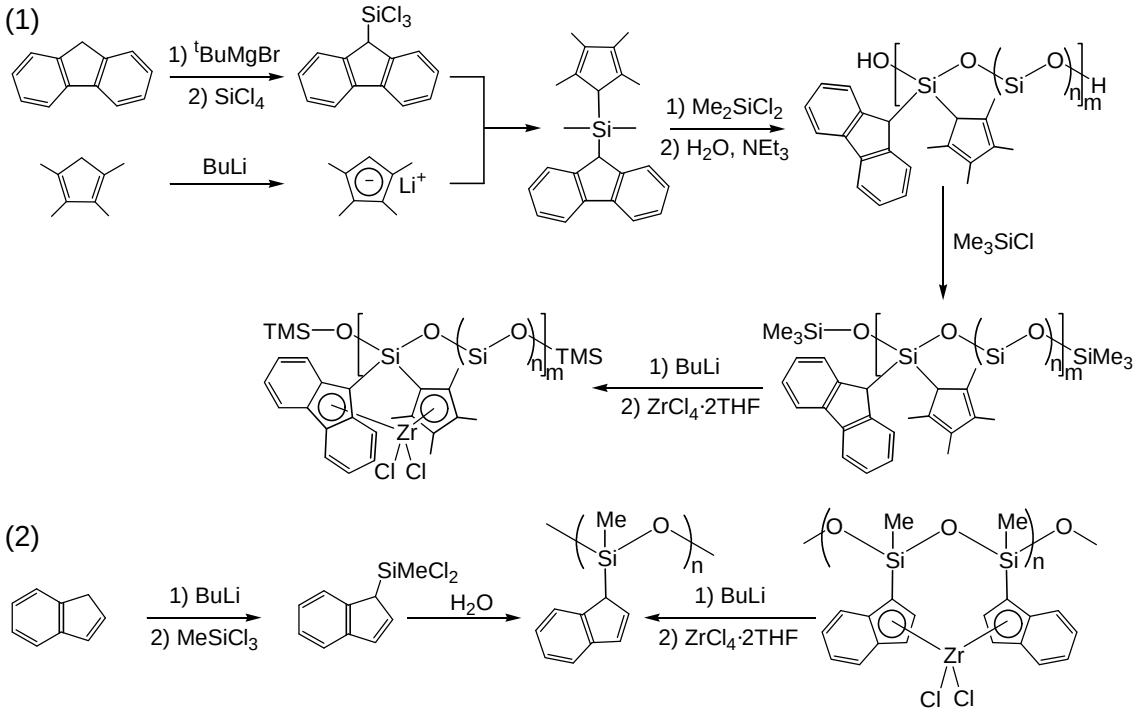

Scheme 1-34 Preparation of Zirconocene Compounds Supported on Polysiloxane Gel [127]

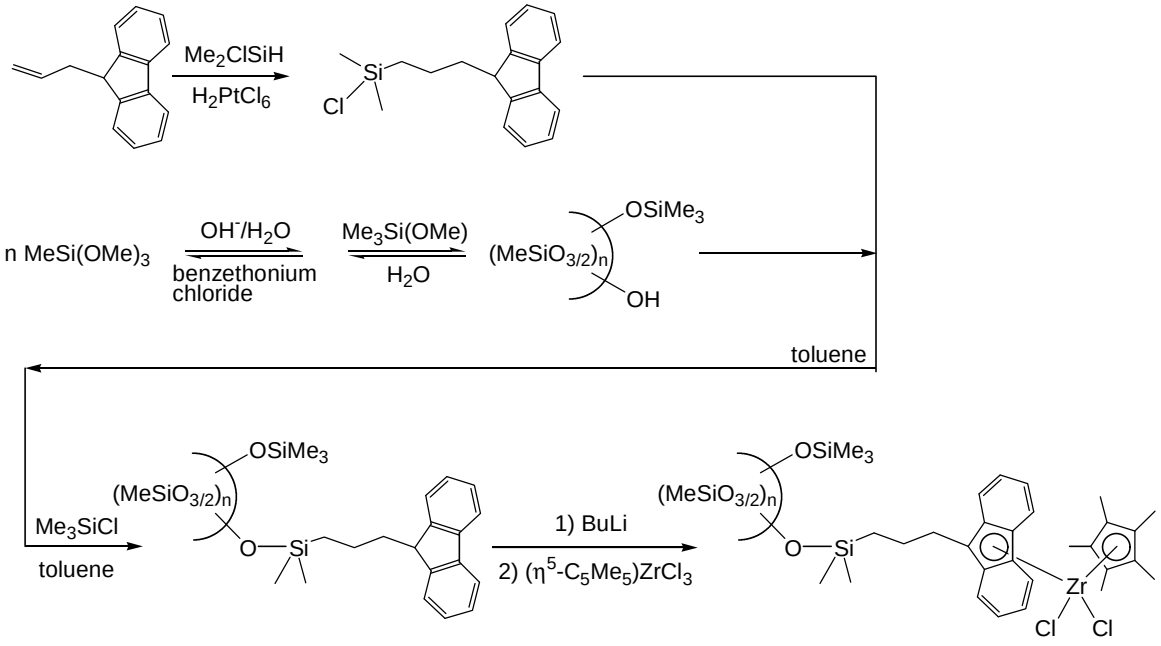

1.4 New Immobilization Strategy and Goals of the Research

1.4.1 Proposal for a New Immobilization Method Using Multiple Short Covalent Tethers

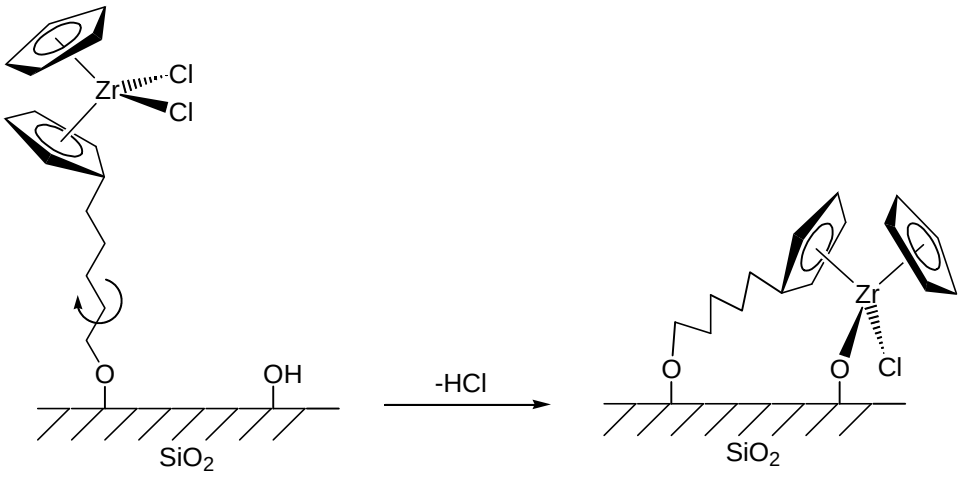

Scheme 1-35 Surface Poisoning Caused by the Flexibility of Single Long Covalent Tether

As discussed in Section 1.3.1, there are three methods for immobilization of metallocene catalysts on silica: direct deposition, pre-alumination, and covalent tethering. The direct deposition method is simple and convenient, but the supported catalysts prepared using this method usually have low polymerization activities due to the influences of the silica surface, e.g., steric hindrance and poisoning effect. In the supported metallocene catalysts prepared using the pre-alumination method, active sites have appreciable freedom of movement on the support, so the catalytic properties of the supported active sites resemble those of the homogeneous analogs, and the polymers produced are similar to those produced by the homogeneous analogs. However, the nature of the weak ionic interactions that bind the active sites to the MAO-covered support is not clear and is difficult to study. The covalent tethering method is expected to avoid the disadvantage of the direct deposition method by putting a covalent spacer between an active site and the support surface. The interface between an active site and the support is a covalent tether, which is somewhat easier to characterize. The flexibility of a long single-tether also

provides the active site a pseudo-solution environment. However, the flexibility of the long single-tether also provides a route for direct interaction of the active site with the surface, so the active site is in a similar situation as that of a active site in a supported catalyst prepared using the direct deposition method (Scheme 1-35).

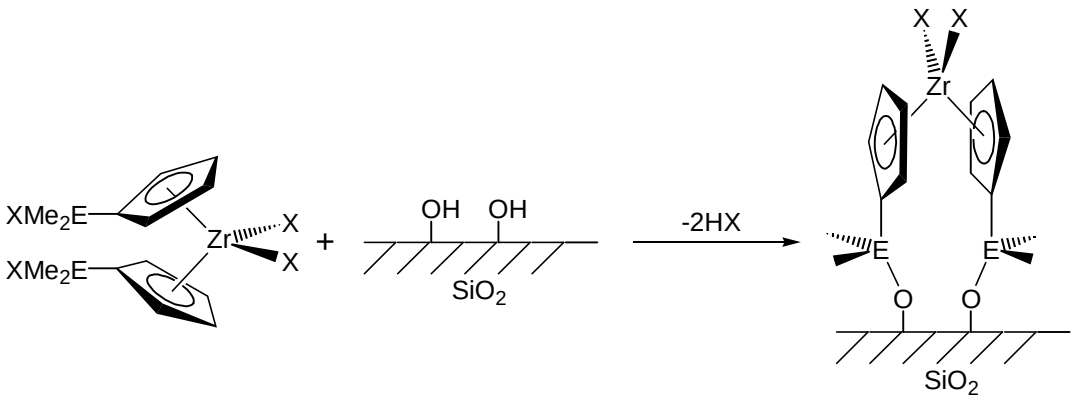

Scheme 1-36 Proposed Immobilization of Functionalized Zirconocene Compound by Two Short Covalent Tethers

Since anchoring a metallocene molecule by only one long single-tether has the possible drawback, we proposed that two or more short single-tethers may solve the problem. As illustrated in the model in Scheme 1-36, a metallocene molecule is bonded to silica by two short single-tethers. The two single-tethers are expected not only to confine movement (translational and rotational) of the molecule, but also to make the metal center in the face-up configuration, i.e., facing away from the silica surface. The face-up configuration ensures sufficient accessibility of the metal center by monomers during polymerization. However, the movement restriction by two single-tethers is not strong enough, the bonded molecule may still takes a face-down configuration as shown in Scheme 1-37. It is expected that more single-tethers would further confine movement of the bonded molecule and eventually fix the molecule on the surface in a face-up configuration, so that the metal center can not interact with the surface directly.

Scheme 1-37 Proposed Face-down Configuration of a Surface Zirconocene Species with Two Single-Tethers

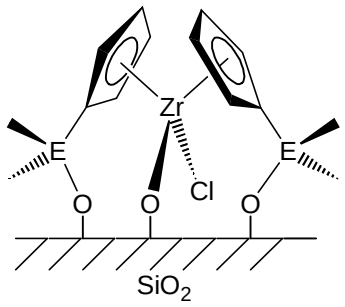

However, the movement restriction by more single-tethers may also cause loss of the favorable pseudo-solution environment of the bonded molecule by one single-tether. Additional single-tethers also increase steric crowding around the labile ligands. One potential solution is to use double-tethers. As shown in the model in Scheme 1-38, the metallocene molecule is bonded to silica through two short double-tethers. On one hand, the two double-tethers have four anchors to the surface, so they should have similar ability to restrict the rotational movement of the bonded molecule as four single-tethers have. On the other hand, there are only two tethers in one molecule, so the steric hindrance around the metal center should be similar to that of the metallocene molecule having two single-tethers. Therefore, with two short double-tethers, it is expected that the bonded metallocene molecule would not rotate to take the face-down configuration as that bonded by four single-tethers, but the steric hindrance of the metallocene molecule with two-double tethers should be much less than that of the metallocene molecule with four single-tethers.

1.4.2 Achievements in the Syntheses of Group 4 Metallocene Compounds Containing Multiple Halosilyl Groups

Preparing metallocene compounds with multiple tether-forming substituents before immobilization is the obvious choice to make silica-supported metallocene compounds with

multiple covalent tethers. The structures of the compounds can be carefully designed before immobilization, and the compounds can be well characterized in homogeneous phases. The only difficulty is to characterize the immobilized metallocene compounds on silica. Because of the results from Deck's group and others, several general methods of preparing group 4 metallocene compounds containing multiple halosilyl substituents are available to provide the precursors to prepare silica-supported metallocene catalysts with multiple covalent tethers.

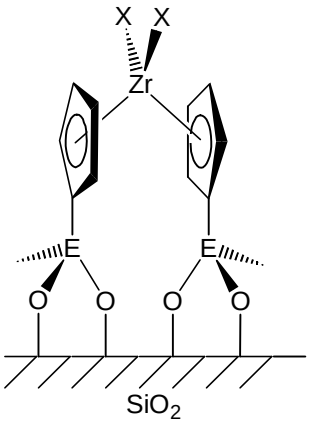

Scheme 1-38 Proposed Configuration of a Surface Zirconocene Species with Two Double-Tethers

Royo and coworkers synthesized bis(chlorodimethylsilyl cyclopentadienyl) zirconium dichloride, (η^5-$ClMe_2Si$-$C_5H_4)_2ZrCl_2$, by the ligand-exchange reaction of $ClMe_2SiC_5H_4SiMe_3$ and $ZrCl_4$ (Scheme 1-39).[128] They found that the compound selectively reacts with water in THF to yield an ansa-zirconocene compound with a disiloxane bridge (Scheme 1-39). This convenient hydrolysis indicates that the Cl-Si bond of the chlorodimethylsilyl ($ClMe_2Si$) group is more labile to nucleophilic attack than the Zr-Cl bonds. Since the hydroxyl groups on silica surface are nucleophiles, it is expected that each $ClMe_2Si$ group can form a single-tether on the surface through a siloxane linkage. Royo and coworkers also made a half titanocene compound with a dichloromethylsilyl (Cl_2MeSi) substituent, which is a possible precursor for a double-

tether (Scheme 1-40).[129] Unfortunately the latter method does not appear to be suitable for preparing similarly substituted zirconocene complexes.

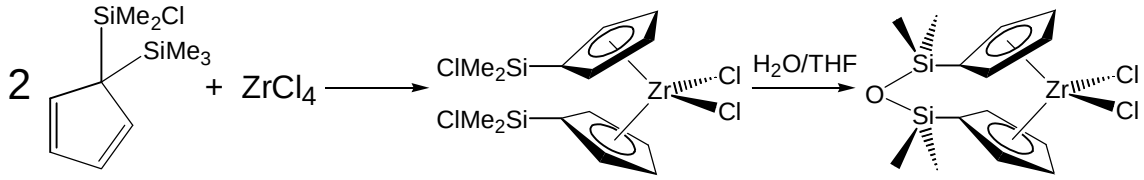

Scheme 1-39 Synthesis of (h^5-$ClMe_2Si$-$C_5H_4)_2ZrCl_2$ by Ligand-exchange Reaction [128]

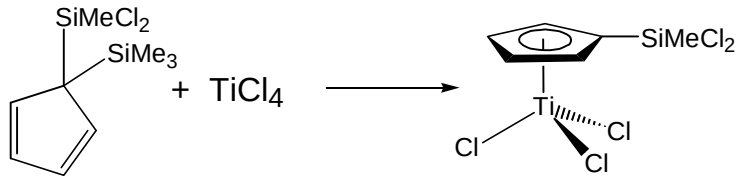

Scheme 1-40 Synthesis of (h^5-Cl_2MeSi-$C_5H_4)TiCl_3$ by Ligand-exchange Reaction [129]

Complementary to the synthesis route developed by Royo's group, in which the halosilyl group is attached on cyclopentadiene before making the desired metallocene compounds, is the route developed by Deck's group. Metallocene compounds containing trimethylsilyl (Me_3Si) groups are synthesized, which are then subjected to halogenation by boron trihalide to convert the Me_3Si groups to halosilyl groups (Scheme 1-41).[130] Typically, two equivalents of trimethylsilyl-cyclopentadienyl lithium ($Me_3SiC_5H_4Li$) react with one equivalent of $ZrCl_4$ in THF at 25 ^oC to afford bis(trimethylsilyl cyclopentadienyl) zirconium dichloride, (η^5-Me_3Si-$C_5H_4)_2ZrCl_2$.[131] The silyl compound reacts with excess of boron tribromide (BBr_3) in $C_2H_4Cl_2$ at 80 ^oC to convert both of the Me_3Si groups to bromodimethylsilyl ($BrMe_2Si$) groups. The reactions are universal for all the group 4 elements. The bromination reaction is selective: only

[128] Ciruelos, S.; Cuenca, T.; Gómez-Sal, P.; Manzanero, A.; Royo, P.: *Organometallics* **14(1)**, 177-185 (1995).
[129] Royo, B.; Royo, P.; Cadenas, L. M.: *J. Organomet. Chem.* **551(1-2)**, 293-297 (1998).
[130] Deck, P. A.; Fisher, T. S.; Downey, J. S.: *Organometallics* **16(6)**, 1193-1196 (1997).

one methyl group on each Me_3Si group is converted. The bromination reaction is also stoichiometric: all the Me_3Si groups are converted. Like the $ClMe_2Si$ group, the $BrMe_2Si$ group also hydrolyzes easily. Moisture will convert $(\eta^5\text{-}BrMe_2Si\text{-}C_5H_4)_2ZrBr_2$ to the disiloxane-bridged compound stoichiometrically in few days, if the compound is left on bench top in air (Scheme 1-41). Zirconocene dichlorides with one, two, or four $BrMe_2Si$ substituents have been prepared by Deck's group. In this research, these compounds are used as precursors to silica-supported zirconocene catalysts with one, two, or four single-tethers.

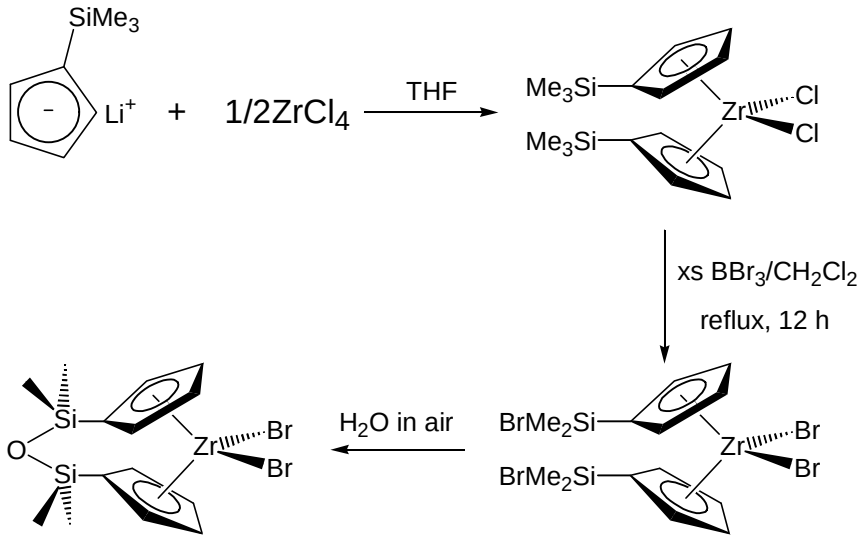

Scheme 1-41 Synthesis and Property of $(\eta^5\text{-}BrMe_2Si\text{-}C_5H_4)_2ZrBr_2$ [130,131]

1.4.3 Goals of the Research

Some metallocene compounds with one or more mono-functional substituents, which could form single-tethers in immobilization, have been prepared. However, few group 4 metallocene compounds are known containing difunctional substituents, which are expected to form double-tethers upon immobilization. Therefore, the first goal of this research is to explore synthetic routes to group 4 metallocene compounds containing double-tether-forming

[131] Antiñolo, A.; Lappert, M. F.; Singh, A.; Winterborn, D. J. W.; Engelhardt, L. M.; Raston, C. L.; White, A. H.; Carty, A. J.; Taylor, N. J.: *J. Chem. Soc. Dalton Trans.* **(6)**, 1463-1472 (1987).

substituents. At the same time, it also enriches the chemistry of functionalized metallocenes. The research will focus on zirconocene compounds.

The second goal of the research is to prepare silica-supported zirconocene catalysts with the zirconocene compounds containing various number and type of tether-forming substituents under different preparation conditions. We aim to investigate the catalytic properties of the immobilized catalysts for ethylene polymerization with MAO as the cocatalyst and to correlate the catalytic properties of the supported catalysts with the number and type of the tether-forming substituents of the zirconocene compounds.

This dissertation includes the following content. In Chapter 2, the synthesis, characterization, and properties of (trimethylstannylcyclopentadienyl cyclopentadienyl)-zirconium dichloride, (η^5-Me_3Sn-C_5H_4)$CpZrCl_2$, are described. The trimethylstannyl (Me_3Sn) group can be converted to a dibromomethylstannyl (Br_2MeSn) group, which we had hoped might be the precursor of a double-tether. In Chapter 3, the synthesis, characterization, and properties of bis[(dibromomethylsilyl)cyclopentadienyl]zirconium dibromide, (η^5-Br_2MeSi-$C_5H_4)_2ZrBr_2$, are described. The dibromomethylsilyl group hydrolyzes readily. Chapter 4 describes the preparations and characterizations of some silica-supported catalysts using the prepared zirconocene compounds containing various number and type of tether-forming substituents. Chapter 4 also includes discussions of the ethylene polymerization data obtained using the prepared silica-supported catalysts with MAO cocatalyst. Chapter 5 presents the results of a model study of the immobilization process using a homogeneous analog. Chapter 6 presents the conclusions of this dissertation and offers suggestions for further experimentation.

Chapter 2 Synthesis and Reactivity of Trimethylstannyl Zirconocene Dichloride [(h^5-Me_3Sn-C_5H_4)$CpZrCl_2$][132]

2.1 Introduction: Comparison between Silicon and Tin

Section 1.4.2 presented some reactivity patterns of Me_3Si-subsituted metallocenes with boron trihalides. To summarize briefly again here, one of the Si-C bonds in each of the Me_3Si substituents on the Me_3Si-substituted group 4 metallocene dichlorides can be cleaved stoichiometrically using excess BBr_3, and the Me_3Si substituents are converted to $BrMe_2Si$ substituents.[130] The $BrMe_2Si$ substituents are interesting to us as precursors for the formation of single tethers in the immobilization of the metallocene compounds on silica. As mentioned in Section 1.4.3, the first goal of the research is to explore more synthetic routes to functionalized zirconocene compounds containing substituents that are precursors to double tethers in the immobilization process. Although Royo and coworkers have reported the synthesis of (η^5-Cl_2MeSi-C_5H_4)$TiCl_3$, in which the Cl_2MeSi substituent is believed to be a precursor to a double tether, this bifunctional silyl substituent can not be formed by halogenation of Me_3Si-substituted zirconocene dichlorides using excess BBr_3,[130] not to mention the weaker congener, BCl_3.[133,134]

The factor that most likely prevents the cleavage of a second Si-C bond in a Me_3Si substituent on zirconocene dichloride by BBr_3 is probably the electron-withdrawing effect of the metallocene. The cleavage of a Si-C bond by boron halide (BX_3) is an electrophilic metathesis, in which BX_3 attacks the most electron-rich Si-C bond. The oxidation state of group 4 elements in metallocene dichlorides is +4, giving a metal-centered noble gas configuration (d^0) and a total valence electron count of 16. After the substitution of the first halide, the halosilyl group

[132] Cheng, X.; Slebodnick, C.; Deck, P. A.; Billodeaux, D. R.; Fronczek, F. R.: *Inorg. Chem.* **39(21)**, 4921-4926 (2000).
[133] Cotton, F. A.; Wilkinson, G.: *Advanced Inorganic Chemistry 5th ed.*, Wiley: New York 1988, 172-176.
[134] Bowmaker, G. A.; Boyd, P. D. W.; Sorrenson, R. J.: *J. Chem. Soc. Faraday Trans. II* **81(7)**, 1023-1034 (1985).

attached to the metallocene is simply too electron-deficient, prohibiting electrophilic attack by a second BX_3 molecule even under forcing conditions. However, similar reactions carried out on Me_3Si-substituted ferrocenes (which are electron-rich, 18-electron species) result not in cleavage of two Si-CH_3 bonds but in the cleavage of the Si-Cp bonds (Scheme 2-1).[130]

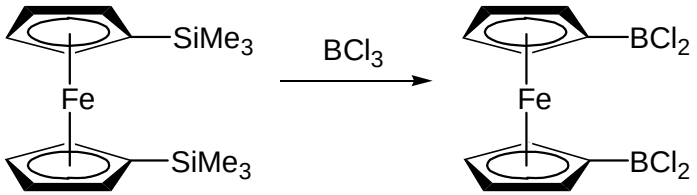

Scheme 2-1 Reaction between (h^5-Me_3Si-$C_5H_4)_2Fe$ and BCl_3 [130]

In order to prepare zirconocene compounds with bifunctional substituents, we explored the following two approaches. The first approach is to replace silicon with a more electron-donating element, or one that might form weaker bonds to carbon. The second approach is to replace the methyl groups on silicon with better leaving groups than methyl groups. To realize the first approach, silicon in the Me_3Si group was replaced by tin. The second approach will be taken up in Chapter 3.

The obvious strategy to select a replacement element for silicon is to find one from the same group. Since elements in a same group have similar properties, the replacement may not change the properties of the original zirconocene compound too much. Group 14 comprises five elements: C, Si, Ge, Sn, and Pb. Table 2-1 lists their ionization potentials.[135] The data show that carbon is more reluctant to donate electrons than silicon, so C is not a good choice. Germanium is more electron-donating than silicon, however, the ionization potential values are close to those of silicon, so their electron-donating abilities will not differ too much. In addition, germanium is expensive. The drawback of lead is its inert electron pair effect, which makes lead unstable in

[135] Harrison, P. G.: *Chemistry of Tin*, P. G. Harrison Ed., Blackie: New York 1989, 9-59.

the +4 state. The normal oxidation state of lead is the +2 state. Therefore, tin is the best choice in the group to replace silicon as a substrate electrophilic halodealkylation.

Table 2-1 Ionization Potentials of Group 14 Elements [135]

element	Ionization Potentials (eV) 1st	2nd	3rd	4th
C	11.260	24.383	47.887	64.492
Si	8.151	16.345	33.492	45.141
Ge	7.899	15.934	34.22	45.71
Sn	7.344	14.632	30.502	40.734
Pb	7.416	15.032	31.937	42.32

The sp^3 covalent radius of Sn(IV) is 1.40 Å, which is much larger than that of silicon (1.18 Å),[136] and the radial distributions of the 5s and 5p orbitals of tin are more diffuse than those of the 3s and 3p orbitals of silicon. These features result in a lower ionization potential (Table 2-1) and a higher polarizability compared to silicon.[137] The atomic trend is reflected in the first ionization potentials of Me_4Sn (9.65 eV) and Me_4Si (10.23 eV).[138] Sn-C bonds are generally weaker than Si-C bonds. For example, the homogeneous dissociation energy of the first Sn-C bond in Me_4Sn is 69.3 kcal/mol, compared to 89.8 kcal/mol in Me_4Si.[139]

The comparison between tin and silicon shows that tin is more "electron rich" than silicon and that Sn-C bonds are weaker than Si-C bonds. Therefore, Sn-CH_3 bonds are more

[136] Huheey, J. E.; Keiter, E. A.; Keiter, R. L.: *Inorganic Chemistry: Principles of Structure and Reactivity 4th ed.*, HarperCollins: New York 1993, 292.
[137] *CRC Handbook of Chemistry and Physics, 80th ed.*, D. R. Lide Ed.-in-Chief, CRC: New York 1999, 10-162.
[138] Aoyama, M.; Masuda, S.; Ohno, K.; Harada, Y.; Yew, M.-C.; Hua, H.-H.; Yong, L.-S.: *J. Phys. Chem.* **93(5)**, 1800-1805 (1989).
[139] Jackson, R. A.: *J. Organomet. Chem.* **166(1)**, 17-19 (1979).

susceptible toward electrophilic cleavage than Si-CH_3 bonds.[140,141,142] The Me_3Sn substituent is expected to be more reactive than Me_3Si in the electrophilic substitution reaction with BX_3. Our hypothesis was that more than one Sn-C bond of the Me_3Sn substituent could be cleaved by BX_3 to make a bifunctional X_2MeSn substituent.

2.2 Synthesis of (h^5-Me_3Sn-C_5H_4)$CpZrCl_2$

2.2.1 Discussion of the Synthetic Route

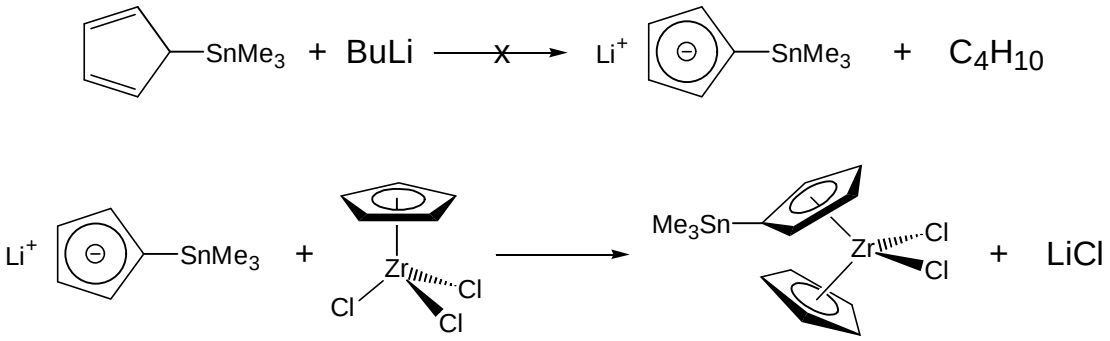

Scheme 2-2 A Failed Route to Synthesize (h^5-Me_3Sn-C_5H_4)$CpZrCl_2$

The monostannylated metallocene (η^5-Me_3Sn-C_5H_4)$CpZrCl_2$ served as a simple substrate for reactivity studies with boron trihalides and with other electrophiles. The first attempt to synthesize this substrate followed a conventional "salt metathesis" reaction (Scheme 2-2), the exchange of a cyclopentadienyl salt (e.g., sodium salt) with a transition metal halide (e.g., chloride). One salt formed after the exchange (e.g., NaCl) is insoluble in the organic solvent and forms a precipitate, leaving the other salt formed after the exchange in solution as the desired metallocene compound. The alkali halide lattice energy and the strong Cp-transition metal bond are the primary driving forces of the metathesis.

[140] Eaborn, C.; Pande, K. C.: *J. Chem. Soc.*, 1566-1571 (1960).
[141] Ponomarev, S. V.; Machigin, E. V.; Lutsenko, I. F.: *Zh. Obshch. Khim.* **36(3)**, 548-552 (1966).
[142] Seyferth, D.: *Prog. Inorg. Chem.* **3**, 129-280 (1962).

To test this route, we need an alkali salt of the Me_3Sn-substituted Cp anion, $(Me_3Sn)C_5H_4$. Normally, a Cp-alkali compound is prepared by reacting the corresponding cyclopentadiene with sodium hydride (NaH) or butyllithium (BuLi). The strong base abstracts a proton from the cyclopentadiene to form the desired cyclopentadienyl anion and either H_2 or butane, respectively. However, in our attempts to prepare the salt of the $(Me_3Sn)C_5H_4$ anion, both of these bases reacted with $(Me_3Sn)C_5H_5$, but only dark-brown sticky materials were obtained, indicating unsuccessful reactions. These results are consistent with the observations of Köhler and coworkers.[143] Due to facile transmetalation, it is not possible to prepare the salts of $(Me_3M)C_5H_4$ anions (when M = Sn or Pb) by a reaction between the corresponding cyclopentadiene and KH or BuLi, even though the M = C, Si, and Ge analogs can be prepared by this reaction. The Me_3Sn or Me_3Pb substituent is more reactive than hydrogen on the cyclopentadiene, so the hydride or butyl anion reacts with the Me_3Sn or Me_3Pb substituent, resulting in the cleavage of the substitute from the cyclopentadiene instead of deprotonation (Scheme 2-3). Therefore, no further attempts were made to synthesize $(\eta^5\text{-}Me_3Sn\text{-}C_5H_4)CpZrCl_2$ following this route.

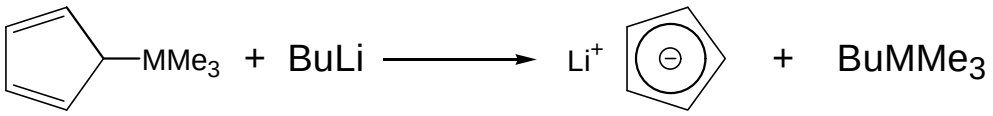

Scheme 2-3 Reason for the Failure of the Route [143]

An alternative route to prepare the salts of $(Me_3M)C_5H_4$ anions (M = Sn and Pb) takes advantage of the reactive nature of the Me_3M substituent on cyclopentadiene.[143] Here, the disubstituted cyclopentadiene, $(Me_3M)_2C_5H_4$, is first prepared from cyclopentadiene (C_5H_6, CpH) and $(Me_3M)NR_2$. The $(Me_3M)_2C_5H_4$ can react with KH or BuLi in THF, and one of the

[143] Köhler, F. H.; Geike, W. A.; Hertkorn, N.: *J. Organomet. Chem.* **334(3)**, 359-367 (1987).

Me_3M substituents on the cyclopentadiene is sacrificed to transmetalation, leaving the other Me_3M substituent on the Cp anion (Scheme 2-4). The salt of the substituted cyclopentadienyl anion can be used in the syntheses of the substituted metallocene compounds by salt metathesis.

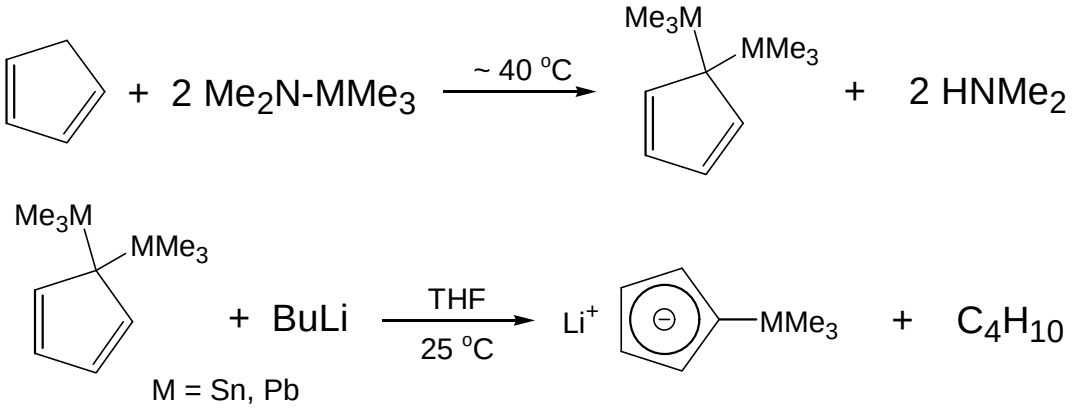

Scheme 2-4 Preparation of Me_3Sn- or Me_3Pb-substituted Cyclopentadienyl Salt by Metal Exchange Reaction [143]

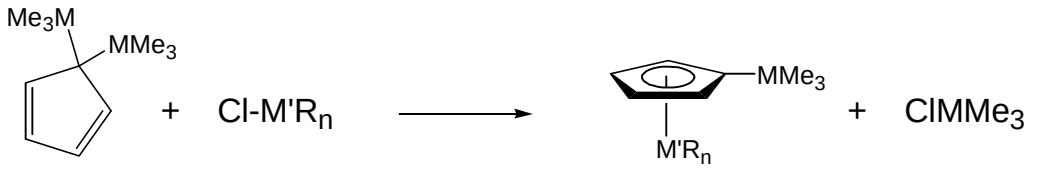

M = Sn, Pb; M' is a transition metal.

Scheme 2-5 Use of the Metal Exchange Reaction in the Synthesis of Me_3Sn- or Me_3Pb-substituted Metallocene Compound

However, due to the reactivity of the Me_3M substituent (M = Sn or Pb), it is not necessary to prepare the substituted anion first in order to carry out the metathesis reaction. The disubstituted cyclopentadiene can be used directly in a modified metathesis procedure (Scheme 2-5). One of the Me_3M groups leaves the cyclopentadiene and combined with one of the halide ligands of the metal salt to form Me_3MX (e.g. X = Cl) and the Me_3M-substituted metallocene compound. Actually, Churakov and Kuz'mina have already synthesized a half titanocene

compound containing a Me_3Sn substituent, (η^5-Me_3Sn-C_5H_4)$TiCl_3$, by the reaction between bis(trimethylstannyl) cyclopentadiene, $(Me_3Sn)_2C_5H_4$, and titanium tetrachloride ($TiCl_4$).[144]

2.2.2 Synthesis and Characterization of (η^5-Me_3Sn-C_5H_4)$CpZrCl_2$

Our synthesis of (η^5-Me_3Sn-C_5H_4)$CpZrCl_2$ followed the modified metathesis route. According to the method developed by Jones and Lappert,[145] $(Me_3Sn)NMe_2$, a light-yellow liquid, was prepared by the reaction of Me_3SnCl and $LiNMe_2$ (THF, reflux). $(Me_3Sn)NMe_2$ is also commercially available from Aldrich but expensive. The preparation of $(Me_3Sn)_2C_5H_4$ followed the method in the literature.[146,147]

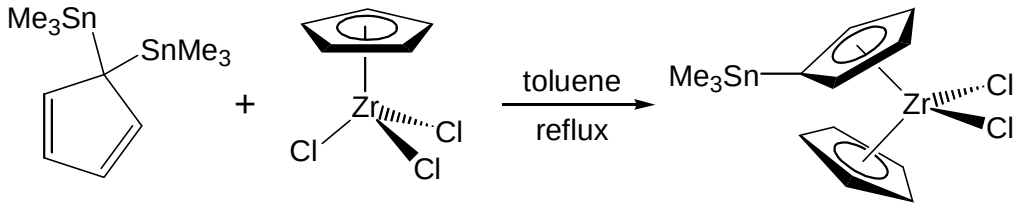

Scheme 2-6 Synthesis of (h^5-Me_3Sn-C_5H_4)$CpZrCl_2$

The zirconocene compound, (η^5-Me_3Sn-C_5H_4)$CpZrCl_2$, was synthesized by a modified procedure (Scheme 2-6) of that described by Churakov and Kuz'mina in the synthesis of (η^5-Me_3Sn-C_5H_4)$TiCl_3$.[144] ^1H NMR analysis of the crude product showed the presence of several species besides the desired compound: unreacted $(Me_3Sn)_2C_5H_4$, the byproduct, Me_3SnCl (0.66 ppm, s), Cp_2ZrCl_2, and (η^5-$ClMe_2Sn$-C_5H_4)$CpZrCl_2$. The formation of the two metallocene species will be discussed in Section 2.2.3. Recrystallization gave the desired stannylated metallocene (η^5-$Me_3SnC_5H_4$)$CpZrCl_2$ in 50% or 78%, using $CpZrCl_3$•DME or $CpZrCl_3$ as the

[144] Churakov, A. V.; Kuz'mina, L. G.: *Acta Cryst.* **C52**, 3037-3038 (1996).
[145] Jones, K.; Lappert, M. F.: *J. Chem. Soc. London*, 1944-1951 (1965).
[146] Jones, K.; Lappert, M. F.: *J. Organomet. Chem.* **3(4)**, 295-307 (1965).
[147] Pribytkova, I. M.; Kisin, A. V.; Luzikov, Yu. N.; Makoveyeva, N. P.; Torocheshnikov, V. N.; Ustynyuk, Yu. A.: *J. Organomet. Chem.* **30(2)**, C57-C60 (1971).

starting material, respectively. The product was identified easily by NMR spectroscopy and elemental microanalysis. The compound is stable in air at ambient temperature.

2.2.3 Discussion of the Synthetic Conditions and Origins of Some Impurities

The synthesis of (η^5-Me_3Sn-C_5H_4)$TiCl_3$ by the reaction between $TiCl_4$ and $(Me_3Sn)_2C_5H_4$ has been carried out at 25 ^oC.[144] However, the reaction between $CpZrCl_3$ (or its DME adduct) and $(Me_3Sn)_2C_5H_4$ did not occur at 25 ^oC (starting materials were recovered according to ^1H NMR analysis). Either the half zirconocene compound is simply less reactive than $TiCl_4$,[128,148] or possibly the insolubility of $CpZrCl_3$ in toluene at 25 ^oC retards the reaction. The reaction using $CpZrCl_3$•DME was apparently slower than that using $CpZrCl_3$, since the yield of the preparation using $CpZrCl_3$•DME was significantly less than that using $CpZrCl_3$ under the same reaction conditions. The ^1H NMR spectra also showed that a significant amount of unreacted $(Me_3Sn)_2C_5H_4$ remained in the crude product when $CpZrCl_3$•DME was used, but not when $CpZrCl_3$ was used. The lower reactivity of the DME adduct is probably due to the electron-donating effect of the DME ligand which decreases the electrophilicity of the zirconium ion.

A frustrating difficulty encountered in the preparation of (η^5-Me_3Sn-C_5H_4)$CpZrCl_2$ was the formation of the chlorodimethylstannyl analog, (η^5-$ClMe_2Sn$-C_5H_4)$CpZrCl_2$. In the first trial of the synthesis of (η^5-Me_3Sn-C_5H_4)$CpZrCl_2$ using $CpZrCl_3$ and $(Me_3Sn)_2C_5H_4$, the quantity of this byproduct was even a little more than that of the desired product. In the recrystallization process, the impurity was isolated instead of the desired compound. The rough positions and pattern of the NMR signals of the crystallized product were consistent with that of (η^5-Me_3Sn-C_5H_4)$CpZrCl_2$, except the integration of the Me_3Sn signal was far too low. Elemental analysis were also inconsistent with (η^5-Me_3Sn-C_5H_4)$CpZrCl_2$. We suspected that the identity of this

[148] Winter, C. H.; Zhou, X.-X.; Dobbs, D. A.; Heeg, M. J.: *Organometallics* **10(1)**, 210-214 (1991).

compound might be (η^5-$ClMe_2Sn$-C_5H_4)$CpZrCl_2$, but we could not rule out a distannoxane-linked dimer, O[-(η^5-Me_2Sn-C_5H_4)$CpZrCl_2$]$_2$. Fortunately we were able to obtain well-formed crystals from a saturated solution in 1 : 2 toluene/hexanes, and X-ray diffraction showed that the compound was the chlorostannyl-substituted complex (Section 2.3.1).

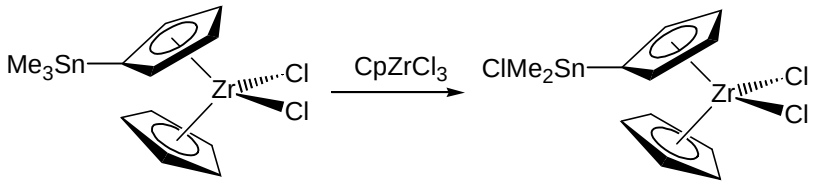

Scheme 2-7 Generation of (h^5-$ClMe_2Sn$-C_5H_4)$CpZrCl_2$ in the Synthesis of (h^5-Me_3Sn-C_5H_4)$CpZrCl_2$

We speculated that (η^5-$ClMe_2Sn$-C_5H_4)$CpZrCl_2$ formed by reaction of (η^5-Me_3Sn-C_5H_4)$CpZrCl_2$ with HCl (generated by adventitious moisture in the reaction). However, a reaction of (η^5-Me_3Sn-C_5H_4)$CpZrCl_2$ with anhydrous HCl in $CDCl_3$ gave Cp_2ZrCl_2 instead, rationalizing the formation of this other impurity in the synthesis of (η^5-Me_3Sn-C_5H_4)$CpZrCl_2$ (see next paragraph). Therefore, we tested some of the more likely impurities in $CpZrCl_3$ (especially $ZrCl_4$) to see if they would convert the Me_3Sn substituent to $ClMe_2Sn$. Metal halides are electrophiles that can halogenate organotin compounds.[149] However, reactions of (η^5-Me_3Sn-C_5H_4)$CpZrCl_2$ with one equivalent of $ZrCl_4$ in toluene showed a complicated mixture of products, as determined by ^{1}H NMR, but neither (η^5-$ClMe_2Sn$-C_5H_4)$CpZrCl_2$ nor (η^5-Me_3Sn-C_5H_4)$CpZrCl_2$ was present. An experiment using one equivalent of $TiCl_4$ in $CDCl_3$ gave similar results, except that a small amount of (η^5-$ClMe_2Sn$-C_5H_4)$CpZrCl_2$ was present. Finally we thought that unreacted $CpZrCl_3$ itself might have been the chlorinating reagent. The reaction of (η^5-Me_3Sn-C_5H_4)$CpZrCl_2$ with one equivalent of $CpZrCl_3$ ($CDCl_3$, 100 ^oC, 15 h) show partial

[149] Wardell, J. L.: *Chemistry of Tin*, P. G. Harrison Ed., Blackie: New York 1989, 145-186.

conversion (about 27%) of (η^5-Me_3Sn-C_5H_4)$CpZrCl_2$ to (η^5-$ClMe_2Sn$-C_5H_4)$CpZrCl_2$. Looking over our notes, we recalled that in the original synthesis of (η^5-Me_3Sn-C_5H_4)$CpZrCl_2$, we found that $CpZrCl_3$ was present in a 15 mol % excess. We conclude that the excess $CpZrCl_3$ further reacted with the product (η^5-Me_3Sn-C_5H_4)$CpZrCl_2$ to generate (η^5-$ClMe_2Sn$-C_5H_4)$CpZrCl_2$ (Scheme 2-7). The chlorination ability of $CpZrCl_3$•DME was much less than that of $CpZrCl_3$, since a significant excess of $CpZrCl_3$•DME generated only a small amount of (η^5-$ClMe_2Sn$-C_5H_4)$CpZrCl_2$ (about 20% as determined by ^{1}H NMR of the crude product).

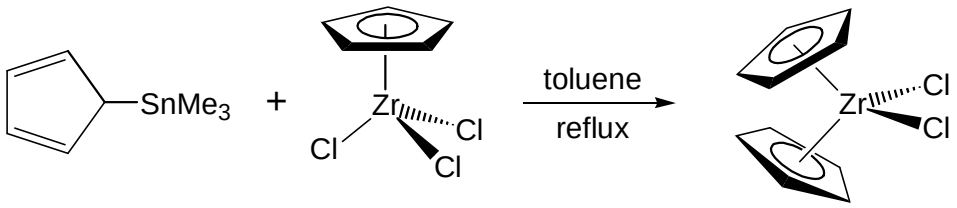

Scheme 2-8 Generation of Cp_2ZrCl_2 in the Synthesis of (h^5-Me_3Sn-C_5H_4)$CpZrCl_2$ (Route One)

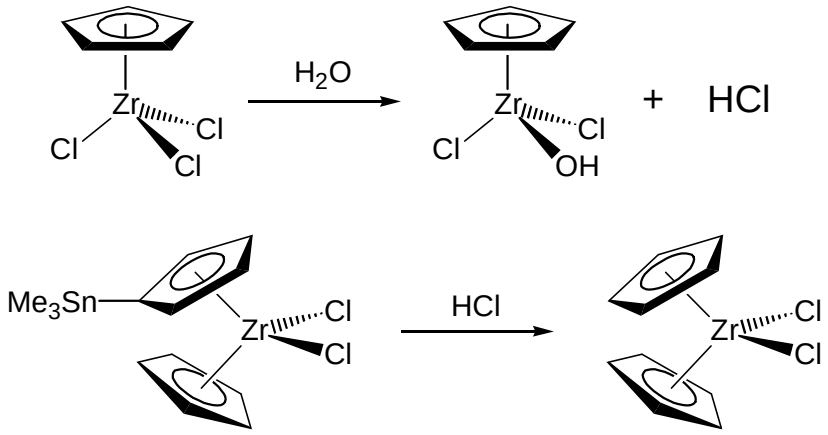

Scheme 2-9 Generation of Cp_2ZrCl_2 in the Synthesis of (h^5-Me_3Sn-C_5H_4)$CpZrCl_2$ (Route Two)

Another impurity observed in the synthesis of (η^5-Me_3Sn-C_5H_4)$CpZrCl_2$ was Cp_2ZrCl_2. There are two possible origins of this impurity. It might originate from the $(Me_3Sn)C_5H_5$ impurity in $(Me_3Sn)_2C_5H_4$, since the metathesis reaction of $(Me_3Sn)C_5H_5$ with $CpZrCl_3$ is similar to that of $(Me_3Sn)_2C_5H_4$ with $CpZrCl_3$, but it generates Cp_2ZrCl_2 instead (Scheme 2-8). The concentration of $(Me_3Sn)C_5H_5$ in the distillation-purified $(Me_3Sn)_2C_5H_4$ was only about 2% to less than 10% to $(Me_3Sn)_2C_5H_4$, so this mechanism was probably operative. However, the ratio of Cp_2ZrCl_2 to (η^5-Me_3Sn-C_5H_4)$CpZrCl_2$ in the raw products were significantly higher than the ratios of $(Me_3Sn)C_5H_5$ to $(Me_3Sn)_2C_5H_4$ in the reactants – nearly 30% in one experiment. As mentioned in the preceding paragraph, adventitious moisture could generate HCl, which reacts with (η^5-Me_3Sn-C_5H_4)$CpZrCl_2$ to cleave the Me_3Sn substituent from the Cp ring to generate Cp_2ZrCl_2 (Scheme 2-9). Stannyl aromatic compounds are known to undergo electrophilic destannylation with Bronsted acids.[150]

2.3 Reactivity of (h^5-Me_3Sn-C_5H_4)$CpZrCl_2$ with Electrophiles

2.3.1 Reaction of (η^5-Me_3Sn-C_5H_4)$CpZrCl_2$ with BCl_3

The reaction of pure (η^5-Me_3Sn-C_5H_4)$CpZrCl_2$ with excess BCl_3 was conducted in an NMR tube and followed by ^1H NMR. After 20 min, the spectrum (Figure 2-1) showed complete disappearance of the starting metallocene, formation of a single metallocene product later identified as (η^5-$ClMe_2Sn$-C_5H_4)$CpZrCl_2$, along with $MeBCl_2$ and Me_2BCl byproducts.[151] No further changes were observed after 6 days. A preparative-scale reaction gave an 82% isolated

[150] a) Asomaning, W. A.; Eaborn, C.; Walton, D. R. M.: *J. Chem. Soc. Perkin Trans. I* **(2)**, 137-138 (1973). b) Eaborn, C.; Jenkins, I. D.; Walton, D. R. M.: *J. Chem. Soc. Perkin Trans. II* **(6)**, 596-600 (1974).

[151] A broad signal at 1.22 ppm was observed if excess BCl_3 was added. Otherwise, a tiny signal at 1.02 ppm was observed. According to the literature, the chemical shifts of Me_2BCl, $MeBCl_2$, Me_2BBr, and $MeBBr_2$ were -1.00 ppm, -1.21 ppm, -1.14 ppm, and -1.42 ppm relative to TMS in CCl_4, respectively. Nöth, H.; Vahrenkamp, H.: *J. Organomet. Chem.* **12(1)**, 23-36 (1968). It is believed that the values are actually +1.00 ppm, +1.21 ppm, +1.14 ppm, and +1.42 ppm based on current chemical shift notation. This interpretation is supported by the proton

yield of (η^5-$ClMe_2Sn$-C_5H_4)$CpZrCl_2$. The compound is stable in air at ambient temperature. Therefore, the reaction between (η^5-Me_3Sn-C_5H_4)$CpZrCl_2$ and BCl_3 was very fast at 25 ^oC but cleaved only one of the three Sn-CH_3 bonds (Scheme 2-10). Importantly, chlorodemethylation of a second Sn-CH_3 bond by BCl_3 is not observed at 25 ^oC.

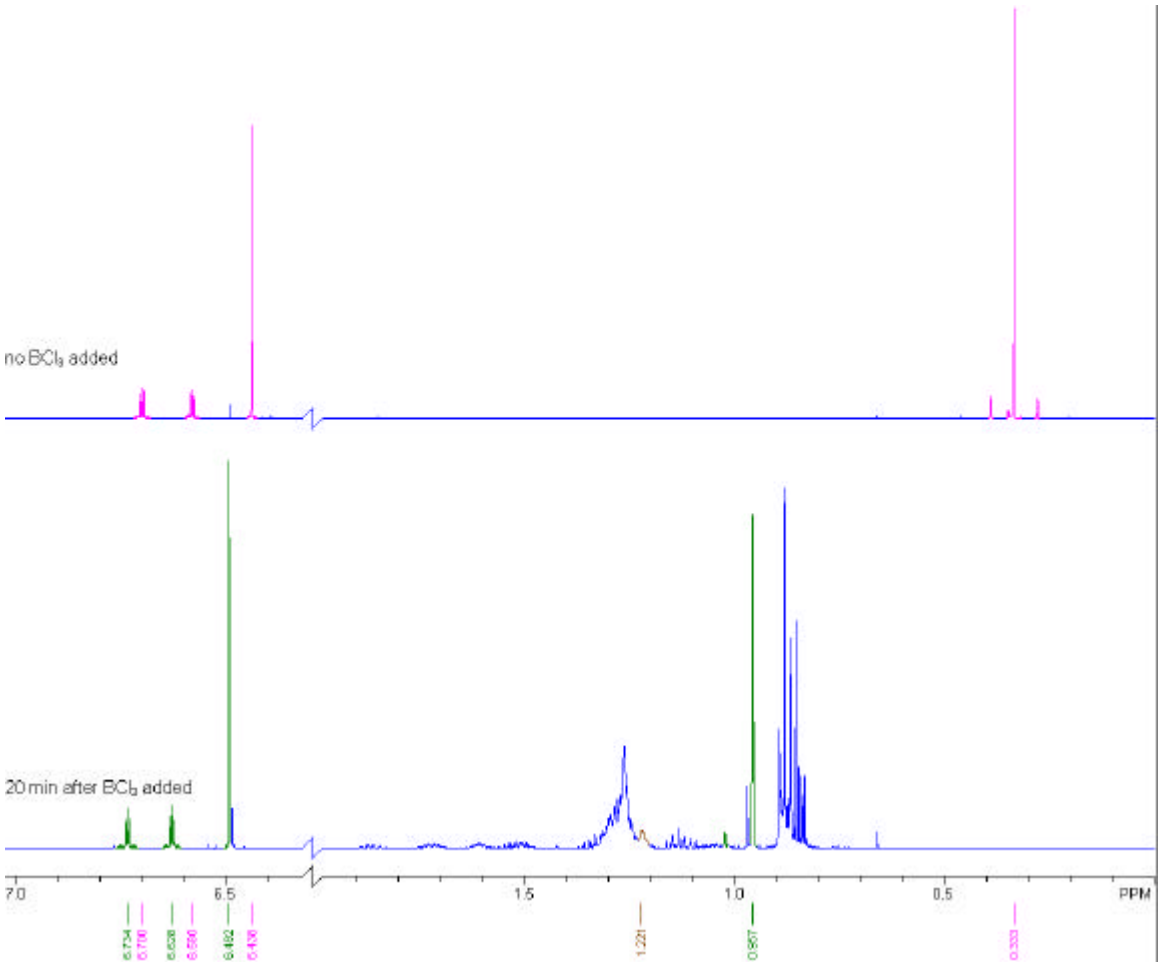

Figure 2-1 The 500 MHz ^1H NMR Spectra of the Reaction between (h^5-Me_3Sn-C_5H_4)$CpZrCl_2$ and BCl_3 in $CDCl_3$

The crystal structure of (η^5-$ClMe_2Sn$-C_5H_4)$CpZrCl_2$ was determined by X-ray crystallography. The molecular structure and selected metric data are shown in Figure 2-2 and Table 2-2. The bond length and bond angle data indicate that the zirconocene "core" of the

---

NMR data for neat Me_2BCl (τ = 9.34) and neat $MeBCl_2$ (τ = 8.88). de Moor, J. E.; van der Kelen, G. P.: *J.*

molecule is nearly identical to that of $(\eta^5\text{-}Me_3Si\text{-}C_5H_4)_2ZrCl_2$.[152] The Sn-$C_6$(ipso) distance (2.135 Å) is a little shorter than that in $(\eta^5\text{-}Me_3Sn\text{-}C_5H_4)TiCl_3$ (2.169 Å).[144] The structure about Sn is typical of tetrahedral Sn compounds with one chloride and three hydrocarbon ligands.[153]

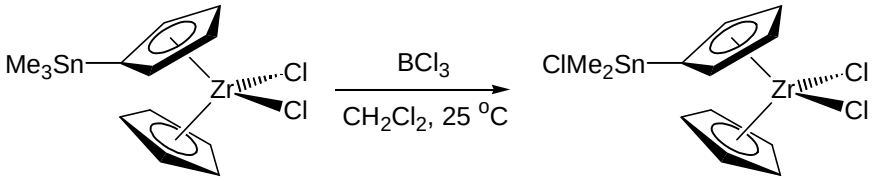

Scheme 2-10 Reaction of $(h^5\text{-}Me_3Sn\text{-}C_5H_4)CpZrCl_2$ with BCl_3

2.3.2 Reaction of $(\eta^5\text{-}Me_3Sn\text{-}C_5H_4)CpZrCl_2$ with BBr_3

The reaction of $(\eta^5\text{-}ClMe_2Sn\text{-}C_5H_4)CpZrCl_2$ with excess BBr_3 in $CDCl_3$ at 25 °C was followed by ^{1}H NMR spectroscopy. The starting material disappeared within 10 min, and the resulting spectrum (Figure 2-3) showed clean conversion to the bromodimethylstannyl-substituted metallocene dibromide, $(\eta^5\text{-}BrMe_2Sn\text{-}C_5H_4)CpZrBr_2$, and BBr_2Me.[151] After about 8 h at 25°C, a new product appeared, which was assigned to $(\eta^5\text{-}Br_2MeSn\text{-}C_5H_4)CpZrBr_2$ (Figure 2-3). After 15 h, the $(\eta^5\text{-}BrMe_2Sn\text{-}C_5H_4)CpZrBr_2$ intermediate was consumed, and only $(\eta^5\text{-}Br_2MeSn\text{-}C_5H_4)CpZrBr_2$ remained. These observations indicated that the transhalogenation of the $ClMe_2Sn$ substituent and the $ZrCl_2$ moiety[154,155] were both very rapid processes (Scheme 2-11). More significantly, since BBr_3 is a stronger electrophile than BCl_3, a second Sn-CH_3 bond can be cleaved slowly by BBr_3 at 25 °C, and the $BrMe_2Sn$ substituent was further converted to Br_2MeSn, which could not be achieved by using BCl_3.

Organomet. Chem. **6(3)**, 235-241 (1966).

[152] In the crystal structure of $(\eta^5\text{-}Me_3Si\text{-}C_5H_4)_2ZrCl_2$, the Cp-Zr distances were 2.199 Å and 2.209 Å, the Cp-Cl distances were 2.476 Å and 2.505 Å, the Cp-Zr-Cp angle was 129.1°, and the Cl-Zr-Cl angle was 93.7°.[131]

[153] The Cl-Sn-C angle ranges from 91°-108° and the C-Sn-C angle ranges from 104°-128° in 41 such tin compounds from the Cambridge Crystallographic Database. The corresponding angles of the molecule are in the middle of the ranges.

Figure 2-2 Thermal Ellipsoid Plot of the Molecular Structure of (h^5-$ClMe_2Sn$-C_5H_4)$CpZrCl_2$

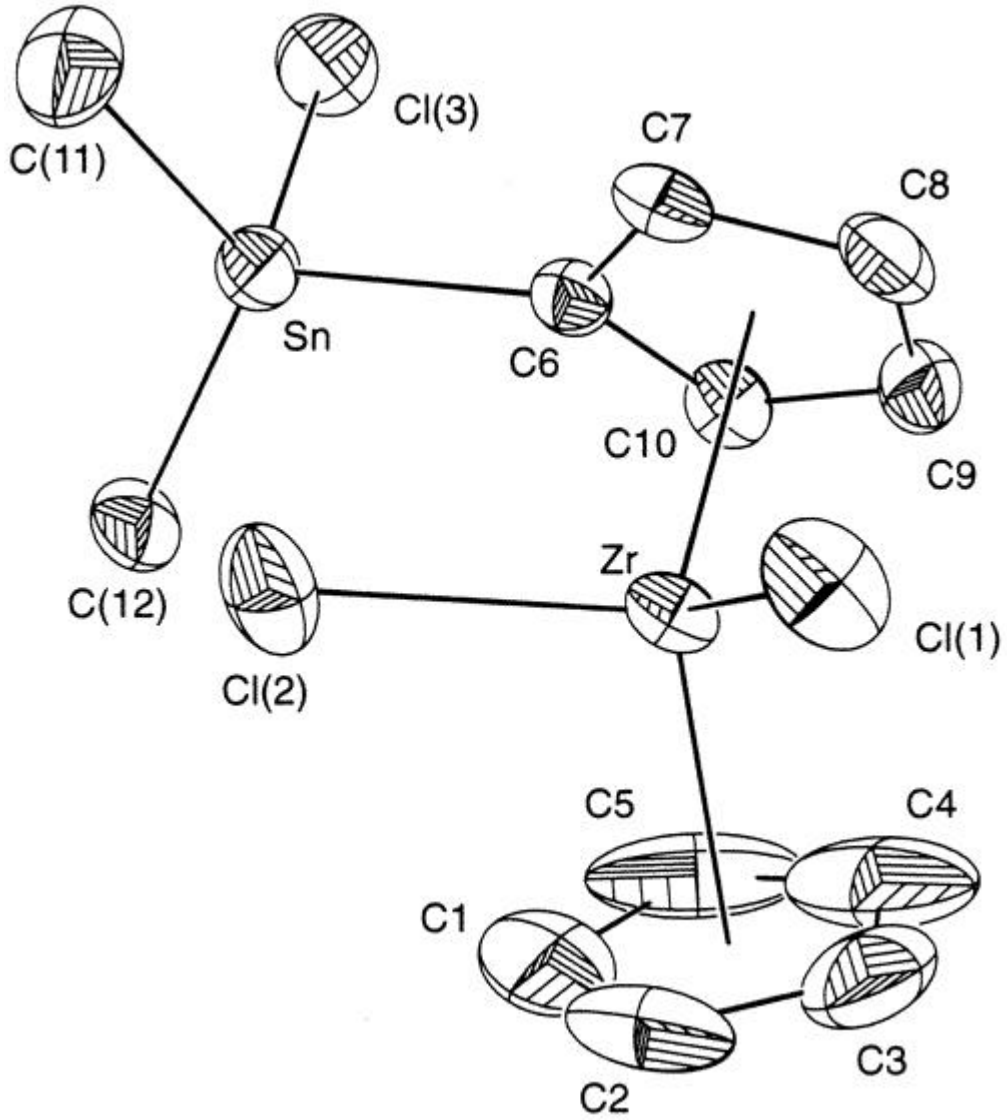

The plot is shown at 50% probability. Hydrogen atoms and disordered toluene solvent molecule omitted. Selected bond distances (Å) and angles (deg): Zr-Cl(1), 2.442(1); Zr-Cl(2), 2.470(1); Zr-Cp(1), 2.193(6); Zr-Cp(2), 2.193(6); Cl(1)-Zr-Cl(2), 95.3(4); Cp(1)-Zr-Cp(2), 129.6(4); Sn-Cl(3), 2.401(2); Sn-C(6), 2.135(4); Sn-C(11), 2.115(5); Sn-C(12), 2.105(4); Cl(3)-Sn-C(6), 97.8(1); Cl(3)-Sn-C(11), 103.8(2); Cl(3)-Sn-C(12), 103.5(2); C(6)-Sn-C(11), 110.5(2); C(6)-Sn-C(12), 116.0(2); C(11)-Sn-C(12), 121.2(2); Cl(3)-Sn-C(6)-C(7), 110.1(3) (torsion). Cp(1) is the centroid of C(1), C(2), C(3), C(4), and C(5). Cp(2) is the centroid of C(6), C(7), C(8), C(9), and C(10).

---

[154] Druce, P. M.; Kingston, B. M.; Lappert, M. F.; Spalding, T. R.; Srivastava, R. C.: *J. Chem. Soc. A* **(14)**, 2106-2110 (1969).

[155] Gassman, P. G.; Winter, C. H.: *Organometallics* **10(5)**, 1592-1598 (1991).

Table 2-2 The Crystallographic Data of (h^5-$ClMe_2Sn$-C_5H_4)$CpZrCl_2$•½toluene and (h^5-Br_2MeSn-C_5H_4)$CpZrBr_2$•THF

	(h^5-$ClMe_2Sn$-C_5H_4)$CpZrCl_2$ •½toluene	(h^5-Br_2MeSn-C_5H_4)$CpZrBr_2$ •THF
chemical formula	$C_{12}H_{15}Cl_3SnZr$•½C_7H_8	$C_{11}H_{12}Br_4SnZr$•C_4H_8O
formula weight	521.57	745.84
a (Å)	21.6517(15)	20.6230(2)
b (Å)	12.8720(10)	8.3330(2)
c (Å)	14.1878(9)	11.9970(4)
b (deg)	103.389(5)	102.5120(10)
V (Å)^3	3846.7(5)	2012.74(9)
Z	8	4
space group	C2/c	$P2_1/c$
T (K)	293(5)	100(2)
l (Mo Ka) (Å)	0.71073	0.71073
r_{calc} (mg m^{-3})[(a)]	1.801	2.461
m (mm^{-1})	2.247	9.698
R[(b)]	0.0384	0.0484
R_w [I > 2s(I)][(c)]	0.0779	0.1189

(a) Experimental crystal densities (r_{obsd}) were not obtained.
(b) $R = S||F_o| - |F_c|| / S|F_o|$, observed data (>2s($I_o$)).
(c) $R_w = [S[w(F_o^2 - F_c^2)^2] / S[w(F_o^2)^2]]^2$, all data.

Scheme 2-11 Reaction of (h^5-$ClMe_2Sn$-C_5H_4)$CpZrCl_2$ with BBr_3

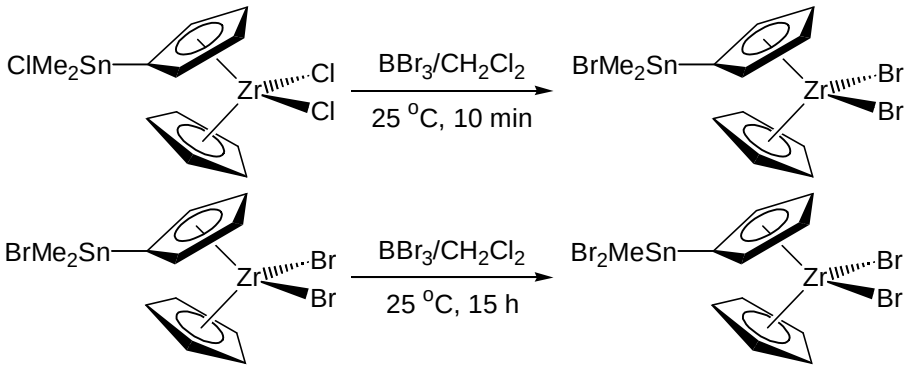

Figure 2-3 The 500 MHz ^{1}H NMR Spectra of the Reaction between (h^5-$ClMe_2Sn$-C_5H_4)$CpZrCl_2$ and BBr_3 in $CDCl_3$

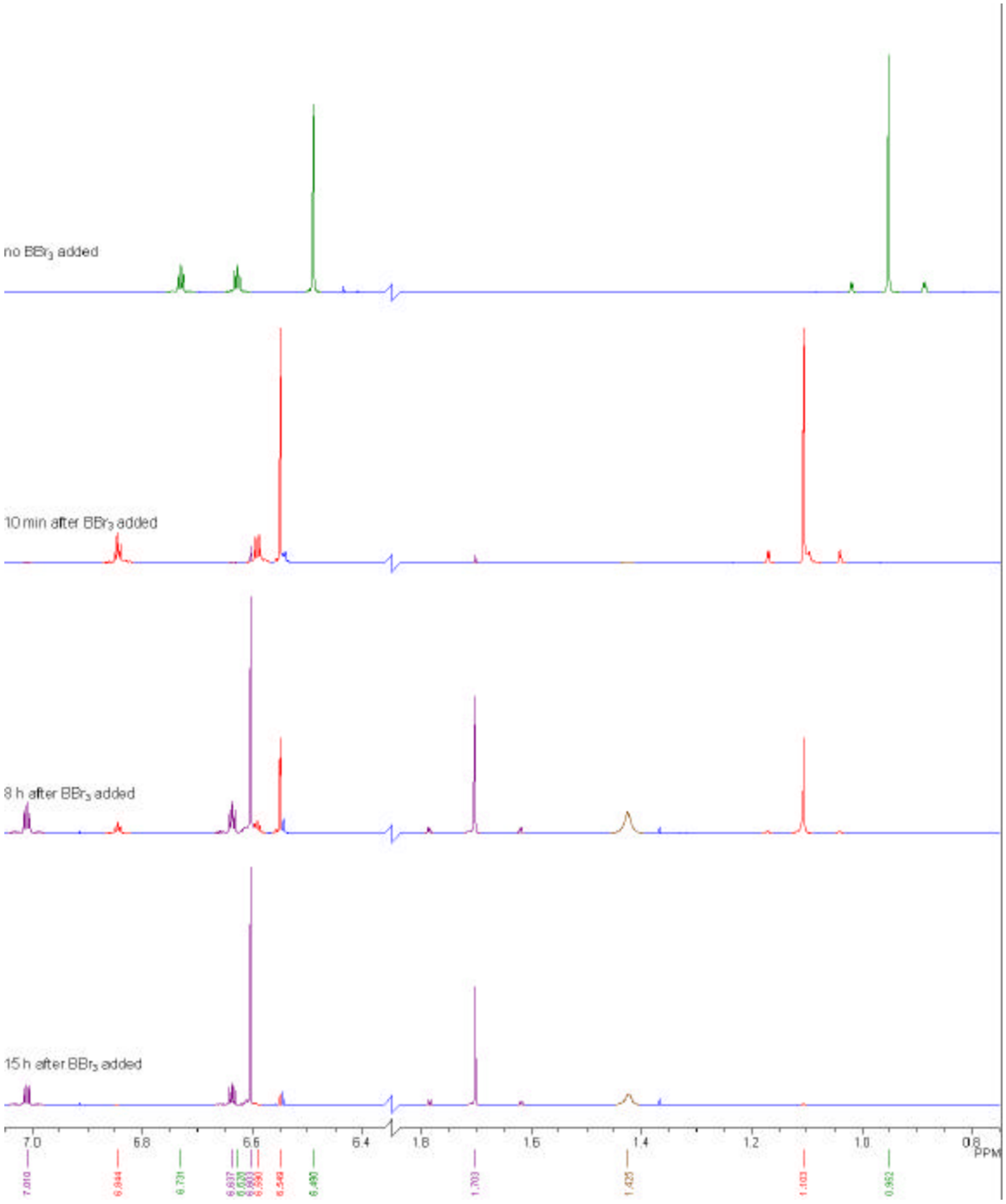

A similar NMR-scale reaction was carried out using (η^5-Me_3Sn-C_5H_4)$CpZrCl_2$ instead. The observations from proton NMR spectra were the same as that using (η^5-$ClMe_2Sn$-

C_5H_4)CpZrCl$_2$. The signals from (η^5-Me$_3$Sn-C_5H_4)CpZrCl$_2$ disappeared in 10 min at 25 ^{o}C, and the signals from (η^5-BrMe$_2$Sn-C_5H_4)CpZrBr$_2$ dominated, which then disappeared gradually, and the signals from (η^5-Br$_2$MeSn-C_5H_4)CpZrBr$_2$ dominated after 15 h. Therefore, similar to BCl$_3$, the cleavage of a first Sn-CH$_3$ bond in (η^5-Me$_3$Sn-C_5H_4)CpZrCl$_2$ by BBr$_3$ was also very fast. In an attempt to see if a third Sn-CH$_3$ bond can be cleaved by BBr$_3$, (η^5-Me$_3$Sn-C_5H_4)CpZrCl$_2$ was treated with excess BBr$_3$ in 1,2-dichloroethane (CH_2ClCH_2Cl, b.p. 83 ^{o}C) and in chlorobenzene (C_6H_5Cl, 132 ^{o}C). In both cases, the major product was (η^5-Br$_2$MeSn-C_5H_4)CpZrBr$_2$, with no evidence for the formation of the tribromostannyl analog. The interconversions of the chlorinated and brominated zirconocene compounds are illustrated in Scheme 2-12. Both the monobromo- and dibromostannyl compounds were also prepared on preparative scales in 82% and 68% isolated yields, respectively. The compounds are air-stable at ambient temperature.

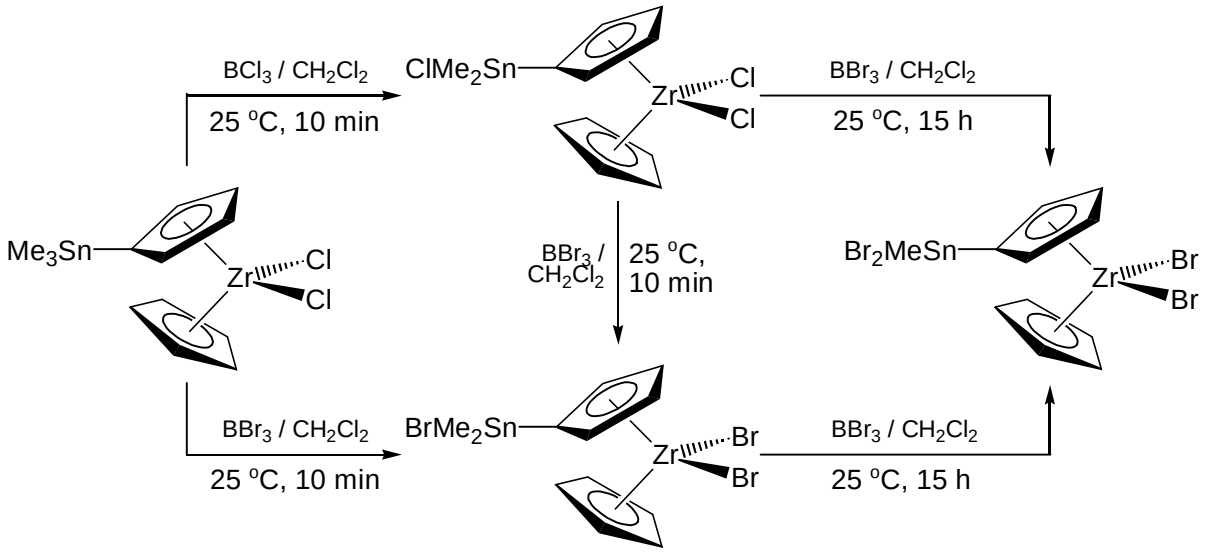

Scheme 2-12 Interconversion among Stannyl- and Halostannyl-Substituted Zirconocene Compounds

Figure 2-4 Thermal Ellipsoid Plot of the Molecular Structure of (h^5-Br_2MeSn-C_5H_4)$CpZrBr_2$•THF

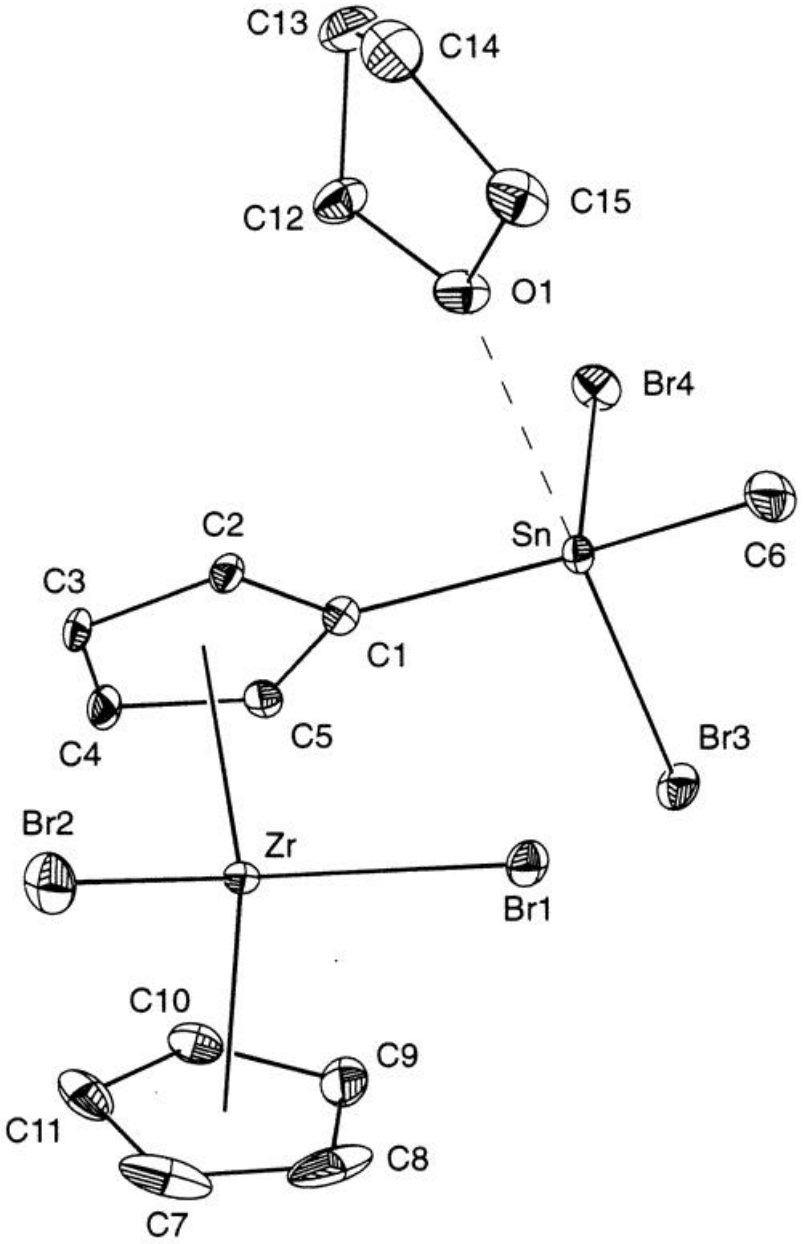

The plot is shown at 50% probability. Hydrogen atoms omitted. Selected bond distances (Å) and angles (deg): Zr-Br(1), 2.6178(5); Zr-Br(2), 2.6001(5); Zr-Cp(1), 2.208(4); Zr-Cp(2), 2.197(4); Br(1)-Zr-Br(2), 95.23(2); Cp(1)-Zr-Cp(2), 128.7(1); Sn-Br(3), 2.5534(5); Sn-Br(4), 2.5139(5); Sn-C(1), 2.113(4); Sn-C(6), 2.111(5); Sn-O(1), 2.655(5); Br(3)-Sn-Br(4), 95.77(2); Br(3)-Sn-C(1), 100.1(1); Br(3)-Sn-C(1), 102.1(2); Br(3)-Sn-O(1), 178.5(2); Br(4)-Sn-C(1), 106.0(1); Br(4)-Sn-C(6), 108.0(1); Br(4)-Sn-O(1), 83.1(2); C(1)-Sn-C(6), 136.9(2); C(1)-Sn-O(1), 79.4(2); C(6)-Sn-O(1), 79.3(2); Br(3)-Sn-C(1)-C(2), -148.0(3) (torsion). Cp(1) is the centroid of C(1), C(2), C(3), C(4), and C(5). Cp(2) is the centroid of C(7), C(8), C(9), C(10), and C(11).

Figure 2-5 Histogram Plot of Sn-O Distances for Trigonal Bipyramidal Complexes Having the General Formula $SnO(CH_3)_nX_{4-n}$

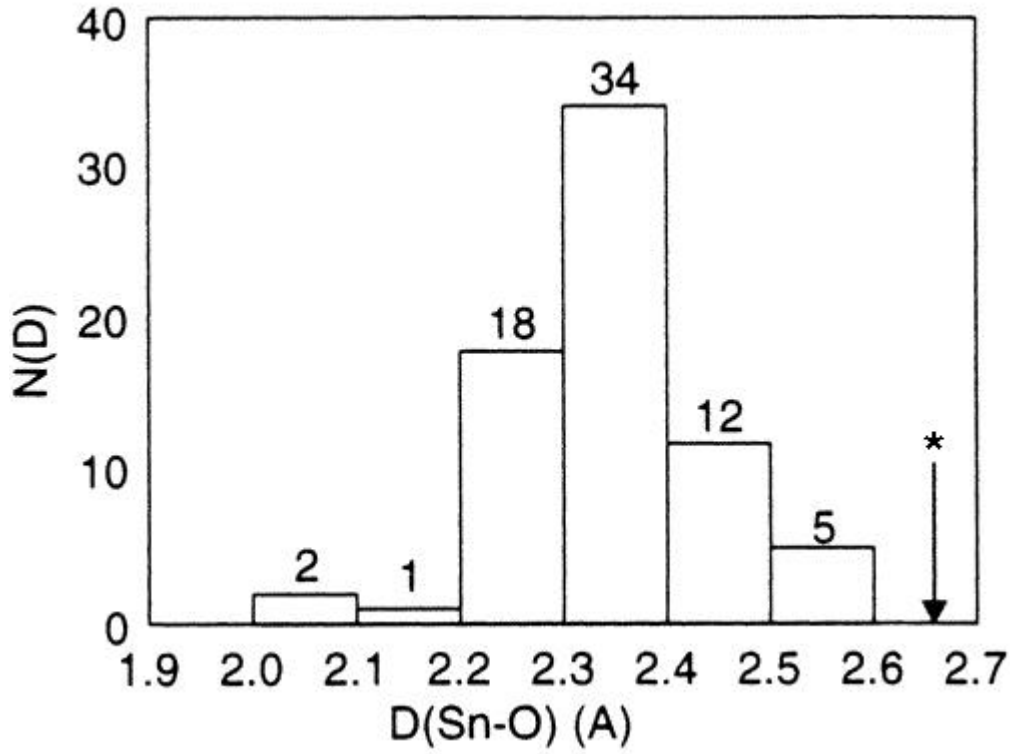

* The Sn-O distance value for $(\eta^5\text{-}Br_2MeSn\text{-}C_5H_4)CpZrBr_2 \bullet THF$.

Histogram plot of Sn-O distances (<2.7 Å) for trigonal bipyramidal complexes having the general formula $SnO(CH_3)_nX_{4-n}$, n = 1-3, X = Cl, Br, or I. Data obtained from the Cambridge Crystallographic Data Center.

The crystal structure of the THF adduct of $(\eta^5\text{-}Br_2MeSn\text{-}C_5H_4)CpZrBr_2$ is shown in Figure 2-4, and selected crystal data are presented in Table 2-2. The oxygen atom of the THF molecule coordinates with the Sn center in the zirconocene molecule, which indicates that the Sn center is electrophilic. The coordination environment of the Sn center is pseudo-trigonal-bipyramidal (tbp), in which the oxygen atom and one of the two bromide ligands occupy the pseudo-axial positions and the rests are in the pseudo-equatorial plane. The structure is distorted from the ideal tbp geometry as shown by a displacement of 0.37 Å of the Sn atom from the equatorial plane away from the coordinated oxygen atom of the THF molecule. The bonding geometries of the zirconocene "core" of the compound resemble those of other unbridged

zirconocene dibromide complexes that had been characterized by X-ray crystallography.[131,156,157] An interesting feature of the adduct is that the Sn-O distance (2.655 Å) is significantly longer than the normal values found in analogous tbp structures containing Sn-O dative bonds. This unusually long distance is presented in Figure 2-5 in the histogram of the Sn-O distances from 72 selected analogous tbp structures selected from the Cambridge Structural Database (CCDC). The 72 structures selected contain Sn atoms that are coordinated by 1-3 halogen ligands, 1-3 hydrocarbyl ligands, and exact one oxygen ligand. Structures whose Sn or O atoms are bridging or whose Sn-O bonds are parts of a ring were excluded. There is no clear structural rationalization for this bond-lengthening effect.

2.3.3 Reactions of (η^5-Me_3Sn-C_5H_4)$CpZrCl_2$ with I_2 and with ICl

Stannyl aromatic compounds can undergo electrophilic aromatic substitution reactions with electrophiles. Due to the weakness of the Sn-C bond, the Sn-Ar bond is cleaved in the reactions instead of the H-Ar bond, resulting in ipso-substituted aromatic compounds. Many such reactions involving the electrophile I_2 or ICl were reported.[158,159,160] For example, ICl converts 3-trimethylstannyl-1,2-dihydrobenzocyclobutene to 3-iodo-1,2-dihydrobenzocyclobutene (Scheme 2-13),[158] and I_2 converts trimethylstannylpyridine to iodopyridine (Scheme 2-14).[159] Protons can also act as the electrophile in the electrophilic aromatic substitution of the stannyl aromatic compounds.[150] For example, regioselective mono-deuterated arenes can be prepared by reaction of the corresponding trimethylstannyl arenes with deuterated acetic acid,

[156] Petoff, J. L. M.; Bruce, M. D.; Waymouth, R. M.; Masood, A.; Lal, T. K.; Quan, R. W.; Behrend, S. J.: *Organometallics* **16(26)**, 5909-5916 (1997).
[157] Bühl, M.; Hopp, G.; von Philipsborn, W.; Beck, S.; Prosenc, M.-H.; Rief, U.; Brintzinger, H.-H.: *Organometallics* **15(2)**, 778-785 (1996).
[158] a) Eaborn, C.; Najam, A. A.; Walton, D. R. M.: *J. Chem. Soc. Chem. Comm.* **(14)**, 840 (1972). b) Eaborn, C.; Najam, A. A.; Walton, D. R. M.: *J. Chem. Soc. Perkin Trans. I* **(19)**, 2481-2484 (1972).
[159] Yamamoto, Y.; Yanagi, A.: *Chem. Pharm. Bull.* **30(5)**, 1731-1737 (1982).
[160] a) Seitz, D. E.; Lee, S.-H.; Hanson, R. N.; Bottaro, J. C.: *Synth. Commun.* **13(2)**, 121-128 (1983). b) Lee, S.-H.; Hanson, R. N.; Seitz, D. E.: *Tetrahedron Lett.* **25(17)**, 1751-1752 (1984).

AcOD/D_2O (Scheme 2-15).[150a] Similarly in our research, HCl was found to cleaved the Cp-$SnMe_3$ bond in (η^5-Me_3Sn-C_5H_4)$CpZrCl_2$ rather than one of the Sn-Me bonds to afford Cp_2ZrCl_2 as described in Section 2.2.3. These results raised the possibility that I_2 or ICl could convert (η^5-Me_3Sn-C_5H_4)$CpZrCl_2$ to (η^5-IC_5H_4)$CpZrCl_2$ by electrophilic aromatic substitution.

Scheme 2-13 Reaction of 3-Me_3Sn-1,2-dihydrobenzocyclobutene with ICl [158]

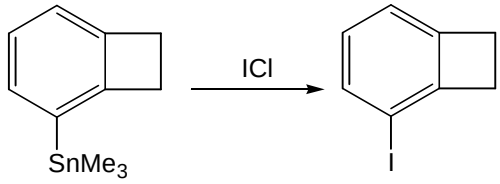

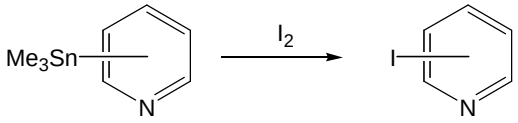

Scheme 2-14 Reaction of Trimethylstannyl Pyridine with I_2 [159]

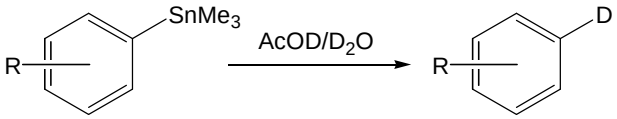

Scheme 2-15 Reaction of Me_3Sn-substituted Arene with AcOD/D_2O [150a]

Figure 2-6 The 500 MHz ^{1}H NMR Spectra of the Reaction between (h^5-Me_3Sn-C_5H_4)$CpZrCl_2$ and I_2

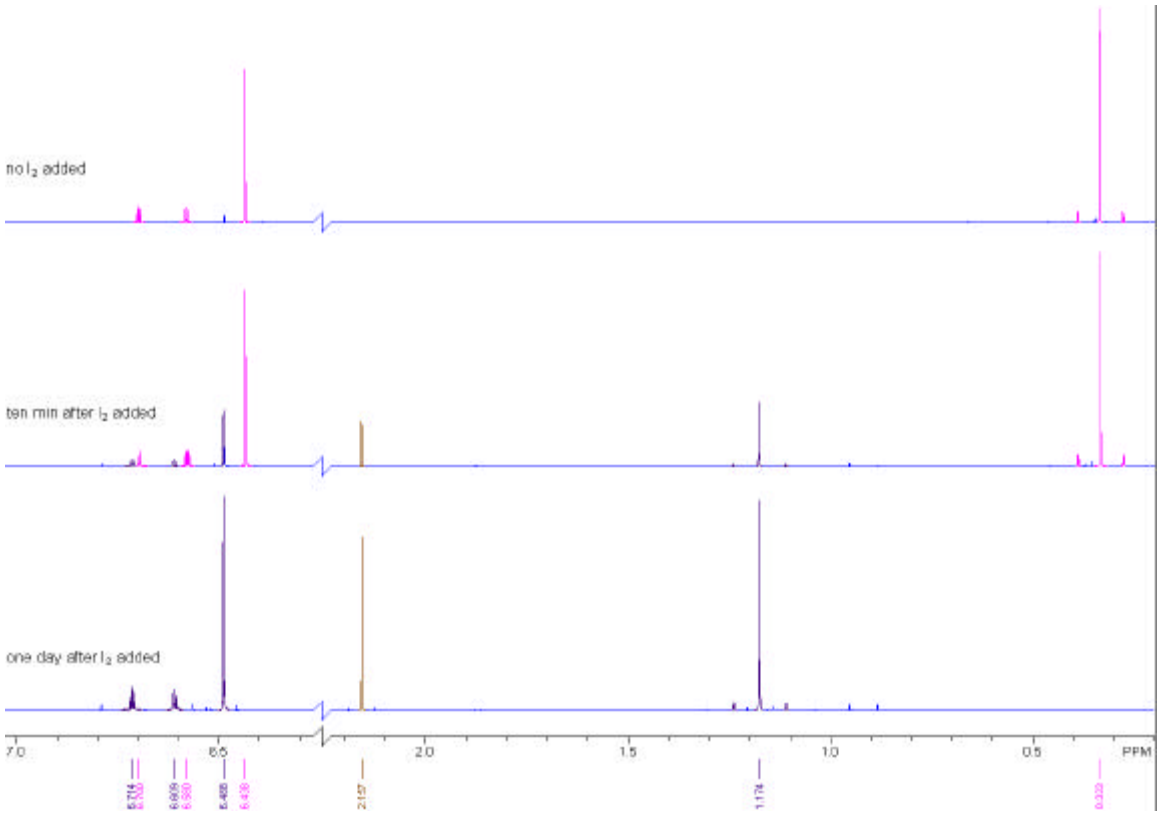

A reaction of (η^5-Me_3Sn-C_5H_4)$CpZrCl_2$ with I_2 was followed by ^{1}H NMR spectroscopy. Ten minutes after the two compounds were mixed in $CDCl_3$ in a J-Young NMR tube, a single product appeared (Figure 2-6), and after one day, conversion of the starting material to this new species was complete. We tentatively assigned the new signals to (η^5-IMe_2Sn-C_5H_4)$CpZrCl_2$. The signal from the byproduct, CH_3I, was also observed as a singlet at 2.16 ppm.[161] Therefore, I_2 did cleave a Sn-C bond in (η^5-Me_3Sn-C_5H_4)$CpZrCl_2$. However, it cleaved one of the Sn-Me bonds instead of the Sn-Cp bond (Scheme 2-16). In contrast to the bromination reaction with BBr_3, in which the two chloride ligands on the zirconium center were replaced immediately by

[161] *The Aldrich Library of ^{13}C AND ^1H FT NMR Spectra 1sted.*, C. J. Pouchert and J. Behnke Eds., Aldrich Chemical: Milwaukee 1993, **1**, 81.

two bromide ligands, the two Zr-Cl bonds were inert toward I_2. Perhaps iodide ligands are too big to coordinate well with the zirconium center due to the steric hindrance from the two Cp rings. More likely, the Zr-Cl exchange reaction is not a truly synchronous s-bond metathesis, but proceeds through a four-centered transition state in which there is a considerable amount of $[Cp_2ZrCl]^+$ $[ClBBr_3]^-$ character. Because I_2 is less electrophilic than BCl_3, I_2 does not engage in this kind of "abstraction exchange". A preparative reaction of (η^5-Me_3Sn-C_5H_4)$CpZrCl_2$ with I_2 gave (η^5-IMe_2Sn-C_5H_4)$CpZrCl_2$ in 48% isolated yield, and the product was fully characterized. The compound is air-stable at ambient temperature.

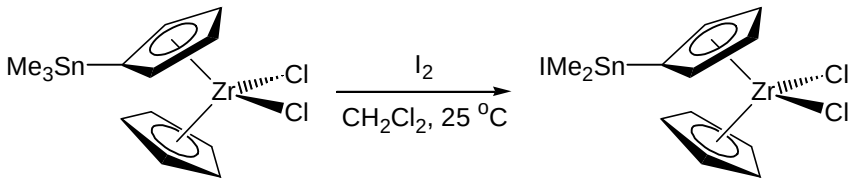

Scheme 2-16 Reaction of (h^5-Me_3Sn-C_5H_4)$CpZrCl_2$ with I_2

The reaction of (η^5-Me_3Sn-C_5H_4)$CpZrCl_2$ with one equivalent of ICl was also followed by ^1H NMR spectroscopy. After 10 min, the spectrum (Figure 2-7) showed that most of the starting material had been converted to (η^5-$ClMe_2Sn$-C_5H_4)$CpZrCl_2$. The byproduct, CH_3I, was also observed at 2.16 ppm. Therefore, unfortunately, ICl also only cleaves one of the Sn-Me bonds instead of the Sn-Cp bond (Scheme 2-17).

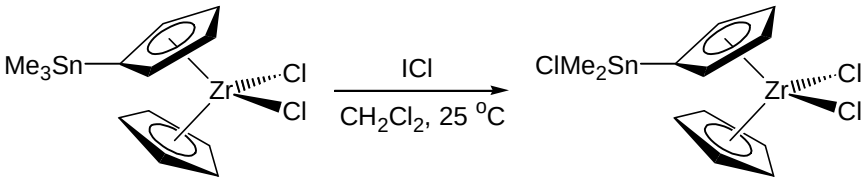

Scheme 2-17 Reaction of (h^5-Me_3Sn-C_5H_4)$CpZrCl_2$ with ICl

Figure 2-7 The 500 MHz ^{1}H NMR Spectra of the Reaction between (h^{5}-Me_3Sn-C_5H_4)$CpZrCl_2$ and ICl

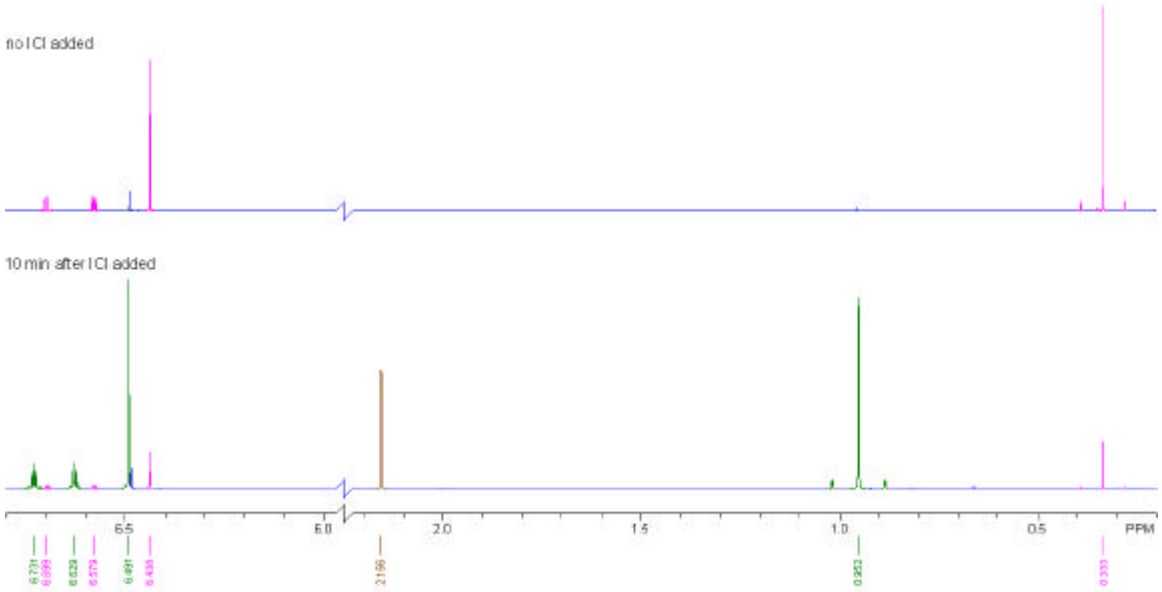

2.3.4 Sn-H and Sn-C Coupling Constants of the Stannyl Complexes

Tin satellites were clearly observed in the proton and ^{13}C NMR spectra of the tin compounds. The ^{2}J coupling constants of the protons in the compounds with ^{117}Sn or ^{119}Sn nuclei were extracted from the proton NMR spectra, as well as the ^{1}J coupling constants of the ^{13}C in the compounds with ^{117}Sn or ^{119}Sn nuclei from the ^{13}C NMR spectra. The data are collected in Table 2-3 together with those from their methyl analogs found in the literature.[162,163,164] Similar to the methyl analogs, change of the substituted halide (Cl, Br, I) on the halostannyl groups of the zirconocene compounds only slightly affects the coupling constants, which decreased with increasing atomic numbers of the substituted halides. As shown by the data of mono-, di-, and tri-bromo-substituted methyl stannanes, the coupling constants increase with increasing number of bromine substituents. The same trend is observed in the

[162] van den Berghe, E. V.; van der Kelen, G. P.: *J. Organomet. Chem.* **6(5)**, 515-521 (1966).
[163] Singh, G.: *J. Organomet. Chem.* **99(2)**, 251-262 (1975).

coupling constants of (η^5-$BrMe_2Sn$-C_5H_4)$CpZrBr_2$ and (η^5-Br_2MeSn-C_5H_4)$CpZrBr_2$. The effect is even greater. The coupling constants of the two compounds in each of the following pairs, (η^5-Me_3Sn-C_5H_4)$CpZrCl_2$ and Me_3SnBr, (η^5-$BrMe_2Sn$-C_5H_4)$CpZrBr_2$ and Me_2SnBr_2, (η^5-Br_2MeSn-C_5H_4)$CpZrBr_2$ and $MeSnBr_3$, are similar. The difference of the first compound from the second compound in each pair is that the zirconocene dihalide moiety in the former is replaced by a bromide substituent in the latter. This observation indicates that the electronic effect of a zirconocene dihalide moiety on the coupling constants is similar to that of a bromide substituent.

Table 2-3 $^2J_{SnH}$ and $^1J_{SnC}$ Coupling Constants for Alkylhalostannanes[(a)]

		^2J (Hz)		^1J (Hz)	
entry	**complex**	**^{119}Sn-^{1}H**	**^{117}Sn-^{1}H**	**^{119}Sn-^{13}C**	**^{117}Sn-^{13}C**
1	(η^5-Me_3Sn-C_5H_4)$CpZrCl_2$	57.5	54.8	374	358
2	(η^5-$ClMe_2Sn$-C_5H_4)$CpZrCl_2$	67.4	64.6	471	451
3	(η^5-$BrMe_2Sn$-C_5H_4)$CpZrBr_2$	66.9	63.7	459	439
4	(η^5-Br_2MeSn-C_5H_4)$CpZrBr_2$	84.8	81.1	584	558
5	(η^5-IMe_2Sn-C_5H_4)$CpZrCl_2$	65.6	62.8	435	415
6	Me_4Sn	54.3[(b)]	52.0[(b)]	338[(c),(d)]	323[(c),(d)]
7	Me_3SnCl	58.5[(b)]	56.0[(b)]	379[(c)]	365[(c)]
8	Me_3SnBr	58.5[(b)]	56.0[(b)]	365[(c)]	349[(c)]
9	Me_2SnBr_2	66.0[(b)]	63.5[(b)]	460[(e)]	420[(e)]
10	$MeSnBr_3$	89.0[(b)]	85.0[(b)]	(f)	(f)

(a) Data for entry 1-5 were determined from spectral satellite positions.
(b) Data obtained in $CDCl_3$ solution.[162]
(c) Data obtained in $CDCl_3$ solution.[163]
(d) Data reported only for ^{119}Sn. Estimated from $J(^{117}Sn\text{-}^{13}C) = J(^{119}Sn\text{-}^{13}C)\delta(^{117}Sn) / \delta(^{119}Sn)$.
(e) Estimated from a single, averaged coupling constant (J = 440 Hz) obtained in CH_2Cl_2.[164]
(f) No reported values found.

[164] Mitchell, T. N.: *J. Organomet. Chem.* **59**, 189-197 (1973).

2.3.5 Reactivities of the Sn-C and Si-C Bonds toward Electrophiles and Their Mechanisms

2.3.5.1 Reactivities of the Sn-CH_3 and Si-CH_3 Bonds toward Electrophiles

As discussed in Section 2.1, since tin is more electron-donating than silicon, and the Sn-C bond is weaker than the Si-C bond, it is expected that cleavage of the Sn-CH_3 bonds in the Me_3Sn-substituted zirconocene compounds should be easier than that of the Si-CH_3 bonds in the Me_3Si-substituted zirconocene compounds. The reactivity differences between the $SnMe_3$ substituent and the $SiMe_3$ substituent toward BX_3 were strikingly demonstrated in the research.

The reactivity of $(\eta^5\text{-}Me_3Si\text{-}C_5H_4)_2ZrCl_2$ toward BCl_3 is very low. Only about 30% of the compound was converted to $(\eta^5\text{-}ClMe_2Si\text{-}C_5H_4)(\eta^5\text{-}Me_3Si\text{-}C_5H_4)ZrCl_2$ when it was reacted with excess BCl_3 in chlorobenzene at about 100 ^oC for 2 days.[130] Therefore, only 15% of the total $SiMe_3$ substituents actually reacted. In comparison, the reaction of $(\eta^5\text{-}Me_3Sn\text{-}C_5H_4)CpZrCl_2$ with BCl_3 was swift at 25 ^oC, and the compound was quantitatively converted to $(\eta^5\text{-}ClMe_2Sn\text{-}C_5H_4)CpZrCl_2$ in a few minutes. In the reaction of $(\eta^5\text{-}Me_3Si\text{-}C_5H_4)_2ZrCl_2$ with excess BBr_3, one of the methyl groups on each $SiMe_3$ substituent was quantitatively replaced by a bromide substituent.[130] However, the reaction was slow. It took about 6 days for the reaction to complete at 25 ^oC. In addition, BBr_3 could not further cleave a second Si-CH_3 bond in each of the silyl substituents. On the contrary, a Me_3Sn substituent in $(\eta^5\text{-}Me_3Sn\text{-}C_5H_4)CpZrCl_2$ was quantitatively converted to a $BrMe_2Sn$ substituent by BBr_3 at 25 ^oC in a few minutes, which is further quantitatively converted to a Br_2MeSn substituent under the same conditions after 15 h.

2.3.5.2 Reactivities of the M-Cp and M-CH_3 Bonds toward Electrophiles

Three types of cleavage were found in the reactions of Me_3M-substituted (M = Si, Sn) metallocene compounds with electrophiles, i.e. cleavage of an M-Me bond, cleavage of an M-Cp bond, and cleavage of a Cp-H bond (Scheme 2-18). As demonstrated in the reactions of (η^5-

Me_3Sn-C_5H_4)$CpZrCl_2$ with many electrophiles (BCl_3, BBr_3, I_2, ICl) and the reactions of (η^5-Me_3Si-C_5H_4)$_2ZrCl_2$ with BCl_3 and BBr_3, M-CH_3 bonds were cleaved as a consequence of the electron-deficiency of the zirconocene dichloride moiety. Cleavage of M-Cp bonds by electrophiles is common in Me_3M-substituted aromatic hydrocarbons.[150,158,159,160,165] Since the ferrocene moiety in (η^5-Me_3Si-C_5H_4)$_2Fe$ is relatively electron-rich, the cleavage by BCl_3 happens on the Si-Cp bonds, resulting in the chloroboryl-substituted ferrocene (Scheme 2-1).[130] Though most electrophilic reactions of the Me_3M-substituted group 4 metallocene compounds occur on one of the M-CH_3 bonds in the Me_3M substituents, HCl cleaved the Sn-Cp bond instead of the Sn-Me bond in the Me_3Sn-substituted zirconocene compound (Scheme 2-9). The cleavage of a Cp-H bond is rare. Manners and coworkers reported that BCl_3 selectively cleaved an ortho-hydrogen to the Me_3Sn substituents in the Me_3Sn-substituted ferrocene, and the ferrocene was ortho-borylated (Scheme 2-19).[166]

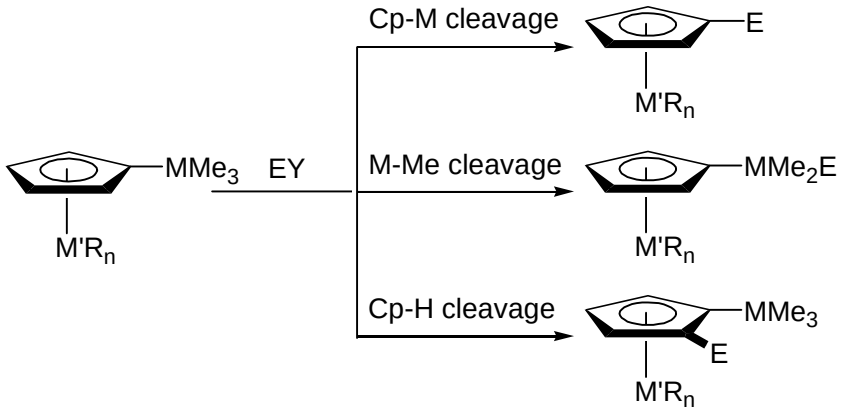

M = Si, Sn; M' is a transition metal.

Scheme 2-18 Cleavage Modes in the Reactions of Me_3Si- or Me_3Sn-substituted Metallocene Compounds with Electrophiles

[165] a) Gross, U.; Kaufmann, D.: *Chem. Ber.* **120(6)**, 991-994 (1987). b) Kaufmann, D.: *Chem. Ber.* **120(6)**, 901-905 (1987). c) Kaufmann, D.: *Chem. Ber.* **120(5)**, 853-854 (1987).
[166] Jäkle, F.; Lough, A. J.; Manners, I.: *J. Chem. Soc. Chem. Commun.* **(5)**, 453-454 (1999).

Scheme 2-19 Reaction of Me_3Sn-substituted Ferrocene with BCl_3 [166]

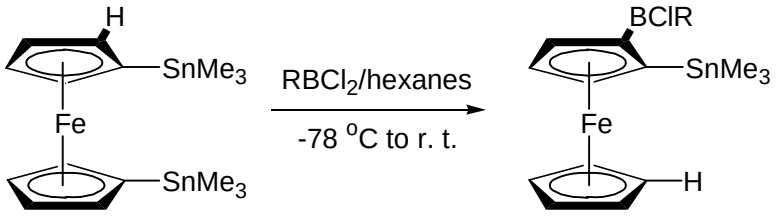

Scheme 2-20 The Intermediate of the Electrophilic Substitution Reaction between a Me_3Si- or Me_3Sn-substituted Metallocene Compound and a Cationic Electrophile

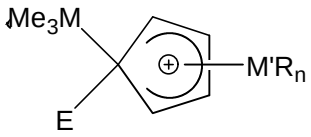

M = Si, Sn
M' is a transition metal.

2.3.5.3 Mechanisms of the Electrophilic Cleavage of the M-Cp and M-CH_3 Bonds

The cleavage of M-Cp bonds in Me_3M-substituted metallocene compounds by Lewis acids is generally believed to be an electrophilic aromatic substitution reaction. Since the ipso carbon atom on the Me_3M-substituted Cp ring is electron-enriched by the Me_3M substituent, electrophilic attack generally occurs on the ipso carbon atom. When an electrophile (E^+) attacks the ipso carbon atom, a Meisenheimer-type intermediate forms (Scheme 2-20),[149] The intermediate is stabilized by the delocalization of the positive charge in the ring. Then, under the assistance of an anionic species, the Me_3M group leaves the Cp ring, and the intermediate becomes the product. The reaction of HCl with (η^5-Me_3Sn-C_5H_4)$CpZrCl_2$ and the reaction of (η^5-Me_3Si-C_5H_4)$_2Fe$ with BCl_3 are believed to follow this mechanism. In the case of BCl_3, which is a neutral electrophile, a zwitterionic intermediate forms, in which the positive charge

(Meisenheimer intermediate) is counterbalanced by a negative charge on boron (Scheme 2-21). The alternative (s-bond metathesis proceeding through a four-centered transition state) is unattractive because of the strong homolytic bond dissociation energies of aryl substituents.

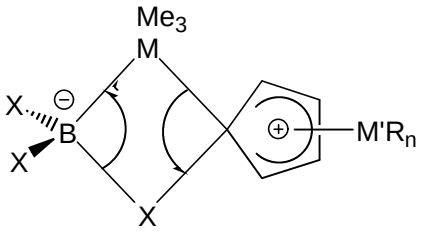

Scheme 2-21 The Intermediate of the Electrophilic Substitution Reaction between a Me_3Si- or Me_3Sn-substituted Metallocene Compound and a Neutral Electrophile

Due to the d^0 electron configuration of the group 4 metals in metallocene dihalides, electrophilic attack on the Me_3M-substituted Cp rings is not favorable. Instead, the electrophiles will attack the methyl groups since they are more electron-rich. The mechanisms of the cleavages are usually S_E2. Three kinds of transition states were proposed (Scheme 2-22).[149,167] The first two transition states result in retention of the configuration of the leaving alkyl group after substitution, and the third transition state causes inversion of the configuration. The second transition state, i.e. four-centered metathesis transition state, is probably the best to explain the mechanism of the electrophilic cleavage of the Sn-CH_3 bonds in (η^5-Me_3Sn-C_5H_4)$CpZrCl_2$ by BX_3. Either of the three transition states could explain the mechanism of the cleavage caused by I_2 or ICl. The mechanisms of the reactions of electrophiles with (η^5-Me_3Sn-C_5H_4)$CpZrCl_2$ would require further study to elucidate in any detail. The reason why HCl cleaves the Sn-Cp bond while the other electrophiles (BCl_3, BBr_3, I_2, ICl) cleave the Sn-CH_3 bonds is unclear.

[167] Matteson, D. S.: *Organometallic Reaction Mechanisms of the Nontransition Elements,* Academic: New York 1974.

Scheme 2-22 S_E2 Mechanisms of the Electrophilic Substitution Reaction Involving Silyl or Stannyl Group [149,167]

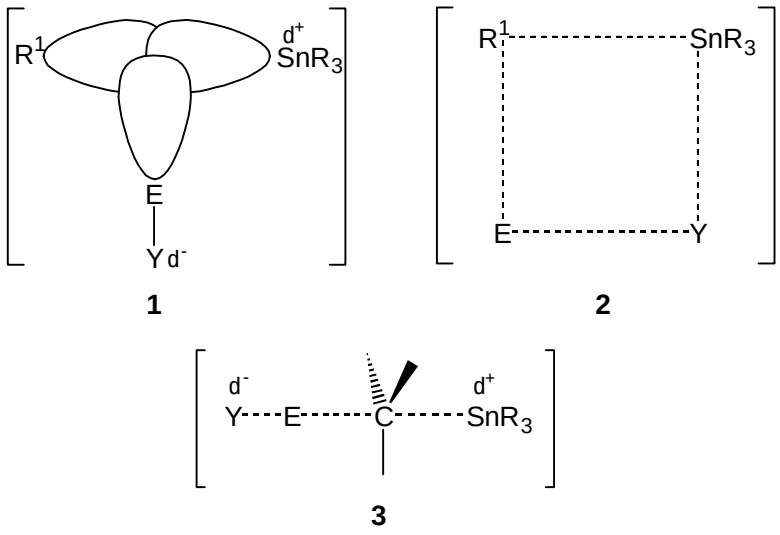

2.4 Comparison of the Reactivity of the Sn-X Bond and the Si-X Bond toward Nucleophiles

It is well documented that halosilyl substituents on the Cp rings of zirconocene compounds are easily hydrolyzed by water to form disiloxane-bridged zirconocene compounds.[128,130,168] However, all the halostannyl substituents investigated in the research are inert to hydrolysis in solid state, as shown by their stability in air. It is well-known that organotin halides undergo a wide range of nucleophilic substitution reactions,[169] including hydrolysis.[170] According to the literature, the hydrolysis with water is an equilibrium process (Scheme 2-23). With the assistance of a base, the hydrolysis becomes complete. A plausible reason for the stability of the halostannyl substituents in solid state is that the equilibrium is in favor of the halostannyl side, so the concentration of the hydrolyzed species is insignificant in the equilibrium. If the zirconocene compounds containing halostannyl substituents are dissolved

[168] Lofthus, O. W.; Slebodnick, C.; Deck, P. A.: *Organometallics* **18(18)**, 3702-3708 (1999).
[169] Molloy, K. C.: *Chemistry of Tin*, P. G. Harrison Ed., Blackie: New York 1989, 187-220.

in solutions, the hydrolysis of the halostannyl substituents will probably occur in the presence of base. Actually, the electrophilicity of the halostannyl substituents has been demonstrated in the crystal structure of the THF adduct of (η^5-Br_2MeSn-C_5H_4)$CpZrBr_2$ shown in Section 2.3.2. The different behaviors of the halosilyl substituents and the halostannyl substituents in zirconocene compounds toward hydrolysis by moisture in air indicate that the halostannyl substituents are much less susceptible to nucleophilic substitution than halosilyl substituents.

$$R_3SnX + H_2O \rightleftharpoons R_3SnOH + HX$$

Scheme 2-23 Hydrolysis Equilibrium of Organotin Halides[170]

2.5 Some Preliminary Results in the Synthesis of (h^5-Me_3Sn-$C_5H_4)_2ZrCl_2$

Similar to the synthesis of the mono-trimethylstannyl zirconocene compound, the synthesis of bis(trimethylstannyl cyclopentadienyl) zirconium dichloride, (η^5-Me_3Sn-$C_5H_4)_2ZrCl_2$, was investigated in the reaction between one equivalent of $ZrCl_4$ or $ZrCl_4$•2THF and two equivalents of $(Me_3Sn)_2C_5H_4$ in CH_2Cl_2, CH_2ClCH_2Cl, THF, or toluene. The proton NMR spectra of the crude products were complicated. Some distinguishable components include Me_3SnCl, (η^5-Me_3Sn-C_5H_4)$CpZrCl_2$, Compound A,[171] and Compound B.[172] Their concentrations in the crude products varied with reaction conditions.

It is very likely that Compound B was (η^5-Me_3Sn-$C_5H_4)_2ZrCl_2$. The corresponding proton chemical shifts of Compound B were very close to those of (η^5-Me_3Sn-C_5H_4)$CpZrCl_2$ but slightly shifted up-field, which was expected since there were two electron-donating Me_3Sn substituents in the former instead of one in the latter, if Compound B was (η^5-Me_3Sn-

---

[170] Neumann, W. P.: *The Organic Chemistry of Tin*, Interscience: New York 1970, 155-160.
[171] ^{1}H NMR ($CDCl_3$): d 6.97 (m), 6.11 (m), 0.85 (s). The measured ratios are approximately 4 : 4 : 6.
[172] ^{1}H NMR ($CDCl_3$): d 6.64 (m), 6.52 (m), 0.32 (s). The measured ratios are approximately 4 : 4 : 17.

$C_5H_4)_2ZrCl_2$. The measured ratios of the signals (4 : 4 : 17) were also consistent with the calculated values (4 : 4 : 18) for (η^5-Me_3Sn-$C_5H_4)_2ZrCl_2$. Since the halostannyl substituents were not considered as good candidates to form tethers in the immobilization process, no further attempts were made to separate and characterize the compounds.

2.6 Experiment Details

General Procedures. Standard inert-atmosphere techniques were used for all procedures. Reaction glassware sealed with either Krytox fluorinated lubricant or Kalrez O-rings and flamed out under vacuum was used for reactions involving boron trihalides. $(CpH)_2$, $(Me_3Sn)NMe_2$, BCl_3 (1.0 M solutions in hexanes or dichloromethane), BBr_3 (neat), and ICl were used as received from Aldrich. I_2 was used as received from Fisher. $CpZrCl_3$ was used as received from Strem Chemical Co. $CpZrCl_3$•DME was prepared according to the procedure of Lund and Livinghouse.[173] Solvents were purified according to the method described by Grubbs and coworkers.[174] A JEOL Eclipse-500 instrument (500 MHz for ^1H, 125 MHz for ^{13}C) was used for all solution NMR measurements. NMR-scale experiments were carried out in J-Young resealable tubes. Elemental analyses were performed by Desert Analytics (Tucson, AZ). Crystal structures were obtained by either a Siemens P4 diffractometer or a Enraf-Nonius Kappa CCD diffractometer.

Preparation of $(Me_3Sn)_2C_5H_4$.[146,147] One equivalent of freshly distilled CpH[175] and two equivalents of $(Me_3Sn)NMe_2$ were mixed, without additional solvent, at 25 ^oC. The mixture was then heated at about 40 ^oC for about 2 h and then fractionally distilled. The first fraction (b.p.

[173] Lund, E. C.; Livinghouse, T.: *Organometallics* **9(9)**, 2426-2427 (1990).
[174] Pangborn, A. B.; Giardello, M. A.; Grubbs, R. H.; Rosen, R. K.; Timmers, F. J.: *Organometallics* **15(5)**, 1518-1520 (1996).

about 60 °C at 5 mmHg) was a pale-yellow liquid that was mostly $(Me_3Sn)C_5H_5$ (lit.[147] b.p. 38 °C at 3 mmHg) as identified by NMR spectroscopy: ^{1}H NMR ($CDCl_3$) δ 6.06 (5 H), 0.06 (9 H).[176] The second fraction (b.p. 98-99 °C at 5 mmHg, lit.[147] b.p. 80 °C at 3 mmHg) was pure $(Me_3Sn)_2C_5H_4$. ^{1}H NMR ($CDCl_3$): δ 6.72 (m, 2 H), 6.47 (m, 2 H), 0.04 (s, 18 H). ^{13}C NMR ($CDCl_3$): δ 135.1 (CH), 126.2 (CH), 53.2 (C), -8.6 (CH_3). NMR spectra were consistent with literature data.[177] The freshly prepared $(Me_3Sn)_2C_5H_4$ was a light-yellow liquid, but it turned yellow-brown gradually. However, the proton NMR spectrum of the yellow-brown liquid was identical to that of the fresh product.

Synthesis of (h^5-Me$_3$Sn-C$_5$H$_4$)CpZrCl$_2$. A suspension of $CpZrCl_3$•DME (1.76 g, 5.00 mmol) and $(Me_3Sn)_2C_5H_4$ (1.96 g, 5.00 mmol) in 30 mL of toluene was stirred under reflux for 15 h. The resulting yellow solution was evaporated, and the yellow residue was recrystallized from hexane/tetrahydrofuran (THF) to obtain 1.13 g (2.50 mmol, 50%) of light golden plates in two crops. An otherwise identical procedure using $CpZrCl_3$ (1.31 g, 5.00 mmol) as the starting material afforded 1.77 g (3.90 mmol, 78%). ^{1}H NMR ($CDCl_3$): δ 6.70 (m, 2 H, C_5H_4), 6.58 (m, 2 H, C_5H_4), 6.44 (s, 5 H, C_5H_5), 0.33 (s, 9 H, $SnMe_3$). ^{13}C NMR ($CDCl_3$): δ 127.1 (CH), 116.9 (CH), 116.1 (C), 115.8 (CH), -7.6 (CH_3). Anal. Calcd for $C_{13}H_{18}Cl_2SnZr$: C, 34.31; H, 3.99. Found: C, 34.52; H, 3.93.

NMR-Scale Reaction of (h^5-Me$_3$Sn-C$_5$H$_4$)CpZrCl$_2$ with BCl$_3$. A small amount of BCl_3 was vacuum-transferred from a 1.0 M hexanes solution to a 10-mg sample of in about 0.7

---

[175] Cyclopentadiene molecules dimerize slowly at room temperature by the Diels-Alder reaction. Commercial cyclopentadiene exists in the dimer form. Cyclopentadiene monomer can be obtained by fractional distillation of the dimer at 186 °C.

[176] a) 5.9 ppm (s, C_5H_5) in $C_2F_2Cl_2$. Kisin, A. V.; Korenevsky, V. A.; Sergeyev, N. M.; Ustynyuk, Yu. A.: *J. Organomet. Chem.* **34(1)**, 93-104 (1972). b) τ = 4.06 (s, C_5H_5), τ = 9.94 (s, $SnMe_3$) in CS_2. Davison, A.; Rakita, P. E.: *Inorg. Chem.* **9(2)**, 289-294 (1970).

[177] ^{13}C NMR (neat): d 134.7 (C1/4), 127.2 (C2/3), 52.6 (C5), -8.2 (CH_3). Grishin, Yu., K.; Luzikov, Yu., N.; Ustynyuk, Yu., A.: *Dokl. Akad. Nauk. SSSR* **216(2)**, 321-324 (1974).

mL of $CDCl_3$ in a J-Young NMR tube. The NMR tube was then refilled with argon, sealed, and shaken vigorously to mix its contents. The ^1H NMR spectrum obtained after 20 min showed a new set of signals assigned to (η^5-$ClMe_2Sn$-C_5H_4)$CpZrCl_2$ at 7.01 (m, 2 H, C_5H_4), 6.64 (m, 2 H, C_5H_4), 6.61 (s, 5 H, C_5H_5), and 1.70 ppm (s, 6 H, $SnMe_2$). A signal arising from the byproduct $MeBCl_2$ was expected at 1.21 ppm, but instead we observed a broad signal at 1.02 ppm, which we assigned to Me_2BCl. Because the initial reaction was limiting in BCl_3, we surmise that the byproduct $MeBCl_2$ reacted further with (η^5-Me_3Sn-C_5H_4)$CpZrCl_2$ to afford Me_2BCl. Then, excess BCl_3 was condensed into the tube. After 10 min, all of the remaining (η^5-Me_3Sn-C_5H_4)$CpZrCl_2$ had reacted to produce (η^5-$ClMe_2Sn$-C_5H_4)$CpZrCl_2$, and $MeBCl_2$ was observed as a broad signal at 1.21 ppm (br s, 3 H, CH_3). No significant change was subsequently observed in the ^1H NMR spectrum after 1 week at 25 °C.

Synthesis of (h^5-$ClMe_2Sn$-C_5H_4)$CpZrCl_2$. A solution of (η^5-Me_3Sn-C_5H_4)$CpZrCl_2$ (0.50 g, 1.1 mmol) and BCl_3 (10 mL, 1.0 M in CH_2Cl_2) in 15 mL of CH_2Cl_2 (including 10 mL of solvent from the BCl_3 solution) was stirred at 25 °C for 10 min. The volatile components were then evaporated. Recrystallization of the residue from hexane/toluene afforded 0.43 g (0.90 mmol, 82%) of silver-gray plates in two crops. ^1H NMR ($CDCl_3$): δ 6.73 (m, 2 H, C_5H_4), 6.63 (m, 2 H, C_5H_4), 6.49 (s, 5 H, C_5H_5), 0.95 (s, 6 H, $SnMe_2$). ^{13}C NMR ($CDCl_3$): δ 130.6 (C), 124.9 (CH), 116.4 (CH), 115.8 (CH), 0.5 (CH_3). Anal. Calcd for $C_{12}H_{15}Cl_3SnZr$: C, 30.31; H, 3.18. Found: C, 30.65; H, 3.04. The NMR data of the compound in C_6D_6 were also obtained.[178] The single crystal used for X-ray diffraction was obtained by dissolving about 25 mg of the compound in about 1.0 mL of 1 : 2 toluene/hexanes, filtering through glass wool, and storing the

[178] ^1H NMR (C_6D_6): d 6.26 (m, 2 H, C_5H_4), 5.80 (s, 5 H, C_5H_5), 5.67 (m, 2 H, C_5H_4), 0.84 (s, 6 H, $SnMe_2$). ^{13}C NMR (C_6D_6): d 165.7 (C), 124.7 (CH), 115.8 (CH), 115.4 (CH), -0.2 (CH_3).

vial (loosely capped) in a refrigerator (5 ^{o}C) for several days. The crystal was found to contain one molecule of toluene every two molecules of metallocene.

Syntheses of (h^5-$BrMe_2Sn$-C_5H_4)$CpZrBr_2$. A solution of (η^5-Me_3Sn-C_5H_4)$CpZrCl_2$ (0.50 g, 1.1 mmol) and BBr_3 (2.0 mL, 21 mmol) in 10 mL of CH_2Cl_2 was stirred at 25 °C for 10 min, and then the volatile components were evaporated. Recrystallization of the residue from hexane/toluene afforded 0.57 g (0.94 mmol, 85%) of light green-yellow plates in two crops. An otherwise identical procedure using (η^5-$ClMe_2Sn$-C_5H_4)$CpZrCl_2$ (0.30 g, 0.63 mmol) as the starting material afforded 0.31 g (0.51 mmol, 82%) of (η^5-$BrMe_2Sn$-C_5H_4)$CpZrBr_2$. ^{1}H NMR ($CDCl_3$): δ 6.85 (m, 2 H, C_5H_4), 6.60 (m, 2 H, C_5H_4), 6.55 (s, 5 H, C_5H_5), 1.10 (s, 6 H, $SnMe_2$). ^{13}C NMR ($CDCl_3$): δ 129.0 (C), 125.5 (CH), 116.2 (CH), 115.3 (CH), 1.5 (CH_3). Anal. Calcd for $C_{12}H_{15}Br_3SnZr$: C, 23.67; H, 2.48. Found: C, 23.47; H, 2.40.

Synthesis of (h^5-Br_2MeSn-C_5H_4)$CpZrBr_2$. A solution of (η^5-Me_3Sn-C_5H_4)$CpZrCl_2$ (0.30 g, 0.66 mmol) and BBr_3 (2.0 mL) in CH_2Cl_2 (10 mL) was stirred at 25 °C for 15 h. The volatile components were then evaporated. Recrystallization of the brown residue from hexane/toluene afforded 0.29 g (0.43 mmol, 66%) of green-yellow plates. An otherwise identical procedure using (η^5-$ClMe_2Sn$-C_5H_4)$CpZrCl_2$ (0.23 g, 0.47 mmol) as the starting material afforded 0.22 g (0.32 mmol, 68%). ^{1}H NMR ($CDCl_3$): d 7.01 (m, 2 H, C_5H_4), 6.64 (m, 2 H, C_5H_4), 6.61 (s, 5 H, C_5H_5), 1.70 (s, 3 H, $SnCH_3$). ^{13}C NMR ($CDCl_3$): d 126.6 (CH), 125.7 (C), 116.5 (CH), 114.3 (CH), 12.0 (CH_3). Anal. Calcd for $C_{11}H_{12}Br_4SnZr$: C, 19.61; H, 1.80. Found: C, 19.80; H, 1.64. The single crystals of (η^5-Br_2MeSn-C_5H_4)$CpZrBr_2$ used for X-ray diffraction were grown from a 1 : 1 mixture of hexanes/THF as follows. A saturated solution of (η^5-Br_2MeSn-C_5H_4)$CpZrBr_2$ in 1 : 1 hexanes/THF was placed in a vial in a refrigerator operating

at 5 ^{o}C. The solution was allowed to evaporate slowly from the loosely capped vial. After several days, green-yellow crystals about 1-2 mm in dimensions appeared in the vial. X-ray diffraction showed that the compound obtained was a mono-THF adduct.

NMR-Scale Reaction of (h^5-Me_3Sn-C_5H_4)$CpZrCl_2$ with I_2. Under a nitrogen counterstream, a small crystal of iodine was added to a 10-mg sample of (η^5-Me_3Sn-C_5H_4)$CpZrCl_2$ dissolved in about 0.7 mL of $CDCl_3$ in a J-Young NMR tube. The NMR tube was sealed and shaken vigorously to mix its contents. The ^{1}H NMR spectrum obtained after 10 min showed partial conversion of the starting material to a single product assigned to (η^5-IMe_2Sn-C_5H_4)$CpZrCl_2$ with signals at 6.72 (m, 2 H, C_5H_4), 6.61 (m, 2 H, C_5H_4), 6.49 (s, 5 H, C_5H_5), and 1.17 ppm (s, 6 H, $SnMe_2$), along with a byproduct that we assigned to CH_3I based on a sharp signal at 2.16 ppm (s, 3 H, CH_3). The spectrum obtained after 1 day showed complete conversion with a concomitant increase in the CH_3I signal.

NMR-Scale Reaction of (h^5-Me_3Sn-C_5H_4)$CpZrCl_2$ with ICl. In a nitrogen glove box, 0.08 mL 1.0 M ICl solution in $CDCl_3$ was added to a 36-mg sample of (η^5-Me_3Sn-C_5H_4)$CpZrCl_2$ dissolved in about 0.7 mL of $CDCl_3$ in a J-Young NMR tube. The tube was sealed and shaken vigorously to mix its contents. The ^{1}H NMR spectrum obtained after 10 min showed that approximately 80% of the starting material had been converted to (η^5-$ClMe_2Sn$-C_5H_4)$CpZrCl_2$. A strong signal arising from the byproduct CH_3I was also observed. Neither (η^5-IMe_2Sn-C_5H_4)$CpZrCl_2$ nor CH_3Cl was detected.

Synthesis of (h^5-IMe_2Sn-C_5H_4)$CpZrCl_2$. A solution of (η^5-Me_3Sn-C_5H_4)$CpZrCl_2$ (0.30 g, 0.66 mmol) and I_2 (0.84 g, 3.3 mmol) in 10 mL of CH_2Cl_2 was stirred at 25 °C for 15 h. The volatile components were evaporated, including most of the excess iodine. Recrystallization of the residue from hexanes/toluene afforded dark red needles. Washing with hexanes and drying

under vacuum afforded 0.18 g (0.32 mmol, 48%) of a pale yellow crystalline solid. ^{1}H NMR ($CDCl_3$): δ 6.72 (m, 2 H, C_5H_4), 6.61 (m, 2 H, C_5H_4), 6.49 (s, 5 H, C_5H_5), 1.17 (s, 6 H, $SnMe_2$). ^{13}C NMR ($CDCl_3$): δ 127.9 (C), 125.4 (CH), 116.3 (CH), 115.5 (CH), 0.8 (CH_3). Anal. Calcd for $C_{12}H_{15}Cl_2ISnZr$: C, 25.42; H, 2.67. Found: C, 25.71; H, 2.65.

2.7 Conclusions

The mono-trimethylstannyl-substituted cyclopentadienyl zirconium dichloride, (η^5-Me_3Sn-C_5H_4)$CpZrCl_2$, can be synthesized by a metal exchange reaction between $CpZrCl_3$ and $(Me_3Sn)_2C_5H_4$. NMR analysis shows that the bis-trimethylstannyl-substituted analog, (η^5-Me_3Sn-$C_5H_4)_2ZrCl_2$, can also be synthesized by the same method, but the synthesis requires further optimization. The Sn-C bonds are more reactive than the Si-C bonds in the cleavage reactions with electrophiles (BCl_3, BBr_3, I_2, ICl, HCl, etc.). However, the Sn-X bonds are much less reactive than the Si-X bonds in nucleophilic substitution reaction. If the halostannyl-substituted zirconocene compounds are used in the immobilization process, nucleophilic substitution reactions between the halostannyl substituents and the surface hydroxyl groups should occur to form tethers. The lower reactivity of the halostannyl substituents in nucleophilic substitution reaction indicates that the immobilization reaction may not be easy. Therefore, the halostannyl substituents are not suitable precursors to form single or double tethers.

Chapter 3 Synthesis and Reactivity of Bis(dibromomethylsilyl) Zirconocene Dibromide [(η^5-Br_2MeSi-C_5H_4)$_2$$ZrBr_2$][179]

3.1 Introduction: Reactivities of Different Si-C bonds toward Electrophilic Cleavage

As discussed in Section 2.1, the Me_3Si substituents in Me_3Si-substituted zirconocene dihalides are converted only to the corresponding monofunctional XMe_2Si substituents in electrophilic substitution reactions with BX_3 (X = Cl, Br). However, bifunctional substituents are desired, since they are expected to form double-tethers in the immobilization of zirconocene dihalides on silica. The double-tethers are expected to be more robust than the single-tethers formed from the monofunctional substituents.

In our efforts to extend the chemistry of the Me_3Si-substituted zirconocene compounds, we explored two new approaches to the synthesis of zirconocene dihalides with bifunctional substituents. In both approaches, we aimed to weaken the Si-C bonds so that more than one might be cleaved in the reactions by BX_3. In the first approach (Chapter 2), the silicon in the Me_3Si substituents was replaced by tin. Sn-C bonds are weaker than the Si-C bonds, and indeed we found that Me_3Sn substituents can be converted to the corresponding bifunctional Br_2MeSn substituents upon treatment with BBr_3. The idea of the second approach is to weaken the Si-C bonds from the carbon side, i.e., to replace the methyl groups in the Me_3Si substituents with other (hopefully more reactive) groups, so that two of the groups in each silyl substituent can be cleaved by BX_3 to form bifunctional X_2MeSi substituents.

First we compared the reactivities of the methyl group and other alkyl groups (e.g. ethyl group and t-butyl group) on silyl substituents in zirconocene dihalides toward electrophilic cleavage by BX_3. $EtMe_2Si$- and $^tBuMe_2Si$-substituted zirconocene dichlorides were synthesized,

[179] Deck, P. A.; Cheng, X.; Stoebenau, E. J.; Slebodnick, C.; Billodeaux, D. R.; Fronczek, F. R.: *Organometallics* **19(25)**, 5404-5409 (2000).

and their reactions with BBr_3 were investigated. This work was started by E. J. Stoebenau, an undergraduate in our group. I followed up on his preliminary results and brought the work into a publishable form.[179] The results of these "departing group" studies were not remarkable. We found that both ethyl group and the t-butyl were less reactive than methyl as departing groups in electrophilic substitution reactions with BX_3, but not sufficiently less reactive to realize useful selectivity. For example, the reaction of $(\eta^5\text{-}EtMe_2Si\text{-}C_5H_4)CpZrCl_2$ with BBr_3 results in about 80% Si-Me bond cleavage and 20% Si-Et bond cleavage. An analogous reaction of $(\eta^5\text{-}{}^tBuMe_2Si\text{-}C_5H_4)CpZrCl_2$, with BBr_3 resulted in about 94% Si-Me bond cleavage and only 6% Si-^{t}Bu bond cleavage. Taking the statistical ratios of the different departing groups into account, the reactivity ratios of Me : Et : ^{t}Bu is about 1.0 : 0.5 : 0.13. The lower reactivities of the Si-Et and Si-^{t}Bu bonds toward BBr_3 were attributed to a steric effect from the ethyl and t-butyl groups. The transition state of the electrophilic substitution reaction is believed to be a four-centered structure (Scheme 3-1). BBr_3 can most easily access the methyl carbon. The Si-C bond is less accessible with either the ethyl or t-butyl group, so the steric hindrance to the approach of BBr_3 increases as the bulk around the a-carbon of the departing group is increased.

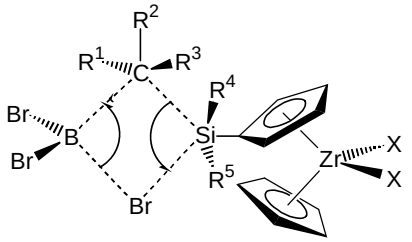

R^1, R^2, R^3 = H or Me
R^4, R^5 = Me, Et, ^{t}Bu

Scheme 3-1 The Transition State Proposed for the Reaction between an Alkylsilyl Substituent on Zirconocene Compound and BBr_3

Because these "higher" alkyl groups were less reactive than methyl groups, we abandoned this approach to the formation of doubly halogenated silyl substituents on group 4

metallocenes. However, Si-phenyl bonds are known to be more reactive than Si-Me bonds in metathesis reactions with BX_3.[165] The reaction of $C_6H_5SiMe_3$ with BCl_3 is rapid, even under mild conditions (Scheme 3-2). The products are exclusively chloromethylsilane (Me_3SiCl) and phenylboron dichloride ($C_6H_5BCl_2$). The selective electrophilic cleavage of the Si-Ph bond is rationalized by invoking a mechanism involving a resonance-stabilized Meisenheimer-type intermediate (Scheme 3-3).[179]

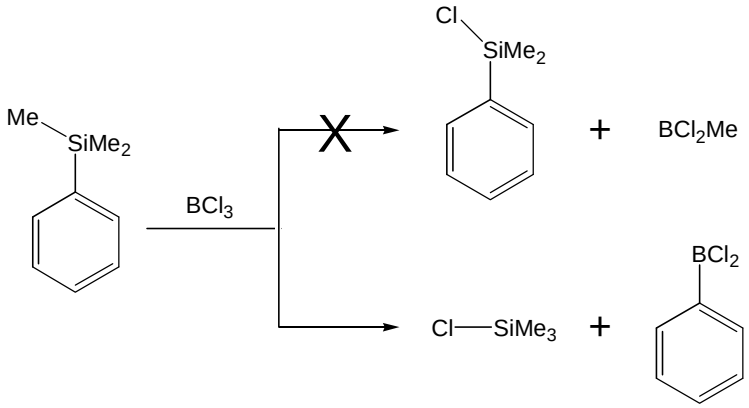

Scheme 3-2 Reaction between Trimethylsilylbenzene and BCl_3 [165c]

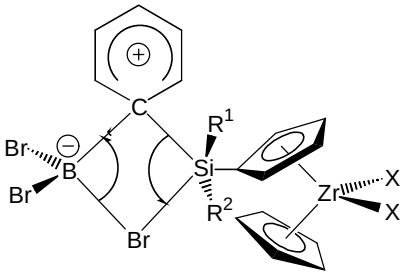

R^1, R^2 = Me or Ph

Scheme 3-3 The Intermediate Proposed for the Reaction between a Phenylsilyl Substituent on a Zirconocene Compound and BBr_3

In order to find out if a Si-Ph bond is also more reactive toward electrophilic cleavage than a Si-Me bond in the silyl-substituted zirconocene compounds, we prepared (η^5-$PhMe_2Si$-$C_5H_4)_2ZrCl_2$[179] and subjected it to BCl_3 in CH_2Cl_2 under reflux for 15 h. Analysis of the

products showed that the reaction was selective: the $PhMe_2Si$ substituents were quantitatively converted exclusively to $ClMe_2Si$ substituents. In comparison, only 30% of (η^5-Me_3Si-$C_5H_4)_2ZrCl_2$ was converted to (η^5-$ClMe_2Si$-C_5H_4)(η^5-Me_3Si-C_5H_4)$ZrCl_2$ in the reaction with BCl_3 in C_6H_5Cl under reflux for two days.[130] Therefore, the Si-Ph bond is much more reactive toward electrophilic cleavage than the Si-Me bond in silyl-substituted zirconocene compounds.

Encouraged by the results from (η^5-$PhMe_2Si$-$C_5H_4)_2ZrCl_2$, we decided to prepare (η^5-Ph_2MeSi-$C_5H_4)_2ZrCl_2$. Hopefully, the reactivity of the Si-Ph bonds toward electrophilic cleavage would be high enough that both phenyl groups on each Ph_2MeSi substituent could be cleaved by BX_3. If the Ph_2MeSi substituents could be converted to X_2MeSi substituents, the resulting compound, (η^5-X_2MeSi-$C_5H_4)_2ZrX_2$, would be functionalized with two potential double-tether-forming substituents.

3.2 Synthesis and Characterization of (η^5-Ph_2MeSi-$C_5H_4)_2ZrCl_2$

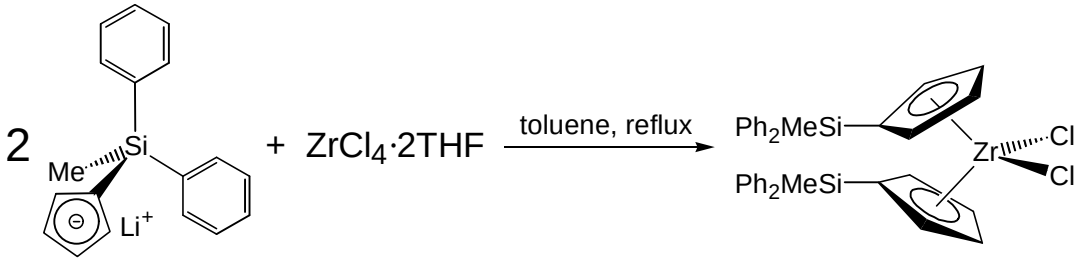

Scheme 3-4 Synthesis of (η^5-Ph_2MeSi-$C_5H_4)_2ZrCl_2$

The synthesis of (η^5-Ph_2MeSi-$C_5H_4)_2ZrCl_2$ follows the conventional metathesis reaction, i.e., reacting two equivalents of Ph_2MeSi-C_5H_4Li with one equivalent of zirconium tetrachloride. In the reaction, the two salts exchange their cations and anions. One product formed after the exchange is LiCl, which is insoluble in the organic solvent. The other product should be the desired zirconocene compound (Scheme 3-4). The experimental details are described in Section 3.5. The desired compound, (η^5-Ph_2MeSi-$C_5H_4)_2ZrCl_2$, was obtained in 60% isolated yield. The

corresponding zirconocene dibromide was also prepared (from $ZrBr_4$) in order to identify that compound as a component in the mixtures analyzed in the experiments in Section 3.3.2. The procedure was nearly the same, except that a slightly lower yield (46%) was obtained. However, this is not an optimized yield. Both compounds were stable in air at ambient temperature as shown by collecting a proton NMR spectra of an intentionally exposed samples.

Table 3-1 Metric Parameters for Crystalline (h^5-Ph_2MeSi-$C_5H_4)_2ZrCl_2$

	Bond Distances (Å)		
Cp(1)-Zr[(a)]	2.210(2)	Si(1)-C(21)	1.881(3)
Cp(2)-Zr[(b)]	2.224(2)	Si(1)-C(31)	1.872(2)
Zr-Cl(1)	2.4253(9)	Si(2)-C(6)	1.876(2)
Zr-Cl(2)	2.4337(8)	Si(2)-C(12)	1.858(4)
Si(1)-C(1)	1.880(2)	Si(2)-C(41)	1.873(3)
Si(1)-C(11)	1.849(4)	Si(2)-C(51)	1.869(2)
	Bond Angles (deg)		
Cp(1)[(a)]-Zr-Cp(2)[(b)]	130.2(2)	C(21)-Si(1)-C(31)	109.1(1)
Cl(1)-Zr-Cl(2)	95.90(3)	C(6)-Si(2)-C(12)	113.5(2)
C(1)-Si(1)-C(11)	111.3(1)	C(6)-Si(2)-C(41)	104.1(1)
C(1)-Si(1)-C(21)	104.5(1)	C(6)-Si(2)-C(51)	107.4(1)
C(1)-Si(1)-C(31)	110.0(2)	C(12)-Si(2)-C(41)	109.5(2)
C(11)-Si(1)-C(21)	110.8(2)	C(12)-Si(2)-C(51)	111.5(2)
C(11)-Si(1)-C(31)	110.9(2)	C(41)-Si(2)-C(51)	110.6(1)
	Torsional Angles (deg)		
C(2)-C(1)-Si(1)-C(11)	177.5	C(7)-C(6)-Si(2)-C(12)	158.3

(a) Cp(1) is the centroid of C(1), C(2), C(3), C(4), and C(5).
(b) Cp(2) is the centroid of C(6), C(7), C(8), C(9), and C(10).

Table 3-2 The Crystallographic Data of (h^5-Ph_2MeSi-$C_5H_4)_2ZrCl_2$ and (h^5-Br_2MeSi-$C_5H_4)_2ZrBr_2$

	(h^5-Ph_2MeSi-$C_5H_4)_2ZrCl_2$	(h^5-Br_2MeSi-$C_5H_4)_2ZrBr_2$
empirical formula	$C_{36}H_{34}Cl_2Si_2Zr$	$C_{12}H_{14}Br_6Si_2Zr$
formula weight	684.93	785.03
diffractometer	Siemens P4	Enraf-Nonius Kappa CCD
cryst dimens (mm)	0.35x0.35x0.35	0.10x0.10x0.12
cryst syst	triclinic	triclinic
a (Å)	10.1109(14)	6.8170(2)
b (Å)	13.0604(18)	14.6660(4)
c (Å)	13.239(2)	22.1520(7)
R (deg)	80.538(12)	105.3520(15)
a (deg)	103.389(5)	91.5380(18)
b (deg)	71.456(10)	90.4540(16)
g (Å)^3	1634.4(4)	2134.66(11)
space group	Pī (No. 2)	Pī (No. 2)
Z	2	4
D_{calc} (Mg m^{-3})	1.392	2.443
abs coeff (mm^{-1})	0.60	11.8
F_{000}	704	1456
l (Mo Ka) (Å)	0.71073	0.71073
temp (K)	293(2)	100(2)
q range for collection	1.60-29.00	1.4-30.00
no. of reflns colld	9883	19436
no. of indep reflns	8610	12401
abs corr method	empirical	multiscan
no. of data/restrts/params	8610/0/506	12401/0/383
R [I > 2s(I)]	0.0373	0.0400
R_w [I > 2s(I)]	0.0785	0.0780
GoF on F^2	0.86	0.85
largest diff peak and hole (e Å^{-3})	0.292, -0.407	1.92, -0.91

Figure 3-1 Thermal Ellipsoid Plot of the Molecular Structure of (h^5-Ph_2MeSi-$C_5H_4)_2ZrCl_2$

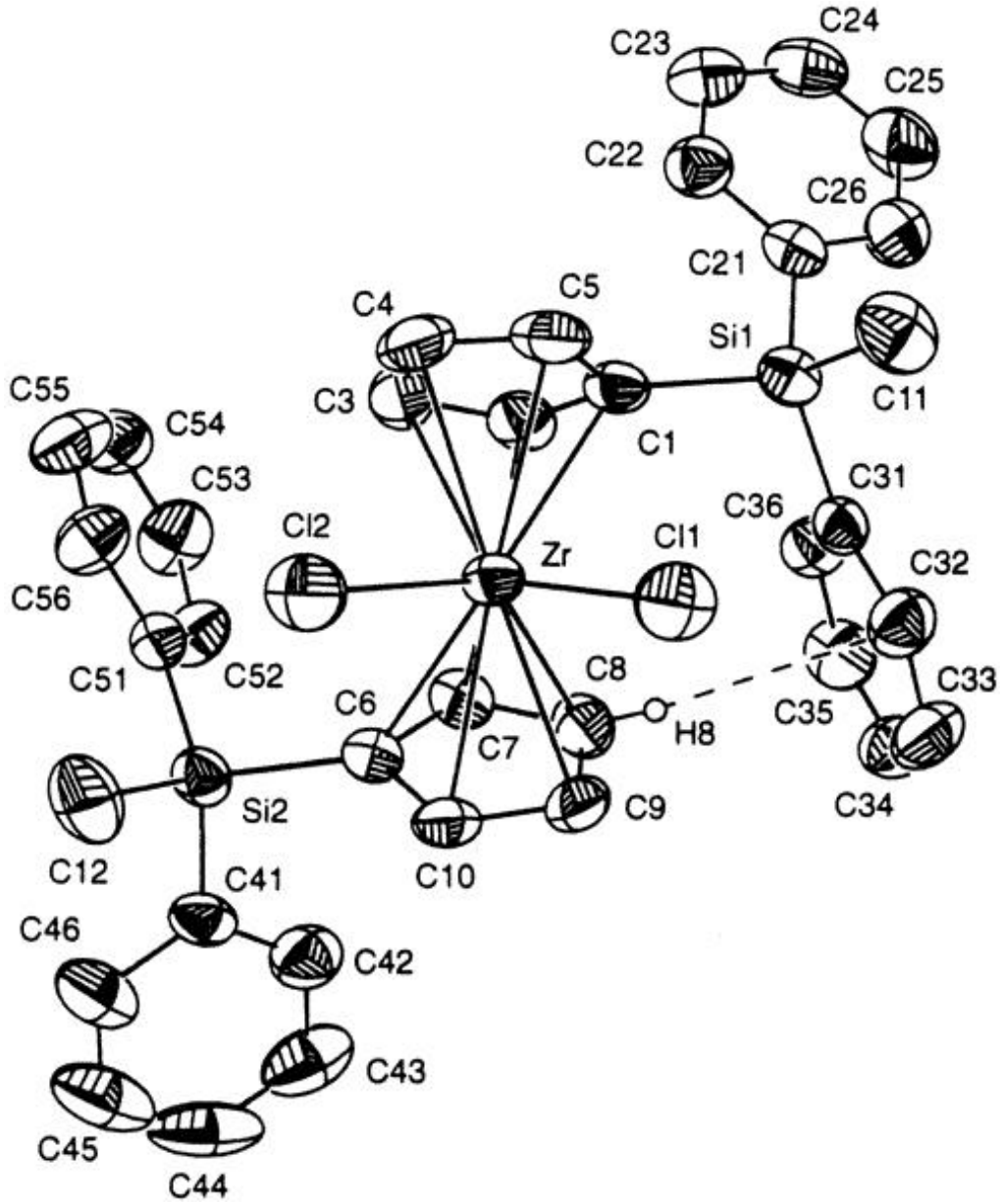

The plot is shown at 50% probability. Hydrogen atoms (except H8) are omitted for clarity. The dashed line is drawn from H(8) to the C(31)-C(36) ring centroid to indicate a "hydrogen bonding" interaction.

The crystal molecular structure of (η^5-Ph_2MeSi-$C_5H_4)_2ZrCl_2$ is presented in Figure 3-1. Selected metric parameters are presented in Table 3-1, and the crystallographic data are collected in Table 3-2. The crystal belongs to the Pī space group, but the conformation of the molecule has approximate C_2 symmetry, which probably minimizes the steric repulsions of the bulky

phenyl groups. An edge-to-face Cp-to-phenyl "hydrogen bonding" contact, which is presented as a dashed line in Figure 3-1, is noted in the molecular structure. The distance of the hydrogen atom H8 to the centroid of the phenyl ring composing of C31-C36 carbon atoms is 2.613 Å, which is almost identical to the distance of H8 to the least squares plane of the phenyl ring (2.602 Å). The two nearly identical distances indicate that the hydrogen atom is well centered on the face of the phenyl ring. The distance value implies an interaction between the hydrogen atom and the phenyl ring.

3.3 Reactivities of (h^5-Ph_2MeSi-$C_5H_4)_2ZrCl_2$ with BCl_3 and BBr_3

3.3.1 Reactivity of (η^5-Ph_2MeSi-$C_5H_4)_2ZrCl_2$ with BCl_3

The reactivity of (η^5-Ph_2MeSi-$C_5H_4)_2ZrCl_2$ with BCl_3 was investigated. In an initial experiment, (η^5-Ph_2MeSi-$C_5H_4)_2ZrCl_2$ was treated with about 80 equivalents of BCl_3 in CH_2Cl_2 under reflux for 15 h. The crude product contained a mixture of the unreacted starting complex and four additional components, as indicated by its ^1H NMR spectrum in $CDCl_3$. Figure 3-2 reveals five signals in the Si-Me region at 1.02, 1.01, 0.99, 0.92, and 0.89 ppm. The signal from (η^5-Ph_2MeSi-$C_5H_4)_2ZrCl_2$ (0.89 ppm) was the most intense, followed by the signals at 0.99 ppm and 0.92 ppm, and then by the signals at 1.02 ppm and 1.01 ppm. Integration of these signals suggested a mole ratio of about 5 : 4 : 4 : 1 : 1. Some of the corresponding signals in the Cp region were well resolved, and others were not (Figure 3-2). Fortunately, we were able to make good assignments based on the SiMe signals alone.

Figure 3-2 The 500 MHz ^{1}H NMR Spectrum of the Product from the Reaction between (h^5-Ph_2MeSi-$C_5H_4)_2ZrCl_2$ and BCl_3 in $CDCl_3$

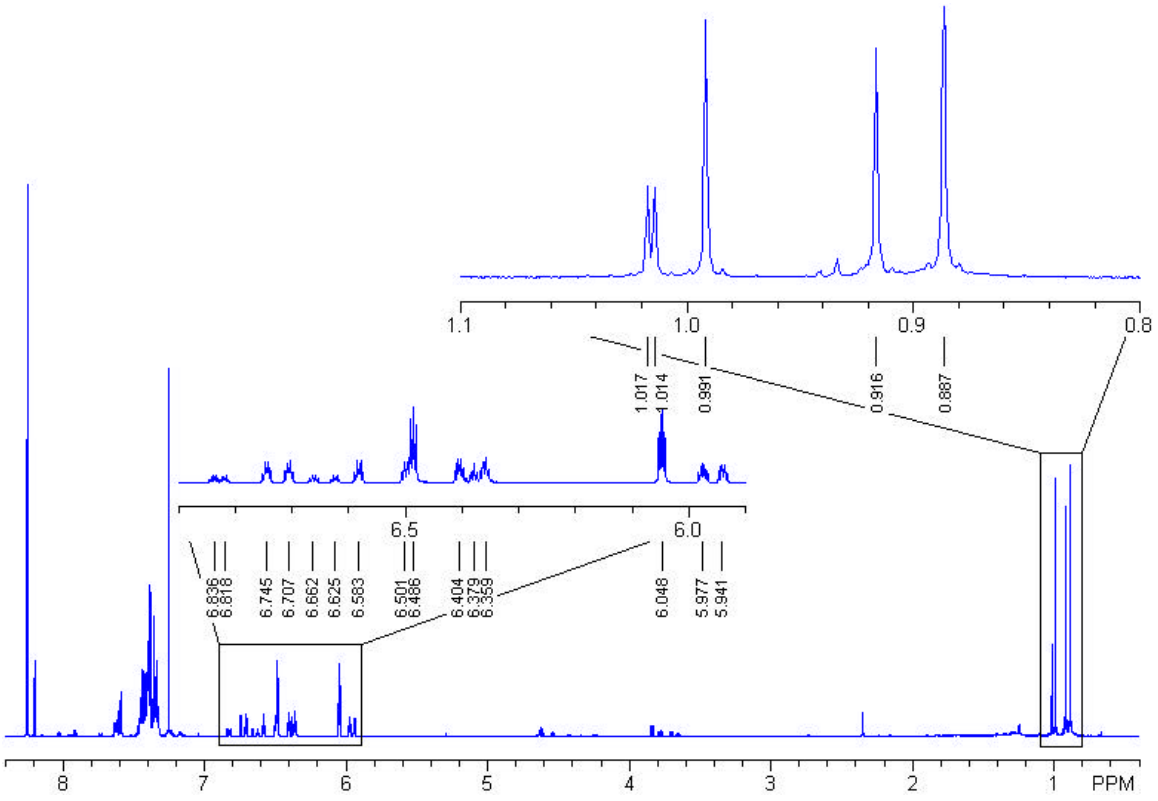

Methyl region assignments:

0.887 ppm: Me-Si in (η^5-Ph_2MeSi-$C_5H_4)_2ZrCl_2$.
0.916 ppm: Me-Si of Ph_2MeSi in (η^5-$ClPhMeSi$-C_5H_4)(η^5-Ph_2MeSi-C_5H_4)$ZrCl_2$.
0.991 ppm: Me-Si of $ClPhMeSi$ in (η^5-$ClPhMeSi$-C_5H_4)(η^5-Ph_2MeSi-C_5H_4)$ZrCl_2$.
1.017 ppm & 1.014 ppm: Me-Si in meso and racemic (η^5-$ClPhMeSi$-$C_5H_4)_2ZrCl_2$ isomers.

Scheme 3-5 Isomers of (h^5-$ClPhMeSi$-$C_5H_4)_2ZrCl_2$

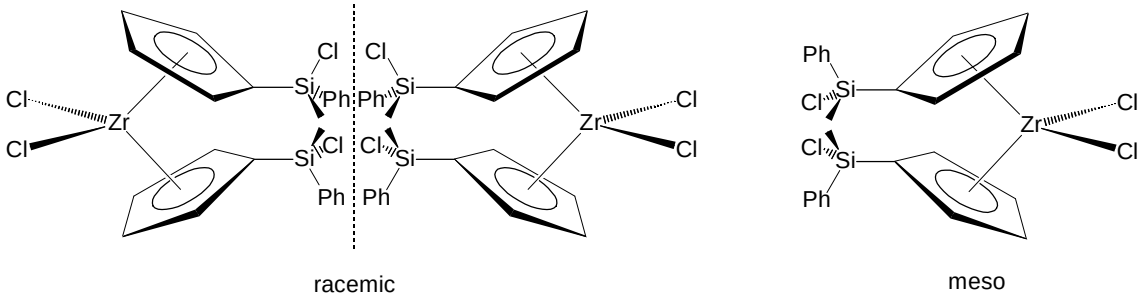

The singlet at 0.89 ppm was assigned to unreacted (η^5-Ph_2MeSi-$C_5H_4)_2ZrCl_2$. The two unresolved singlets at 1.02 ppm and 1.01 ppm of equivalent intensity were assigned to the two diastereomers (meso and racemic) of (η^5-$ClPhMeSi$-$C_5H_4)_2ZrCl_2$ (Scheme 3-5). These two singlets could not arise from a Cl_2MeSi group, because the chemical shift would be expected further downfield -- near that of the fully-characterized Br_2MeSi-substituted zirconocene dibromide analog (SiMe at 1.46 ppm). This analysis excludes (η^5-Cl_2MeSi-$C_5H_4)_2ZrCl_2$, (η^5-$ClPhMeSi$-C_5H_4)(η^5-Cl_2MeSi-C_5H_4)$ZrCl_2$, and (η^5-Cl_2MeSi-C_5H_4)(η^5-Ph_2MeSi-C_5H_4)$ZrCl_2$. The two singlets at 0.99 ppm and 0.92 ppm of equivalent intensity were assigned to (η^5-$ClPhMeSi$-C_5H_4)(η^5-Ph_2MeSi-C_5H_4)$ZrCl_2$. The singlet at 0.92 ppm was probably from the Ph_2MeSi group since the chemical shift was close to that of the methyl groups in (η^5-Ph_2MeSi-$C_5H_4)_2ZrCl_2$ (0.89 ppm), and the singlet at 0.99 ppm was probably from the ClPhMeSi group.

If the assignments are correct, an interesting question is raised. Why is the reactivity of (η^5-Ph_2MeSi-$C_5H_4)_2ZrCl_2$ toward BCl_3 so much less than that of (η^5-$PhMe_2Si$-$C_5H_4)_2ZrCl_2$? As described in Section 3.1, the reaction of (η^5-$PhMe_2Si$-$C_5H_4)_2ZrCl_2$ with BCl_3 was carried out under the same conditions as those of the reaction of (η^5-Ph_2MeSi-$C_5H_4)_2ZrCl_2$ with BCl_3. However, the former reaction stoichiometrically and selectively converted (η^5-$PhMe_2Si$-$C_5H_4)_2ZrCl_2$ to (η^5-$ClMe_2Si$-$C_5H_4)_2ZrCl_2$, while the latter reaction only converted a small portion of (η^5-Ph_2MeSi-$C_5H_4)_2ZrCl_2$ to (η^5-$ClPhMeSi$-$C_5H_4)_2ZrCl_2$. One possible explanation is that replacing a methyl group with a phenyl group decreases bond-rotational degrees of freedom in the four-centered "Meisenheimer" intermediate. In other words, the phenyl group may introduce steric strain into the geometry of the transition state leading to the key intermediate. Another possibility is that a phenyl group is electron-withdrawing relative to a methyl group, slowing down the first phenyl exchange.

Figure 3-3 The 500 MHz ^{1}H NMR Spectrum of the Product from the Reaction between (h^5-Ph_2MeSi-$C_5H_4)_2ZrCl_2$ and BBr_3 in $CDCl_3$

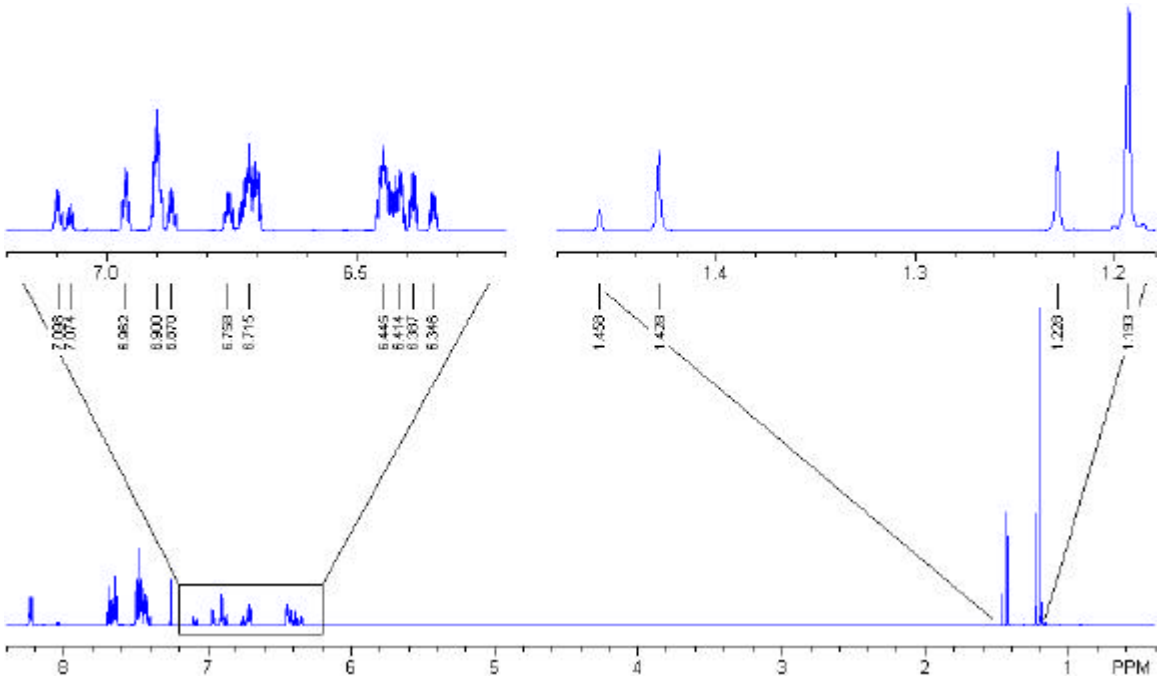

Methyl region assignments:

1.193 ppm: Me-Si in (η^5-BrPhMeSi-$C_5H_4)_2ZrBr_2$.
1.228 ppm: Me-Si of BrPhMeSi in (η^5-Br_2MeSi-C_5H_4)(η^5-BrPhMeSi-C_5H_4)$ZrBr_2$.
1.428 ppm: Me-Si of Br_2MeSi in (η^5-Br_2MeSi-C_5H_4)(η^5-BrPhMeSi-C_5H_4)$ZrBr_2$.
1.458 ppm: Me-Si in (η^5-Br_2MeSi-$C_5H_4)_2ZrBr_2$.

3.3.2 Reactivity of (η^5-Ph_2MeSi-$C_5H_4)_2ZrCl_2$ with BBr_3, Synthesis and Structure of (η^5-Br_2MeSi-$C_5H_4)_2ZrBr_2$

The compound (η^5-Ph_2MeSi-$C_5H_4)_2ZrCl_2$ was also treated with BBr_3. In an initial experiment, a solution of (η^5-Ph_2MeSi-$C_5H_4)_2ZrCl_2$ in CH_2Cl_2 was treated with excess BBr_3 under reflux for 15 h. ^{1}H NMR analysis of the crude product in $CDCl_3$ was also very complicated (Figure 3-3). The Cp region contained a lot of multiplet signals that were not resolved. However, the Si-Me region was relatively simple, comprising four well-resolved singlets at 1.46, 1.43, 1.23, and 1.19 ppm, whose intensity ratios were approximately 1 : 4 : 4 : 12, respectively.

The singlet at 1.46 ppm was assigned to the desired bis-dibromomethylsilyl-substituted zirconocene compound, (η^5-Br_2MeSi-$C_5H_4)_2ZrBr_2$ (later confirmed). The singlet at 1.19 ppm was not from the simple transhalogenated compound (η^5-Ph_2MeSi-$C_5H_4)_2ZrBr_2$, whose methyl signal would be found at 0.87 ppm (Section 3.5). Instead, the signal at 1.19 ppm was assigned to (η^5-BrPhMeSi-$C_5H_4)_2ZrBr_2$. The position of the signal was roughly half way in between the methyl signal of (η^5-Ph_2MeSi-$C_5H_4)_2ZrCl_2$ (0.89 ppm) and that of (η^5-Br_2MeSi-$C_5H_4)_2ZrBr_2$ (1.46 ppm), suggesting that one phenyl group was replaced by bromine. In a similar way, the two singlets of the same intensity at 1.43 ppm and 1.23 ppm were assigned to (η^5-Br_2MeSi-C_5H_4)(η^5-BrPhMeSi-C_5H_4)$ZrBr_2$. We tried to prepare (η^5-BrPhMeSi-$C_5H_4)_2ZrBr_2$ by a stoichiometric reaction of (η^5-Ph_2MeSi-$C_5H_4)_2ZrCl_2$ and exactly four equivalents of BBr_3. However, the proton NMR spectrum of the crude product still showed a mixture of the above four components with other impurities.

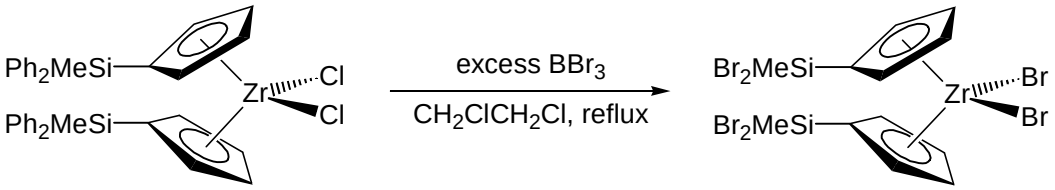

Scheme 3-6 Bromination of (η^5-Ph_2MeSi-$C_5H_4)_2ZrCl_2$

In an optimized reaction of (η^5-Ph_2MeSi-$C_5H_4)_2ZrCl_2$ with excess BBr_3, the two compounds were refluxed in CH_2ClCH_2Cl instead of using CH_2Cl_2. The boiling point of CH_2ClCH_2Cl is 83 ^oC, much higher than that of CH_2Cl_2 at 40 ^oC, so Si-Ph bonds of (η^5-Ph_2MeSi-$C_5H_4)_2ZrCl_2$ should be cleaved more rapidly by BBr_3. The proton NMR spectrum of the crude product from the reaction showed complete conversion of (η^5-Ph_2MeSi-$C_5H_4)_2ZrCl_2$ to (η^5-Br_2MeSi-$C_5H_4)_2ZrBr_2$, which was identified by a multiplet at 7.07 ppm, a multiplet at 6.73 ppm, and a singlet at 1.46 ppm (4 : 4 : 6 ratio). This compound was then prepared on a larger

(0.50 mmol) scale, following a similar method, to obtain a 79% isolated yield of pure, crystalline, product. We conclude that the reactivity of the Si-Ph bond with BBr_3 is high enough that both of the phenyl groups on the Ph_2MeSi substituent were replaced by bromine (Scheme 3-6). Like other halosilyl-substituted zirconocene compounds, $(\eta^5\text{-}Br_2MeSi\text{-}C_5H_4)_2ZrBr_2$ is not air-stable at ambient temperature. The yellow-green needles gradually turned into a yellow-gray powdery solid over several days when exposed to air in a weighing dish covered with a beaker.

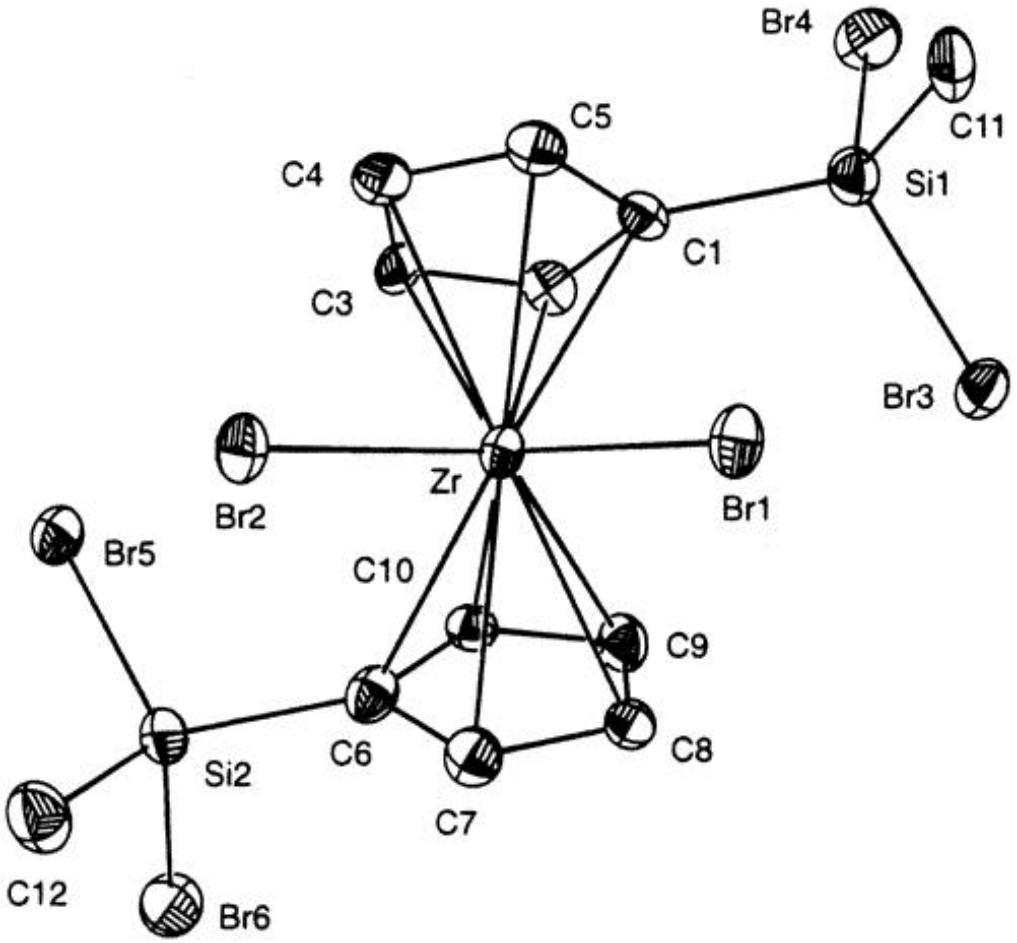

The plot is shown at 50% probability. Hydrogen atoms are omitted for clarity.

Figure 3-4 Thermal Ellipsoid Plot of the Molecular Structure of $(h^5\text{-}Br_2MeSi\text{-}C_5H_4)_2ZrBr_2$

The molecular structure of $(\eta^5\text{-}Br_2MeSi\text{-}C_5H_4)_2ZrBr_2$ was determined by X-ray crystallography (data in Table 3-2 and Table 3-3). A thermal ellipsoid plot of the molecular structure of $(\eta^5\text{-}Br_2MeSi\text{-}C_5H_4)_2ZrBr_2$ is shown in Figure 3-4. Like its Ph_2MeSi-substituted

precursor, the compound crystallizes in the Pī space group, and individual (η^5-Br_2MeSi-$C_5H_4)_2ZrBr_2$ molecules also adopt approximate C_2 symmetry. The conformation can be rationalized using an argument regarding the minimization of the overall polarity of the molecule. As shown in Figure 3-4, in the conformation, the electrostatic dipole moment of the $ZrBr_2$ moiety can be represented by an arrow coming out of the paper plane, while that of the two Br_2MeSi substituents are represented by two arrows going into the paper plane. Therefore, the opposite dipole moments compensate each other to give the whole molecule a minimized overall polarity. Several weak Cp-H···Br-Zr and Cp-H···Br-Si interactions were found in the packing diagrams, whose distances range from 2.85 Å to 3.20 Å. These weak "hydrogen-bonding" interactions probably contributed to the observed structure.

Table 3-3 Metric Parameters for Crystalline (h^5-Br_2MeSi-$C_5H_4)_2ZrBr_2$[(a)]

	Bond Distances (Å)		
Cp(1)[(b)]-Zr	2.205(3)	Si(1)-Br(3)	2.218(2)
Cp(2)[(c)]-Zr	2.206(3)	Si(1)-Br(4)	2.223(2)
Zr-Br(1)	2.6018(8)	Si(2)-C(6)	1.841(6)
Zr-Br(2)	2.6013(8)	Si(2)-C(12)	1.823(6)
Si(1)-C(1)	1.841(6)	Si(2)-Br(5)	2.219(2)
Si(1)-C(11)	1.831(6)	Si(2)-Br(6)	2.231(2)
	Bond Angles (deg)		
Cp(1)[(b)]-Zr-Cp(2)[(c)]	129.7(2)	Br(3)-Si(1)-Br(4)	105.2(6)
Br(1)-Zr-Br(2)	95.31(2)	C(6)-Si(2)-C(12)	116.4(3)
C(1)-Si(1)-C(11)	114.1(3)	C(6)-Si(2)-Br(5)	110.1(2)
C(1)-Si(1)-Br(3)	112.2(2)	C(6)-Si(2)-Br(6)	104.1(2)
C(1)-Si(1)-Br(4)	105.2(2)	C(12)-Si(2)-Br(5)	111.5(2)
C(11)-Si(1)-Br(3)	110.5(2)	C(12)-Si(2)-Br(6)	108.6(2)
C(11)-Si(1)-Br(4)	109.1(2)	Br(5)-Si(2)-Br(5)	105.2(6)
	Torsional Angles (deg)		
C(2)-C(1)-Si(1)-C(11)	1.9(4)	C(7)-C(6)-Si(2)-C(12)	19.2(6)

(a) Data are shown for one of two nearly identical molecules in the asymmetric unit.
(b) Cp(1) is the centroid of C(1), C(2), C(3), C(4), and C(5).
(c) Cp(2) is the centroid of C(6), C(7), C(8), C(9), and C(10).

3.4 Characterization of a Polymeric Zirconocene Compound with a Polysiloxane Backbone

3.4.1 Characterization of the "Gray Solid"

3.4.1.1 Analytical and Spectroscopic Evidences for the Polymeric Structure

After exposition to air, the moisture-sensitive compound, $(\eta^5\text{-}Br_2MeSi\text{-}C_5H_4)_2ZrBr_2$, turns gradually from green-yellow crystalline material to yellow-gray powdery solid, which we call the "gray solid". Elemental analysis of the "gray solid" was consistent with the empirical formula $(C_{12}H_{14}Br_2O_2Si_2Zr)_n$, resulting from hydrolysis of all Si-Br bonds and condensation of the resulting silanols to form disiloxanes. The ^1H NMR spectrum of the solid in $CDCl_3$ was dominated by five signals: four multiplets at 7.10, 7.02, 6.90, 6.52 ppm, and a singlet at 0.44 ppm (2 : 2 : 2 : 2 : 6 ratio). Weak impurity signals were also observed. Corresponding chemical shifts in THF-d_8 were 7.18 (4 H), 6.83 (2 H), 6.53 (2 H), and 0.45 ppm (3 H).

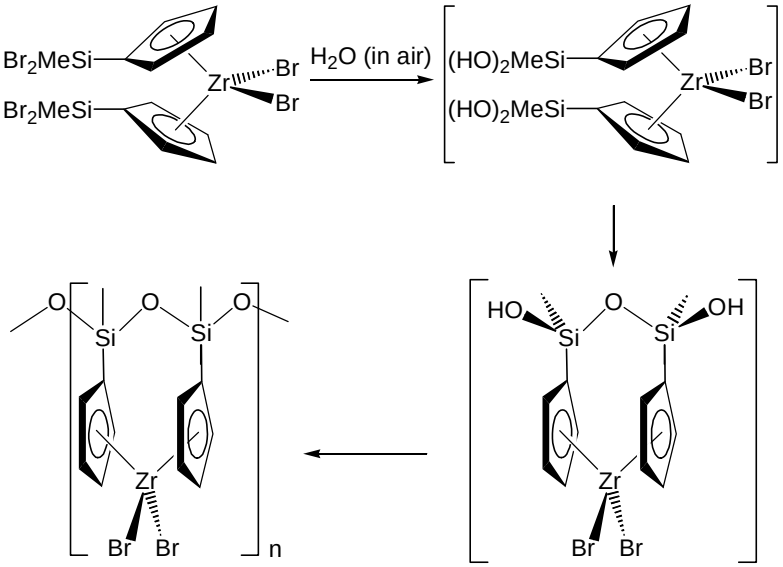

Scheme 3-7 Hydrolysis of (h^5-Br_2MeSi-$C_5H_4)_2ZrBr_2$

It is known that halosilyl-substituted group 4 metallocene compounds undergo facile hydrolysis reaction with water. For example, the reaction of $(\eta^5\text{-}BrMe_2Si\text{-}C_5H_4)_2ZrBr_2$ with

moisture in air affords a disiloxane-bridged compound, [(μ-O)(-η^5-Me_2Si-$C_5H_4)_2$]$ZrBr_2$, which was presumably formed by a hydrolysis reaction to give (η^5-$HOMe_2Si$-$C_5H_4)_2ZrBr_2$ followed by condensation (Scheme 1-41).[130] Therefore, based on the structural similarities of the halosilyl-substituted metallocene compounds and (η^5-Br_2MeSi-$C_5H_4)_2ZrBr_2$, we proposed that the "gray solid" had an oligomeric or polymeric structure with single-strand polysiloxane backbones, $(C_{12}H_{14}Br_2O_2Si_2Zr)_n$, presumably formed by hydrolysis followed by condensation (Scheme 3-7). The analytical data of the solid were consistent with the proposed structure. The simple pattern of the proton NMR spectra also suggested a stereoregular molecular structure.

The solid-state ^{13}C CPMAS NMR spectra of [(μ-O)(-η^5-Me_2Si-$C_5H_4)_2$]$ZrBr_2$, the "gray solid", and the precipitate prepared from hydrolysis of (η^5-Br_2MeSi-$C_5H_4)_2ZrBr_2$ in toluene solution were compared (Figure 3-5). An evolution of the spectra was observed. The spectrum of solid [(μ-O)(-η^5-Me_2Si-$C_5H_4)_2$]$ZrBr_2$ had better resolved signals. The spectrum of the precipitate looked like a broadened and smoothed version of that of solid [(μ-O)(-η^5-Me_2Si-$C_5H_4)_2$]$ZrBr_2$. The spectrum of the "gray solid" looked like a further broadened and smoothed version. The similarities in the ^{13}C CPMAS NMR spectra, especially in the Cp region, indicate that the "gray solid", the precipitate, and [(μ-O)(-η^5-Me_2Si-$C_5H_4)_2$]$ZrBr_2$ had similar molecular structures. Since the solid was considered as oligomer or polymer of the proposed polymeric structure, and [(μ-O)(-η^5-Me_2Si-$C_5H_4)_2$]$ZrBr_2$ can be considered as an analog of the monomer of the proposed polymeric structure, the precipitate probably contained lower degree of oligomers of the proposed polymeric structure.

Figure 3-5 Comparison of the 75.5 MHz CPMAS ^{13}C NMR Spectra of [(m-O)(-h^5-Me$_2$Si-C$_5$H$_4$)$_2$]ZrBr$_2$ and the Polymeric Zirconocene Compound

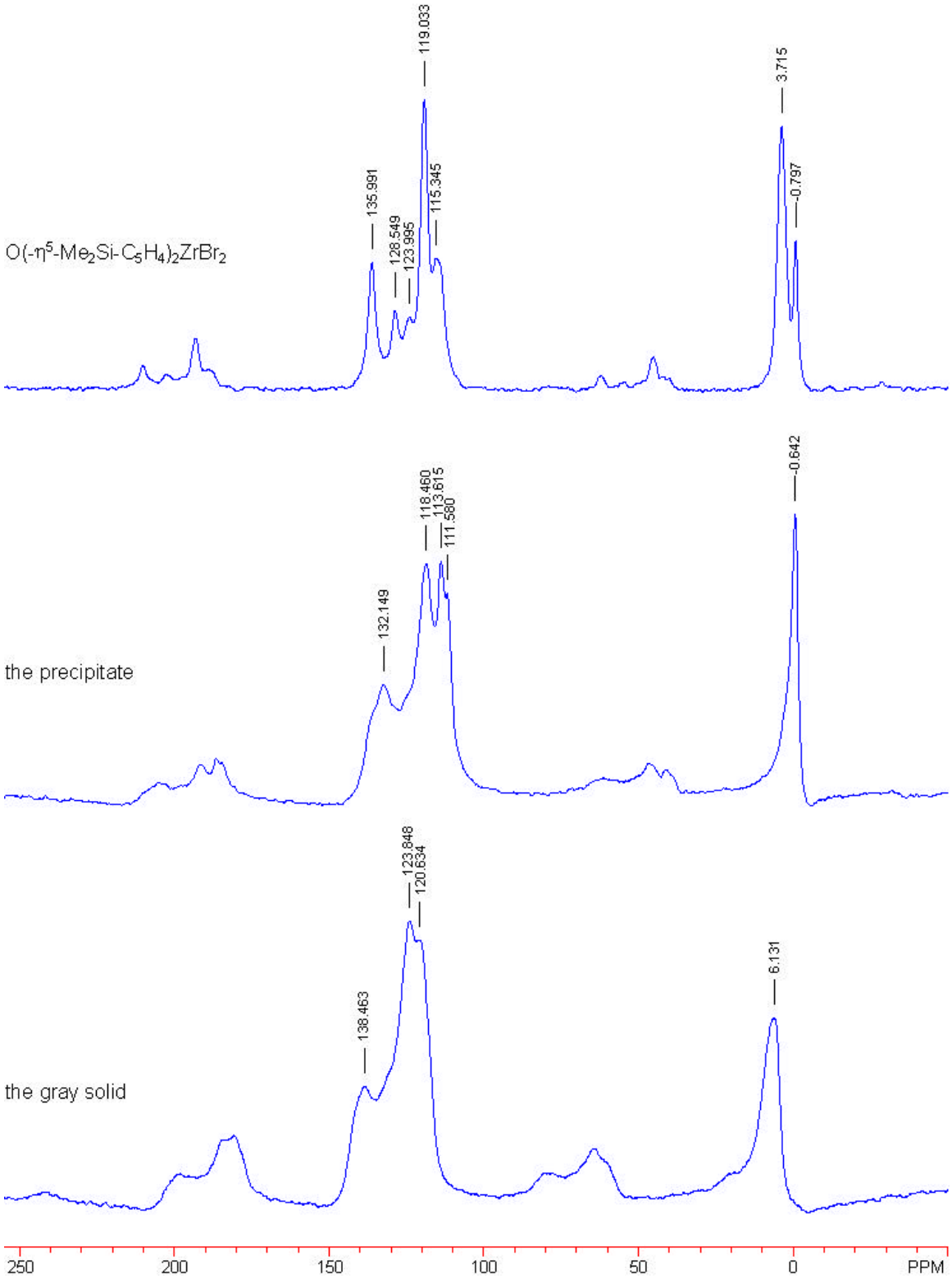

Figure 3-6 Comparison of the FT-IR Spectra of [(μ-O)(-h^5-Me$_2$Si-C$_5$H$_4$)$_2$]ZrBr$_2$ and the Polymeric Zirconocene Compound

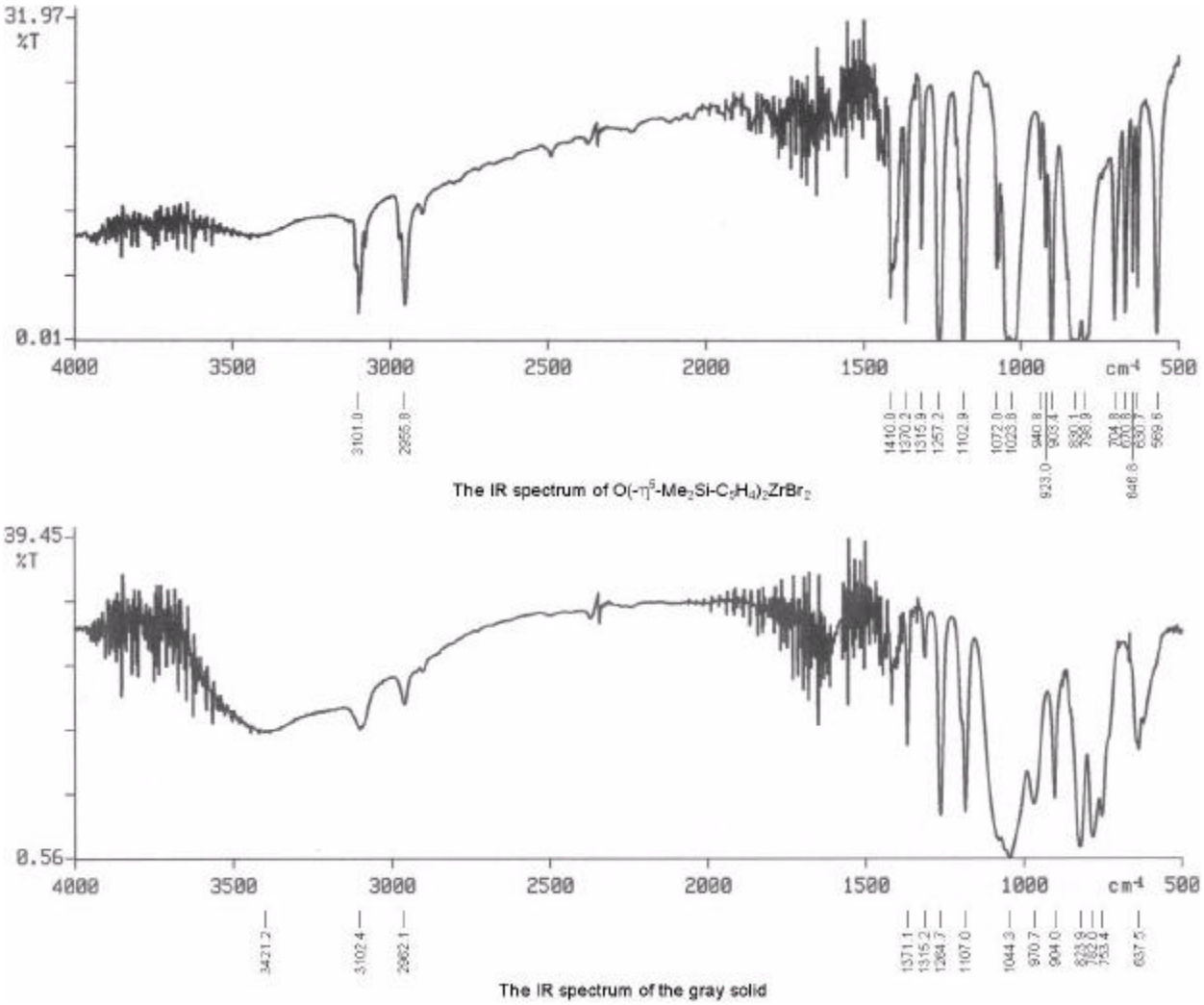

MALDI-TOF MS of the "gray solid" showed the existence of fragments containing two repeat units (M/Z = 995) and unidentified fragments derived from fragments containing 3 ~ 4 repeat units. Especially, the fragments at M/Z = 846, M/Z = 1343, and M/Z = 1840 were all 149 mass units away from the two-repeat-unit fragments, three-repeat-unit fragments (M/Z = 1492.5), and the four-repeat-unit fragments (M/Z = 1990), respectively, indicating that they were formed from their parent fragments (not observed) by loss of a same fragment that was not identified. The MALDI-TOF MS results indicated that the "gray solid" was composed of at least

oligomeric structures. Due to its poor solubility, the molecular weight of the gray solid could not be determined by GPC. FT-IR spectra of the gray solid and of [(μ-O)(-η^5-Me_2Si-C_5H_4)$_2$]ZrBr_2 were obtained from KBr pellets (Figure 3-6). Some similar features were found in both spectra. The band at 3101.0 cm^{-1} in the spectrum of [(μ-O)(-η^5-Me_2Si-C_5H_4)$_2$]ZrBr_2 (3102.4 cm^{-1}; values for the "gray solid" in parentheses) was from the C-H stretching of the methyl groups. The band at 2955.8 (2962.1) cm^{-1} was from the C-H stretching of the Cp rings. The Si-Me stretching was observed at 1257.2 (1264.7) cm^{-1}, and the Si-Me bending was probably at 830.1 and 798.9 (823.9, 782.0, and 753.4) cm^{-1}. The vibrations related to the Si-O-Si linkages were observed at 1102.9 and 1023.8 (1107.0 and 1044.3) cm^{-1}. The broad band at 3420 cm^{-1} in the spectrum of the "gray solid" was probably from remaining hydroxyl groups in the solid.[180]

3.4.1.2 Elucidation of the Steric Configuration of the Polymeric Structure

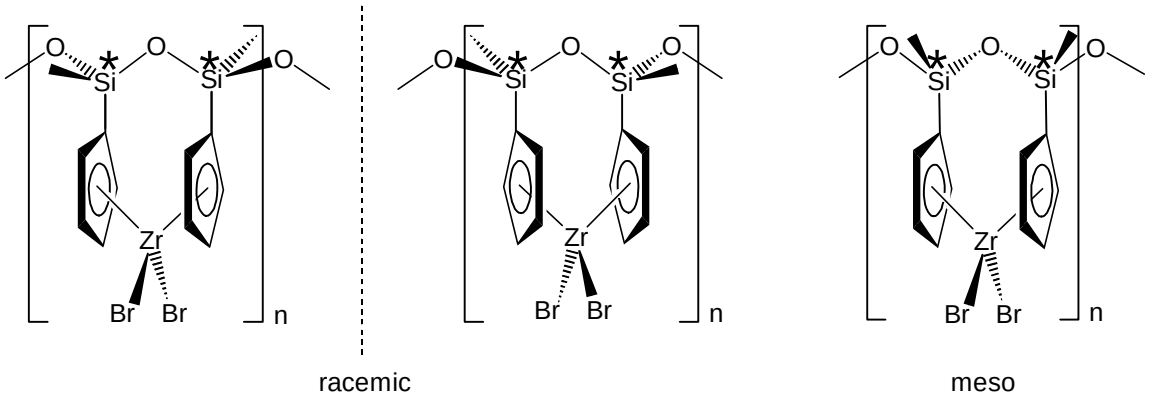

Scheme 3-8 Stereoisomers of the Polymeric Zirconocene Compound

Although no direct evidence was found to verify the structure of the gray solid, all the characterization results were consistent with the proposed single-strand polysiloxane-backbone structure. If the configuration of the polysiloxane backbone is considered, two steric isomers are possible, i.e., the meso and the racemic isomers (Scheme 3-8). The meso isomer has a mirror

[180] *Silicone Compounds Register and Review*, B. Arkles, et al. Eds, Petrarch Systems 1987.

plane and the racemic isomer has a C_2 axis, so both isomers should show four multiplet proton signals in the Cp region and one singlet proton signal in the methyl region. Therefore, it is not possible to distinguish the two isomers from their NMR spectra.

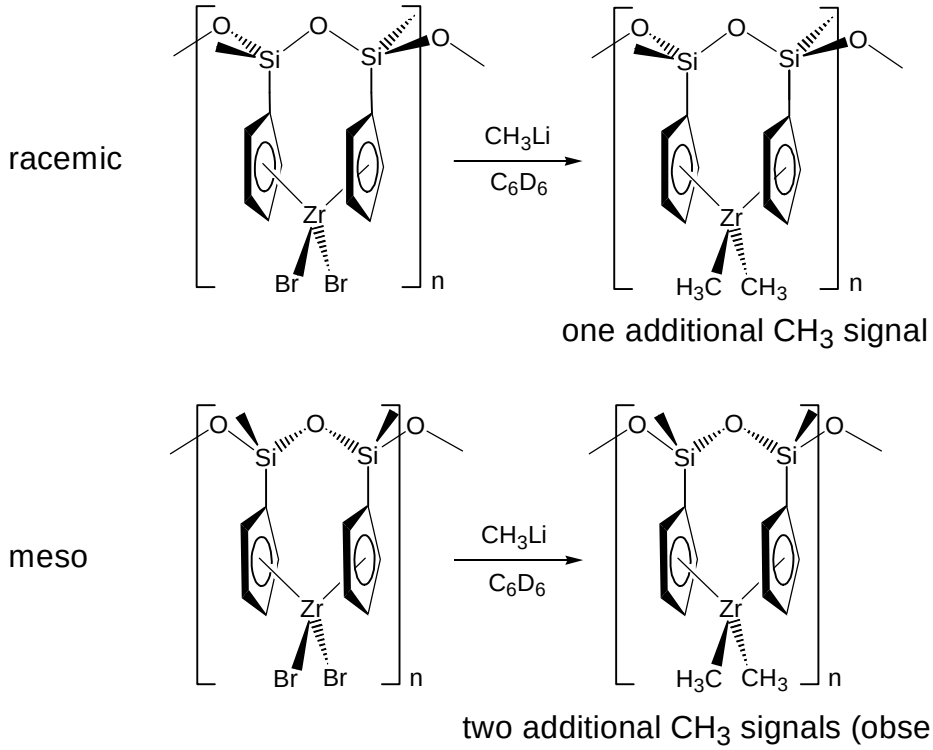

Scheme 3-9 Methylation of the Stereoisomers of the Polymeric Zirconocene Compound

To find out which isomer the "gray solid" contained, the $ZrBr_2$ moiety was converted to $ZrMe_2$ using methyllithium. The ^1H NMR spectra showed that the weak singlet at 0.35 ppm in the $ZrBr_2$ species was much stronger in the $ZrMe_2$ species (indicating higher solubility) and shifted to 0.37 ppm. As shown in Scheme 3-9, the presence of two equally integrating Zr-Me signals argues against a racemic (C_2-symmetric) metallocene, which requires two homotopic methyl groups. Instead, the spectrum favors a meso (C_s-symmetric) metallocene moiety, which has diastereotopic methyl groups. From this analysis of the $ZrMe_2$ derivative, we can safely infer the same symmetry in the starting $ZrBr_2$ species (the "gray solid"). Double-strand

polysiloxane backbones were also ruled out. Local repeat unit symmetries and the expected number of NMR signals are shown in Scheme 3-10 for three canonical structures.

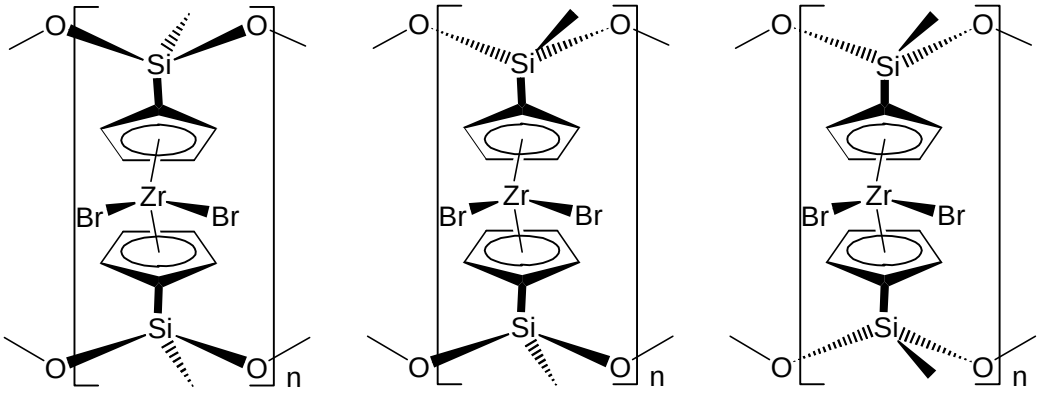

Scheme 3-10 Possible Double-strand Isomers of the Polymeric Zirconocene Compound

Similar polymeric zirconocene compounds with polysiloxane backbones have been prepared in other laboratories. Some examples were presented in Section 1.3.2. However, unlike the polymeric zirconocene compound in this research, which formed by polymerization of the functionalized zirconocene compound, the polymeric zirconocene compounds in the literature were formed by reaction of functionalized polysiloxane chains with zirconium salts. The former had stereoregular structure according to our spectroscopic evidence, while the latter contained various zirconocene moieties in the polymer structures.[126]

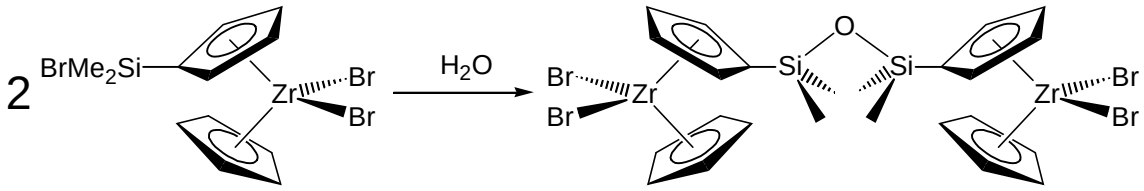

Scheme 3-11 Hydrolysis of (h^5-$BrMe_2Si$-C_5H_4)$CpZrBr_2$

3.4.1.3 Comparison of the Formation Modes of Disiloxane Bridges in Different Halosilyl-Substituted Zirconocene Compounds

It is interesting to compare the structures of the hydrolysis products of several halosilyl-substituted zirconocene compounds: (η^5-$BrMe_2Si$-C_5H_4)$CpZrBr_2$, (η^5-$BrMe_2Si$-C_5H_4)$_2ZrBr_2$, [η^5-1,3-($BrMe_2Si$)$_2C_5H_3$]$_2ZrBr_2$, and (η^5-Br_2MeSi-C_5H_4)$_2ZrBr_2$. Unpublished results obtained by Huaiying Kang in our group showed that the mono-$BrMe_2Si$-substituted zirconocene compound, (η^5-$BrMe_2Si$-C_5H_4)$CpZrBr_2$, is converted to a complex with two zirconocene moieties linked together by a disiloxane bridge when it was hydrolyzed (Scheme 3-11). The bis-$BrMe_2Si$-substituted zirconocene compound, (η^5-$BrMe_2Si$-C_5H_4)$_2ZrBr_2$, forms the ansa-zirconocene compound with a disiloxane bridge, [(μ-O)(-η^5-Me_2Si-C_5H_4)$_2$]$ZrBr_2$ (Scheme 1-41), whereas the tetrakis-$BrMe_2Si$-substituted zirconocene compound, [η^5-1,3-($BrMe_2Si$)$_2C_5H_3$]$_2ZrBr_2$, forms an ansa-zirconocene compound with two disiloxane bridges (Scheme 3-12).[130] In this research, the bis-Br_2MeSi-substituted zirconocene compound, (η^5-Br_2MeSi-C_5H_4)$_2ZrBr_2$, formed the polymeric zirconocene compound with a polysiloxane backbone.

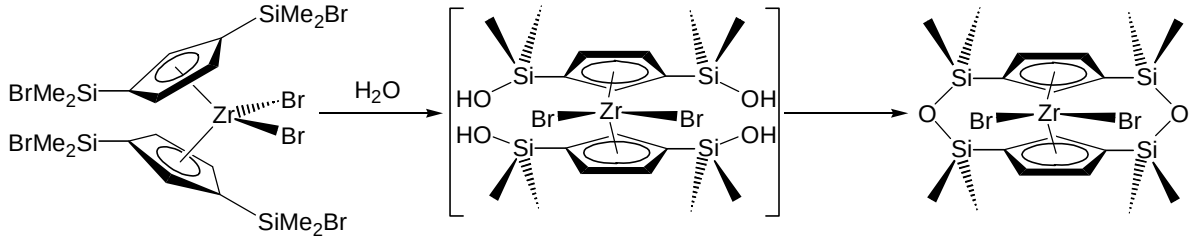

Scheme 3-12 Hydrolysis of [η^5-1,3-($BrMe_2Si$)$_2C_5H_3$]$_2ZrBr_2$ [130]

Scheme 3-13 Hypothetical Oligomeric Structure from the Hydrolysis of (h^5-$BrMe_2Si$-$C_5H_4)_2ZrBr_2$

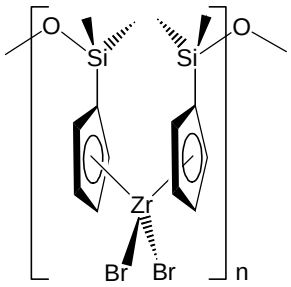

The most striking trend in these hydrolysis results is the pronounced tendency to form intramolecular disiloxane linkages. For example, (η^5-$BrMe_2Si$-$C_5H_4)_2ZrBr_2$ could form intermolecular disiloxane bridges with two other such molecules (Scheme 3-13), but the single intramolecular disiloxane bridge is formed exclusively. Plausible reasons for the preference of ring closure over oligomerization include the proximity of the two opposing $BrMe_2Si$ functional groups and the entropic advantage of the intramolecular reaction over the intermolecular reaction, which is analogous to the chelate effect. Additional evidence for the mechanism of intramolecular disiloxane formation comes from [η^5-1,3-$(BrMe_2Si)_2C_5H_3]_2ZrBr_2$, which exclusively forms two intramolecular disiloxane bridges (in nearly quantitative yield) instead of intermolecular bridges. Here, we find that the four $BrMe_2Si$ substituents are exclusively in the eclipsed configuration rather than the staggered configuration. Upon condensation to form a disiloxane bridge, the metallocene may adopt an eclipsed conformation (Scheme 3-14), so that the first disiloxane bridge can assist the formation of the second one. Otherwise, if the first intramolecular bridge is formed when the molecule is in the staggered configuration, the second intramolecular bridge can not form due to the spatial separation of the remaining two $SiMe_2OH$ groups, and oligomerization would ensue. This theory suggests that the silicon atoms are already "lined up" for ring closure in the crystalline state. However, a crystal structure of [η^5-1,3-

$(BrMe_2Si)_2C_5H_3]_2TiBr_2$ (synthesized by H.-Y. Kang; crystallography by A. Rheingold) showed that intramolecular and intermolecular Si-Si distances are comparable. Alternatively, disiloxane formation might be reversible, and the "double-strapped" compound could simply be thermodynamically favored; double ring closure is favored entropically (chelate effect) and enthalpically (no strain). The situation with $(\eta^5\text{-}Br_2MeSi\text{-}C_5H_4)_2ZrBr_2$ is different. Presumably, formation of the first intramolecular disiloxane bridge is entropically favored. However, no matter how the first intramolecular bridge is formed, the first bridge prohibits the formation of the second intramolecular bridge, since the remaining two $SiMe_2OH$ groups are directed away from the metallocene after the first bridge is formed (Scheme 3-7). They are forced to form intermolecular disiloxane bridges with other molecules, resulting in the polysiloxane chain structure.

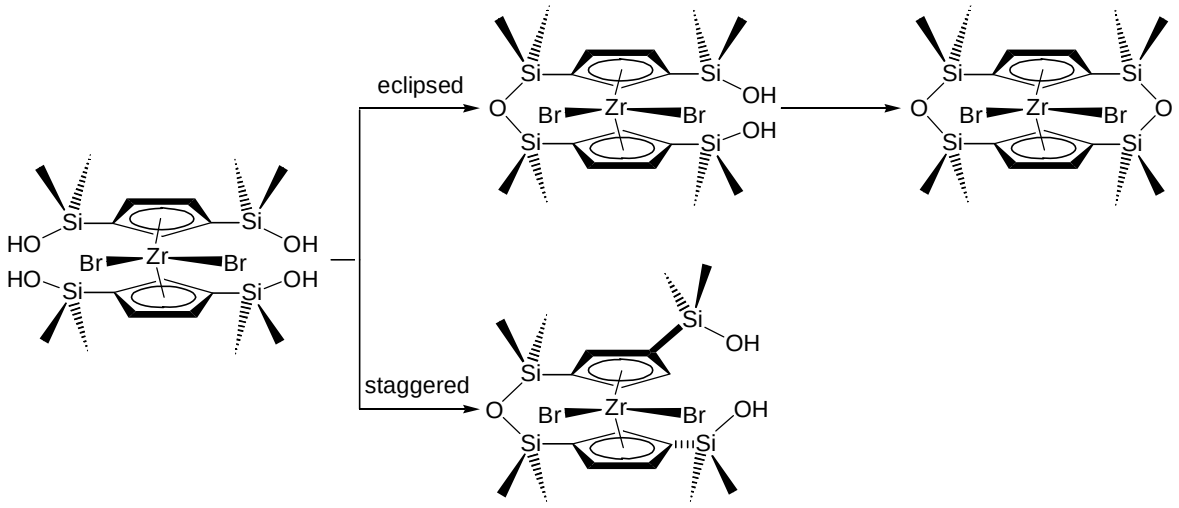

Scheme 3-14 Eclipsed and Staggered Condensation Modes in the Hydrolysis of [h^5-1,3-$(BrMe_2Si)_2C_5H_3]_2ZrBr_2$

3.4.2 Ethylene Polymerization Catalyzed by the Polysiloxane-based Zirconocene Compound

The catalytic activity of the gray solid for ethylene polymerization was evaluated and compared with other similar zirconocene compounds. Since the gray solid has a little solubility

in toluene, the polymerization experiments were carried out in a glass bench-top reactor using the solution process in toluene. MAO was used as the cocatalyst.

Table 3-4 Ethylene Polymerization Data for Some Homogeneous Zirconocene Compounds

Pre-catalyst Compound	Activity[(a)] (kg/mol(Zr)/h	M_p ($x10^{-5}$)	M_n ($x10^{-5}$)	M_w ($x10^{-5}$)	M_z ($x10^{-5}$)	PDI (M_w/M_n)
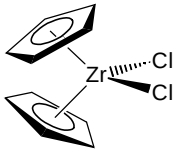	$16(1) \times 10^4$	3.98	2.30	5.30	9.72	2.30
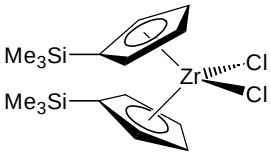	$9.3(7) \times 10^4$	6.93	4.11	11.0	20.8	2.67
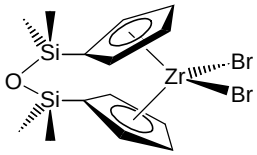	$7.0(5) \times 10^4$	6.34	4.09	10.2	20.4	2.48
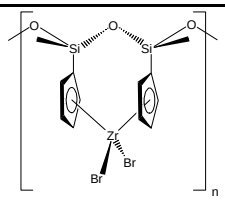 (b)	$11(1) \times 10^4$	4.42	2.77	6.50	13.3	2.34
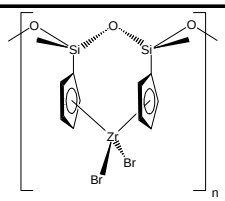 (c)	$8.5(2) \times 10^4$	4.44	2.73	6.47	13.9	2.36

(a) Polymerization conditions: MAO cocatalyst, Al/Zr = 5000, 1 atm C_2H_4, t = 5 min.
(b) $5.0x10^{-7}$ mol/L stock solution in toluene not filtered, looked clear.
(c) $5.0x10^{-7}$ mol/L stock solution in toluene filtered to ensure homogeneity.

Table 3-4 includes the activity data for ethylene polymerization and GPC data of the polyethylene products from several homogeneous zirconocene catalysts with MAO cocatalyst:

Cp_2ZrCl_2, $(\eta^5\text{-}Me_3Si\text{-}C_5H_4)_2ZrBr_2$, $[(\mu\text{-}O)(\text{-}\eta^5\text{-}Me_2Si\text{-}C_5H_4)_2]ZrBr_2$, and the polymeric zirconocene compound. The four catalysts had similar activities for ethylene polymerization. Especially, the polymeric zirconocene compound has a surprisingly high activity close to the activity of the classic Kaminsky catalyst (Cp_2ZrCl_2/MAO) and higher than that of the monomeric analog, $[(\mu\text{-}O)(\text{-}\eta^5\text{-}Me_2Si\text{-}C_5H_4)_2]ZrBr_2$. The results of Noh and coworkers showed that the activities of the binuclear zirconocene compounds for ethylene polymerization decreased with decreasing length of the spacer between the two zirconium centers.[181] Since two neighboring active centers would compete for the limited monomer resource around them and might also undergo bi-molecular deactivation, larger separation between them favored higher activity. If the same rationale applied here, the polymeric zirconocene compound, in which the active centers neighbor to each other, should have lower activity than that of the monomeric analog, $[(\mu\text{-}O)(\text{-}\eta^5\text{-}Me_2Si\text{-}C_5H_4)_2]ZrBr_2$. However, the exact structure of the catalyst in toluene after it was reacted with MAO is not clear. It is possible that the active species was no longer polymeric, though we suspect that the cleavage of Si-O-Si bonds by MAO was insignificant (Chapter 5). The catalyst prepared from an unfiltered solution of the polymeric zirconocene compound had slightly higher activity than that of a filtered solution. The unfiltered solution probably contained some active species that were undissolved but too small to be visible.

The molecular weight of the polyethylene from the polymeric zirconocene compound was slightly higher than that from Cp_2ZrCl_2, but lower than that from $(\eta^5\text{-}Me_3Si\text{-}C_5H_4)_2ZrBr_2$. The PDI value of the polyethylene from the polymeric zirconocene compound was close to those from the other three homogeneous zirconocene catalysts. The low PDI value indicates that the polymeric zirconocene catalyst behaved like a normal homogeneous zirconocene catalyst. In

[181] Noh, S.-K.; Kim, S.-C.; Lee, D.-H.; Yoon, K.-B.; Lee, H.-B.: *Bull. Korean Chem. Soc.* **18(6)**, 618-622 (1997).

comparison, the polymer products from polysiloxane-supported zirconocene catalysts in the literature have suggested multi-site catalyst structure.[126]

3.5 Experimental Details

General Procedures. Standard inert atmosphere techniques were used for all manipulations. Swivel-frit vessels sealed with Kalrez O-rings and interfaced to a high-vacuum line were used for reactions involving boron trihalides. $ZrCl_4$, $ZrBr_4$, $(CpH)_2$, BuLi (1.6 M solution in hexanes), BCl_3 (1.0 M solution in CH_2Cl_2), BBr_3 (neat), and $Ph_2MeSiCl$ were used as received from Aldrich. CH_3Li powder was obtained from 1.4 M solution in ether ordered from Aldrich by evaporation. NaH dispersion in mineral oil was ordered from Aldrich, which was washed with hexanes and dried to get NaH powder. MAO powder was obtained by evaporating a 30% solution in toluene from Albemarle. CpNa was prepared from NaH and freshly distilled CpH.[175] $ZrCl_4$•2THF was prepared according to Manzer's procedure.[182] Solvents were purified according to the method described by Grubbs and coworkers.[174] Solution NMR spectra were recorded on a JEOL Eclipse-500 instrument (500 MHz for ^1H, 125 MHz for ^{13}C). ^{13}C CPMAS NMR spectra were recorded on a MSL-300 instrument (75.5 MHz for ^{13}C). FT-IR spectra were recorded on a Perkin Elmer-1600 instrument. MALDI-TOF MS experiments were carried out on a Kratos Kompact SEQ spectrometer. Elemental analyses were performed by either Desert Analytics (Tucson, AZ) or Oneida Research Services (Whitesboro, NY). GPC analyses of polymer samples were carried out by Dow Chemical (Midland, MI). Crystal structures were obtained by either a Siemens P4 diffractometer or a Enraf-Nonius Kappa CCD diffractometer.

Preparation of Ph_2MeSi-C_5H_4Li.[179,183] The lithium salt of the cyclopentadienyl ligand (Ph_2MeSi-C_5H_4Li) was prepared according to the route shown in Scheme 3-15. First,

[182] Manzer, L. E.: *Inorg. Synth.* **21**, 135-140 (1987).
[183] Kira, M.; Watanabe, M.; Sakurai, H.: *J. Am. Chem. Soc.* **99(24)**, 7780-7785 (1977).

(diphenylmethylsilyl)cyclopentadiene (Ph_2MeSi-C_5H_5) was prepared from cyclopentadienyl-sodium (CpNa) and (chlorodiphenylmethyl)silane ($Ph_2MeSiCl$) using the reported method.[183] Our procedure follows. To a solution of CpNa (3.28 g, 37.2 mmol) in THF at 0 ^oC was added $Ph_2MeSiCl$ (8.68 g, 37.3 mmol) using a syringe. The ice-bath was removed and the solution was stirred for 15 h and then evaporated. The residue was hydrolyzed with a mixture of hexane and H_2O. The water layer was separated. The hexane layer was dried over anhydrous $MgSO_4$, filtered, and evaporated to afford a yellow oil. Distillation (b.p. 107-123 ^oC at 0.07 torr, lit. b.p. 128 ^oC at 0.5 torr) afforded 6.15 g (23.4 mmol, 63%) of a colorless oil, which was found to be mostly Ph_2MeSi-C_5H_5 by ^1H NMR analysis. A solution of distilled Ph_2MeSi-C_5H_5 (4.77 g, 18.2 mmol) in hexanes at 25 ^oC was treated with excess butyllithium (1.6 M in hexanes, 15 mL, 24 mmol) with stirring for 15 h. The pale precipitate formed was collected on a filter, washed with pentane, and dried under vacuum to afford 3.95 g (14.7 mmol, 81%) of the desired organolithium compound as a white powder, which was found to be pure by NMR analysis. ^1H NMR (THF-d_8): δ 7.55 (m, 4 H), 7.20 (m, 6 H), 6.08 (m, 2 H), 5.98 (m, 2 H), 0.66 (s, 3 H). ^{13}C NMR (THF-d_8): δ 141.7 (C), 134.9 (CH), 127.7 (CH), 126.9 (CH), 112.9 (CH), 106.5 (CH), 103.5(C), -2.5 (CH_3). Anal. Calcd for $C_{18}H_{17}LiSi$: C, 80.56; H, 6.39. Found: C, 70.93, H, 6.09. We suspect the poor analysis results from inorganic impurities such as LiOH or LiCl in the product.

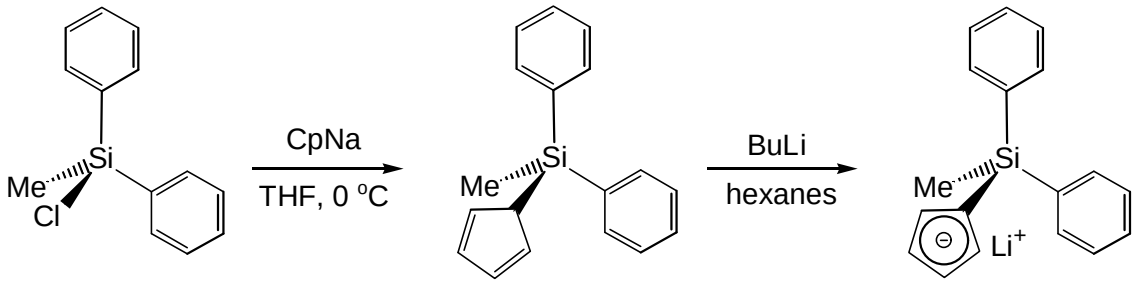

Scheme 3-15 Preparation of Ph_2MeSi-C_5H_4Li [183]

Synthesis of (h^5-Ph_2MeSi-$C_5H_4)_2ZrCl_2$. A suspension of $ZrCl_4$•2THF (1.13 g, 3.00 mmol) and Ph_2MeSi-C_5H_4Li (1.70 g, 6.40 mmol) in toluene (60 mL) was heated under reflux for 3 h. The resulting orange mixture was cooled and filtered. Evaporation of the filtrate afforded an orange residue, which was recrystallized from toluene to produce 1.22 g (1.80 mmol, 60%) of yellow crystals in three crops. ^{1}H NMR ($CDCl_3$): δ 7.37 (m, 20 H, C_6H_5), 6.49 (m, 4 H, C_5H_4), 6.05 (m, 4 H, C_5H_4), 0.89 (s, 6 H, $SiCH_3$). ^{13}C NMR ($CDCl_3$): δ 136.0 (C), 135.2 (CH), 129.8 (CH), 128.0 (CH), 125.8 (CH), 120.7 (C) 119.5 (CH), -3.5 (CH_3). Anal. Calcd for $C_{36}H_{34}Cl_2Si_2Zr$: C, 63.13; H, 5.00. Found: C, 63.45; H, 5.11. Crystals suitable for single-crystal X-ray diffraction were grown by allowing a hot toluene solution of the complex to cool and stand at room temperature.

Synthesis of (h^5-Ph_2MeSi-$C_5H_4)_2ZrBr_2$. The synthesis of (η^5-Ph_2MeSi-$C_5H_4)_2ZrBr_2$ used the THF adduct of zirconium tetrabromide, $ZrBr_4$•2THF, and Ph_2MeSi-C_5H_4Li. $ZrBr_4$•2THF was prepared by adding THF (12.2 mL, 0.150 mol) to a rapidly stirred suspension of $ZrBr_4$ (20.5 g, 50.0 mmol) in 100 mL CH_2Cl_2 maintained at 0 ^{o}C.[182] The resulting yellow mixture was stirred at 25 ^{o}C overnight. The suspension was filtered, and the product was washed with CH_2Cl_2 and dried under vacuum to afford 9.45 g of an off-white powder. Some additional product was obtained by concentrating the filtrate. ^{1}H NMR (acetone-d_6): δ 1.78 (m, 8 H), 3.63 (m, 8 H). Anal. Calcd for $C_8H_{16}Br_4O_2Zr$: C, 17.31; H, 2.91. Found: C, 17.05; H, 2.95. The ^{1}H NMR spectra shown in Figure 3-7 distinguish clearly the coordinated THF from a spectrum of free THF (1.78 and 3.61 ppm). Although the chemical shifts of free and bound THF are nearly the same, the coupling patterns are distinctive. The procedure to synthesize (η^5-Ph_2MeSi-$C_5H_4)_2ZrBr_2$ was the same as that to synthesize (η^5-Ph_2MeSi-$C_5H_4)_2ZrCl_2$. A yellow suspension of 2.78 g $ZrBr_4$•2THF (5.00 mmol) and 2.68 g Ph_2MeSi-C_5H_4Li (10.0 mmol) in 50 mL

anhydrous toluene was refluxed for 15 h. The suspension was then filtered and the yellow solution was evaporated in vacuum. The residue was recrystallized from toluene to afford 1.79 g yellow-green crystallites (2.31 mmol, 46%). ^{1}H NMR ($CDCl_3$): δ 7.36 (m, 20 H, C_6H_5), 6.52 (m, 4 H, C_5H_4), 6.21 (m, 4 H, C_5H_4), 0.87 ppm (s, 6 H, $SiCH_3$). ^{13}C NMR ($CDCl_3$): δ 135.8 (C), 135.1 (CH), 129.9 (CH), 128.1 (CH), 126.4 (CH), 120.0 (CH), 118.8 (C), and -3.2 ppm ($SiCH_3$). Anal. Calcd for $C_{36}H_{34}Br_2Si_2Zr$: C, 55.87; H, 4.43. Found: C, 56.26; H, 4.40.

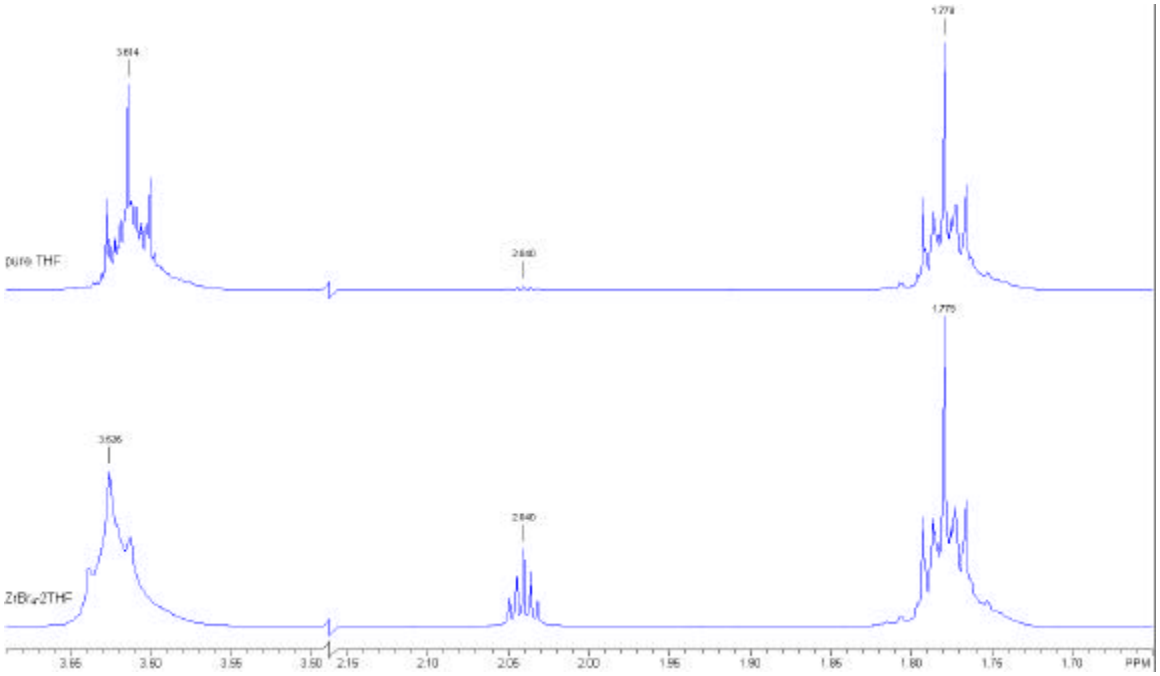

Figure 3-7 Comparison of the 500 MHz ^{1}H NMR Spectra of THF and $ZrBr_4$•2THF

Reaction of (h^5-Ph_2MeSi-$C_5H_4)_2ZrCl_2$ with BCl_3. A solution of (η^5-Ph_2MeSi-$C_5H_4)_2ZrCl_2$ (0.31 g, 0.45 mmol) in CH_2Cl_2 was treated with BCl_3 (3.6 mL, 1.0 M in CH_2Cl_2, 36 mmol). The solution was refluxed for 15 h in a Kalrez o-ring sealed reactor. After cooling, the volatile components were evaporated. The black residue was extracted with hot CH_2Cl_2/hexanes, the filtrate was evaporated, and the residue was then analyzed by ^{1}H NMR. The analysis of the complicated mixture is described in the text (Section 3.3.1).

Synthesis of (h^5-Br_2MeSi-$C_5H_4)_2ZrBr_2$. 2.0 mL of pure BBr_3 (21 mmol) was injected into a solution of 0.34 g (η^5-Ph_2MeSi-$C_5H_4)_2ZrCl_2$ (0.50 mmol) in CH_2ClCH_2Cl at 25 ^oC. The solution mixture was refluxed for 15 h, and then the volatile components were evaporated. The solid residue was recrystallized from hexanes/CH_2Cl_2 to afford 0.31 g (0.39 mmol, 79%) of yellow-green needles. ^1H NMR ($CDCl_3$): δ 7.07 (m, 4 H, C_5H_4), 6.73 (m, 4 H, C_5H_4), 1.46 (s, 6 H, $SiCH_3$). ^{13}C NMR ($CDCl_3$): δ 126.7 (CH), 118.04 (CH), 118.00 (C), 10.2 ($SiCH_3$). Anal. Calcd for $C_{12}H_{14}Br_6Si_2Zr$: C, 18.36; H, 1.80. Found: C, 18.51; H, 1.65. Single crystals of (η^5-Br_2MeSi-$C_5H_4)_2ZrBr_2$ suitable for X-ray crystallography were grown by adding CH_2Cl_2 to a hot suspension of (η^5-Br_2MeSi-$C_5H_4)_2ZrBr_2$ in hexanes until all of the (η^5-Br_2MeSi-$C_5H_4)_2ZrBr_2$ was dissolved, and then allowing the hot, saturated solution to cool to 25 ^oC.

Synthesis of $(C_{12}H_{14}Br_2O_2Si_2Zr)_n$. A sample of ($\eta^5$-$Br_2MeSi$-$C_5H_4)_2ZrBr_2$ (0.356 g, 0.453 mmol) was exposed to air for several days to afford 0.224 g of a yellow-gray solid. The weight loss (calcd 36.6%, found 37.1%) and the elemental analysis (Anal. Calcd for $C_{12}H_{14}Br_2O_2Si_2Zr$: C, 28.97; H, 2.84; Found: C, 28.59; H, 2.49) were consistent with the replacement of two bromine atoms by oxygen. The "gray solid" was only sparingly soluble in common solvents, such as $CDCl_3$, THF-d_8, hexanes, toluene, and benzene. Of these, THF affords the highest solubility (3.5 mg in 2 mL of THF-d_8). The hydrolysis of (η^5-Br_2MeSi-$C_5H_4)_2ZrBr_2$ in toluene solution was also investigated. Pure (η^5-Br_2MeSi-$C_5H_4)_2ZrBr_2$ (430 mg, 0.55 mmol) was dissolved in 30 mL toluene, about 4 equivalents of deionized water (0.040 mL, 2.2 mmol) was then added to the solution by a micro-syringe. The water added did not dissolve in toluene but formed drops. After the mixture was stirred rigorously to allow sufficient reaction at 25 ^oC for 15 h, an orange precipitate was formed. The suspension was centrifuged, and the precipitate was separated from the solution, washed with CH_2Cl_2, and dried in vacuum. The

mass of the precipitate was 83 mg, less than 20% of that of the starting (η^5-Br_2MeSi-$C_5H_4)_2ZrBr_2$.

Methylation of the "Gray Solid". A small portion of the gray solid (5 mg) was suspended in 10 mL of C_6D_6 in a sealed vial in the glove box. The solid did not dissolve completely. The suspension was allowed to settle, and then about 0.8 mL of the supernatant was decanted into a J-Young NMR tube. ^{1}H NMR spectrum in C_6D_6 showed only a very weak signal at 0.35 ppm (SiMe). Then, methyllithium (8.8 mg) was added to the vial. The mixture was stirred at 25 ^{o}C for 15 h. The suspension was allowed to settle. The supernatant was subjected to ^{1}H NMR analysis. ^{1}H NMR (C_6D_6, stronger signals): δ 6.37 (m, 2 H), 6.32 (m, 2 H), 6.16 (m, 2 H), 6.13 (m, 2 H), 0.37 (s, 6 H), -0.01 (s, 3 H), -0.05 (s, 3 H).

Solution Ethylene Polymerization Procedure. The diagram in Figure 3-8 shows the setup of the reactor and the procedure of a typical solution polymerization experiment. The capacity of the glass kettle is about one liter. The kettle has two parts, which are sealed with an o-ring flange. The upper part of the kettle is fitted with a thermocouple, a Teflon-sealed overhead stirrer shaft, a gas outlet (for nitrogen or vacuum), a gas dispersion tube for introducing ethylene monomer, and a utility port that could be either sealed with a septum or opened to introduce catalysts and other reagents. In a typical polymerization experiment, the glass parts of the reactor were well baked in an oven. The parts were assembled into a reactor, which was then evacuated when it was still hot. The reactor was back-filled with N_2, into which about 400 mL of anhydrous toluene was transferred. The toluene in the reactor was stirred and regulated at 50 ^{o}C using a servo-controlled water bath under N_2 protection, and about 50 mg of MAO was added as the scavenger for residual O_2 and H_2O in the reactor. Then, purified ethylene was introduced through the dispersion tube to saturate the toluene and to stabilize the monomer flow. After the

temperature was stabilized at 50 ^{o}C, an aliquot of typically 1.00 mL of a solution containing a predetermined amount of a catalyst was injected into the reactor through the septum to initiate the polymerization. The catalyst solution was prepared in glove box by mixing typically 1.00 mL of a stock solution of a zirconocene compound of a known concentration with excess MAO (typically Al:Zr = 5000) in a 10-mL volumetric flask. The mixture was then diluted with toluene to the mark and stirred sufficiently. The polymerization time was accurately controlled using a stopwatch, and the polymerization was terminated by injecting a large quantity of 5% HCl in methanol into the reactor when the desired polymerization time was reached. The amount of catalyst used in each experiment was controlled and fast stirring was applied, so that the temperature jump at the beginning of each polymerization experiment was only about 1 ^{o}C or less. The polyethylene product from each experiment was separated from the solvent by filtration, washed with methanol, and dried at about 75 ^{o}C in vacuum oven overnight. The mass of the polyethylene product from each experiment was then measured, and the mean and standard deviation in the activity of each catalyst was calculated from the yields of three identical experiments. Since the solubility of the polymeric zirconocene compound in toluene is low, though the stock solution prepared by dissolving 2.5 mg of the gray solid in toluene (total volume was 10.00 mL, 5.0×10^{-7} mol/mL) looked clear, two activity values were obtained using the as-prepared stock solution and the stock solution that was filtered through a glass frit, respectively. The polyethylene products were also sent to Dow Chemical Company (Midland, Michigan) for GPC analysis to get their molecular weights (M_n and M_w), polydispersity indices (PDI, M_w/M_n), and molecular weight distribution curves.

Figure 3-8 The Apparatus for the Homogeneous Polymerization Experiment

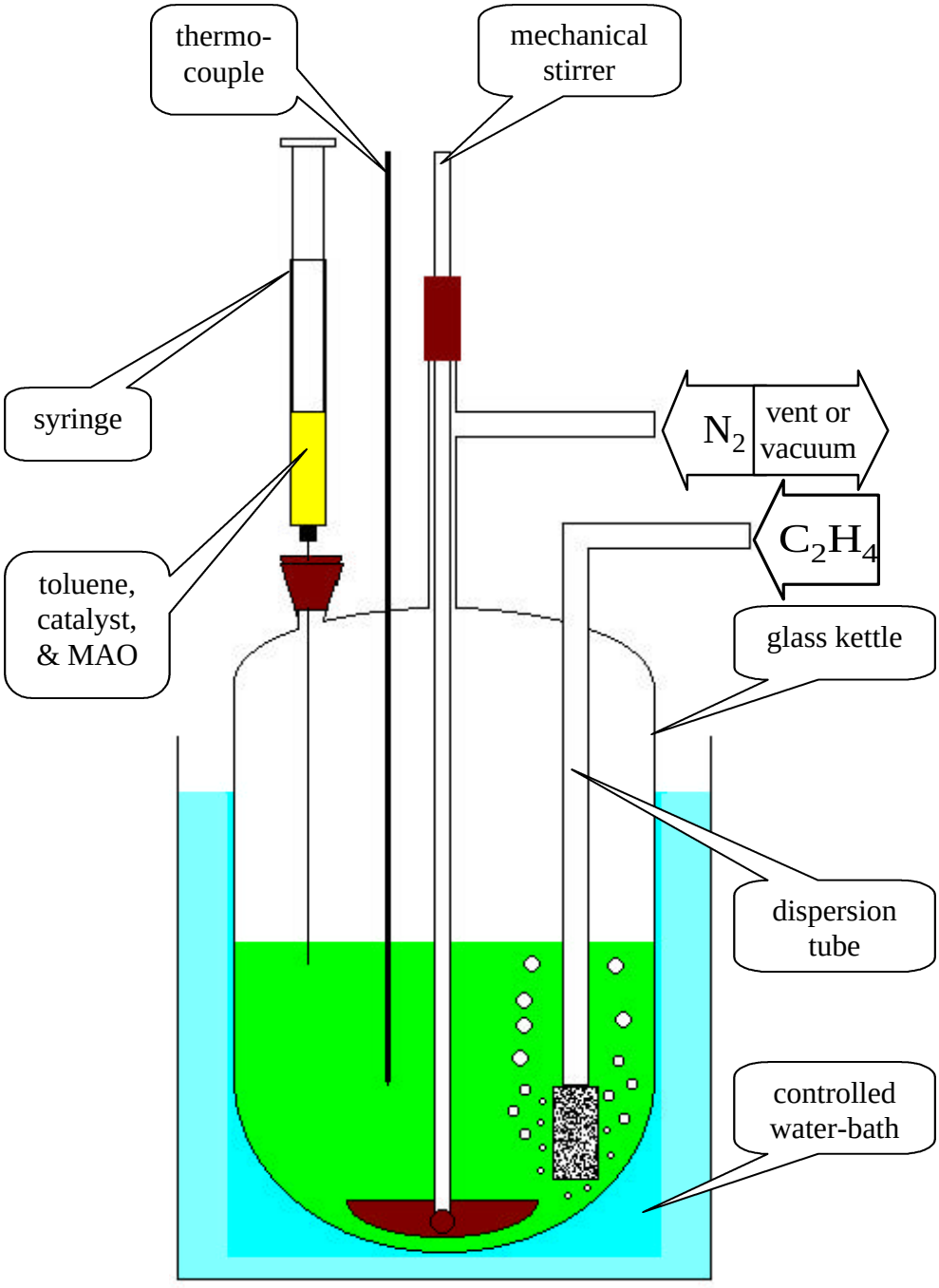

3.6 Conclusions

The Ph_2MeSi-substituted zirconocene compound, $(\eta^5\text{-}Ph_2MeSi\text{-}C_5H_4)_2ZrCl_2$, was synthesized by the metathesis reaction of $Ph_2MeSi\text{-}C_5H_4Li$ with $ZrCl_4$•2THF. The Si-Ph bonds

were more reactive than the Si-Me bonds toward electrophilic cleavage by BCl_3 and BBr_3. The fully brominated compound, $(\eta^5\text{-}Br_2MeSi\text{-}C_5H_4)_2ZrBr_2$, was synthesized by the reaction of $(\eta^5\text{-}Ph_2MeSi\text{-}C_5H_4)_2ZrCl_2$ with BBr_3 in CH_2ClCH_2Cl under reflux. Similar to other halosilyl-substituted zirconocene compounds, $(\eta^5\text{-}Br_2MeSi\text{-}C_5H_4)_2ZrBr_2$ also hydrolyzed easily with moisture in air and formed a gray solid that was barely soluble in common solvents. Based on the analytic and spectroscopic evidence as well as the hydrolysis chemistry of similar halosilyl-substituted zirconocene compounds, the gray solid was proposed to be a polymeric zirconocene compound with a stereoregular polysiloxane backbone. The gray solid had an activity for ethylene polymerization close to that of Cp_2ZrCl_2 with MAO cocatalyst. The narrow polydispersity of the polyethylene produced by the gray solid indicated that the polymeric zirconocene catalyst behaved like homogeneous zirconocene catalysts.

Chapter 4 Immobilization of Zirconocene Compounds on Silica and Ethylene Polymerization Using the Immobilized Catalysts

4.1 Pretreatment of Silica and Immobilization of the Zirconocene Compounds

Some general features of silica were presented in Section 1.3.1.1. Due to its porous structure and large surface area, amorphous silica is most commonly used to prepare immobilized metallocene catalysts. Many brands of amorphous silica are available commercially. We used Grace 948 silica, which is a white fluffy powder with an average particle size of 55.7 μm, a pore volume of 1.6 mL/g, and a surface area of 309 m^2/g.

The as-purchased silica contained a large quantity of surface hydroxyl groups and adsorbed water molecules, which are harmful to polymerization. Studies elsewhere showed that supported metallocene catalysts prepared using silica that was not sufficiently dehydrated had poor activities.[89,90,184] On the other hand, the zirconocene compounds in this research require surface hydroxyl groups to form covalent tethers, and a sufficient surface density of hydroxyl groups on silica is necessary for the formation of multiple tethers. Therefore, it is necessary to dehydrate the as-purchased silica properly before it is used in the preparation of immobilized zirconocene catalysts in this research. In the crystal structure of $(\eta^5\text{-}Br_2MeSi\text{-}C_5H_4)_2ZrBr_2$, the distance between the two Si atoms is 0.7640 nm. Since the molecule is flexible in solution, when the molecule is immobilized on silica, the distance may change in order to adapt to the distance between hydroxyl groups on silica. According to calculated and experimental data in the literature,[86,185] amorphous silica dehydrated at 500 ^oC in vacuum (about $2x10^{-5}$ torr) has a surface density of 2-3 hydroxyl groups per square nanometer, assuming a random distribution of the hydroxyl groups. A surface density of 2-3 OH/nm^2 on silica is about right for the immobilization

[184] Collins, S.; Kelly, W. M.; Holden, D. A.: *Macromolecules* **25(6)**, 1780-1785 (1992).
[185] Shapiro, I.; Weiss, H. G.: *J. Phys. Chem.* **57**, 219-221 (1953).

of (η^5-$BrMe_2Si$-$C_5H_4)_2ZrBr_2$ or (η^5-Br_2MeSi-$C_5H_4)_2ZrBr_2$ molecules. Therefore, the silica samples used in this research were all dehydrated at 500 ^oC in vacuum.

Functionalized metallocenes were immobilized on the partially dehydroxylated silica (PDS) in the presence or absence of NEt_3 (HBr scavenger). From a series of preliminary experiments, we found that NEt_3 facilitated the immobilization under mild conditions (1 h, 25 ^oC), whereas harsher conditions (15 h, 50 ^oC) were required in the absence of NEt_3. It remains unclear whether NEt_3 merely scavenges HBr after formation of an Si-O-Si linkage (preventing the reverse reaction), or if the NEt_3 serves to deprotonate surface silanol groups, activating them toward nucleophilic attack on the metallocene functional groups.

One primary means of determining the success of immobilization was to analyze, using ^1H NMR, the residues obtained after washing the metallocene-treated silica with dichloromethane. Of course, when NEt_3 was used, $HNEt_3Br$ dominated the residue spectrum. Some unknown minor impurities were also observed, but the signals from the original functionalized zirconocene compounds were never observed. Therefore, the residues were not further characterized, and we assumed that the sample of the zirconocene compound was totally immobilized onto silica in each preparation using NEt_3. The zirconium loading was calculated from the amounts of the samples used.

In the preparations where no NEt_3 was added, the proton NMR spectrum of the yellow residue in $CDCl_3$ showed several weak multiplets in the Cp region and a dense cluster of signals centered at 0.44 ppm in the Si-Me region. The proton NMR spectrum suggested that the yellow residue was a mixture of some oligomeric zirconocene compounds with structures similar to the hydrolysis product of (η^5-Br_2MeSi-$C_5H_4)_2ZrBr_2$ discussed in Section 3.4. Therefore, the zirconium loadings of the immobilized products could not be calculated from the amounts of the

zirconocene compound and the silica used in the preparation. The amount of zirconium in the residue was also too small to weigh accurately. Therefore the zirconium loadings of these silica samples were determined using elemental analysis.

Figure 4-1 The Apparatus for the Slurry Polymerization Experiment

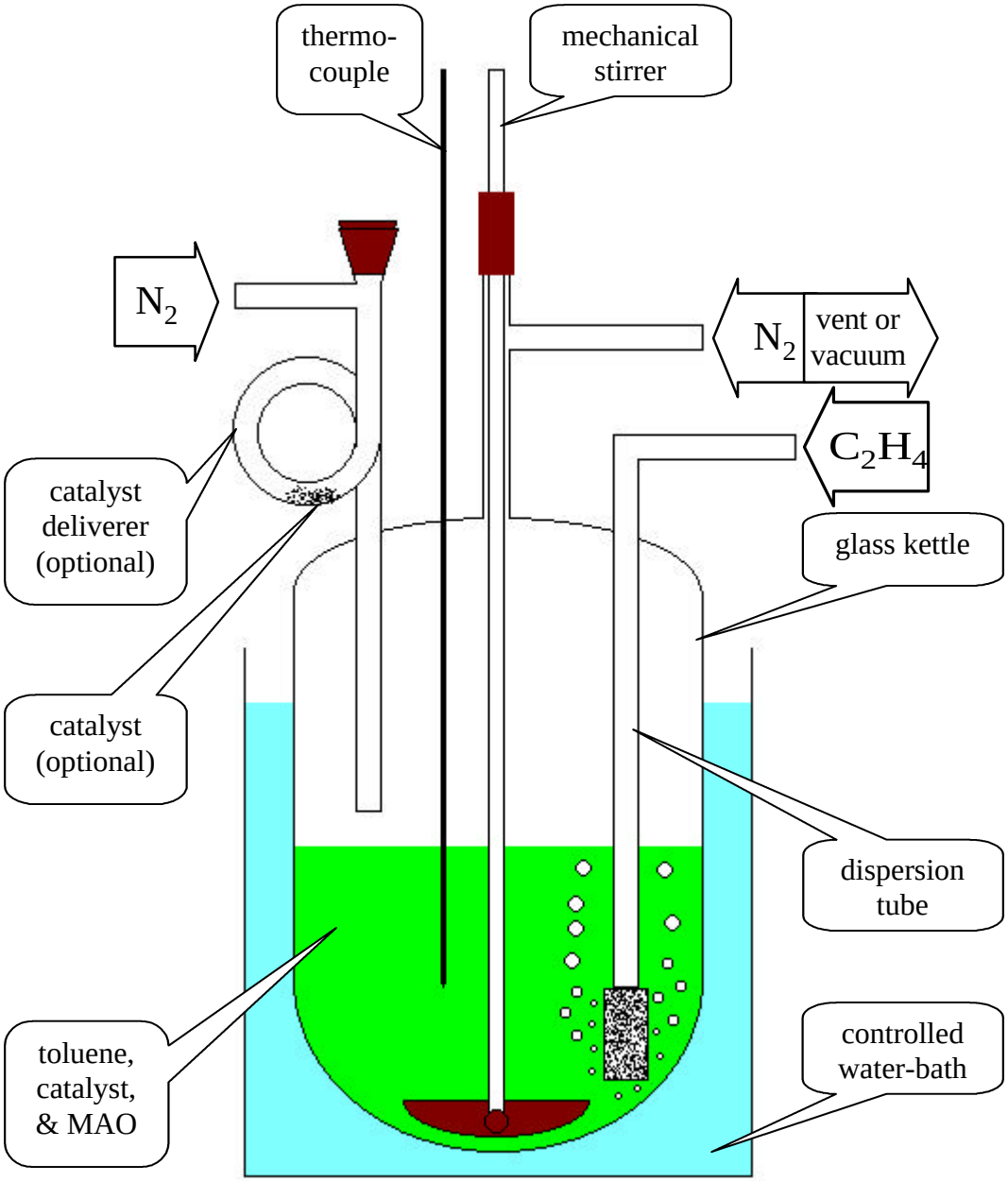

4.2 Descriptions of the Activity Evaluation Experiment and the Leaching Experiment

The catalytic activities of the immobilized zirconocene catalysts were evaluated for ethylene polymerization using MAO as the cocatalyst. The activity evaluation experiments were carried out using the slurry polymerization process in a bench-top reactor. The diagram of the set-up of the reactor used in the research for the slurry polymerization experiments is shown in Figure 4-1. Details of the polymerization reactions are provided in Section 4.5, but here we briefly summarize and discuss the two main methods by which catalysts were tested for activity. In our preliminary method, the reactor was charged with toluene and MAO and saturated with ethylene, and then a small catalyst charge was blown into the reactor using a spiral tube. In our improved method, the reactor was charged with catalyst and MAO first, then toluene, and then polymerization was initiated by the inrush of ethylene. In the second method, we were careful to pre-heat the toluene before adding it to the reactor, so that the catalyst would not be exposed to MAO solution too long. We found that the "preliminary" method provided much lower activities, probably because an immobilized catalyst needs a significant initiation period to be wetted by solvent and activated by MAO. In the second method, wetting and activation probably occur during the few minutes prior to the reaction when the temperature is being stabilized.

We also devised an experimental means of determining whether the catalysts could be "leached" from the support during activation and/or polymerization. To analyze for leaching, we set up an apparatus (Figure 4-2) in which the catalyst could be pretreated with MAO solution at 50 ^{o}C for 10 min, which modeled the reaction conditions. Then, the catalyst slurry was filtered into the reactor. Any activity in the filtrate would be a sensitive test for catalyst leaching. The results of those experiments are discussed in detail in Section 4.4.2.

Figure 4-2 The Apparatus for the Leaching Experiment

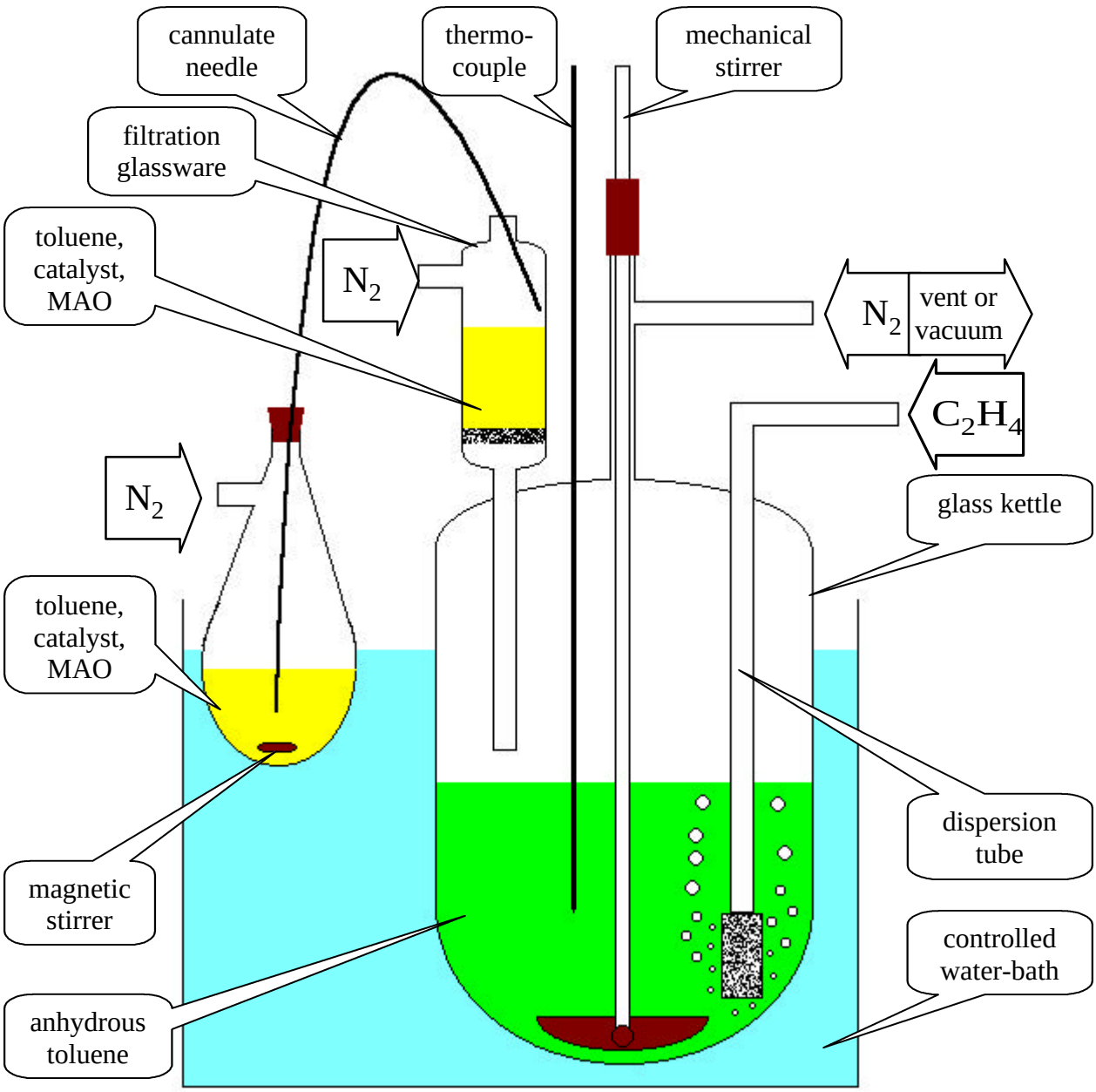

4.3 Ethylene Polymerization Results of Different Immobilized Zirconocene Catalysts

The major goal of the polymerization experiments using the immobilized zirconocene catalysts was to investigate the effects of the number and structure of the tethers of the precursor zirconocene compounds on the performance of the immobilized catalysts. Besides, in the

immobilization process, many factors may also affect the performance of the immobilized catalysts, so it is necessary to investigate the effects of these factors in order to optimize the immobilization process. Therefore, some immobilized zirconocene catalysts using the same precursor zirconocene compound were prepared under different immobilization conditions, and their catalytic performance for ethylene polymerization was investigated. The results are discussed in the following sections.

4.3.1 Effect of Tether Number and Structure

Table 4-1 Ethylene Polymerization Data for Some Immobilized Zirconocene Compounds Containing Different Tethers

Precursor of Immobilized Catalyst	Activity (kg/mol(Zr)/h	M_p ($x10^{-5}$)	M_n ($x10^{-5}$)	M_w ($x10^{-5}$)	M_z ($x10^{-5}$)	PDI (M_w/M_n)
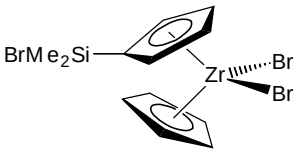	5.8(4) x 10^3	5.17	3.62	8.66	18.0	5.10
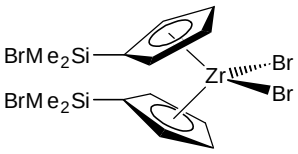	1.32(9) x 10^3	5.63	1.26	8.39	21.7	6.65
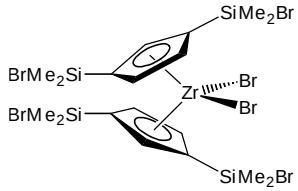	3.1(1) x 10^2	4.30	1.10	7.82	22.1	7.09
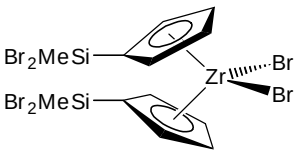	6.0(6) x 10^2	5.95	1.69	9.02	21.5	5.32

- Immobilized catalysts were prepared using excess NEt_3, and the Zr loadings were all about 1.1%.

The ethylene polymerization data in Table 4-1 are those of several immobilized zirconocene catalysts that were prepared using precursor zirconocene compounds of different tether numbers and structures, i.e., (η^5-$BrMe_2Si$-C_5H_4)$CpZrBr_2$, (η^5-$BrMe_2Si$-C_5H_4)$_2ZrBr_2$, [η^5-1,3-($BrMe_2Si$)$_2C_5H_3$]$_2ZrBr_2$, and (η^5-Br_2MeSi-C_5H_4)$_2ZrBr_2$, which can theoretically form one single-tether, two single-tethers, four single-tethers, and two double-tethers, respectively. The preparation conditions of the immobilized catalysts were the same. The zirconium loadings were all about 1.1%, and excess NEt_3 was used in the immobilization of all the catalysts.

The data show that the activities of the immobilized catalysts for ethylene polymerization were much lower than that of the homogeneous Cp_2ZrCl_2 catalyst ($1.6x10^5$ kg/mol/h) with MAO cocatalyst. This is a common phenomenon for immobilized catalysts, probably due to the reduced accessibility of the active centers on the support surface. The activities of the immobilize catalysts decreased with increasing number of single-tethers: the activity of immobilized (η^5-$BrMe_2Si$-C_5H_4)$CpZrBr_2$ was almost 20 times that of immobilized [η^5-1,3-($BrMe_2Si$)$_2C_5H_3$]$_2ZrBr_2$. This result probably suggests that the flexibility of an active center on the support surface decreases with increasing number of tethers, and thus, the catalytic activity also decreases with increasing number of tethers. The activity of immobilized (η^5-Br_2MeSi-C_5H_4)$_2ZrBr_2$ was twice that of immobilized [η^5-1,3-($BrMe_2Si$)$_2C_5H_3$]$_2ZrBr_2$, but about half that of immobilized (η^5-$BrMe_2Si$-C_5H_4)$_2ZrBr_2$. A speculative explanation of this result is that two double-tethers allow more flexibility than four single-tethers, but one double-tether is still less flexible than one single-tether. All of these "conclusions" are predicated on the assumption that the compounds are supported in the hypothesized "face-up" manner. Nevertheless, we believe the flexibility difference causes the activity difference of the immobilized catalysts. The molecular weights of the polyethylene products were similar. The large polydispersity indices

(PDI) indicate that the molecular weight distributions of the polyethylene products were broad and in some cases bimodal. Therefore, the immobilized zirconocene catalysts still have multi-site behavior. However, it is worth pointing out that the PDI of the polyethylene product from immobilized $(\eta^5\text{-}Br_2MeSi\text{-}C_5H_4)_2ZrBr_2$ was significantly lower than those of the other polyethylene products. ^1H NMR analysis showed that the polymer products were highly linear.

4.3.2 Effect of Triethylamine

Three immobilized catalysts using the same precursor zirconocene compound, $(\eta^5\text{-}Br_2MeSi\text{-}C_5H_4)_2ZrBr_2$, were prepared. The difference among the three immobilized catalysts were that the first one was prepared using an excess of NEt_3 in a room-temperature immobilization process, the second one was prepared using an exactly stoichiometric amount of NEt_3, and the third one was prepared without NEt_3 but at higher temperatures and longer reaction times.

Table 4-2 Ethylene Polymerization Data for Several Immobilized $(h^5\text{-}Br_2MeSi\text{-}C_5H_4)_2ZrBr_2$ Prepared Using Different Amount of NEt_3

Quantity of NEt_3 Used in Preparation	Activity (kg/mol(Zr)/h	M_p ($x10^{-5}$)	M_n ($x10^{-5}$)	M_w ($x10^{-5}$)	M_z ($x10^{-5}$)	PDI (M_w/M_n)
Excess NEt_3	6.0(6) x 10^2	5.95	1.69	9.02	21.5	5.32
Stoichiometric NEt_3	1.0(2) x 10^3	6.84	0.61	9.75	22.3	16.0
No NEt_3 But Refluxed	2.35(6) x 10^3	5.80	1.47	8.55	20.7	5.81

- The Zr loadings in the first two immobilized catalysts were about 1.1%, and the Zr loading in the immobilized catalyst prepared without NEt_3 was 0.42% as determined by elemental analysis.

The data in Table 4-2 show that the activities of the immobilized catalysts increased with decreasing amount of NEt_3 used. The activity of the immobilized catalyst prepared without using NEt_3 was about four times that of the immobilized catalyst prepared using excess NEt_3. It should be noted that the zirconium loading of the immobilized catalyst prepared without using NEt_3 (0.42%), which was determined by elemental analysis, was significantly lower than those prepared using NEt_3 (1.1%). The result can probably be explained by the different reactivities of the Si-Br bonds and Zr-Br bonds in $(\eta^5\text{-}Br_2MeSi\text{-}C_5H_4)_2ZrBr_2$ molecules. As mentioned in Section 1.4.2, the Si-Br bond is more susceptible to nucleophilic substitution than the Zr-Br bond. The model study described in Section 5.1 also showed that the Si-OH group in $^tBuMe_2SiOH$ only react with the Si-Br bond in $(\eta^5\text{-}BrMe_2Si\text{-}C_5H_4)CpZrBr_2$ to form $[\eta^5\text{-}(^tBuMe_2SiO)Me_2Si\text{-}C_5H_4]CpZrBr_2$, and the Zr-Br bonds were intact, if no NEt_3 was used in the reaction. Therefore, it is reasonable to assume that the zirconocene molecules in the immobilized catalyst prepared without using NEt_3 was bonded to the support only through the Si-O-Si linkages of the tethers. However, when NEt_3 was used in the preparation, especially excess amount of NEt_3 was used, the Zr-Br bonds may also react with surface hydroxyl groups to form Si-O-Zr linkage between the metal center and the support surface, which would poison the metal center and cause decrease of the activity. The model study in Section 5.1 also found more complicated products in the reaction between $^tBuMe_2SiOH$ and $(\eta^5\text{-}BrMe_2Si\text{-}C_5H_4)CpZrBr_2$, if NEt_3 was used. The molecular weights of the polyethylene products from the immobilized catalysts prepared using different amount of NEt_3 had no significant difference. However, the PDI of the immobilized catalyst prepared using stoichiometric amount of NEt_3 was much higher than the other two. The molecular weight distribution curve showed two components in the

polymer product from the immobilized catalyst prepared using stoichiometric amount of NEt_3. Possibly, this procedure resulted in a combination of tethering arrangements.

4.3.3 Effect of Zirconium Loading

It was frequently found in the literature that high loading of a metallocene precursor on a supporting material decreased the polymerization activity of the immobilized catalyst,[92] presumably due to the interaction between two active centers on the support surface if they locate close enough to each other. In order to investigate the effect of zirconium loading to the activity of the immobilized catalysts in this research, two immobilized zirconocene catalysts were prepared using $(\eta^5\text{-}Br_2MeSi\text{-}C_5H_4)_2ZrBr_2$ as the precursor compound. The zirconium loading of one immobilized catalyst was 1.1%, and that of the other was about 0.28%. The other immobilization conditions were the same, e.g., excess NEt_3 were used in both preparations.

Table 4-3 Ethylene Polymerization Data for Immobilized $(h^5\text{-}Br_2MeSi\text{-}C_5H_4)_2ZrBr_2$ of Different Zr Loadings

Zr Loading on Silica	Activity (kg/mol(Zr)/h	M_p ($x10^{-5}$)	M_n ($x10^{-5}$)	M_w ($x10^{-5}$)	M_z ($x10^{-5}$)	PDI (M_w/M_n)
1.1%	$6.0(6) \times 10^2$	5.95	1.69	9.02	21.5	5.32
0.28%	$1.08(7) \times 10^3$	4.53	1.09	7.94	19.1	7.29

- The immobilized catalysts were prepared using excess NEt_3.

The polymerization data showed that ethylene polymerization activity of the immobilized catalysts of 0.28% zirconium loading was indeed significantly higher than that of the immobilized catalyst of 1.1% zirconium loading (Table 4-3). The molecular weights of the polyethylene product from the 1.1% immobilized catalyst was significantly higher than that from

the 0.28% immobilized catalyst, but the PDI of the polyethylene product from the 1.1% immobilized catalyst was significantly smaller than that from the 0.28% immobilized catalyst.

4.4 Catalyst Leaching of the Immobilized Zirconocene Catalysts

4.4.1 Catalyst Leaching of Immobilized Metallocene Catalysts in the Literature

An important aspect of the immobilized metallocene catalysts is the stability of the active species on the supports. Unstable active species of the immobilized catalysts may leave or migrate on the support during polymerization, causing many problems. In the slurry polymerization process, if unstable active species leave the support and become free in the solution, they just act as homogeneous catalyst and polymerize monomers. The polymer produced by the freed active species in solution causes poor morphology of the polymer product and reactor fouling. Reactor fouling means that the polymer produced by the freed active species will adhere to the surface of the mechanical stirrer or the internal surface of the reactor and form a polymer layer, so the efficiency of the stirrer and the heat-transfer efficiency of the reactor were greatly reduced. In the gas-phase polymerization process, the migration of unstable active species from interior of the catalyst particles to the surface will result in polymer product of poor molecular weight distribution and micro-structural dispersion, etc. Both poor morphology and reactor fouling are manifestations of "catalyst leaching". Catalyst leaching has been found in many immobilized catalysts.

Table 4-4 lists the results of the leaching experiments of some silica-supported metallocene catalysts found in the literature. The silica-supported metallocene catalysts that have been investigated for catalyst leaching include examples prepared by each of the three major preparation methods, i.e., direct deposition, pre-alumination, and covalent tethering. Some of the results are contradictory. Tait and coworkers deposited Cp_2ZrCl_2 directly on unmodified

silica, which was dehydrated at 450 ^{o}C. The product was treated with MAO solution and then filtered. They found that the filtrate was highly active for ethylene polymerization.[186] Similarly, after the silica-supported Cp_2ZrMe_2 prepared by the directed deposition method was treated with MAO solution, the filtered solution could polymerize ethylene with high activity.[187] Semikolenova and Zakharov also found that the polyethylene from the filtered solution determined the properties of the polyethylene product of the immobilized catalyst. On the contrary, Sacchi, et al. found no significant ethylene polymerization activity from the filtered solution obtained by treatment of Cp_2ZrCl_2/SiO_2 with MAO solution, while the filtered solid Cp_2ZrCl_2/SiO_2, was highly active for ethylene polymerization.[188]

Kaminsky and Strübel prepared silica-supported Cp_2ZrCl_2 by the pre-alumination method.[189] After the immobilized catalyst was treated with MAO solution, they found that the ethylene polymerization activity of the filtered solution was about 37% of the activity of the original immobilized catalyst with MAO cocatalyst. ICP-OES analysis showed about 40% loss of zirconium from the immobilized catalyst after treatment with MAO solution. Toluene alone did not abstract zirconocene species away from the support. Similar results were obtained by Semikolenova and Zakharov,[187] as well as Sacchi and coworkers.[188] On the other hand, the immobilized $SiO_2/MAO/Cp_2ZrCl_2$ catalyst prepared by Janiak and Rieger using the pre-alumination method was stable when it was abstracted with heptane.[190] No polymerization activity was observed from the filtered solution. The stability was attributed to the low solubility of Cp_2ZrCl_2 in heptane.[189] Chien and He investigated the stability of $SiO_2/MAO/(\mu$-

[186] Tait, P. J. T.; Monteiro, M. G. K.; Yang, M.; Richardson, J. L.: *Proceedings Metallocenes '96*, Houston 1996.
[187] Semikolenova, N. V.; Zakharov, V. A.: *Macromol. Chem. Phys.* **198(9)**, 2889-2897 (1997).
[188] Sacchi, M. C.; Zucchi, D.; Tritto, I.; Locatelli, P.: *Macromol. Rapid Commun.* **16(8)**, 581-590 (1995).
[189] Kaminsky, W.; Strübel, C.: *J. Mol. Catal. A Chem.* **128(1-3)**, 191-200 (1998).
[190] Janiak, C.; Rieger, B.: *Angew. Makromol. Chem.* **215**, 47-57 (1994).

C_2H_4)Ind_2ZrCl_2, and they found no polymerization activity from the filtered solution after the immobilized catalyst was treated with MAO.[76]

Table 4-4 Catalyst Leaching Experiments Found in the Literature

Immobilized Catalyst	Method	Treatment of Silica	Preparation Conditions	Leaching Experiment Conditions	Activity from Leaching Experiment	Ref
Cp_2ZrCl_2/SiO_2	direct deposition	silica dehydrated at 450 ^oC	Zr = 2.5%	contact with MAO at 22 ^oC for 100 min	filtrate was 5- to 7-fold more reactive than the solid	186
Cp_2ZrMe_2/SiO_2	direct deposition	silica calcinated at 450 ^oC for 3 h & dehydrated at 700 ^oC for 2 h	stir in toluene at 20 ^oC for 30 min, Zr = 3.0%	Al/Zr = 100, stir in toluene at 70 ^oC for 30 min	11.0 kg/g(Zr)/h 80% Zr abstracted	187
Cp_2ZrCl_2/SiO_2	direct deposition	silica calcinated at 650 ^oC for 5 h	stir in toluene at 70 ^oC for 16 h, Zr = 0.60%	Al/Zr = 500, stir in toluene at 50 ^oC for 30 min	trace PE when Al/Zr = 500, no PE when Al/Zr = 300	188
Cp_2ZrCl_2/ MAO/SiO_2	pre-alumination	silica calcinated at 600 ^oC for 6 h & dried at 80 ^oC for 12 h, stir with MAO in toluene at 25 ^oC for 1 h, Al = 3.9 mmol/g	stir in toluene at 25 ^oC for 1 h, Zr = 0.07 mmol/g	Al/Zr = 230, stir in toluene at 30 ^oC for 30 min	37% of the activity of original solid catalyst	189
Cp_2ZrMe_2/ MAO/SiO_2	pre-alumination	silica calcinated at 450 ^oC for 3 h & dehydrated at 700 ^oC for 2 h, stir with MAO in toluene at 20 ^oC for 30 min, Al = 4.6%	stir in toluene at 20 ^oC for 30 min, Zr = 1.8%	Al/Zr = 100, stir in toluene at 70 ^oC for 30 min	22.0 kg/g(Zr)/h 60% Zr abstracted	187
Cp_2ZrCl_2/ MAO/SiO_2	pre-alumination	silica calcinated at 650 ^oC for 5 h, stir with MAO in toluene at 30 ^oC for 30 min, Al = 16%	stir in toluene at 30 ^oC for 30 min, Zr = 0.38%	Al/Zr = 300, stir in toluene at 50 ^oC for 30 min	17g/g	188

Continued on next page.

Table 4-4 Catalyst Leaching Experiments Found in the Literature (Continued)

Immobilized Catalyst	Method	Treatment of Silica	Preparation Conditions	Leaching Experiment Conditions	Activity from Leaching Experiment	Ref
Cp_2ZrCl_2/ MAO/SiO_2	pre-alumination	silica dehydrated at 180 ^oC for 5 h stir with MAO in toluene at 50 ^oC for 2 h, Al = 18%	stir in toluene at 25 ^oC 2-4 h, then stir with MAO in toluene at 25 ^oC for 30 min, distill off solvent, Zr = 0.5-2.0%	extracted with heptane	no activity even after adding more MAO	190
$Et[Ind]_2ZrCl_2$/ MAO/SiO_2	pre-alumination	silica heated at 350 ^oC for 18 h & dehydrated at 200 ^oC for 4 h, stir with MAO in toluene at 50 ^oC for 4 h, Al = 9%	stir in toluene at 25 ^oC overnight, Zr = 0.62%	Al/Zr = 12500, stir in toluene at 25 ^oC for 10 min	no activity, the extracted solid is the same as the original	76
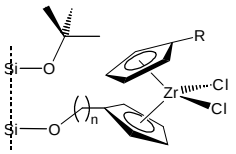	covalent tethering	silica dehydrated at 800 ^oC for 15 h	stir in hexane at 85 ^oC for 3 h, Zr = 1.4%	Al/Zr = 120, stir in hexane at 40 ^oC for 1 h	3% Zr abstracted	104
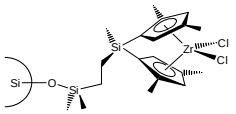	covalent tethering	silica dehydrated at 500 ^oC for 16 h	stir in toluene at 25 ^oC overnight in the presence of NEt_3, Zr = 0.78%	Al/Zr = 100, stir in toluene at 70 ^oC for 30 min	no activity	103

Catalyst leaching experiments were also carried out using some immobilized catalysts prepared by the covalent tethering method. Lee and Oh prepared silica-supported Cp_2ZrCl_2 with Si-O-C tethers (Scheme 1-27).[104] About 3% of the zirconium content was abstracted from the immobilized catalyst by MAO, as indicated by ICP analysis. Suzuki and coworkers immobilized a C_2-symmetric silylene-bridged zirconocene compound on silica through a Si-O-Si linkage (Scheme 1-25).[103] They found no catalyst leaching when the immobilized catalyst was treated with MAO solution.

Therefore, immobilized metallocene catalysts prepared by all the three methods had some degree of catalyst leaching when the immobilized catalysts were contacted with MAO, though there were some contradictory examples.

4.4.2 Catalyst Leaching of the Immobilized Zirconocene Catalysts in This Research

Catalyst leaching was also found in the immobilized zirconocene catalysts in this research. The procedure of the leaching experiments was described in Section 4.5. The immobilized zirconocene catalyst sample used in a leaching experiment was from the same batch of the immobilized catalyst used in the slurry polymerization experiment to obtain the activity data. If there was any significant ethylene polymerization activity in a leaching experiment, the yield was converted to the approximate nominal activity of the immobilized catalyst for catalyst leaching. Since only about half of the solution was used in the polymerization in a leaching experiment, the yield was multiplied by two to estimate the total amount of leaching. The actual yield was then divided by the polymerization time and the total molar quantity of the zirconocene compound in the sample of the immobilized catalyst used in the leaching experiment to obtain the nominal activity of the immobilized catalyst in the leaching experiment. The adjective “nominal” is used because the polymerization activity in a leaching experiment was actually caused by the active species that get into the solution in the leaching experiment. However, the actual quantity of the freed active species in solution was not known, so the total molar quantity of the zirconocene compound in the sample of the immobilized catalyst used in the leaching experiment was used in the activity calculation for convenience.

Table 4-5 Results of the Leaching Experiments

Precursor of Immobilized Catalyst	Nominal Activity (kg/mol(Zr)/h	M_p ($x10^{-5}$)	M_n ($x10^{-5}$)	M_w ($x10^{-5}$)	M_z ($x10^{-5}$)	PDI (M_w/M_n)
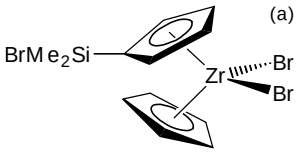 (a)	8.2×10^3	5.58	1.03	7.99	17.7	2.22
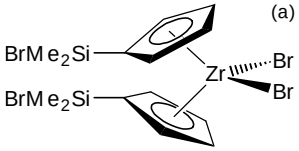 (a)	1.5×10^3	4.59	2.24	8.55	20.7	3.81
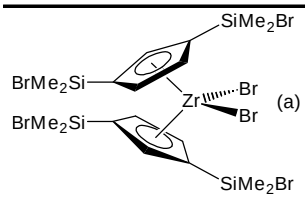 (a)	5.2 x 10	2.30	1.04	3.32	7.32	3.18
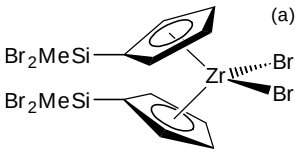 (a)	5.8×10^2	5.91	3.55	9.46	20.6	2.66
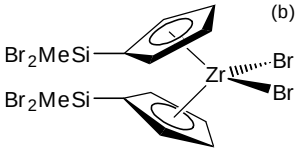 (b)	2.5×10^3	7.03	4.72	11.6	22.6	2.45
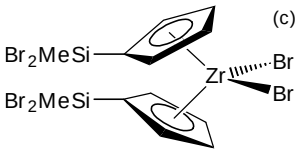 (c)	1.92×10^3	6.30	2.21	8.63	18.9	3.90

(a) Prepared using excess NEt_3, and the Zr loading was about 1.1%.
(b) Prepared without NEt_3, and the Zr loading was 0.42% according to elemental analysis.
(c) Prepared using excess NEt_3, and the Zr loading was about 0.28%.

The results of the leaching experiments of different immobilized zirconocene catalysts in this research are listed in Table 4-5. Most of the nominal activities were comparable to the

activity data of the corresponding original immobilized catalysts. Therefore, catalyst leaching of the active species occurred in the slurry polymerization of most of the immobilized zirconocene catalysts. However, the nominal activity of the immobilized catalyst prepared using [η^5-1,3-$(BrMe_2Si)_2C_5H_3]_2ZrBr_2$ was much lower than the activity of the original immobilized catalyst, suggesting that increase of tether numbers increases the stability of the active species on the support. The PDI of the polyethylene products from the leaching experiments were close to the values of homogeneous metallocene catalysts, which were much lower than those of the polyethylene products from the slurry polymerization experiments using the corresponding original immobilized catalysts. Since the freed active species were actually homogeneous, so it is not surprising that the PDI of the polyethylene products were close to the values of homogeneous metallocene catalysts. The different PDI values of the polyethylene products from the leaching experiment and the slurry polymerization experiment of a same immobilized zirconocene catalyst indicate that the activity of an immobilized catalyst in the slurry polymerization experiment contained the contribution from the freed active species as well as the contribution from the active species that was still on the support. Though, the contribution from the freed active species was dominant in most of the immobilized zirconocene catalysts.

It is interesting to evaluate how much active species was indeed freed from the support in the leaching experiment. In a special leaching experiment of immobilized (η^5-Br_2MeSi-$C_5H_4)_2ZrBr_2$ (1.1% Zr) prepared by the described immobilization process using excess NEt_3, a sample of 0.10 g of the immobilized catalyst was mixed with 3.34 g MAO (Al/Zr ratio was 5000) in toluene in a glass apparatus protected under Ar at 50 ^oC for 10 minutes. The mixture was then filtered through a frit, and the solvent was evaporated in vacuum. A sample of the residue (mostly MAO) from the filtered solution was sent for elemental analysis. Trace analysis

of the sample did not find any zirconium content in the sample. In other words, the zirconium content in the sample was below the detection limit (0.01%). However, a portion of the same residue was dissolved in anhydrous toluene and subjected to the solution ethylene polymerization experiment, which was repeated once, significant amount of polyethylene was obtained in both experiments. Clearly, polymerization activity is more sensitive than ICP.

In a rough estimation, the actual activity of the freed active species is assumed to be the same as that of $(\eta^5\text{-}Me_3Si\text{-}C_5H_4)_2ZrCl_2$ ($9.3x10^4$ kg/mol/h, Table 3-4). The nominal activity of the immobilized $(\eta^5\text{-}Br_2MeSi\text{-}C_5H_4)_2ZrBr_2$ in the leaching experiment ($5.8x10^2$ kg/mol/h) was actually caused by the freed active species, so only about 0.62 percent ($5.8x10^2$ / $9.3x10^4$) of the total zirconocene loading in the immobilized catalyst sample was leached. In the case of the special leaching experiment, it means $6.8x10^{-6}$ g (0.10 x 1.1% x 0.62%) of the zirconium content was abstracted into the solution, which was obviously not detectable since the active zirconium species was dissolved in 3.34 g MAO. Therefore, due to the high activity of the homogeneous active species, only a tiny amount of freed active species caused significant polymer yield in the leaching experiments. Most zirconocene species were still stable on the support in the leaching experiments.

4.5 Experimental Details

General Procedures. Grace 948 silica was ordered from Grace Davison (Baltimore, MD). MAO powder was obtained by evaporating a 30% solution in toluene from Albemarle. NEt_3 was ordered from Aldrich and was distilled from CaH_2 before use. Solvents were purified according to the method described by Grubbs and coworkers.[174] Solution NMR spectra were recorded on a JEOL Eclipse-500 instrument (500 MHz for ^1H, 125 MHz for ^{13}C). Elemental

analyses were performed by Desert Analytics (Tucson, AZ). GPC analyses of polymer samples were carried out by Dow Chemical (Midland, MI).

Dehydration of Silica. Grace 948 silica was gently packed inside a clean quartz tube, which was then sealed with quartz wool at both ends. The loaded tube was fitted into a larger quartz tube open at one end. The larger tube was then put into a tube furnace, so that the silica was in the middle of the homogeneous temperature zone of the furnace. The tube was cautiously evacuated, ultimately reaching about $1x10^{-5}$ torr. Then, the tube furnace was heated up at a rate of 20 ^{o}C/min to 500 ^{o}C. After 6 h at 500 ^{o}C, the furnace was allowed to cool overnight, with the tube still under vacuum. The cooled sample was transferred to a nitrogen glove box.

Typical Metallocene Immobilization Procedure. In the glove box, dehydrated silica (200~400 mg) and a functionalized zirconocene compound (10~40 mg) were transferred into a swivel frit apparatus. On the vacuum line, anhydrous CH_2Cl_2 (about 20 mL) was transferred onto the solid from P_2O_5. In the "excess NEt_3" preparations, an excess (2 mL) of triethylamine (freshly distilled from CaH_2) was injected into the flask under an Ar counterstream, and the mixture was stirred for one hour under Ar at 25 ^{o}C and then filtered. In the "no NEt_3" preparations, no NEt_3 was added, and the mixture was stirred under reflux for 15 h and then filtered. In either case (excess NEt_3 or no NEt_3), the filtrate was evaporated, leaving a residue. The silica collected on the filter was washed with CH_2Cl_2 three times, dried in vacuum at 25 ^{o}C overnight, and transferred to the glove box. The white filtrate residue was analyzed by ^{1}H NMR. In the "excess NEt_3" preparations, $HNEt_3Br$ was identified by its characteristic spectrum: ^{1}H NMR ($CDCl_3$): δ 11.2 (br s, 1 H, NH), 3.12 (m, 6 H, CH_2), 1.44 (t, 9 H, CH_3). Metallocene byproduct species were observed in the spectra of the residues from the "no NEt_3" preparations. These are described in the text.

Slurry Polymerization Procedure. In a typical slurry polymerization experiment, the glass parts of the reactor were dried thoroughly in an oven and transferred into a glove box when they were still hot. The glass kettle was the same as that used in the solution polymerization experiments described in Section 3.4.2. The accessories fixed on the kettle were the same as those used in the solution polymerization experiments, except that, in the preliminary development of the activity measurement experiments, the fourth inlet was fixed with a specially designed glass deliverer to deliver the catalyst powder into the reactor. The reactor was assembled in the glove box, and a measured amount of an immobilized zirconocene catalyst sample and an excess of MAO (typically Al:Zr = 5000) were loaded into the reactor. Outside the glove box, a solution of MAO (50 mg) in about 400 mL of anhydrous toluene at 50 ^{o}C was transferred into the reactor under N_2. The mixture was stirred and the temperature was allowed to stabilize at 50 ^{o}C in water-bath for about 10 minutes. Then, purified ethylene gas was introduced into the suspension to initiate the polymerization. The temperature would drop 1-2 degrees initially and then return to 50 ^{o}C with the help of the water-bath. Fast stirring was applied to ensure rapid mixing of the slurry polymerization. The polymerization time was accurately controlled using a stopwatch, and the polymerization was terminated by injecting a large quantity of 5% HCl in methanol into the reactor when the desired polymerization time was reached (typically 10 minutes). The polyethylene product from each experiment was separated from the solvent by filtration, washed with methanol, and dried at about 75 ^{o}C in vacuum oven overnight. The experiment for each catalyst was repeated at least twice to obtain the average activity value and the standard deviation. In the preliminary development of the activity measurement experiments, the catalyst was delivered into the reactor by another method. The measured catalyst sample was not put into the reactor with MAO in the glove box but put into a

specially designed glass deliverer as shown in Figure 4-1. The reactor with MAO inside was taken out of the glove box. About 400 mL anhydrous toluene was added. Then, the sealed deliverer with the catalyst powder inside was taken out of the glove box and assembled onto the reactor. The toluene in the reactor was stirred and water-bathed to 50 ^{o}C. Then, purified ethylene was introduced to saturate the toluene through the dispersion tube and form a stable flow. After the temperature was stabilized at 50 ^{o}C again, the valve of the deliverer was opened and the catalyst powder was blown into the toluene solution by N_2 to initiate polymerization. The rest part of the experiment was the same as the normal process. This preliminary process was not used later, since the activity of an immobilized catalyst measured using this method was significantly lower than that using the other method. The lower activity is probably because an immobilized catalyst needs a significant initiation period to be wetted by solvent and activated by MAO. In the preliminary method, the wetting and activating time was counted in the polymerization time.

Procedure for the Leaching Experiments. The diagram of the set-up of the reactor used for a leaching experiment is shown in Figure 4-2. The glass kettle and the accessories fixed on the kettle were the same as those used in other polymerization experiments, except that the fourth inlet on the kettle was fitted with a specially designed glass filter. In a typical leaching experiment, the glass parts of the reactor and two Schlenk flasks were dried thoroughly in an oven and transferred into a glove box when they were still hot. The reactor was assembled in the glove box, and about 50 mg of scavenger MAO was put into the reactor. The same amount of an immobilized zirconocene catalyst from the same batch as that used in the slurry polymerization was taken and transferred to a Schlenk flask. Excess MAO (typically Al:Zr = 5000) was put into the other Schlenk flask. The reactor was then taken out of the glove box, and about 350 mL of

anhydrous toluene was transferred into the reactor. The toluene in the reactor was water-bathed to 50 ^{o}C. In the meantime, the sealed Schlenk flask containing MAO was taken out of the glove box, and about 100 mL of anhydrous toluene was transferred into the flask under N_2 protection. The toluene in the Schlenk flask was also water-bathed to 50 ^{o}C. Then, the sealed Schlenk flask with the catalyst inside was taken out of the glove box, and the toluene solution of MAO at 50 ^{o}C in the other Schlenk flask was transferred into the Schlenk flask containing the catalyst. The mixture was stirred and water-bathed at 50 ^{o}C for about 10 minutes. Then, about half of the mixture was transferred, using a canulla, to the glass filter mounted on the reactor. N_2 was applied to the liquid in the filter to push the liquid through into the reactor. After the temperature of the solution in the reactor was again stabilized at 50 ^{o}C, purified ethylene was introduced into the reactor. The temperature would drop 1-2 degrees initially and then return to 50 ^{o}C. Fast stirring was applied to the solution. The reaction time was the same as that of a normal slurry polymerization (typically 10 minutes). The reaction was terminated by injecting large quantity of 5% HCl in methanol into the reactor when the desired time was reached. Any polyethylene product obtained was separated from the solvent by filtration, washed with methanol, and dried at about 75 ^{o}C in vacuum oven overnight. The experiment for each catalyst was repeated at least once to obtain an average leaching activity value.

GPC Measurements of Molecular Weights. Samples of the polyethylene products from different immobilized zirconocene catalysts were sent to Dow Chemical in Midland, Michigan for Gel Permeation Chromatography (GPC) analysis. GPC analyses were carried out by Judy Gunderson. In a typical GPC experiment, a polymer sample is dissolved in 1,2,4-trichlorobenzene at 130 ^{o}C and filtered to remove any insoluble component. The filtered solution is then passed through a chromatographic column, which separates different fractions in

the polymer sample according to the size exclusion principle. The column is filled with particles of porous material. When a polymer solution is passing through the column, polymer molecules of larger hydrodynamic volume in the mobile phase are more difficult to get into the pores, so they bypass the particles through the large inter-particle space and are eluted through the column quickly by solvent. However, polymer particles of smaller hydrodynamic volume can easily get into the pores, so they are retained in the pores for a period of time. Therefore, their elution time is longer. Each polymer fraction eluted from the column is detected by refractive index. In a simplified model, the hydrodynamic volume of a polymer fraction is proportional to its molecular weight. The detector has been calibrated using standard polymer samples of known molecular weights, so the molecular weight of each fraction can be determined, from which the average molecular weights and the molecular weight distribution curve of the polymer sample can be obtained. In a more strict treatment, the structure of a polymer molecule (branch structure and branching frequency) also affects its hydrodynamic volume. Therefore, it is much more complicated to analyze the molecular weights of branched polymer. However, based on the NMR analysis results of selected samples, the polyethylene products from the immobilized zirconocene catalysts in this research are highly linear, so the molecular weights obtained from the GPC analysis are their real molecular weights. The molecular weight data of the polyethylene products from different immobilized zirconocene catalysts are discussed together with the activity data in Section 4.3.

Proton NMR Study of the Chain Structures of the Polyethylene Products. It is well known that polyethylene products from metallocene catalysts are highly linear. To find out if the polyethylene products from the immobilized zirconocene catalysts in this research are also highly linear, some selected polyethylene samples were subjected to proton NMR analysis. If a

polyethylene sample is highly linear, most of the hydrogen atoms in the chains are the CH_2 hydrogen atoms in the middle of the chains, so their chemical shift is essentially the same. Some other hydrogen atoms do exist in highly linear polyethylene, e.g., those in the terminal CH_3 groups (including branch terminae), those in the CH_2 groups near the chain terminals, and those in the CH groups at the branch heads on the chains. However, compared to the quantity of the hydrogen atoms in the CH_2 groups in the middle of linear chains, the quantity of the other hydrogen atoms in highly linear polyethylene are so low that their ratios to the hydrogen atoms in the CH_2 groups in the middle of linear chains is out of the dynamic range of the NMR experiment. Therefore, the signals from the other hydrogen atoms can not be observed in the proton NMR spectrum of highly linear polyethylene, and only a singlet from the hydrogen atoms in the CH_2 groups in the middle of linear chains can be observed. On the other hand, if a polyethylene sample is highly branching, the quantities of the other hydrogen atoms in the polyethylene chains are significant compared to that of the CH_2 hydrogen atoms in the middle of the chains, so the proton NMR spectrum should show several signals representing different hydrogen atoms in the polymer chains. Polyethylene samples from the immobilized catalysts may contain silica, so they need to be pretreated before the NMR analysis. A polyethylene sample was dissolved in hot o-dichlorobenzene, and then the hot solution was filtered. The filtration was slow and very difficult. Due to the temperature drop during filtration, polyethylene precipitated out of the solution and blocked the frit. Only part of the solution was filtered, to which, some methanol was added to precipitate the dissolved polyethylene. Then, the polyethylene precipitate was separated from the solvent by filtration and dried in vacuum. The pretreated polyethylene precipitate was mixed with some 1,1,2,2-$C_2D_2Cl_4$ in a J-Young NMR tube, which can be sealed. The mixture could form a homogeneous solution when 1,1,2,2-

$C_2D_2Cl_4$ started boiling in the tube heated with a heat gun. The boiling point of 1,1,2,2-$C_2D_2Cl_4$ is 146 ^oC. The proton NMR spectra of the polyethylene samples were obtained in a 500-MHz NMR instrument at 140 ^oC. The spectra of the selected polyethylene products showed only a major singlet signal at 1.35 ppm and a tiny signal at 1.41 ppm, besides the solvent signal at 5.98 ppm, which indicated that the polyethylene products from the immobilized zirconocene catalysts were highly linear. The tiny signal at 1.41 ppm was from dissolved water. The ^1H NMR spectrum of a polymer sample obtained after intentionally adding some water to the NMR tube showed that the signal at 1.41 ppm was much enhanced, and the rest signals were unchanged.

4.6 Conclusions

The immobilized zirconocene catalysts prepared using precursor zirconocene compounds containing different numbers and structures of tethers were active for ethylene polymerization with MAO cocatalyst. The activities were much lower than those of typical homogeneous zirconocene catalysts. Increased number of tethers on a precursor molecule decreased the polymerization activity. A precursor molecule with two double-tethers was more active than that with four single-tethers, possibly due to increased conformational flexibility in the supported surface. Use of NEt_3 in the immobilization process poisoned the immobilized catalyst, causing decrease of the activity. The immobilized catalyst of lower zirconium loading showed enhanced polymerization activity than that of higher zirconium loading. Catalyst leaching was observed in all of our immobilized zirconocene catalysts. Though, the freed active species was only a very small portion of the total zirconocene compound loaded on the sample of an immobilized catalyst, since the freed species were highly active, their contribution to the activity of the immobilized catalyst was overwhelming. Increased tethers numbers increased the stability of the active species on the support, so the amount of freed active species was reduced.

Chapter 5 Model Studies and Stabilities of the Si-O-Si Bonds

5.1 Reaction of (h^5-$BrMe_2Si$-C_5H_4)$CpZrBr_2$ with $^tBuMe_2SiOH$

It was observed that the Si-X bonds in halosilyl-substituted zirconocene compounds are much more reactive than the Zr-X bonds in the reactions with nucleophiles. Only the Si-X bonds react with water in air. Therefore, it was assumed that only the Si-X bonds react with surface hydroxyl groups on silica to form tethers, and the Zr-X bonds are intact during the immobilization. However, due to the difficulties in characterization of the immobilized surface zirconocene species, the assumption was difficult to prove directly. A model study was carried out to provide some indirect evidence for this assumption.

In the model study, a silanol molecule, $^tBuMe_2SiOH$, was considered to be the homogeneous analog of a surface hydroxyl group on silica. The reaction between $^tBuMe_2SiOH$ and (η^5-$BrMe_2Si$-C_5H_4)$CpZrBr_2$ was carried out to mimic the immobilization reaction on silica surface. In one reaction, 100 mg of (η^5-$BrMe_2Si$-C_5H_4)$CpZrBr_2$ (0.19 mmol) was dissolved in about 20 mL CH_2Cl_2 in a flask under Ar. Then, 2.0 mL of 0.10 mol/L $^tBuMe_2SiOH$ solution in CH_2Cl_2 (0.20 mmol) was added to the flask under Ar. The mixture was refluxed overnight. After evaporation of the volatile components in vacuum, a gray residue was obtained. The proton NMR spectrum of the residue in $CDCl_3$ showed a major set of signals with several minor impurity signals. The major signals were a multiplet at 6.84 ppm, a multiplet at 6.60 ppm, a singlet at 6.55 ppm, a singlet at 0.89 ppm, a singlet at 0.36 ppm, and a singlet at 0.06 ppm. Their integration ratios were approximately 2.5 : 2.1 : 4.9 : 9.6 : 6.1 : 6.1, respectively, which were close to 2 : 2 : 5 : 9 : 6 : 6, the ratios for [η^5-($^tBuMe_2SiO$)Me_2Si-C_5H_4]$CpZrBr_2$. The chemical shifts of the signals were consistent with the structure of [η^5-($^tBuMe_2SiO$)Me_2Si-C_5H_4]$CpZrBr_2$. The singlet at 0.89 ppm and that at 0.06 ppm were assigned to the protons of the t-butyl group

and those of the two methyl groups on the $^{t}BuMe_2SiO$ group, respectively, since they were very close to the corresponding chemical shifts in $^{t}BuMe_2SiOH$.[191] Based on the corresponding signals in the proton NMR spectrum of (η^5-$BrMe_2Si$-C_5H_4)$CpZrBr_2$,[192] the two multiplets at 6.84 ppm and 6.60 ppm were assigned to the four protons of two kinds on the substituted Cp ring, and the singlet at 6.55 ppm was assigned to the five protons on the unsubstituted Cp ring. The remaining singlet at 0.36 ppm was assigned to the six protons of the two methyl groups of the silyl substituent on the Cp ring.

Recrystallization of the gray residue in hexanes gave only some white non-crystalline precipitate, whose proton NMR spectrum in $CDCl_3$ showed that it contained minor amount of [η^5-($^{t}BuMe_2SiO$)Me_2Si-C_5H_4]$CpZrBr_2$ and a major compound represented by four signals, i.e., a multiplet at 6.83 ppm, a multiplet at 6.58 ppm, a singlet at 6.52 ppm, and a singlet at 0.40 ppm, whose integration ratios were 3.7 : 3.7 : 8.1 : 10.6, respectively. The signals corresponded to the minor impurity signals in the proton NMR spectrum of the crude gray residue. The compound was identified to be the complex with two zirconocene moieties linked together by a disiloxane bridge (Scheme 3-11). The corresponding five ^{13}C NMR signals in $CDCl_3$ were found at 125.3 ppm (CH), 123.3 ppm (C), 117.8 ppm (CH), 116.1 ppm (CH), and 2.2 ppm (CH_3).

Proton NMR spectrum of the residue after evaporation of the solvent in the filtered mother liquor indicated that the residue was pure [η^5-($^{t}BuMe_2SiO$)Me_2Si-C_5H_4]$CpZrBr_2$. The yield was not obtained. The ^{13}C NMR spectrum of the pure product was also obtained in $CDCl_3$: 125.3 ppm (CH), 123.0 ppm (C), 118.6 ppm (CH), 116.0 ppm (CH), 25.8 ppm (CH_3), 18.2 ppm

[191] Chemical shifts of $^{t}BuMe_2SiOH$: ^1H NMR ($CDCl_3$): δ 12.0 (br s, 1 H, OH), 0.89 (s, 9 H, CCH_3), 0.07 (s, 6 H, $SiCH_3$). ^{13}C NMR ($CDCl_3$): δ 25.7 (CH_3), 18.0 (C), -3.5 (CH_3).

[192] Chemical shifts of (η^5-$BrMe_2Si$-C_5H_4)$CpZrBr_2$: ^1H NMR ($CDCl_3$): δ 6.91 (m, 2 H, C_5H_4), 6.60 (m, 2 H, C_5H_4), 6.57 (s, 5 H, C_5H_5), 0.93 (s, 6 H, $SiCH_3$). ^{13}C NMR ($CDCl_3$): δ 125.5 (CH), 123.8 (C), 116.9 (CH), 116.3 (CH), 4.4 (CH_3).

(C), 2.5 ppm (CH_3), and -2.7 ppm (CH_3). The chemical shifts were consistent with the corresponding chemical shifts of $^tBuMe_2SiOH$ and (η^5-$BrMe_2Si$-C_5H_4)$CpZrBr_2$.[191,192] The ^1H and ^{13}C NMR spectra of the pure product in C_6D_6 were also obtained.[193]

In another reaction between $^tBuMe_2SiOH$ and (η^5-$BrMe_2Si$-C_5H_4)$CpZrBr_2$, excess NEt_3 was used, and the mixture was only reacted at 25 ^oC for one hour. The residue after evaporation of the volatile components was a yellow-brown sticky material. The proton NMR spectrum of the residue was much more complicated than that of the residue from the reaction under reflux condition. After washing the residue with hexanes, the proton NMR spectrum in $CDCl_3$ showed that the washed and filtered solid was $HNEt_3Br$. Some yellow residue was obtained after evaporation of the filtered washing hexanes. The proton NMR spectrum in $CDCl_3$ showed that the yellow residue contained primarily [η^5-($^tBuMe_2SiO$)Me_2Si-C_5H_4]$CpZrBr_2$, and minor amount of the disiloxane-bridged binuclear zirconocene compound (Scheme 3-11), as well as some unidentified impurities (less than 30% of the major product). The unidentified impurities were tentatively assigned to products in which not only the bromine atoms of the Si-Br bond but also the bromine atoms of the Zr-Br bonds were replaced by $^tBuMe_2SiO$ groups or NEt_3, with the assistance of excess NEt_3.

Therefore, under the reflux condition or with the assistance of excess NEt_3, the major product from the reaction between $^tBuMe_2SiOH$ and (η^5-$BrMe_2Si$-C_5H_4)$CpZrBr_2$ was [η^5-($^tBuMe_2SiO$)Me_2Si-C_5H_4]$CpZrBr_2$. A minor byproduct, the disiloxane-bridged binuclear zirconocene compound was also produced (Scheme 5-1). The results of the model reactions in

[193] Chemical shifts of [η^5-($^tBuMe_2SiO$)Me_2Si-C_5H_4]$CpZrBr_2$: ^1H NMR (C_6D_6): d 6.55 (m, 2 H, C_5H_4), 6.07 (s, 5 H, C_5H_5), 6.02 (m, 2 H, C_5H_4), 0.92 (s, 9 H, CCH_3), 0.41 (s, 6 H, $SiCH_3$), 0.04 (s, 6 H, $SiCH_3$). ^{13}C NMR (C_6D_6): d 125.2 (CH), 117.0 (CH), 115.5 (CH), 25.7 (CH_3), 2.2 (CH_3), -2.9 (CH_3). The two tertiary carbon signals were lost due to low sample concentration.

solution support the existence of the assumed immobilization reaction between halosilyl-substituted zirconocene compounds and surface hydroxyl groups.

5.2 Stabilities of the Si-O-Si Bonds in the Reaction with MAO in Some Model Systems

The results of the leaching experiments of the immobilized zirconocene catalysts discussed in Section 4.4.2 indicate that a small portion of active species was abstracted from silica upon interacting with MAO presumably through cleavage of the Si-O-Si bonds of the tethers. The abstracted active species was highly active, to which most of the activity of the immobilized catalyst was contributed. Therefore, it was important for us to investigate the stabilities of the Si-O-Si bonds in some model systems.

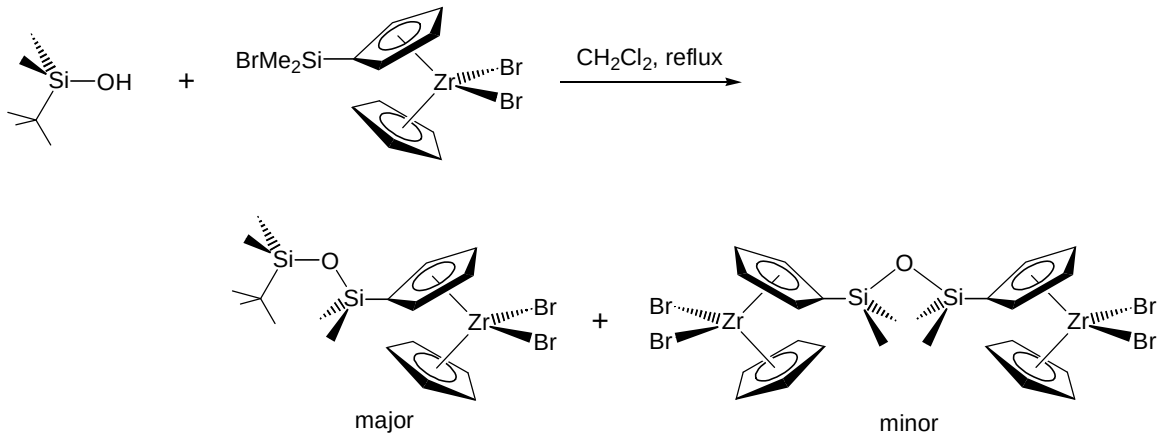

Scheme 5-1 Reaction between ^{t}BuMe$_2$SiOH and (η^5-BrMe$_2$Si-C$_5$H$_4$)CpZrBr$_2$

5.2.1 Reaction of [η^5-(^{t}BuMe$_2$SiO)Me$_2$Si-C$_5$H$_4$]CpZrBr$_2$ with MAO

The reaction of [η^5-(^{t}BuMe$_2$SiO)Me$_2$Si-C$_5$H$_4$]CpZrBr$_2$ with MAO in $CDCl_3$ was difficult to study. The proton NMR spectrum obtained within 20 minutes after the mixing of the two chemicals in $CDCl_3$ in a J-Young NMR tube at 50 ^{o}C was complicated. In addition, the yellow solution in the tube after mixing the two chemicals became dark brown gradually in several hours, and then a dark brown precipitate appeared. The NMR spectra of the mixture changed with the change of the color. The reaction of (η^5-Me$_3$Si-C$_5$H$_4$)CpZrCl$_2$ with MAO in $CDCl_3$ had

the same color-change course, and the proton NMR spectra were also complicated and changed with the color change. Similar results were also obtained in C_6D_6. Even the reaction between Cp_2ZrCl_2 and MAO in C_6D_6 showed the color change. We were not able to obtain conclusive evidence about the stability of these "model" Si-O-Si compounds, so we decided to simplify the model as much as possible.

5.2.2 Reaction of Hexamethyldisiloxane with MAO

Hexamethyldisiloxane (Me_3Si-O-$SiMe_3$) is the simplest compound that contains a Si-O-Si bond. The stability of this Si-O-Si bond in the reaction with MAO may partially reflect the stability of the Si-O-Si bonds of the tethers of the immobilized zirconocene catalysts. In a reaction, 38 mg Me_3Si-O-$SiMe_3$ was dissolved in C_6D_6 in a J-Young NMR tube, and 137 mg MAO was added to the tube in a glove box. The molar ratio between Me_3Si-O-$SiMe_3$ and MAO was about 1 : 10. The NMR tube was then sealed and heated at 50 ^oC overnight. The proton NMR spectrum of the resulted mixture showed five weak signals at around 0 ppm (0.055 ppm, 0.022 ppm, 0.014 ppm, 0.005 ppm, and -0.005 ppm) besides the huge signal of Me_3Si-O-$SiMe_3$ at 0.115 ppm and the broad band of MAO centered at -0.254 ppm (Figure 5-1). Among the five signals, two signals of about the same intensity at 0.055 ppm and 0.005 ppm were unlikely the satellites of the huge signal at 0.115 ppm due to their chemical shifts and distinguishing intensities. They were probably from the reaction products of Me_3Si-O-$SiMe_3$ with MAO, i.e., Me_3Si-O-MAO and $SiMe_4$ (Scheme 5-2).

Scheme 5-2 Reaction between of Me_3Si-O-$SiMe_3$ and MAO

$$Me_3Si\text{-}O\text{-}SiMe_3 + CH_3\text{-}MAO \longrightarrow Me_3Si\text{-}O\text{-}MAO + SiMe_4$$

Figure 5-1 500 MHz ^{1}H NMR Spectrum of the Reaction between Me_3Si-O-$SiMe_3$ and MAO

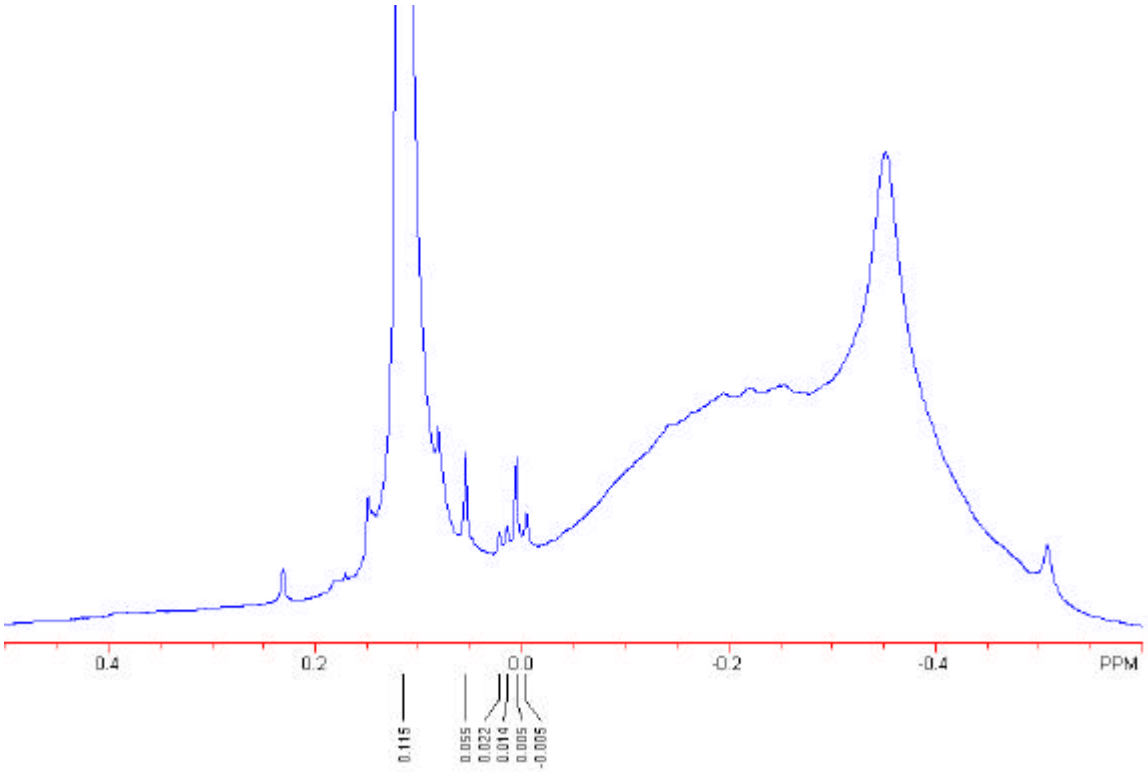

Figure 5-2 500 MHz ^{1}H NMR Spectrum of the Reaction between Me_3Si-O-$SiMe_3$ and MAO with Pure $SiMe_4$ Added

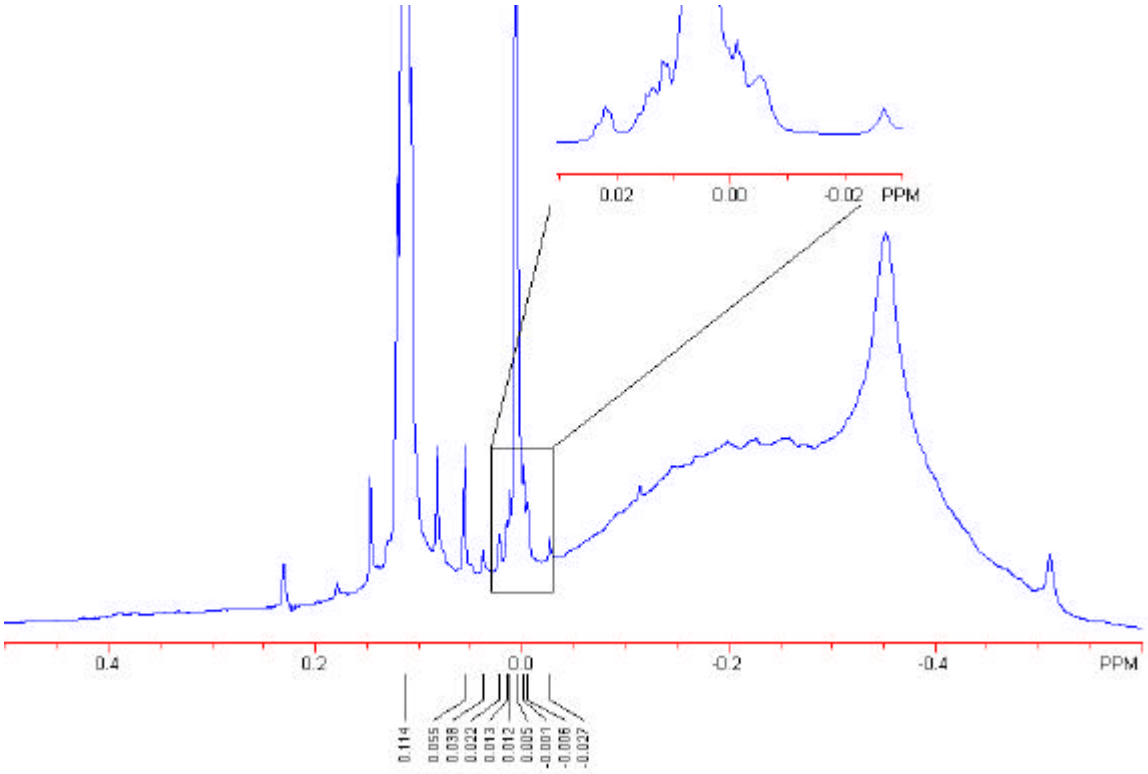

The signal at 0.005 ppm was suspected to be from $SiMe_4$. To confirm the suspicous, a little pure $SiMe_4$ was diffused from high vacuum line into the NMR tube containing the reaction mixture. The proton NMR spectrum of the reaction mixture after addition of $SiMe_4$ showed that the signal at 0.005 ppm was enhanced tremendously. The other four signals were still there (Figure 5-2). Four additional signals at 0.038 ppm, 0.012 ppm, -0.001 ppm, and -0.027 ppm were probably the satellites of the $SiMe_4$ signal. The NMR evidence showed that a little portion (2.1% in a rough NMR integration estimation) of $Me_3Si\text{-}O\text{-}SiMe_3$ was indeed reacted with MAO, and $SiMe_4$ was produced.

5.2.3 Reaction of the Immobilized Decylchlorosilane with MAO

Suzuki and coworkers claimed that they observed no catalyst leaching in the reaction between MAO and their immobilized ansa-zirconocene catalyst with a single covalent tether bonded to silica by a Si-O-Si bond.[103] Their results are in some ways in contradiction with the results in this research. The difference between their tether and the tethers used in this research is that their tether has an alkyl spacer between the Si-O-Si bond and the zirconocene moiety, but the tethers in this research have no such spacers. To investigate whether such kind of Si-O-Si bonds is stable in the reaction with MAO, the following reactions were carried out.

In a Schlenk flask, 1.0 mL 0.05 mol/L decylchlorosilanol in toluene was added to a slurry of 0.50 g dehydrated silica in 10 mL anhydrous toluene. Freshly distilled NEt_3 (2 mL) was added to the mixture, and the mixture was stirred for one hour at 25 ^oC. Then, the product silica with immobilized decylchlorosilanol was filtered, washed with toluene, and dried in vacuum. Proton NMR spectrum of the residue from the filtered solution showed that the residue contained the byproduct of $HNEt_3Cl$. The product silica with immobilized decylchlorosilanol (0.20 g) and 2.3 g MAO (Al : silanol = 2000) were dispersed in 30 mL of 50 ^oC anhydrous toluene. The

mixture was stirred at 50 ^{o}C for 30 min and then filtered. The filtered solution was evaporated to obtain solid MAO. The product MAO, which might contain trace amount of leached decyl species, was dissolved in 20 mL CH_2Cl_2 and hydrolyzed with excess deionized water. A white slurry of alumina gel was obtained, which was dried and extracted with pentane. The pentane extract and the slurry were subjected to MS analysis. The spectrum showed a complex sequence of fragments in the range of 100-200 amu, but no clear assignments could be made.

5.3 Conclusions

The model studies showed that the SiOH group of $^{t}BuMe_2SiOH$ reacts predominantly with the Si-Br bond of (η^5-$BrMe_2Si$-C_5H_4)$CpZrBr_2$ instead of the Zr-Br bonds, indicating that the expected immobilization reaction between surface hydroxyl groups of silica and the halosilyl-substituted zirconocene compounds was reasonable. The complicated reaction of [η^5-($^{t}BuMe_2SiO$)Me_2Si-C_5H_4]$CpZrBr_2$ with MAO made the study of the stability of the Si-O-Si bond very difficult. NMR analysis of the products from the reaction between Me_3Si-O-$SiMe_3$ and MAO indicated the cleavage of Si-O-Si bonds in Me_3Si-O-$SiMe_3$.

Chapter 6 Conclusions and Future Work

The first goal of this research was to explore synthetic routes to prepare zirconocene compounds containing double-tether-forming substituents. Two approaches were proposed. The first approach is to replace Si in the Me_3Si-substituted zirconocene compounds with Sn, since the Sn-C bond is weaker than the Si-C bond. The second approach is to replace the methyl groups in the Me_3Si substituents with more reactive phenyl groups. The results from the investigation of the first approach showed that the Sn-Me bonds in the Me_3Sn-substituted zirconocene compound were indeed more reactive in electrophilic substitution reaction than the Si-Me bonds in the Me_3Si-substituted zirconocene compounds. The conversion of a Me_3Sn substituent to a Br_2MeSn substituent is convenient, while a Me_3Si substituent can only be converted to a $BrMe_2Si$ substituent. However, the Sn-Br bonds were much less reactive than the Si-Br bonds in nucleophilic substitution reaction, implying that the Br_2MeSn substituents are not useful for the formation of double-tethers in the immobilization reaction on silica. The results from the investigation of the second approach showed that the Si-Ph bonds in the phenylsilyl-substituted zirconocene compounds are more reactive in electrophilic substitution reaction than the Si-Me bonds. The conversion of a Ph_2MeSi substituent to a Br_2MeSi substituent is convenient. The Br_2MeSi substituents are also very reactive in nucleophilic substitution reaction, so they were selected as promising candidates to form double-tethers in the immobilization reaction.

The second goal of this research is to prepare silica-supported zirconocene catalysts with the zirconocene compounds containing various tether-forming substituents and investigate their catalytic properties for polymerization with MAO cocatalyst. The results from the research indicated that the zirconocene compounds could be immobilized on silica. The immobilized zirconocene catalysts were active for ethylene polymerization with MAO cocatalyst. Their

activities were much lower than those of homogeneous zirconocene catalysts. Catalyst leaching was found in the immobilized zirconocene catalysts. Though the amount of active species that left silica support during slurry polymerization was very small, the contributions of the leached active species to the activities of the immobilized zirconocene catalysts were great. Increased number of tethers of a zirconocene molecule reduced catalyst leaching.

Two new immobilization strategies are proposed for the future work of the immobilization of the halosilyl-substituted zirconocene compounds.

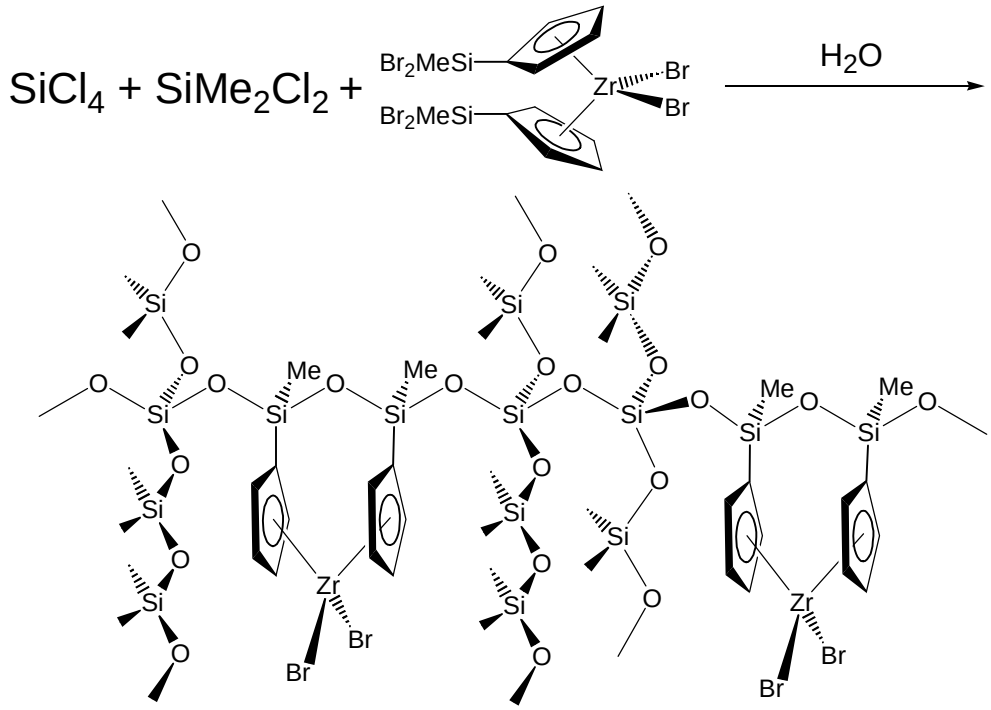

Scheme 6-1 Proposed Formation of Silica Gel Containing Zirconocene Molecules

The first proposal is to immobilize a halosilyl-substituted zirconocene compound by integrating the silyl substituents of the molecules of a zirconocene compound into the network of a silica sol-gel. For example, $(\eta^5\text{-}Br_2MeSi\text{-}C_5H_4)_2ZrBr_2$ molecules form the polymeric structure described in Section 3.4, when they are hydrolyzed. Silica gel can be prepared by hydrolysis of $SiCl_4$ or $Si(OR)_4$. If $SiCl_4$ is hydrolyzed in the presence of $(\eta^5\text{-}Br_2MeSi\text{-}C_5H_4)_2ZrBr_2$, the ($\eta^5$-

$Br_2MeSi\text{-}C_5H_4)_2ZrBr_2$ molecules should be integrated into the three dimensional network of the formed silica gel (Scheme 6-1). The silica gel network should increase the stability of the zirconocene molecule. The leaching experiment results showed that the Si-O-Si bonds were very stable and only a very small portion of the Si-O-Si bonds was cleaved in the reaction with MAO. The Si-O-Si bonds formed in the immobilization reaction in this research were different from the Si-O-Si bonds of the silica support. However, when the zirconocene molecules are integrated into the silica gel network, the Si-O-Si bonds that bind the zirconocene molecules to the gel network are almost the same as the common network-constructing Si-O-Si bonds in the gel network formed among the hydrolyzed $SiCl_4$ molecules. It is very unlikely that all of the four Si-O-Si bonds that bind one particular zirconocene molecule in the silica gel network are cleaved by MAO, so catalyst leaching in the immobilized zirconocene catalyst prepared by this method should be minimized. In the development of this new immobilization method, besides the gelation conditions that need to be systematically investigated to optimize the immobilized catalysts, halosilanes of different numbers of halogen groups can also be used in the formation of silica gel to investigate their influences on the catalytic behaviors of the formed immobilized catalysts. The gelation is a condensation polymerization process. The functionality of $SiCl_4$, $SiMeCl_3$, $SiMe_2Cl_2$, and $SiMe_3Cl$ are four, three, two, and one, respectively, so pure $SiCl_4$ or $SiMeCl_3$ can gelatinize during hydrolysis, but pure $SiMe_2Cl_2$ or $SiMe_3Cl$ can not. However, $SiMe_2Cl_2$ and $SiMe_3Cl$ are also useful. The function of $SiMe_2Cl_2$ in the silica gel network is to extend chains, and that of $SiMe_3Cl$ is to terminate chains. If a mixture of $SiCl_4$ and $SiMe_2Cl_2$ is used in the formation of silica gel integrated with $(\eta^5\text{-}Br_2MeSi\text{-}C_5H_4)_2ZrBr_2$, the increase of the ratio of $SiMe_2Cl_2$ will increase the chain lengths between cross-links in the formed network and thus increase the free space around the integrated zirconocene molecules. Therefore, the

integrated molecules should have higher degree of motion freedom, and they should be more accessible to MAO and monomer molecules. Since $SiMe_3Cl$ can terminate chains, certain amount of $SiMe_3Cl$ can be added to the gelation system to control the size of the silica gel network, as well as to protect the chain ends with Me_3SiO caps.

The second proposal is to develop a new immobilization method to immobilize the metallocene compounds, which is a combination of the pre-alumination method and the covalent-tethering method. The polymerization results showed that the immobilized zirconocene catalysts still had multi-site behavior, which was reflected by the broad molecular distributions of the polyethylene products. Since silica surface is of multi-site nature, it is difficult to remove the multi-site behavior of the immobilized catalysts, if the precursor molecules are immobilized on unmodified silica. The pre-alumination method is an immobilization method that can remove the multi-site behavior. In the method, silica is treated with MAO before the immobilization of the precursor molecules. The modified silica surface is covered with MAO, which covers the multiple sites of the silica surface and makes the modified silica surface uniform. Therefore, the precursor molecules immobilized on the MAO-modified silica should have the same environment, which is similar to the environment in solution, so the polymers produced by the immobilized catalysts prepared by the pre-alumination method should resemble those produced by homogeneous catalysts. However, catalyst leaching was also found in the immobilized metallocene catalysts prepared by the pre-alumination method. The results of the leaching experiments in this research showed that the Si-O-Si bonds were stable, so the idea of the proposed new immobilization method is to combine the stability of covalent tethers and the surface homogeneity of pre-aluminated silica. In the new immobilization method, silica is treated with MAO first, then the pre-aluminated silica is reacted with a zirconocene precursor

with tether-forming substituents, e.g. (η^5-$BrMe_2Si$-C_5H_4)$CpZrBr_2$, to form the immobilized zirconocene catalyst. The precursor molecule is expected to have not only direct ionic interaction with the surface MAO but also a covalent tether formed by the reaction between the Si-Br bond and the surface MAO (Scheme 6-2). The covalent tether is expected to make the zirconocene molecule more stable on the modified silica. At the same time, surrounded by surface MAO, the zirconocene molecule is still in a pseudo-homogeneous environment. Therefore, the immobilized catalyst is expected not only to have no or less catalyst leaching, but also to have similar catalytic behaviors to the homogeneous catalysts, e.g., high activity and narrow MWD. In the development of this new immobilization method, the spacer length, the tether number, and the tether type can be systematically changed to investigate their influences on the catalytic behaviors of the immobilized catalysts.

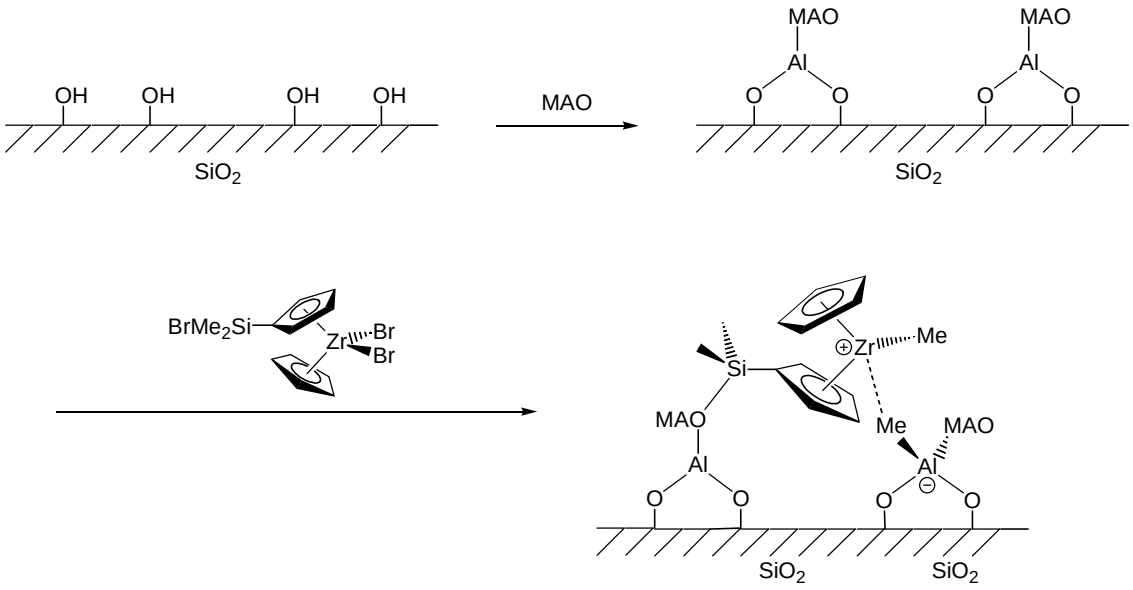

Scheme 6-2 Proposed Immobilization of Functionalized Zirconocene Compound on MAO-modified Silica

Vita

Current Position, 1999-2001

Ph. D. Candidate in Chemistry
Department of Chemistry
Virginia Polytechnic Institute and State University
Blacksburg, Virginia 24060, United States of America
Dissertation: The Use of Functionalized Zirconocenes as Precursors to Silica-Supported Zirconocene Olefin Polymerization Catalysts.
Advisor: Prof. Paul A. Deck

Graduate Education, 1993-1999

1996-1999
Department of Chemistry
Virginia Polytechnic Institute and State University
Blacksburg, Virginia 24060, United States of America
Degree: M. S. in Chemistry, March 1999.
Thesis: Synthesis of Nanometer-sized Y_2O_3 Particles in AOT/Isooctane Reverse Micelle Solution
Advisor: Prof. Brian M. Tissue

1993-1996
Department of Materials Science
Fudan University
Shanghai 200433, People's Republic of China
Degree: M. S. in Materials Chemistry, June 1996.
Thesis: Synthesis and Characterization of Superfine $InBO_3$:Eu and YBO_3:Eu Phosphors
Advisor: Prof. Jinggeng Huang

Undergraduate Education, 1989-1993

1989-1993
Department of Chemistry
Nanjing University
Nanjing, Jiangsu 210090, People's Republic of China.
Degree: B. S. in Chemistry, July 1993
Research Project: Modification and Characterization of Clay Catalysts for p-Alkylation of Phenol with C_6-C_8 Alkenes
Advisors: Prof. Yichun Yan and Prof. Wenxia Shen